Universidad de Huelva

Departamento de Trabajo Social, Sociología y Salud Pública

Industrial environmental pollution as a determinant of the bioacumulation of metal(loid)s in Huelva

Memoria para optar al grado de doctor
presentada por:

Manuel Contreras Llanes

Fecha de lectura: 17 de junio de 2025

Bajo la dirección del doctor:

Juan Alguacil Ojeda

Huelva, 2025

DOCTORAL THESIS

INDUSTRIAL ENVIRONMENTAL POLLUTION AS A DETERMINANT OF THE BIOACUMULATION OF METAL(LOID)S IN HUELVA

Manuel Contreras Llanes

Doctoral Thesis

Industrial environmental pollution as a determinant of the bioacumulation of metal(loid)s in Huelva

Contaminación ambiental industrial como determinante de la bioacumulación de metal(oid)es en Huelva.

Manuel Contreras Llanes

Directors:
Juan Alguacil Ojeda

Tutor:
Juan Alguacil Ojeda

Doctoral Program in Health Sciences

Programa de Doctorado en Ciencias de la Salud

2025

Universidad de Huelva

Funding

This work has been partially supported by both, the Andalusian Government, '2018 Special Action of the Andalusian Government: Support to the Huelva Phosphogypsum Experts Committee'; and by Huelva University local funds to support research groups during 2018 to 2023.

Spanish Government Department of Science and Technology (MINECO), through the project 'Fluxes of radionuclides emitted by the phosphogypsum piles located at Huelva; assessment of the dispersion, radiological risks and remediation proposals' (Ref.: CTM2015-68628-R)

Government of Andalusia through the project 'Characterisation and modelling of the phosphogypsum stacks from Huelva for their environmental management and control' (Ref.: P10-RNM-6300) and 'Phosphogypsum: from the environmental assessment as a waste to its revaluation as a resource' (Ref.: P12-RNM-2260). In addition, Andalusian Public Foundation for Progress and Health through the project 'Incorporation of Huelva into the Population-Based Multicase-Control Study (Breast, Colorectal, Gastro-Oesophageal, and Prostate Cancer)' (Ref.: PI-0571 2010) and 'Identification of breast cancer risk factors in south-western Andalusia' (Ref.: PI-0306 2011). The Health Research Fund (FIS) by Government of Andalusia through the project 'Bladder cancer in south-western Andalusia: The role of environmental exposure' (Ref.: PI071160) and 'Association between occupational exposure and cancer in the MultiCase-Control Cancer Study MCC-Spain' (Ref.: PI12/00265).

On the other hand, the research contract awarded through the selection of doctoral research personnel was essential for the preparation of this thesis; reference DOC_01664, called by Resolution of May 21, 2020 of the General Secretariat of Universities, Research and Technology, corresponding to the aid granted to universities and public research entities by Resolution of December 30, 2019 within the scope of the Andalusian Plan for Research, Development and Innovation (PAIDI 2020). These grants, provided for in the aforementioned call, are co-financed by the European Union within the framework of the European Social Fund Operational Program of Andalusia 2014-2020.

Furthermore, some of the research has been carried out at the Department of Anatomy, School of Medicine, Pamukkale Üniversitesi (Pamukkale, Türkiye), with the help of the Prof. Dr Mehmet Bülent Özdemir.

A mis padres,
Manuel y Concha
, y a mi sobrino Juan Manuel

Que los vientos te empujen siempre hacia delante y
el sol te dé en la cara, y los vientos del destino te hagan
volar para así bailar con las estrellas

Agradecimientos

Al finalizar este camino lleno de esfuerzo y dedicación, quiero aprovechar la oportunidad para expresar mi más sincero agradecimiento a todas las personas que, de una manera u otra, han dejado su huella en la realización de esta tesis.

En primer lugar, mis palabras más profundas van dirigidas a mis PADRES, los pilares de mi existencia. Gracias por darme las herramientas para crecer como persona, por vuestro amor incondicional, por todos los valores que me habéis inculcado, así como los innumerables sacrificios que habéis hecho por mí. Vuestro apoyo me ha llevado hasta aquí. OS QUIERO y ADMIRO más de lo que puedo expresar con palabras.

Mi querida ABUELITA CARMEN merece una mención especial. Tu cariño, ternura y tus risas han sido un faro de luz constante en mi vida. Junto con ella se encuentra su gran amiga, Chiquita, que siempre vive en mis pensamientos y corazón. Guiarme y alumbrarme el camino desde el firmamento.

A mi familia en general, gracias por cada palabra de aliento, especialmente a mis titas Manuela y María, mi tío Juan Antonio, mis primos y, por supuesto, a mi queridísimo sobrino Juan Manuel. No puedo olvidar mencionar a dos ejemplos de vida, Hugo y “la rubia de los ajos”.

A mi director de tesis, el Dr. Juan Alguacil Ojeda, gracias por su guía inquebrantable y por mostrarme el camino en el mundo de la investigación en Salud. A mi compañera, amiga y “codirectora” la Dra. Vanessa Santos Sánchez sin tu ayuda, compresión, ánimo, apoyo, etc. este camino hubiera sido imposible. Mi gratitud también se extiende a mis compañeros del Departamento, en especial a Pepa, quienes siempre tuvieron una mano dispuesta para ayudar y compartieron conmigo momentos que hicieron este viaje más llevadero.

Tampoco podría olvidar a Lorenzo Lidueña, cuya ayuda con los aspectos administrativos fue esencial, y a Pablo Hidalgo, un AMIGO, por su apoyo incondicional y constante.

Finalmente, a mis AMIGOS, la familia que se elige, a quienes considero un regalo invaluable. Pajáres, Raúl, Mac, Tomás, Marieke, Dirk, Dunia, y mis compañeros de

pedaladas, sois una parte fundamental de mi vida y de este logro. ¡Gracias a todos por estar ahí siempre!

This PhD thesis is presented according to the Compendium of Publications mode, regulated under art. 35 of the Regulation of Official Doctoral Studies of the University of Huelva of 17th December 2024. The articles have been published with the express approval of the Director/Tutor of this PhD thesis and carried out further to the enrolment of doctoral studies. Moreover, this thesis is also eligible for the mention of International Doctorate of the University of Huelva, according to art. 36 of the Regulation, '*...that part of the doctoral thesis, at least the summary and the conclusions, be written and defended in one of the usual languages for scientific communication in its field of knowledge, different from any of the official languages in Spain*', thus, the thesis is completely written in English, although the Summary and the Conclusions of the study are also presented in Spanish.

Publications

1. **Contreras-Llanes, M.**, Santos-Sánchez, V., Alguacil, J. and Castillo, J.M., 2024. Delineating distinct sediment pollution signatures from diverse sources in a heavily contaminated estuary near an area of high cancer and cardiovascular mortality. Sci. Total Environ. 957, 177715. https://doi.org/10.1016/j.scitotenv.2024.177715

2. **Contreras-Llanes, M.**, Santos-Sánchez, V., Alguacil, J. and Rodríguez, R., 2025b. Influence of phosphogypsum waste on rainwater chemistry in a highly polluted area with high mortality rates in Huelva metropolitan area, Spain. *Sustainability*, 17, 3102. https://doi.org/10.3390/su17073102

3. **Contreras-Llanes, M**., Alguacil, J., Capelo, R., Gómez-Ariza, J.L., García-Pérez, J., Pérez-Gómez, B., Martin-Olmedo, P. and Santos-Sánchez, V., 2025a. Internal cumulated dose of toxic metal(loid)s in a population residing near a Naturally Occurring Radioactive Material waste stacks and an industrial heavily polluted area with high mortality rates in Spain. J. Xenobiot. 15, 29. https://doi.org/10.3390/jox15010029

Structure of the thesis

This doctoral thesis is structured into six sections. The first section, titled 'Introduction', presents the background of the problem, a detailed explanation of the study area, the main pollution sources, the potential relationship between industrial and mining pollution and the health effects on the residents of Huelva.

The thematic unity of the thesis is justified in Section 2. This section establishes a comprehensive and compelling rationale for the thematic integration present throughout the work.

In the following Section 3 called 'Objectives', the main objective and the specific objectives of the thesis are showed.

Section 4, titled 'Methodology', provides a comprehensive and detailed presentation of the materials and methods employed in the study. Firstly, sampling materials and sample pre-treatment are described. Then, the measuring techniques used for the characterisation of the wastes and materials have been summarised. Finally, the techniques used to evaluate the technological properties and the potential environmental risks are shown.

The discussion is described in Section 5, which is divided into five sub-sections, constitutes the core of this thesis and presents the results. The first sub-section (5.1) identifies specific pollution signatures from local pollution sources in marsh sediments using geochemical tracers in the highly polluted Odiel–Tinto Estuary, prior to the implementation of the approved restoration plan, RESTORE 2030, for the affected marshes. This study has been published in Science of the Total Environment (Contreras-Llanes et al., 2024).

Sub-section (5.2) focuses on investigating the distribution of suspended pollutant particles originating from the phosphogypsum stacks to determine their radius of influence on the chemical composition of rainwater in the Huelva metropolitan area. This work has been published in Sustainability (Contreras-Llanes et al., 2025b).

Sub-section (5.3), reports the association between Huelva's residents proximity to local pollution sources of metal(loid) and their bioaccumulation in toenails. This work has been published in Journal of Xenobiotics (Contreras-Llanes et al., 2025a).

Last sub-sections include the strength and limitation (5.4) of the study.

Finally, Sections 6 and 7 present the main conclusions of this thesis in English and Spanish respectively, along with proposed research lines for the future.

Additionally, this thesis includes an annex that presents both an extended abstract and full version of each paper (Annex I), the document proving the quartile and impact index of the publications included in the thesis, corresponding to the year of publication or the latest available (Annex II), as well as a list of other publications derived from the thesis (Annex III).

List of abbreviations

AMD	Acid mine drainage
APHEA	Air Pollution and Health, a European Approach
BDU	Andalusian Public Healthcare database
CIDERTA	Research and Development of Agri-Food Resources and Technologies Centre
CLL	Chronic lymphocytic leukaemia
EC	Electrical conductivity
Eh	Redox potential
GIS	Geographic information system
IAEA	International Atomic Energy Agency
IC	Ion chromatography
ICP-MS	Inductively coupled plasma mass spectroscopy
ICP-OES	Inductively coupled plasma optical emission spectroscopy
IDL	Instrumental detection limits
IDW	Inverse distance weighting
IQC	Internal quality controls
KED	Kinetic energy discrimination
LOD	Low limits of detection
MCC-Spain	Multicase-control study, Spain
NMMAPS	National Morbidity, Mortality, and Air Pollution Study
NORM	Naturally occurring radioactive material
PC	Principal component
PCA	Principal component analysis
PG	Phosphogypsum
PM_{10}	Particulate matter (ø < 10 µm)
ppb	Parts per billion (ppb)
ppm	Parts per million (ppm)
ppt	Parts per thousand (ppt),
PTFE	Polytetrafluoroethylene
SPSS	Statistical Package for the Social Sciences

WHO	World Health Organisation
WMO	World Meteorological Organisation

List of figures

List of tables

Abstract

Introduction: Huelva City, in SW Spain, encompasses chemical plants, refineries, fertiliser production facilities, and one of the largest phosphogypsum stacks globally, in addition to mining operations within the Iberian Pyrite Belt, that contribute to significant environmental pollution. The city faces higher mortality rates for cancers and heart diseases compared to the rest of Spain, as well as social inequalities. Understanding the sources, routes of exposure and impact of industrial and mining pollution is crucial for protecting public health and the environment, and to evaluate the potential contribution of industrial pollution to the mortality.

Objective: To study the association between the location of industrial pollution sources and their environmental pollution sites, and the bioaccumulation of metal(loid)s on Huelva City's population.

Methology: Seventy sediment samples were collected from six different marshes in the Odiel-Tinto Estuary and one in the nearby unpolluted Piedras River Estuary in March 2021. The sediment textures were analysed, and pH, electrical conductivity (EC), and redox potential (Eh) were measured, while the concentrations of 48 chemical elements were determined. To assess the deposition of metal(loid)s in rainwater, 612 rainwater samples were collected using 17 rain gauges around the metropolitan area of Huelva from January 2021 to December 2022. pH, EC, major ions, and trace metals were detected in the soluble fraction of the rainwater. Fifty-five participants aged 20 to 85 from the city of Huelva were included in the MCC-Spain study. The elemental content of 16 metal(loid)s was analysed in toenail samples. Spatial variability in metal(loid) concentrations was studied using kriging.

Results: A unique pollution signature for PG stacks was identified, characterised by 20 elements including Gd, U, As, and Zn. AMD from mining waste deposits showed six key elements like Fe, Pb, and Mn. Sulphur marked AMD influence in the Tinto River, while beryllium indicated agricultural impact. Rainwater quality varied spatially, with enrichment of toxic metal(loid)s like As, Cr, and Ni near PG stacks, exceeding WHO guidelines for drinking water. Marine and industrial emissions also contributed to pollution. Huelva residents' toenails showed higher levels of As, Co, Cr, Ni, and Se

compared to unpolluted areas, correlating with proximity to PG stacks and industrial complexes.

Conclusions: We identified distinct pollution signatures for PG stacks, separating metal exposure from other sources like AMD in the Odiel and Tinto Rivers and agricultural areas. Contributes to understanding the influence of various pollution sources in the Odiel-Tinto Estuary, establishing a baseline for assessing environmental and health impacts. Spatial variability in sediments and rainwater chemistry showed decreasing concentrations of harmful elements as distance from PG stacks increases. Higher levels of hazardous elements in Huelva residents' toenails were governed by anthropogenic factors, with distinct spatial variations in exposure. The research consistently demonstrates the influence of exposure sources on salt marsh sediments and rainfall in Huelva, identifying contamination hotspots and their impact on residents' metal(loid)s bioaccumulation. These findings underscore the need for targeted remediation efforts and continued monitoring to control the environmental and health impacts of industrial activities in Huelva.

Resumen

Introducción: La ciudad de Huelva, en el suroeste de España, cuenta con plantas químicas, refinerías, instalaciones de producción de fertilizantes y uno de los mayores depósitos de fosfoyeso a nivel mundial, además de operaciones mineras dentro del Cinturón Piritoso Ibérico, que contribuyen a una contaminación ambiental significativa. La ciudad enfrenta tasas de mortalidad altas por cáncer y enfermedades cardíacas en comparación con el resto de España, así como desigualdades sociales. Conocer las fuentes, rutas de exposición e impacto de la contaminación industrial y minera es crucial para proteger la salud pública y el medio ambiente, y para evaluar la posible contribución de la contaminación industrial a la mortalidad.

Objetivo: Estudiar la asociación entre la ubicación de las fuentes de contaminación industrial y sus sitios de contaminación ambiental, y la bioacumulación de metal(oid)es en la población de la ciudad de Huelva.

Metodología: Se recogieron 70 muestras de sedimento de 6 marismas diferentes en el Estuario Odiel-Tinto y una en el cercano Estuario del Río Piedras, no contaminado. Se analizaron las texturas de los sedimentos, y se midieron el pH, la conductividad eléctrica (EC) y el potencial redox (Eh), y se determinaron las concentraciones de 48 elementos químicos. Para evaluar la deposición de metal(oid)es en el agua de lluvia, se recogieron 612 muestras de agua de lluvia utilizando 17 pluviómetros alrededor del área metropolitana de Huelva desde enero de 2021 hasta diciembre de 2022. Se midió pH, EC, iones principales y metales traza en la fracción soluble del agua de lluvia. Se incluyeron 55 participantes de entre 20 y 85 años de la ciudad de Huelva del estudio MCC-Spain. Se analizó el contenido elemental de 16 metal(oid)es en muestras de uñas de los pies. La variabilidad espacial en metal(oid)es se estudió utilizando kriging.

Resultados: Se identificó una firma de contaminación única para los depósitos de fosfoyeso, caracterizada por 20 elementos, incluyendo Gd, U, As y Zn. El drenaje ácido de minas (AMD) de los depósitos de residuos mineros mostró seis elementos clave como Fe, Pb y Mn. El azufre marcó la influencia del AMD en el río Tinto, y el berilio indicó un impacto agrícola. La calidad del agua de lluvia varió espacialmente, con un enriquecimiento de metal(oid)es tóxicos como As, Cr y Ni cerca de los depósitos de

fosfoyesos, superando las directrices de la OMS para agua potable. Las emisiones marinas e industriales también contribuyeron a la contaminación. Las uñas de los pies de los residentes de Huelva mostraron niveles más altos de As, Co, Cr, Ni y Se en comparación con áreas no contaminadas, correlacionándose con la proximidad a los depósitos de fosfoyesos y complejos industriales.

Conclusiones: Se identificaron firmas de contaminación distintas para los depósitos de fosfoyeso, separando la exposición a metales de otras fuentes como la AMD en los ríos Odiel y Tinto y áreas agrícolas. Se ha establecido una línea base para evaluar los impactos ambientales y en la salud. La variabilidad espacial en la química de los sedimentos y el agua de lluvia mostró concentraciones decrecientes de elementos dañinos a medida que aumenta la distancia de los depósitos de fosfoyeso. Los niveles más altos de elementos peligrosos en las uñas de los residentes de Huelva fueron determinados por factores antropogénicos, con variaciones espaciales distintas en la exposición. Se demuestra la influencia de las fuentes de exposición en los sedimentos de marismas salinas y la lluvia en Huelva, identificando puntos críticos de contaminación y su impacto en la bioacumulación de metal(loid)s en los residentes. Estos hallazgos subrayan la necesidad de esfuerzos de remediación específicos y un monitoreo continuo para controlar los impactos ambientales y en la salud de las actividades industriales en Huelva.

General index

1. Introduction

1. Introduction

1.1. Environmental pollution and health effects

Environmental pollution constitutes a profound global challenge, exerting extensive and detrimental effects on human health. The pervasive presence of pollutants in the atmosphere, hydrosphere, and lithosphere has led to an array of adverse health outcomes, ranging from respiratory and cardiovascular diseases to neurological disorders and cancers (Briffa et al., 2020; Fuller et al., 2022).

The health impacts related to occupational exposure to harmful elements, such as heavy metals, have been extensively examined. Consequently, concerns about the health risks associated with exposure to heavy metals like Cd, Hg, Mn, and Pb, as well as elements like As, have significantly intensified. This heightened concern stems from their potential toxic effects (Briffa et al., 2020) and their propensity to accumulate in target organs (Gil and Pla, 2001).

However, the most concerning issue from a public health perspective currently is the exposure to low doses of contaminant mixtures in non-occupationally exposed populations, particularly those residing close to anthropogenic polluted areas. This exposure occurs through the inhalation of pollutants and the consumption of contaminated water and food. Vulnerable populations, including children, the elderly, and those with pre-existing health conditions, are particularly at risk (Briffa et al., 2020; Fuller et al., 2022).

Industrial and mining pollution has emerged as one of the most pressing environmental and public health challenges of the 21st century. The rapid industrialisation and urbanisation witnessed globally have led to significant economic growth and development. However, this progress has come at a substantial cost to the environment and human health (Fuller et al., 2022). Industrial and mining activities release a myriad of pollutants into the air, water, and soil, which can have detrimental effects on ecosystems and human populations (Fuller et al., 2022).

Mining activities release dust and particulate matter into the air, which can cause respiratory diseases, cardiovascular disorders, and other health issues. Moreover, acid mine drainage (AMD) and heavy metals from mining operations contaminate water sources, leading to toxic water that affects both human health and aquatic life. In addition, mining can lead to soil erosion and contamination with heavy metals, which can enter the food chain and cause health problems. On the other hand, industrial activities emit pollutants like sulphur dioxide (SO_2), nitrogen dioxide (NO_2), and particulate matter (PM_{10}), which degrade air quality and cause respiratory and cardiovascular diseases. Additionally, industrial waste discharges into water bodies can lead to contamination with chemicals and heavy metals, affecting drinking water quality and aquatic ecosystems. Furthermore, these activities can lead to soil contamination with hazardous substances, which can affect agriculture and food safety.

Numerous studies have delved into the health risks associated with industrial and mining pollution. The health impacts of industrial and mining pollution are profound and multifaceted (Briffa et al., 2020; Fuller et al., 2022). The epidemiological evidence that long-term exposure to particulate matter air pollution contributes to an increased risk of mortality comes from cohort survival studies of individuals. Since the 1970s, the connection between cardiopulmonary diseases and exceedingly high concentrations of particulate matter air pollution has been generally acknowledged (Dockery and Pope, 1994; Evans et al., 1984; Özkaynak and Thurston, 1987; Pope et al., 1995; Pope and Dockery, 2006). This phenomenon is primarily due to well-documented rises in morbidity and mortality resulting from extreme episodes of particulate matter air pollution, particularly in heavily industrialised or mining areas. In addition, a recent meta-analysis of existing cohort studies presents substantial evidence of detrimental links between long-term particle matter air exposition and mortality rates from cardiopulmonary diseases and lung cancer (Pope et al., 2020). On the other hand, the European project titled 'Air Pollution and Health, a European Approach (APHEA)' was a large multi-city time series study, which has investigated the short-term effects of particulate matter air pollution in Europe (Anderson et al., 1997). The results confirm that air pollution is associated with chronic obstructive pulmonary disease in European cities with widely varying climates. Similarly, the National Morbidity, Mortality, and Air

Pollution Study (NMMAPS) has examined the short-term impacts of ambient air pollution on daily mortality and morbidity rates across the United States (Samet et al., 2000). The findings suggested an increase of cardiovascular diseases, pneumonia and chronic obstructive pulmonary disease for each 10 μg m^{-3} increment in particle matter concentrations in the air.

Furthermore, comprehensive reviews synthesise findings from studies on human health risk assessments at heavy metal-contaminated sites around the world (Han et al., 2025; Rahman et al., 2021). The findings indicate that industrial pollution significantly increases death rates, while factors like economic growth, healthcare access, and sanitation facilities decrease death rates. Besides, the main health impacts produce by industrial and mining pollution are respiratory, cardiovascular, and neurological diseases and cancers (Briffa et al., 2020; Fuller et al., 2022). Exposure to metal(loid)s from mining and industrial activities can cause respiratory diseases such as asthma, bronchitis, and lung cancer, and other cardiovascular diseases, including heart attacks and strokes (Briffa et al., 2020; Fuller et al., 2022). Moreover, exposure to toxic substances like heavy metals can cause neurological impairments, including cognitive deficits and developmental delays in children (Aguilera et al., 2010; Rodríguez-Barranco et al., 2014). These studies investigate the levels of heavy metals in children's hair and urine, linking high cadmium levels to cognitive behaviour changes and other health issues. Finally, long-term exposure to industrial and mining pollutants has been linked to various forms of cancer, including lung, bladder, and skin cancer (Fuller et al., 2022). This research focuses on the health risks posed by heavy metal contamination in industrial areas, emphasising the acute and chronic conditions that arise from long-term exposure. Other studies have focused in the relation between industrial air pollution and public health in urban areas (Alguacil et al., 2014; Benach et al., 2003; Lopez-Abente et al., 2001). The results revealed a strong correlation between industrial air pollution and mortality rates for heart disease and various cancers in urban populations, with a specific focus on vulnerable groups. These studies provide a solid foundation for understanding the health impacts of industrial and mining pollution. They highlight the importance of comprehensive risk assessments, diversified approaches to studying pollutants, and the need for further research to protect vulnerable populations.

1.2. Environment and health risk assessment

This is the process of assessing the potential harm to the environment and human health caused by toxic substances generated from human activities, or natural phenomena, released to the environment. Therefore, understanding the distribution of contaminants in highly polluted environment and the surrounding areas is crucial for several reasons:

1. **Risk assessment:** Identifying where contaminants are concentrated in the environment helps assess the potential risks to human health and the ecosystem. This information is vital for protecting populations and wildlife living close to these polluted areas.

2. **Source identification:** Knowing the distribution patterns can help trace the sources of pollution. This is essential for implementing effective control measures and preventing further contamination and health effects.

3. **Regulatory compliance:** Monitoring contaminant levels and their distribution helps ensure that industries and other polluters comply with environmental regulations and standards.

4. **Long-term monitoring:** Understanding how contaminants spread and persist in the environment is important for long-term monitoring and management of pollution. Moreover, assessing long-term exposure at the individual level using bioindicators, such as toenails, which provide long-term exposure of mineral metabolism reflecting a period of 6 ± 18 months (Bencko et al., 1995; Gutiérrez-González et al., 2019; Salcedo-Bellido et al., 2021), is essential for understanding the impact of the metal(loid)s on the health of Huelva's residents.

5. **Remediation planning:** Effective restoration strategies depend on a clear understanding of contaminant distribution. This ensures that efforts are targeted and resources are used efficiently.

6. **Public awareness:** Providing information about contaminant distribution can raise public awareness and encourage community involvement in environmental protection efforts.

By knowing where contaminants are and how they move, we can better protect our health and the environment. Therefore, it is important to carry out biomonitoring studies of metal(loid)s to evaluate the possible health risks. In this sense, geostatistical methods utilising spatial data are frequently employed to identify spatial patterns. Their primary goal is to offer unbiased estimates of a sampled variable at locations that have not been sampled (Webster et al., 2001). Kriging, a subset of geostatistical techniques, interpolates unknown values from nearby known ones, producing a continuous surface of estimated values across the entire area of interest. This method is a powerful geostatistical technique used in health exposure studies to estimate and predict environmental exposures across different geographic areas. Kriging is used to estimate exposure to various environmental pollutants, such as metal(loid)s in air, soil or water, and assess their potential health impacts (Michael et al., 2019; Shit et al., 2016; Whitworth et al., 2011; Zou et al., 2011). Moreover, this technique helps in mapping disease incidence or risk by interpolating data from regional counts to create continuous risk surfaces. This is useful for identifying disease hotspots and understanding spatial patterns in health data (Berke, 2004). However, there are limited published studies using these spatial analysis techniques to examine the internal cumulated dose of metal(loid)s in toenails and associate them with exposure to pollution sources in contaminated areas (Zierold et al., 2021).

1.3. The case of the city of Huelva

Huelva City located in south-western Spain, with approximately 150,000 inhabitants, lies 500 m away from the Odiel–Tinto Estuary (Figure 1), which ranks as one of the world's most heavily polluted areas mainly by industrial and mining factors (Morillo et al., 2008; Sáenz et al., 2003). A confluence of stressors gives this estuary unique characteristic. The Odiel-Tinto Estuary is highly polluted primarily due to AMD from the extensive mining activities in the Iberian Pyrite Belt, which is documented as one of the most significant polymetallic sulphide mining districts in the world (Leistel et al., 1998; Pérez-López et al., 2023). Palaeozoic sedimentary and volcanic rocks abundant in pyrite (FeS_2) and various other sulphide minerals mainly form the Odiel and Tinto basins' bedrock (Achterberg et al., 2003). Therefore, this region has been mined for over 4,500 years, leading to the release of large quantities of metal(loid)s into the Odiel and Tinto Rivers, which drain the region from north to south, carrying them to the Odiel–Tinto Estuary (Blasco et al., 2000; Santos Bermejo et al., 2003). The oxidation of sulphide minerals, such as pyrite, results in highly acidic water that carries dissolved metals like Al, Cu, Fe, Mn, and Zn (Figure 2a; Blasco et al., 2000; Santos Bermejo et al., 2003). These pollutants are transported by these rivers and eventually accumulate in the estuary, causing significant environmental degradation (Morillo et al., 2008; Sáenz et al., 2003). Furthermore, an area of 12,600 m^2 exists in the Odiel marshes that is severely contaminated with these metal(loid)s originating from AMD produced by mineral wastes from an abandoned foundry, which is located next to a residential area (Figure 1). This area was declared contaminated by the Andalusian Government in 2007 (https://www.juntadeandalucia.es/boja/2007/168/9). This area is subject to rainfall and rising river levels during spring tides (Figure 2b; Davila et al., 2019). Therefore, the tidal regime is pivotal in the containment and spread of contaminants (Hierro et al., 2014), while bioavailable metals significantly contribute to sediment toxicity (Rosado et al., 2016; Sáenz et al., 2003).

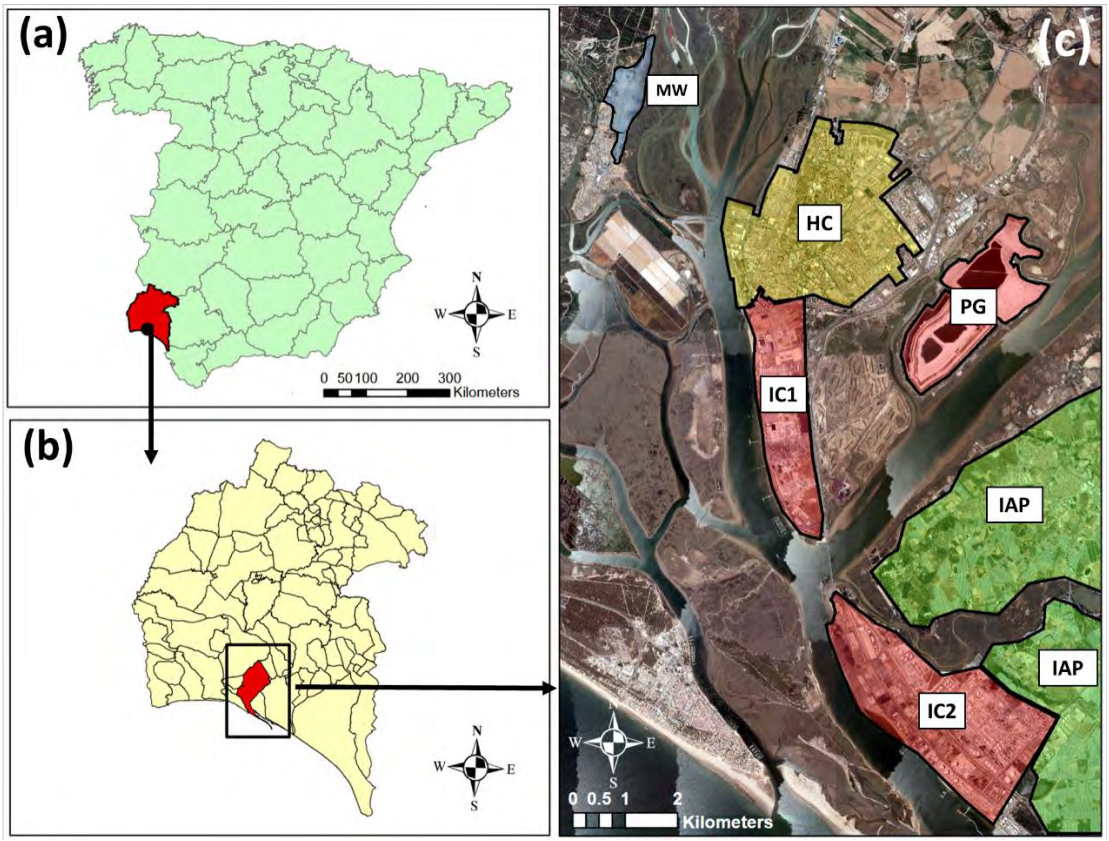

Figure 1. *(a) Location map of Huelva province (SW Spain); (b) location map of Huelva City; (c) orthophotograph highlighting the residential area of Huelva City (HC), phosphogypsum stacks (PG), industrial complex 'Polo Químico de Promoción y Desarrollo de Huelva—Punta del Sebo' (IC1), and industrial complex 'Nuevo Puerto Palos de la Frontera' (IC2), mineral wastes from an abandoned foundry (MW), and intensive agricultural practices (IAP).*

On the other hand, Huelva has been a highly industrialised city since the mid-1960s, hosting two important industrial complexes: 'Polo Químico de Promoción y Desarrollo de Huelva – Punta del Sebo' (Figures 1,2c), and 'Nuevo Puerto Palos de la Frontera' (Figures 1,2d), both situated in the Odiel–Tinto Estuary. Some of the most polluting industries located in these chemical parks include leading Spanish copper and fertiliser producers, a thermal power plant, and an oil refinery, among others (Blasco et al., 2000; Torre et al., 2019). These industries emit various pollutants, including NO_2, SO_2, and PM_{10}, which degrade air quality. Some studies have evaluated the air quality of Huelva City (Alastuey et al., 2006; Chen at al., 2016; González-Castanedo et al., 2014; Querol et al., 2002; Sánchez de la Campa et al., 2007, 2015, 2018), and the chemical analysis showed that PM_{10} at Huelva is characterised by high As, Cd, Cu, Pb, PO_4^{3-}, SO_4^{2-}, and Zn levels, as expected from the industrial activities. In addition, large quantities of industrial

pollutants have been discharged in the Odiel-Tinto Estuary from these factories increasing the pollution of both the sediments and the water in the estuary (Borrego et al., 2022; Elbaz-Poulichet et al., 1999; Hierro et al., 2014). Although, the most significant industrial pollution problem, in terms of mass, in this estuary is the phosphogypsum (PG) stacks (Lieberman et al., 2020; Pérez-López et al., 2010). PG is an industrial waste of the phosphoric acid production process by wet acid method originates from the reaction of powdered phosphate rock with sulphuric acid in a reactor (Contreras, 2017). This chemical reaction produces phosphoric acid, used exclusively in the fertiliser manufacture, and calcium sulphate, called PG. This process has been ongoing for decades (1968-2010), leading to the accumulation of large quantities of PG in large stacks on the salt marshes of the Tinto River covering a vast area of about 1,200 hectares and containing 100 million tonnes (Figures 1,2e), which ranks as one of the most important in the world (Contreras-Llanes et al., 2015; Contreras, 2017; Lieberman et al., 2020; Pérez-López et al., 2010; Rentería-Villalobos et al., 2010). PG originates from phosphate rock, which carries metal(loid)s and natural radionuclides that concentrate within PG (Rentería-Villalobos et al., 2010). Therefore, PG is classified as naturally occurring radioactive material (NORM) according International Atomic Energy Agency (IAEA) due to the high activity concentration of natural radionuclides from the ^{238}U decay series (IAEA, 2004). In addition, other extremely-polluted waste has been also deposited in these stacks increasing the potential harmful pollutants (Lieberman et al., 2020; Pérez-López et al., 2010). These factors combined make the PG stacks contain a multitude of harmful substances, such as organic substances, metal(loid)s and other potentially toxic elements (As, Cd, Cr, F^-, Fe, NH^{4+}, Ni, P, Pb, SO_4^{2-}, and Zn), and natural radionuclides, including the highly radiotoxic ^{210}Pb, ^{210}Pb, and ^{226}Ra (Contreras-Llanes et al., 2015; Contreras, 2017; Lieberman et al., 2020; Pérez-Lópezet al., 2010; Rentería-Villalobos et al., 2010), which have been linked to health problems (Silva et al., 2022). While extensive research has been done on the chemical characterisation of the water and saltmarshes in the Odiel-Tinto Estuary (Millán-Becerro et al., 2023; Pérez-López et al., 2016), the specific pollution profiles affecting the tidal marshes of this human-affected estuary have not been thoroughly characterised yet. Furthermore, gases with relatively high concentrations of radon (^{222}Rn) and hydrogen fluoride (HF)—one of the

most toxic gaseous compounds—to the atmosphere are emitted from PG stacks (López-Coto et al., 2014; Torres-Sánchez et al., 2019, 2020). Thus, PG stacks can release these pollutants into the air and water, significantly contributing to the pollution levels. Understanding these spatial distributions and conducting environmental risk assessments are crucial for the site's management and future remediation efforts.

Figure 2. *Photographs of the main pollution sources identified in the Odiel–Tinto Estuary (Spain) [(a) AMD; (b) mineral wastes from an abandoned foundry; (c) industrial complex 'Polo Químico de Promoción y Desarrollo de Huelva—Punta del Sebo' (IC1); (d) industrial complex 'Nuevo Puerto Palos de la Frontera' (IC2); (e) PG stacks; (f) intensive agricultural practices].*

Additionally, the Odiel–Tinto Estuary is impacted by agrochemical runoff resulting from intensive agricultural practices on nearby farmlands; Huelva is the Europe's largest producer of strawberries and the second in the world (Figure 2f; Barba-Brioso et al., 2010; Sainz et al., 2004;). Finally, the estuary receives sewage discharge from Huelva City and other towns situated along the edge of the estuary channel (Torre et al., 2019).

These factors combined make Huelva one of the most polluted cities in Spain, with significant implications for public health and the environment. In this sense, previous studies revealed that Huelva has higher cancer and heart disease mortality rates for both men and women compared to the rest of Spain (Alguacil et al., 2014; Benach et al., 2003; Lopez-Abente et al., 2001). Additionally, the Spanish National Atlas of Mortality indicates significantly greater standard mortality ratios in Huelva City between 1989 and 2014 in both men and women for acute myocardial infarction, heart failure, cerebrovascular diseases, bladder cancer, and other cardiovascular diseases. Furthermore, breast cancer in women and lung cancer in men were notably higher during this period (Martínez-Beneito et al., 2024). Moreover, previous studies examining the urinary and hair levels of heavy metals (As, Cd, Cr, Cu, and Ni) in children from Huelva city have shown that the average Cd levels were higher than those reported in other European studies (Aguilera et al, 2010; Rodríguez-Barranco et al., 2014). These studies also indicated that children with elevated Cd concentrations exhibited notable cognitive behaviour changes. Additionally, industry workers in Huelva city displayed high levels of arsenic and other metals, even after accounting for fish and seafood consumption (Silva-Caicedo et al., 2024). Furthermore, a recent exploratory study further linked environmental exposure to heavy metals with neurobehavioral performance in children from Huelva (Capelo et al., 2024). Although, there is support on the scientific literature for a deleterious effect for human heath due to industrial and mining pollution exposure (Alguacil et al., 2014; Briffa et al., 2020), the matter remains indeterminate in Huelva City.

This situation has sparked social mobilisation and legal actions, primarily targeting the PG stacks, which is located on the highly permeable marshes just 500 meters from Huelva City, despite other sources of exposure. In response to pressure from citizens,

associations, and environmentalists, judicial authorities mandated the cessation of PG stockpiling in December 2010. Additionally, governmental authorities demanded the fertiliser company to create a restoration protocol plan for the affected marshes that has been approved, known as RESTORE 2030 (https://restore2030.com/), which is currently being carried out. A committee of national scientific experts, coordinated by the University of Huelva, determined that the RESTORE 2030 plan was insufficient for fully restoring saltmarshes (Scientific Committee, 2024).

Considering the elevated mortality rates in Huelva City coincide with pollution from industrial and mining activities, it is crucial to study the depositional signatures of specific metal(loid)s to identify the various pollution sources in this contaminated area. Although comprehensive studies have been conducted on the air quality in Huelva City (Alastuey et al., 2006; Chen at al., 2016; González-Castanedo et al., 2014; Querol et al., 2002; Sánchez de la Campa et al., 2007, 2015, 2018), and other focused on sediment and water characterisation in Odiel-Tinto Estuary (Borrego et al., 2022; Elbaz-Poulichet et al., 1999; Hierro et al., 2014; Lieberman et al., 2020; Millán-Becerro et al., 2023; Morillo et al., 2008; Pérez-López et al., 2010, 2016; Rentería-Villalobos et al., 2010; Sáenz et al., 2003), the specific sediments and rainwater chemical profile using geochemical tracers in this area have not yet been characterised in detail. Monitoring sediments and rainwater can help assess the potential impact of the industrial and mining activities to the ecosystem, which is crucial to evaluate the impact of future restoration plans, such as RESTORE 2030. In addition, the restoration labours may result in resuspension of coarse particles from the PG stacks, which may have a significant impact on the surrounding environment. Therefore, the environment risk assessments are critical to evaluate the improvement of restoration plans, such as RESTORE 2030. Furthermore, the measurement of exposure at the individual level is a critical aspect in studying the role of these metal(loid)s in the health of the citizens of Huelva City, the issue remains uncertain.

2. Justification

Huelva City faces a significant and multifaceted environmental problem, stemming from various sources of contamination, including industrial and mining activities (Morillo et al., 2008; Sáenz et al., 2003). The area is particularly affected by emissions of pollutants in the air, water, and soil from the two chemical complexes, PG stacks, mining waste from an abandoned foundry, and other pollution sources such as intensive agriculture and sewage discharge (Morillo et al., 2008; Sáenz et al., 2003). These environmental challenges have profound implications for public health and ecological balance. Additionally, Huelva City experiences a high mortality rate, with many deaths attributed to respiratory and cardiovascular diseases, as well as cancer (Alguacil et al., 2014; Benach et al., 2003; Lopez-Abente et al., 2001; Martínez-Beneito et al., 2024). Given the well-established link between environmental degradation and adverse health outcomes, there is considerable concern among the local population (Briffa et al., 2020; Fuller et al., 2022). A substantial portion of this concern is directed towards the PG stacks, which is a major source of harmful elements such as metal(loid)s and radioactive elements. The presence of these hazardous substances poses significant risks to public health and the environment, requiring urgent and comprehensive evaluation to mitigate their impact. However, despite this concern, there are no individual-based studies providing direct evidence of a causal association in Huelva City between environmental pollution and excess mortality.

An environmental and health risk assessment characterises the exposure sources, defines the routes of exposure, and evaluates whether contaminants reach the population. On the other hand, this procedure analyses whether the known effects of these pollutants, when accumulated in the body, are present with a higher incidence on the target population. Finally, studies are conducted to assess the association between sources of contamination and disease in the study population. Nevertheless, executing all of these tasks in Huelva City proves to be a formidable task, owing to the relatively small population size and the administration's lack of proactive engagement.

The present work humbly aims to fill some gaps in the information chain to explore the intricate relationship between industrial/mining pollution and health outcomes in Huelva City. Moreover, this thesis is distinctive due to utilise spatial data and techniques like Kriging to identify contaminant distribution patterns. In addition, uses bioindicators, such as toenail analysis, to assess long-term exposure to contaminants in a sample of the general population. Finally, we conduct the first epidemiological study to assess the association between proximity to industrial and mining pollution sources among Huelva's residents.

By determining the spatial distribution of metal(loid)s, both within the estuary, where they were accumulated in the sediments, and through the atmospheric dispersion of particulate matter by air, which were transported to their final deposition, this research endeavours to provide a comprehensive understanding of the scope and scale of the problem. Moreover, this analysis is further complemented by studying the association between the levels of accumulated exposure to these metal(loid)s in the toenails of Huelva's general population and their spatial proximity to local pollution sources. Furthermore, it offers a valuable tool to differentiate between various pollution sources, assess the most affected areas, assign responsibility to the different polluting entities, and establish a baseline to evaluate the impact of the RESTORE 2030 restoration plan and other innovative solutions to mitigate the adverse effects of industrial and mining pollution on public health.

Although these efforts denote only modest progress and significant gaps persist that warrant further inquiry, this study provides information that was previously inaccessible. The magnitude of work necessary to complete all required studies needed to study whether there is a causal link between Huelva's estuary environmental pollution and a higher mortality of the Huelva population extends beyond what is generally expected for a doctoral thesis.

3. Objectives

3.1. Main objective

To study the association between the location of industrial pollution sources and their environmental pollution sites, and the bioaccumulation of metal(loid)s on Huelva City's population.

3.2. Specific objectives

a) To assess the environmental exposure pathways, including sediments and rainwater, in the metropolitan area of Huelva, and the internal accumulated dose of toxic metal(loid)s among the inhabitants of Huelva City (Contreras-Llanes et al., 2024; 2025a,b).

b) To identify specific pollution signatures in marsh sediments using geochemical tracers within the highly polluted Odiel–Tinto Estuary, aiming to determine the extent of environmental exposure to toxic metal(loid)s. (Contreras-Llanes et al., 2024).

c) To investigate the distribution of the suspended pollutant particles originating from the PG stacks and other local pollution sources to identify the radius of influence on the rainwater chemical fallen in Huelva metropolitan area (Contreras-Llanes et al., 2025b).

d) To examine the internal accumulated dose of toxic metal(loid)s in the nails from general population of Huelva City (Contreras-Llanes et al., 2025a).

e) To analyse the association between the spatial proximity patterns to the local industrial sources of pollutants with the levels of cumulated exposure of metal(loid)s in the toenails of the general population of Huelva (Contreras-Llanes et al., 2025a).

f) To establish a reference starting point of metal(loid)s levels levels in marsh sediments within the Odiel-Tinto Estuary, rainwater collected in the Huelva metropolitan area, and toenails from the population of Huelva City, in order toenail on the Huelva City population to assess the impact of the RESTORE 2030

restoration plan for the Odiel-Tinto Estuary (Contreras-Llanes et al., 2024; 2025a,b).

4. Methodology

4.1. Study design

We used a cross-sectional epidemiological study with geographical-correlation analyses as a basis [specific objectives a), d) and f)], combined with environmental specific-site chemical-tracers characterisation and geographical dispersion analyses [specific objectives b), c) and e)].

4.2. Study publications' samples and population sources

This thesis concentrates on the Odiel-Tinto Estuary, an area characterised by very poor environmental quality owing to anthropogenic pollution sources such as industrial and mining activities. The health effects of pollutants generated by these activities, including trace elements and radionuclides, are well documented. However, to date, no studies conclusively determine that the elevated mortality and morbidity rates in Huelva City are attributable to the high levels of pollution. Therefore, it is crucial to understand how contaminants are distributed across the air, soil, and water to gain a holistic view of the environmental challenges in this area. Identifying the flow of contaminants is imperative to understand the potential environmental exposure pathways. This is a preliminary step before assessing the accumulated levels of these metals in the general population residing in this area, taking into account the proximity to previously identified sources of exposure. With this comprehensive information, the relationship between anthropogenic pollution determinants and bioaccumulation in the general population of Huelva might be now elucidated.

This work comprises two studies that spatially determine the exposure pathways, in addition to another study that measures the bioaccumulation of metals in the general population in relation to their proximity to the identified exposure sources:

4.2.1. Paper #1: Delineating distinct sediment pollution signatures from diverse sources in a heavily contaminated estuary near an area of high cancer and cardiovascular mortality

The distinct pollution signatures in marsh sediments by utilising geochemical tracers in the severely contaminated Odiel-Tinto Estuary have been identified. This research differentiated between pollution sources, measured the most affected marsh areas, attributed responsibility to various polluters within the estuary, and established a baseline for assessing the impact of the RESTORE 2030 restoration plan in the Odiel-Tinto Estuary.

Representative samples of sediments covering the entirety of the Odiel-Tinto Estuary, including primary sources of contamination and other strategic locations, have been meticulously studied. The estuarine sediments serve as the final repository for hazardous elements, which are transported by the water from various pollution sources and ultimately accumulate in different zones of the estuary. The accumulation of metals in the sediments is influenced by the distance from contamination sources. Additionally, the tidal and fluvial dynamics within the estuary significantly contribute to the distribution of these hazardous elements. Understanding these factors is crucial for assessing the impact of contamination and for developing effective environmental management strategies.

4.2.2. Paper #2: Influence of phosphogypsum waste on rainwater chemistry in a highly polluted area with high mortality rates in Huelva metropolitan area, Spain

Environmental exposure to metal(loid)s has been characterised through this study, including the analysis of the effect of PG stacks and other relevant factors on rainwater quality. This study identified the specific pollution influence on the chemical profile of rainwater fallen in the metropolitan area of Huelva.

To investigate the atmospheric distribution of these contaminants, we have identified the exposure pathways of the particulate matter that precipitates with the rain. Our study includes all the major population centres around the Odiel-Tinto Estuary, considering the distribution of industrial sources and the prevailing wind direction.

4.2.3. Paper #3: Internal cumulated dose of toxic metal(loid)s in a population residing near naturally occurring radioactive material waste stacks and an industrial heavily polluted area with high mortality rates in Spain

A cross-sectional epidemiological study has been conducted to examine the association between cumulative exposure levels to 16 metal(loid)s (Al, As, Cd, Co, Cr, Cu, Fe, Mn, Mo, Ni, Pb, Se, Tl, U, V, and Zn) measured in toenail samples from a representative sample (n = 55 participants) of the general control population of Huelva City, who participated in the multicase-control (MCC-Spain) study, and the spatial proximity patterns to local pollution sources.

We have utilised the 2012 MCC study, which provided us with a database of metal levels in the nails of 55 control individuals. These individuals were selected to be representative of the general population of Huelva City and met the criteria established for this study. The city of Huelva City was chosen because, for a thesis project, it is not feasible to conduct a new sampling of all population centres, a task that exceeds the scope of a doctoral thesis. Moreover, Huelva is the closest city to the main contamination sources (PG stacks and industrial complexes), and it is the main urban area, with 150,000 residents, while the other centres do not exceed 15,000 inhabitants each.

4.3. Study area and population

A detailed description of the study areas and the population examined is provided in this section.

4.3.1. Paper #1: Delineating distinct sediment pollution signatures from diverse sources in a heavily contaminated estuary near an area of high cancer and cardiovascular mortality

This investigation was conducted in seven low to mid-tide marsh areas, six of them (A1-6) within the Odiel-Tinto estuary and another in the Piedras River estuary (A7), both located in the province of Huelva, Spain (Figure 3). Table 1 presents the geographical coordinates for each sampling area (A1-7). The estuary suffers bi-daily flooding caused by semi-diurnal mesotidal tides (with an equinox mean tidal range of 2.97 m; Figueroa et al., 2003).

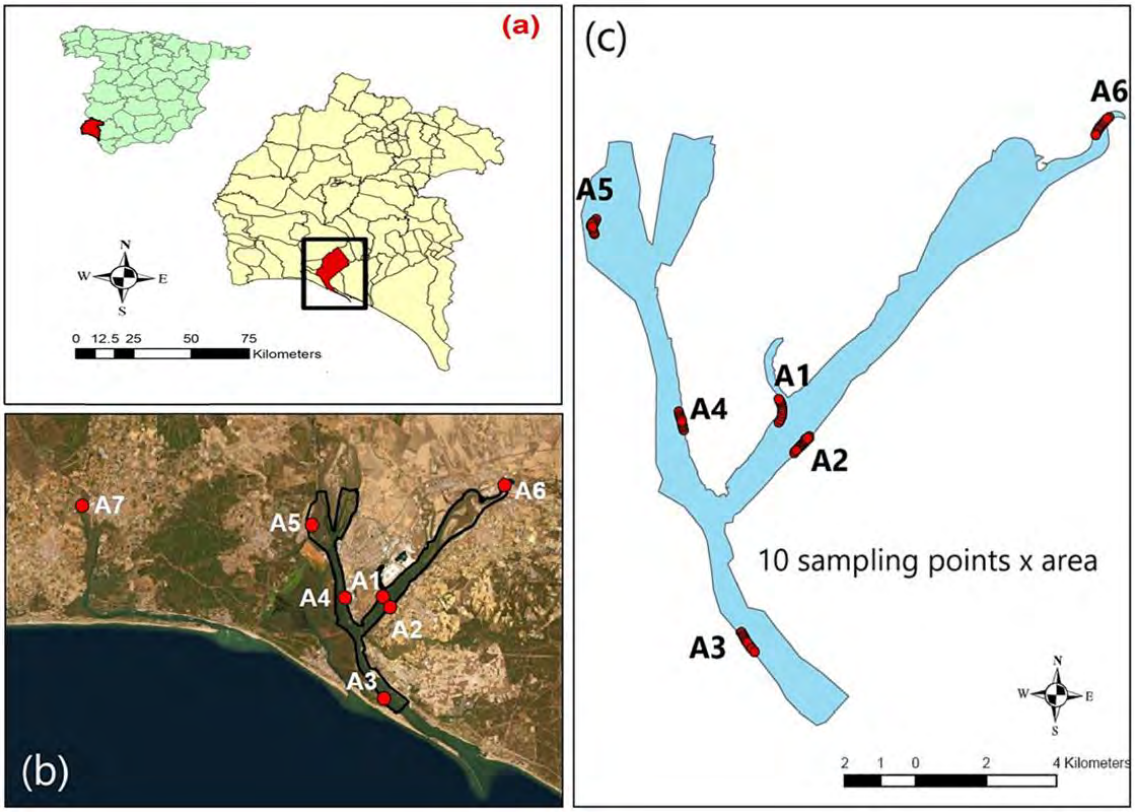

Figure 3. *(a) Location map of Huelva (SW-Spain), (b) orthophotograph highlighting the sampled salt marsh areas (marked in red) within the Odiel-Tinto (A1–6) and Piedras River (A7) estuaries, and (c) specific sediment sampling points in the Odiel-Tinto Estuary.*

Summary of sampling salt marsh areas in the Odiel-Tinto and Piedras River estuaries:

Sampling point A1: The first salt marsh area is positioned within the area locally referred to as 'Estero del Rincón' placed on the Tinto River's right bank and in close

proximity to the PG stacks (Figure 3). This area is predominantly occupied by *Atriplex portulacoides L., Sarcocornia perennis* (Mill.) A.J. Scott, *Spartina densiflora* Brongn (an exotic invasive cordgrass), along with sparse clumps of native *Spartina maritima* (Curtis) Fernald (Figure 4).

Table 1. *Geographical coordinates (latitude and longitude) of sampling areas in the estuaries of Odiel-Tinto and Piedras Rivers. 10 sampling points were selected in each selected area.*

Code	Latitude, longitude (°)	Code	Latitude, longitude (°)	Code	Latitude, longitude (°)
A1-1	37.231945, -6.922102	**A2-1**	37.226751, -6.914179	**A3-1**	37.176331, -6.929251
A1-2	37.232637, -6.921619	**A2-2**	37.226640, -6.914018	**A3-2**	37.176438, -6.929456
A1-3	37.233508, -6.921211	**A2-3**	37.226572, -6.913911	**A3-3**	37.176515, -6.929579
A1-4	37.234285, -6.921168	**A2-4**	37.226504, -6.913814	**A3-4**	37.176545, -6.929745
A1-5	37.235114, -6.921157	**A2-5**	37.226286, -6.913943	**A3-5**	37.176430, -6.929268
A1-6	37.235797, -6.921243	**A2-6**	37.226619, -6.913476	**A3-6**	37.176511, -6.929407
A1-7	37.236497, -6.921511	**A2-7**	37.226722, -6.913621	**A3-7**	37.176614, -6.929520
A1-8	37.237027, -6.921811	**A2-8**	37.226692, -6.913444	**A3-8**	37.176665, -6.929659
A1-9	37.237403, -6.922036	**A2-9**	37.226863, -6.913262	**A3-9**	37.176639, -6.929761
A1-10	37.237779, -6.922422	**A2-10**	37.226884, -6.913037	**A3-10**	37.176581, -6.929819
A4-1	37.231050, -6.953260	**A5-1**	37.279193, -6.984398	**A6-1**	37.310880, -6.821850
A4-2	37.231167, -6.953311	**A5-2**	37.279230, -6.984390	**A6-2**	37.310961, -6.821751
A4-3	37.231101, -6.953031	**A5-3**	37.279247, -6.984363	**A6-3**	37.311029, -6.821652
A4-4	37.231236, -6.953034	**A5-4**	37.279268, -6.984374	**A6-4**	37.311084, -6.821566
A4-5	37.231339, -6.953074	**A5-5**	37.279054, -6.984193	**A6-5**	37.311144, -6.821456
A4-6	37.231427, -6.953125	**A5-6**	37.279071, -6.984157	**A6-6**	37.311191, -6.821397
A4-7	37.231506, -6.953181	**A5-7**	37.279096, -6.984140	**A6-7**	37.311229, -6.821330
A4-8	37.231549, -6.953217	**A5-8**	37.279116, -6.984112	**A6-8**	37.311274, -6.821255
A4-9	37.231604, -6.953269	**A5-9**	37.279006, -6.983974	**A6-9**	37.311317, -6.821191
A4-10	37.231698, -6.953355	**A5-10**	37.279031, -6.983978	**A6-10**	37.311353, -6.821145
A7-1	37.284265, -7.175764				
A7-2	37.284282, -7.175815				
A7-3	37.284297, -7.175877				
A7-4	37.284322, -7.175908				
A7-5	37.284361, -7.175833				
A7-6	37.284411, -7.175880				
A7-7	37.284445, -7.175775				
A7-8	37.284404, -7.175729				
A7-9	37.284415, -7.175679				
A7-10	37.284422, -7.175955				

Sampling point A2: This area, opposite to A1, is also located within the 'Estero del Rincón' area placed on the Tinto River's left bank close to intensive agriculture farms (Figure 3). *S. perennis, A. portulacoides, S. maritima and S. densiflora* are the dominant species in this salt marsh area (Figure 4).

Sampling area A3: This is placed near the mouth of the Odiel-Tinto Estuary on right bank of the main channel of this estuary, which is locally known as the 'Canal del Padre Santo' (Figure 3). This salt marsh area is the nerviest to the industrial complex 'Nuevo Puerto Palos de la Frontera' and is predominately inhabited by *S. densiflora*, along with sparse clumps of *S. maritima* (Figure 4).

Sampling area A4: This salt marsh area is located on the right bank of the Odiel River near the industrial complex 'Polo Químico de Promoción y Desarrollo de Huelva—Punta del Sebo' (IC1; Figure 3). This area, ecologically restored in 1992 (Curado et al., 2014), is nowadays extensively occupied with uninterrupted prairies *S. maritima* (Figure 4).

Sampling area A5: This point is situated north of the estuary, upstream and on the left bank of the Odiel River, near a 12,600 m² area containing mineral waste of an abandoned foundry (Figure 2; Davila et al., 2019). The area is exposed to rain and rising river levels during spring tides and is mainly covered with *A. portulacoides* and *S. densiflora* (Figure 4).

Sampling area A6: This area is situated upstream and on the left bank of the Tinto River Located (Figure 3). This area has high levels of AMD pollution (Curado et al., 2010) and is mainly covered by *A. portulacoides, Phragmites australis* (Cav.) *Trin. ex Steud*. and *S. densiflora* (Figure 4).

Sampling area A7: This salt marsh is situated within the Piedras River Estuary, which is relatively unpolluted compared to the Odiel-Tinto Estuary (Figure 3). This area has not been impacted by industrial and mining activities, receiving only minimal discharges from surrounding agricultural farms (Lario et al., 2016). The marsh and is primarily occupied by different *Sarcocornia taxa, A. portulacoides*, and isolated patches of *S. maritima* and *S. densiflora* (Figure 4).

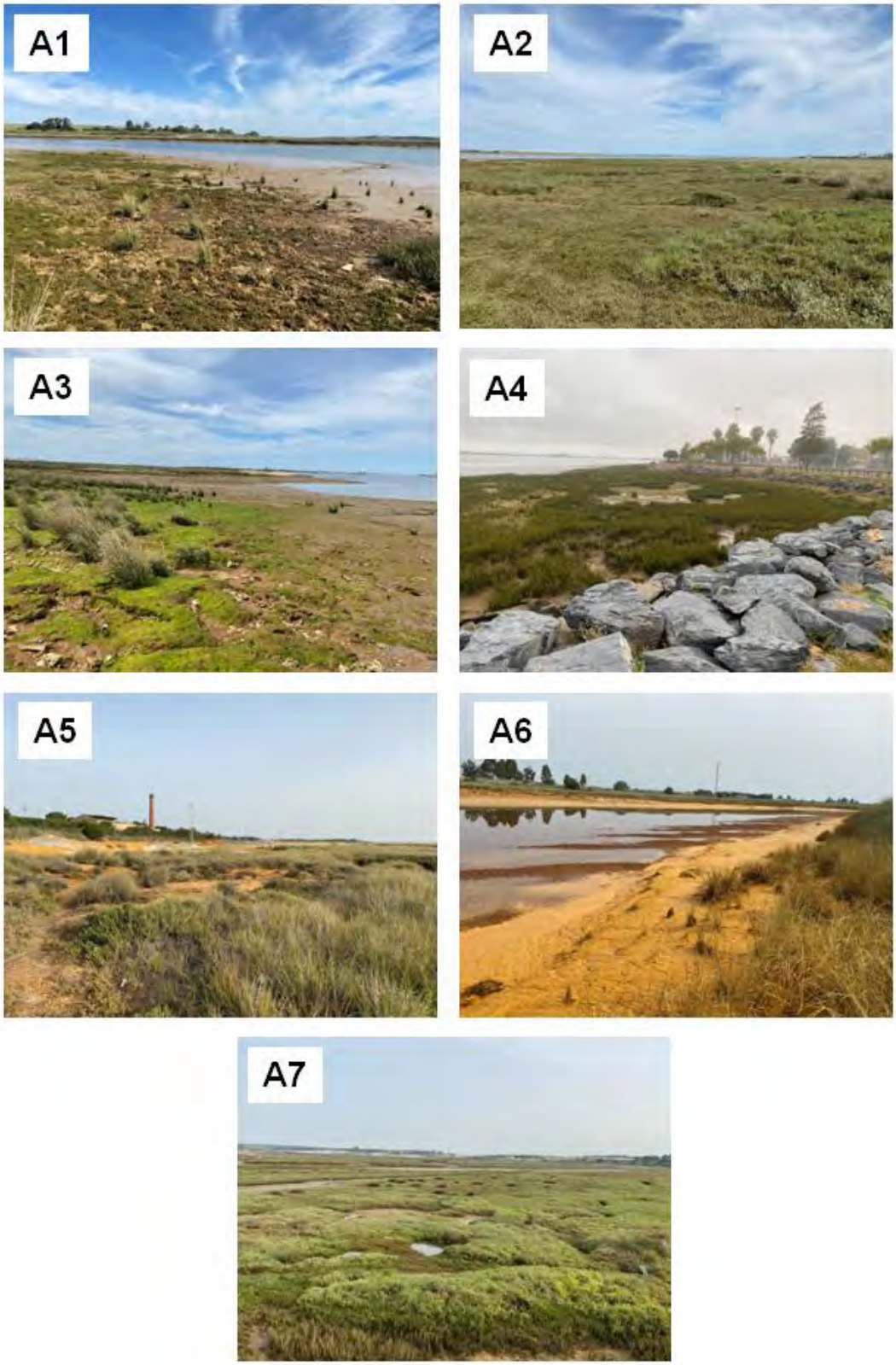

Figure 4. *Study salt marsh areas in the Estuary of Odiel-Tinto Rivers (A1-6) and the Estuary of Piedras River (A7).*

4.3.2. Paper #2: Influence of phosphogypsum waste on rainwater chemistry in a highly polluted area with high mortality rates in Huelva metropolitan area, Spain

This study was conducted across 17 sampling points, with 16 of them (AD, AL, CA, CM, CO, EP, GI, JR, MO, FB, FE, PF, PI, PU, RA, and SJ) situated within the Odiel-Tinto estuary. An additional point was located in an unpolluted area in the village of Matalascañas (MN) within the 'Doñana' national reserve park. Both locations are in the province of Huelva, Spain (Figure 5). Table 2 presents the geographical coordinates for each sampling point. The area experiences a Mediterranean climate with Atlantic Ocean influence, featuring mild, humid winters (average January temperature of 11°C; annual precipitation of 505.6 mm) and warm, dry summers (average August temperature of 25°C with little to no rainfall).

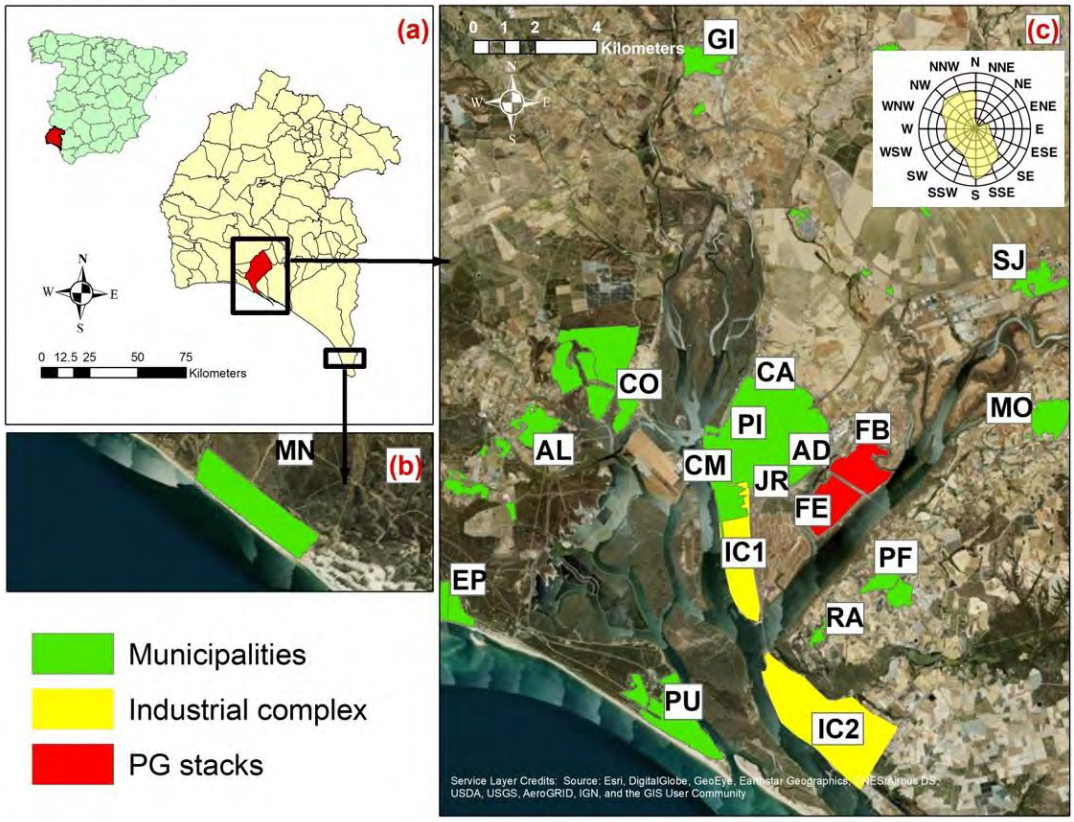

Figure 5. *(a) Location map of Huelva (SW-Spain), (b) orthophotograph highlighting the placement of rain gauges within the village of Matalcañas (MN), and (c) across the Huelva metropolitan area (AD, AL, CA, CM, CO, EP, GI, JR, MO, FB, FE, PF, PI, PU, RA, and SJ). FB marks the centre of the PG stacks, while IC1 represents the industrial complex 'Polo Químico de Promoción y Desarrollo de Huelva – Punta del Sebo', and IC2 refers to the industrial complex 'Nuevo Puerto Palos de la Frontera'. The wind rose diagram covering January 2021 to December 2022 is also included.*

Table 2. *Geographical coordinates (latitude, longitude and elevation) of rainwater sampling point in the metropolitan area of Huelva.*

Code	Latitude (°)	Longitude (°)	Elevation (m)
SJ	37.315963535041625	-6.844673348116906	8.5
MO	37.27404096136433	-6.843628148847764	44.5
PF	37.22583528815851	-6.896610148954115	24.0
GI	37.37291101622668	-6.962827144750453	25.5
AL	37.26338721519359	-7.025648933455252	35.5
CO	37.275718999899304	-6.992748844197898	18.0
PU	37.186582388719046	-6.964988380772668	13.5
EP	37.217220068425966	-7.050034465212165	15.0
PI	37.26993722045656	-6.946403313043633	63.5
JR	37.25690041972183	-6.929071660979101	15.5
CM	37.253299763961465	-6.95769898099551	15.5
AD	37.264498497363334	-6.916356203810738	6.5
FB	37.25738537638599	-6.912615145675258	6.5
FE	37.242528887473554	-6.922759271839377	10.5
MÑ	37.01649575587383	-6.569597437247151	7.5
RA	37.20012123768613	-6.921093453988427	25.5
CA	37.271689672788135	-6.925285909334211	22.5

The sampling points were chosen to encompass the most densely populated centres in the Odiel-Tinto Estuary, considering the varied land uses and human activities, such as industrial, mining, urban, and agricultural areas, as well as the predominant wind direction (Figure 5). A Hellman rain gauge was installed in each sampling point at public institutions, private companies, and residential addresses. Furthermore, owing to the significant size of Huelva City and its proximity to the PG stacks, five rain gauges were meticulously positioned to provide thorough coverage of the entire region. As illustrated in Figure 5, the PG stacks (FB) rain gauge was chosen as the central point of the affected area. Its coordinates, referenced to latitude (°), longitude (°), and elevation (m) reference system, are: 37.25738537638599, -6.912615145675258, 6.5. Detailed information of the sampling network is provided in Table 3.

Table 3. *Main characteristics of the rain gauges.*

Code	Rain gauges location	R (L m^{-2} y^{-1})	D_E (m)	D_C (m)	D_{PG} (m)	Context	Facility situation
SJ	San Juan city	315,4	8542	19130	8880	Urban	High school
MO	Moguer city	399,6	5040	14500	6404	Urban	Primary school
PF	Palos de la Frontera city	333,6	1335	7575	3778	Urban	Primary school
GI	Gibraleón city	354,3	12456	19995	13584	Urban	High school
AL	Aljaraque city	538,0	5083	6385	10053	Urban	High school
CO	Corrales village	378,5	1928	8668	7396	Urban	Primary school
PU	Punta Umbria city	354,1	40	1120	9130	Urban	High school
EP	El Portil village	435,4		900	12980	Urban	Dwelling house
PI	IES Pintor Pedro Gómez, Huelva city	352,0	1272	9924	3289	Urban	High school
JR	CEIP Juan Ramón Jímenez, Huelva city	323,2	2370	9430	1465	Urban	Primary school
CM	Casa del Mar, Huelva city	305,5	157	7770	4028	Urban	
AD	Adif-mercancias, Huelva city	327,8	2157	10675	855	Industrial	Train cargo terminal
FB	PG stacks, Huelva city	295,6	1360	10221	0	Waste	PG stacks
FE	PG stacks border, Huelva city	299,4	820	8365	1878	Salt marsh	Weather station
MN	Matalascañas village	333,1		854	40540	Rural	Researching centre
RA	Campus 'la Rábida', La Rábida village	313,4	1295	4005	6400	Rural	University
CA	Campus 'el Carmen', Huelva city	318,8	3150	11014	1945	Urban	University

R: annual average rainfall in the period 2021-2022; DE: distance to the Tinto-Odiel Estuary; DC: distance to the coast; DPG: distance to the PG stacks.

4.3.3. Paper #3: Internal cumulated dose of toxic metal(loid)s in a population residing near naturally occurring radioactive material waste stacks and an industrial heavily polluted area with high mortality rates in Spain

This study was conducted on a representative sample (n = 55 participants) of the general population-based controls from Huelva City (Figure 6; Table 4), recruited as part of the population-based multicase-control (MCC-Spain) study (http://www.mccspain.org). The MCC-Spain study was concentrated on 12 Spanish provinces (Asturias, Barcelona, Cantabria, Girona, Granada, Guipúzcoa, Huelva, León, Madrid, Murcia, Navarra, and Valencia) from September 2008 to December 2013. The aim of this study was to explore environmental and genetic factors associated with common tumours or cancers (breast, chronic lymphocytic leukaemia (CLL), colorectal,

gastric, and prostate) with unusual epidemiological features (Castaño-Vinyals et al., 2015; Gutiérrez-González et al., 2022). Cases were recruited from the 23 cooperating hospitals. Moreover, these control controls were arbitrarily selected from the Andalusian Public Healthcare Database (BDU) within the hospitals' catchment areas and invited to participate. Both, cases and controls, aged 20 to 85 years, residing in the catchment area for at least 6 months before the study, had the capability to complete the epidemiological survey, and matched in frequency to all tumour and cancer cases, ensuring distribution by sex and age in 5-year age groups. Every province enrolled cases of a minimum of two distinct types of tumours. Written informed consent was obtained from each participant, as well as from the ethical and research committees. The study adhered to the principles outlined in the Declaration of Helsinki.

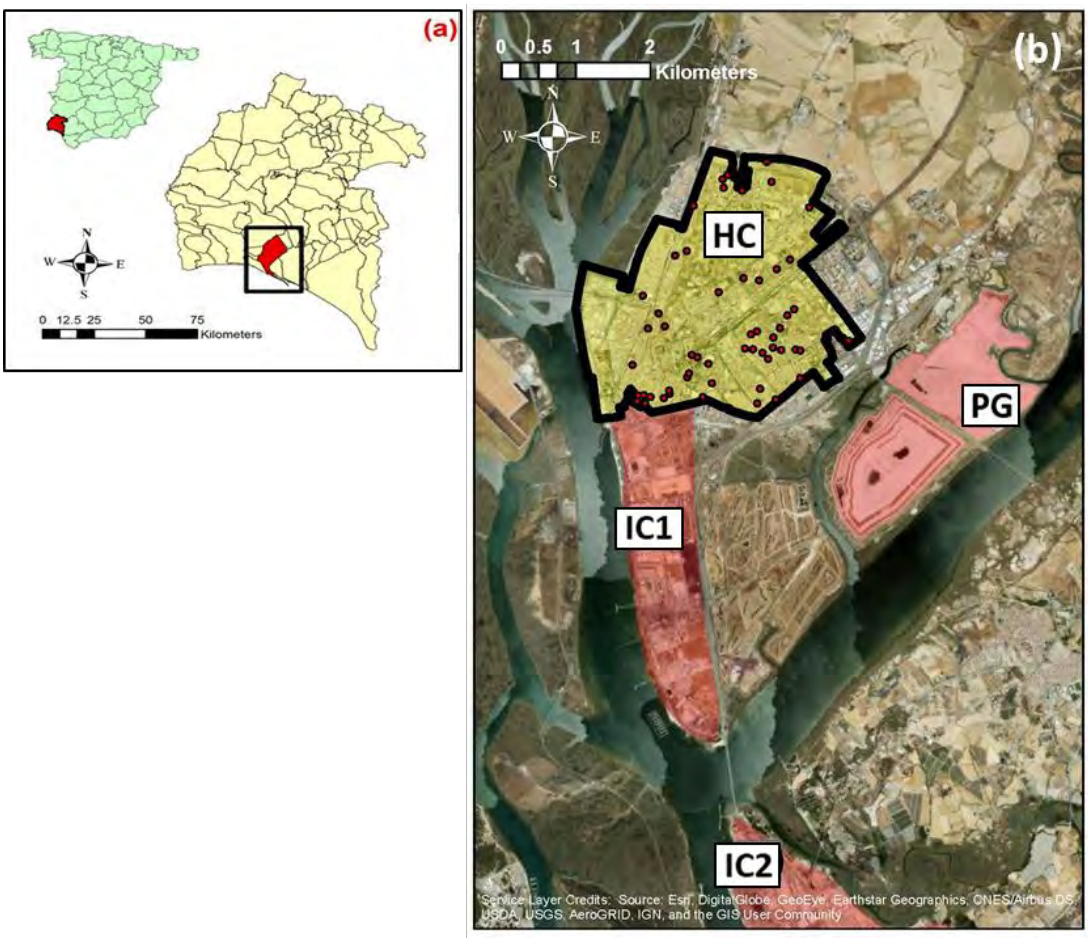

Figure 6. *(a) Location map of Huelva Province (SW-Spain); (b) orthophotograph highlighting the residential area of Huelva City (HC), phosphogypsum stacks (PG), industrial complex 'Polo Químico de Promoción y Desarrollo de Huelva—Punta del Sebo' (IC1), and industrial complex 'Nuevo Puerto Palos de la Frontera' (IC2). Dots represent the locations of participants on a map of the residence area of Huelva City.*

Table 4. *Geographical coordinates (latitude and longitude) of participants residing in the city of Huelva.*

Code	Latitude	Longitude	Code	Latitude	Longitude	Code	Latitude	Longitude
4131207	37,26221	-6,93058	4131501	37,26477	-6,93311	4131758	37,26716	-6,93111
4130674	37,25723	-6,93573	4133761	37,28503	-6,93618	4131525	37,26441	-6,95054
4133492	37,28263	-6,93532	4131702	37,26597	-6,95158	4130502	37,25507	-6,95427
4132551	37,27374	-6,94770	4133530	37,28273	-6,94272	4132490	37,27314	-6,94943
4130588	37,25587	-6,95324	4131372	37,26358	-6,93403	4130606	37,25617	-6,9494
4130832	37,25829	-6,94680	4131103	37,26078	-6,94538	4130475	37,25487	-6,95301
4131203	37,26210	-6,93280	4133144	37,2797	-6,92946	4133371	37,2814	-6,9397
4131415	37,26385	-6,93744	4132302	37,27196	-6,93398	4132151	37,27051	-6,93659
4132180	37,27069	-6,93892	4130584	37,25581	-6,95413	4130550	37,25564	-6,95024
4131327	37,26355	-6,92265	4130584	37,25581	-6,95413	4131234	37,26234	-6,93404
4131080	37,26093	-6,93467	4130530	37,25602	-6,93331	4133412	37,28168	-6,94251
4130560	37,25565	-6,95226	4130560	37,25592	-6,94433	4133584	37,28324	-6,94201
4131496	37,26406	-6,95306	4133169	37,27934	-6,94696	4130750	37,25768	-6,94304
4131197	37,26214	-6,92990	4131222	37,26209	-6,93827	4130474	37,25543	-6,93606
4130884	37,25876	-6,94660	4130999	37,25952	-6,95519	4131457	37,26426	-6,93655
4131014	37,26003	-6,94372	4131676	37,26639	-6,93209	4130818	37,25873	-6,92975
4131134	37,26103	-6,94626	4131162	37,26164	-6,9356	4130648	37,25654	-6,94949
4131212	37,26203	-6,937068	4132434	37,27322	-6,93203			
4131990	37,26886	-6,942631	4131942	37,26805	-6,95409			

4.4. Sampling procedures and pre-treatments

In this section, a description of the sampling procedures and sample pre-treatments will be detailed.

4.4.1. Paper #1: Delineating distinct sediment pollution signatures from diverse sources in a heavily contaminated estuary near an area of high cancer and cardiovascular mortality

In March 2021, ten representative salt marsh sediment samples (approximately 2.5 x 10^{-4} m^3) were randomly selected and directly taken from each sampling area (A1-A7). Each sediment sample was collected 10 cm deep, coinciding with the rooting zone of the halophytes present in this area, and placed in clean plastic bags. These samples were then stored in a freezer at -20°C until the pre-treatment procedure. Upon the completion of the sampling procedure, a total of 70 samples were obtained.

Sample pre-treatments procedure is summarised in Figure 7. A total of 5-10 grams of each sediment sample were placed into petri dishes, which were then placed in a drying oven at 35°C for one week. Subsequently, at least 3 grams of completely dry sediment samples were ground to a particle size smaller than 500 µm. The samples were then stored in clean airtight plastic bags, properly labelled, and preserved in the freezer at -20°C to ensure their chemical properties remained unaltered until analysis, which was conducted as soon as possible after sampling, typically within a fortnight. Just before analysis, sediments samples were thawed, placed into a Teflon reactor, and designed for microwave-assisted digestion and digested with HNO_3 at 220°C using a microwave (UltraWAVE. Millestone Srl). Following digestion, the samples were diluted to 50 mL. Finally, the extracts were filtered through a 0.45 µm polytetrafluoroethylene (PTFE) membrane filter.

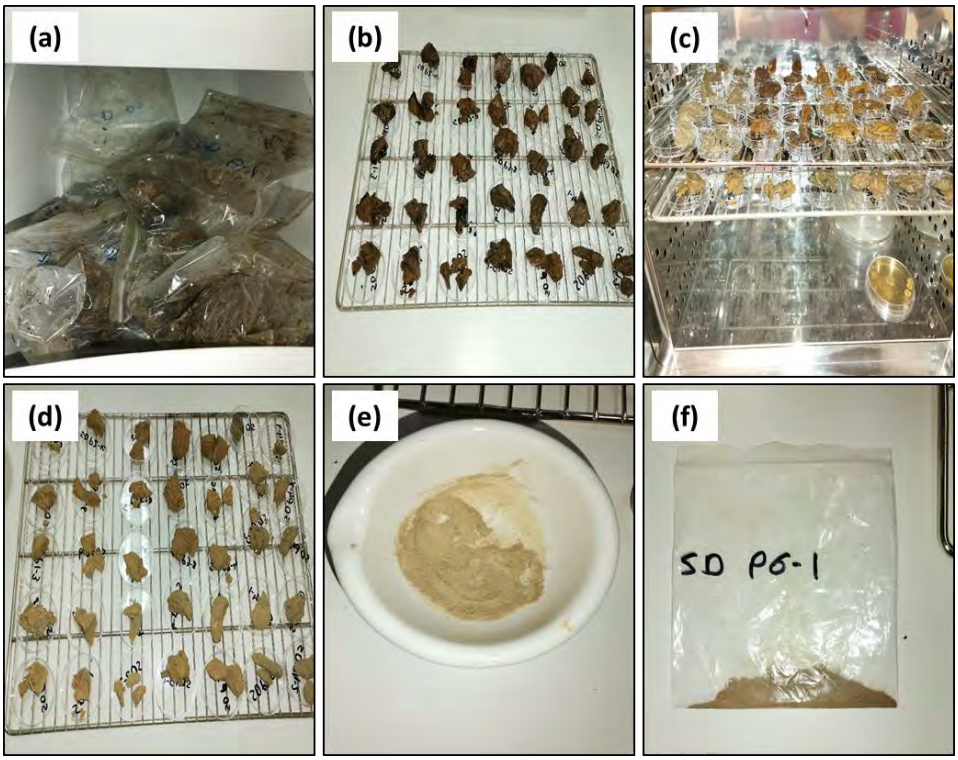

Figure 7. *Photographs of the main steps involved in the sampling pre-treatment procedure for salt marsh sediment samples. [(a) frozen sediment samples; (b) samples placed into petri dishes; (c) samples paced in a drying oven; (d) dried samples; (e) grounded sediment; (f) sediment sample stored in airtight plastic bags].*

4.4.2. Paper #2: Influence of phosphogypsum waste on rainwater chemistry in a highly polluted area with high mortality rates in Huelva metropolitan area, Spain

The rainwater samples were collected using 17 Hellman rain gauges over the period January 2021-December 2022, based on specific rainfall events. This timeframe ensured that each sampling area was monitored for at least two full hydrologic years. A basis rain event was defined as rainfall of at least 1 mm following a minimum 24-hour dry period.

A Hellmann rain gauge is a traditional and widely utilised device for measuring rainfall, renowned for its precision and reliability. It comprises two plastic vessels connected together. The upper vessel, known as the receiver, has a bevelled collection mouth of 200 cm^2 that leads into a funnel designed to minimise splashing (Figure 8a). The lower vessel, referred to as the protector, gathers the water from the funnel using an isolated container in the centre, creating an air chamber around it to help reduce evaporation of the collected water. In addition, the exterior parts are made in light grey to reduce the thermal load (Figure 8a,b). In addition, it features a plastic graduated cylinder (DIN 58667B, 0-10 mm, scaled in 1/10 mm precipitation height; Figure 8c) for taking rainfall readings and brackets for attaching the instrument to a post, fence, or other support structure at a height of 1.5 m according to the World Meteorological Organisation (WMO) standard (Figure 8b). The collected precipitation is directed into a collection container through the funnel, and the measuring cylinder is used to accurately determine the height of the rainfall. Following a prolonged dry period, which is typical in this region, it is crucial to thoroughly clean the rain gauge with deionised water and perform maintenance before the onset of the wet season. This ensures that the composition of single-event samples can be regarded as wet-only deposition.

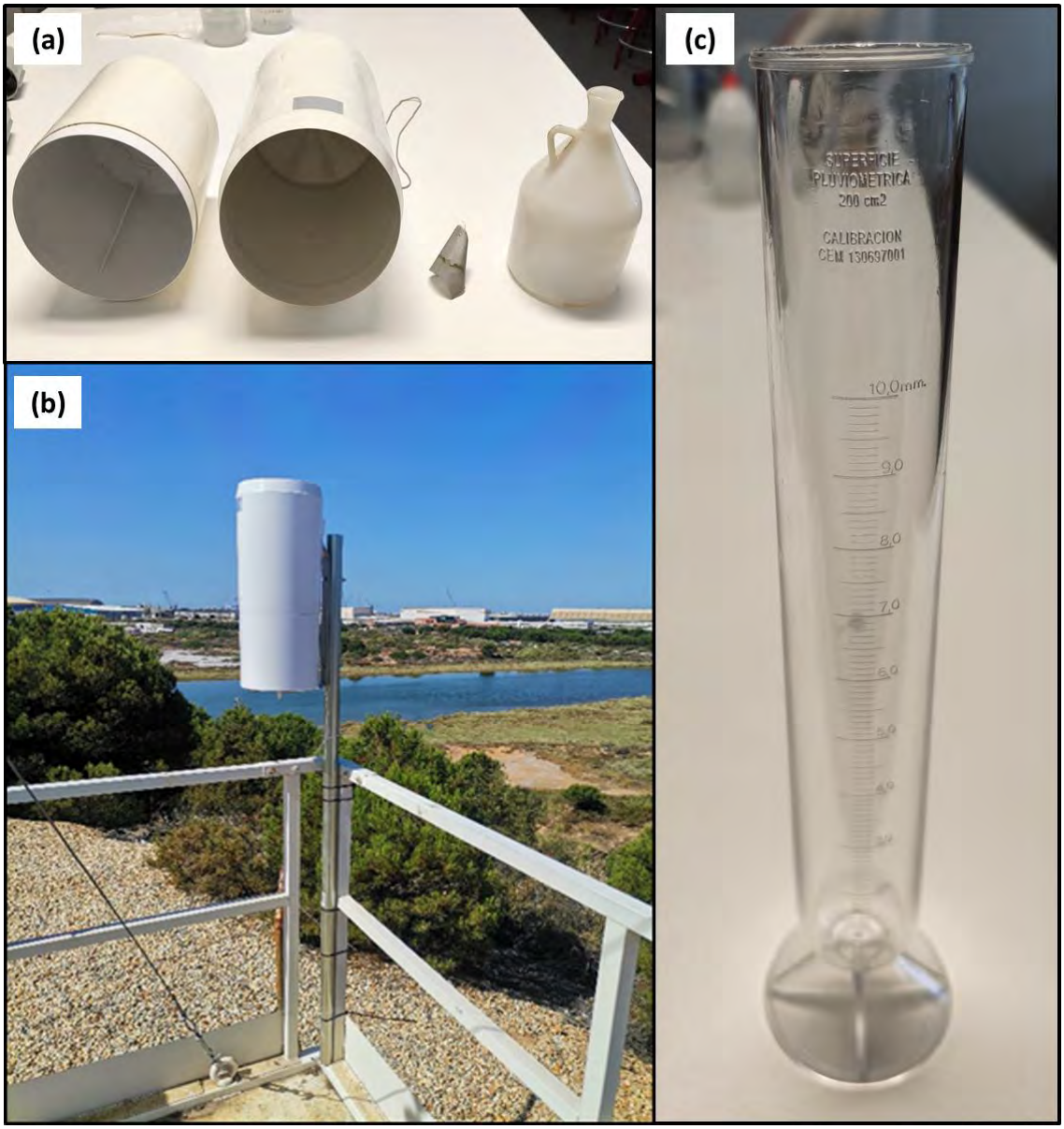

Figure 8. *Photographs of (a) the main part of the Hellman rain gauge; (b) a Hellman rain gauge installed in a sampling point; (c) plastic graduated cylinder (DIN 58667B).*

After a rain event, sample collections were conducted promptly, typically the following day. The rainwater contained in the collection container was then collected and measured using the measuring cylinder. Subsequently, the interior walls of the rain gauge were meticulously cleaned multiple times with the collected rainwater sample to gather the particulate matter present on them, which was then preserved in clean plastic bottles. Following the collection procedure, the rain gauges were subjected to a comprehensive wash using deionised water.

In the laboratory, the samples were subjected to filtration using 0.45 mm PTFE membrane filter to remove insoluble particles. Then, four replicates were made for each sample and placed in clean plastic bottles. At this stage, both the pH and electrical conductivity were measured, with the procedure to be detailed further in subsequent sections. Once these parameters were measured, two of the four replicas were acidified with nitric acid ≥ 99% (T) suprapur supplied by Honeywell™ (Wabash, Indiana, United States), until pH level was reduced to below 2.5. The replicates were meticulously labelled to clearly differentiate between the acidified and non-acidified samples. Finally, the samples were then stored in the fridge below 4°C to ensure their chemical properties remained unaltered until analysis, which was conducted as soon as possible after pre-treatment, typically within a fortnight. Upon the completion of the sampling and pre-treatment procedures, a total of 612 samples were obtained.

Conversely, concerning the metal(loid)s monitored in this study, several factors significantly influence the quality of rainwater sampling from these devices (Alcolea et al., 2015):

- ✓ Hostile environment due to the presence of intense road traffic, ashes, dust, particles of plant and animal origin, mainly bird droppings.
- ✓ Inadequate maintenance and irregular cleaning of the device, particularly after prolonged dry periods.
- ✓ Materials used in the construction of the rain gauge.
- ✓ Minimal quantities of rainwater collected after each precipitation event.

A quality score ranging from 1 to 5 (1 = poor, 5 = excellent) was assigned to each sampling point taking into consideration these various factors (Table 5). This 5-point likert scale reflects a range of average scores, demonstrating the challenge of obtaining meaningful data from rain gauges with the lowest scores (1) compared to those with the highest scores (5). This 5-point Likert scale illustrates different average scores, what obviously makes difficult to get useful data in the rain gauges with the lowest scores (1) but not in these with the highest result (5). Consistency in temporal and spatial observations is crucial for extracting valuable insights from any analysis. A minimum

acceptable score of 3 is required to achieve this consistency. The Likert scale reveals an average score of 3.5, which is higher than the minimum acceptable score of 3. AL, FB, FE, and MO achieved the highest quality score (5), followed by CO, GI, MN, PF, and PI with scores of 4. Conversely, sampling points with the lowest quality index (1), PU and SJ, are most affected by these previous factors that may introduce additional pollutants in the collected sample.

Table 5. *5-point Likert scale, which captures the range of average scores assigned to the rain gauges based on their level of exposure to pollution sources.*

Code	Exposure to pollution sources	QS*
SJ	Traffic-related air pollution Industrial activities Organic material from birds and vegetation	1
MO	Industrial activities Intensive agricultural activities	5
PF	Industrial activities Intensive agricultural activities	4
GI	Intensive agricultural activities	4
AL	Organic material from vegetation	5
CO	Mining waste	4
PU	Industrial activities Organic material from birds and vegetation	1
EP	Organic material from vegetation	2
PI	Organic material from vegetation	4
JR	Traffic-related air pollution Urban emissions	3
CM	Traffic-related air pollution Urban emissions	3
AD	Traffic-related air pollution Industrial activities	3
FB	PG stacks	5
FE	PG stacks	5
MN	Organic material from vegetation	4
RA	Industrial activities	3
CA	Traffic-related air pollution Organic material from birds and vegetation Urban emissions	3

* Quality score 1 = poor, 5 = excellent.

4.4.3. Paper #3: Internal cumulated dose of toxic metal(loid)s in a population residing near naturally occurring radioactive material waste stacks and an industrial heavily polluted area with high mortality rates in Spain

Upon the completion of the epidemiological survey, toenail samples from both feet were collected from the 55 participants, who were part of the general population-based controls from Huelva City. For this purpose, clean stainless steel nail clippers were used within a two-week period following recruitment, from September 2008 to December 2013. The toenail clippings were then placed in a clean plastic bag, properly labelled and stored at room temperature until pre-treatment. Furthermore, anthropometric measurements and additional information were gathered in accordance with the study protocol, which received approval from the recruiting centres.

Initially, toenail samples (50-100 mg) underwent two washes with 2 mL of a 5% (weight/volume) Triton water solution. Subsequently, samples were rinsed twice using 2 mL of Milli-Q water, followed by two washes with 2 mL of acetone. A supplementary ultrasound treatment for 5 minutes was then carried out. Next, the samples were air-dried and then digested with 800 µL of an Ultra Trace Metals grade quality mixture (4:1) of HNO_3 and H_2O_2, using a Teflon reactor designed for microwave-assisted digestion. The mineralisation process was performed using a UltraWAVE system provided by Milestone Srl (Sorisole, Bergamo, Italy). The procedure involved starting at room temperature and applying 400 W of power, ramping up the temperature to 160°C over a period of 15 minutes, and then maintaining this temperature for an additional 20 minutes. Finally, the extracts were passed through a 0.45 µm PTFE membrane filter before undergoing analysis.

4.5. Chemical and physical laboratory techniques

In this section, we will outline the measurements techniques and equipment used in the chemical and spatial characterisation of the collected samples. Moreover, the quality control measures applied to ensure the reliability of the results are summarised below. Finally, the statistical analysis procedures were detailed.

4.5.1. Electrical conductivity (EC), redox potential (Eh), pH

4.5.1.1. Paper #1: Delineating distinct sediment pollution signatures from diverse sources in a heavily contaminated estuary near an area of high cancer and cardiovascular mortality

In the Odiel-Tinto Estuary, pH levels in low salinity conditions and competitive desorption in high salinity conditions are critical environmental factors that influence the movement of anions and cations (Kerl et al., 2023). Therefore, electrical conductivity (EC) as an indicator of salinity, pH, and redox potential (Eh) were measured in salt marsh sediment samples with a digital multimeter LAQUA PC220 (HORIBA Advanced Techno Co., Ltd., Kyoto, Japan). These parameters were measured using a mixture of sediment and distilled water in a 1:2 ratio, which was stirred at approximately 1,200 rpm for 24 hours.

The multimeter was calibrated daily with standard solutions of 4.01, 7.00, and 9.21 pH units, to account for both basic and acidic sediments, and with solutions of 147 mS cm^{-1} and 1413 mS cm^{-1}, which encompassed the range of EC values of the sediments. The results, adjusted to a reference temperature of 25°C, were obtained through temperature conversion.

4.5.1.2. Paper #2: Influence of phosphogypsum waste on rainwater chemistry in a highly polluted area with high mortality rates in Huelva metropolitan area, Spain

The pH is a critical parameter of rainwater chemistry, as it influences various other characteristics like EC. Its measurement is one of the most commonly performed tests in rainwater quality (Dunea et al., 2021). Moreover, the bioavailability of metals in salt marshes is affected by salinity levels (Conesa et al., 2011). The EC and pH of the rainwater samples were measured by directly immersing the sensor of the digital multimeter model LAQUA PC220 provided by HORIBA Advanced Techno Co., Ltd. (Tokyo, Japan) within 24 h after being collected.

The multimeter was calibrated daily with standard solutions of 4.01, 7.00 and 9.21 pH units, to account for both basic and acidic rainwaters, and with solutions of 147 mS cm^{-1} and 1413 mS cm^{-1}, which encompassed the range of EC values of the rainwaters.

The results, adjusted to a reference temperature of 25°C, were obtained through temperature conversion.

4.5.2. Texture by Bouyoucos,

4.5.2.1. Paper #2: Influence of phosphogypsum waste on rainwater chemistry in a highly polluted area with high mortality rates in Huelva metropolitan area, Spain

Soil can be divided into twelve soil textures, defined by the distribution of particle sizes (sand: 2000-63 µm; silt: 63-2 µm; clay: <2 µm), see Figure 9 (Osman, 2012). It plays a pivotal role in soil degradation, as soils with varying textures exhibit different levels of susceptibility to the movement of contaminants (Guo et al., 2022).

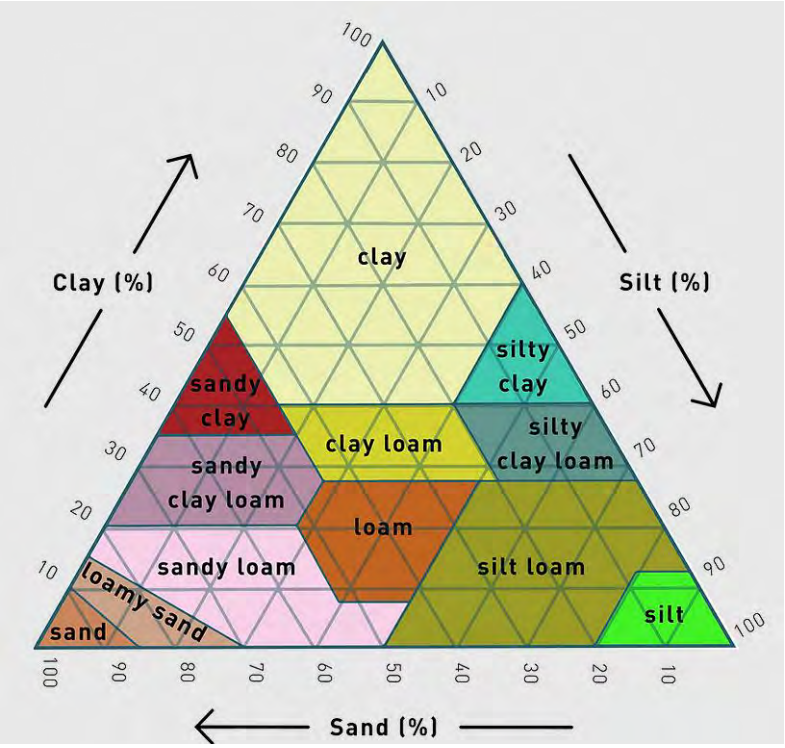

Figure 9. *Soil texture triangle (adapted from Osman, 2012)*

The composition of sand, silt and clay in salt marsh sediments were determined using the Bouyoucos method (Bouyoucos, 1936). According to this method, the particle size of solids in the suspension is determined by measuring the density of the solution with a hydrometer.

Firstly, 50 g of dry salt marsh sediment were placed into a glass flask. Secondly, 100 mL of a 5% Calgon solution was added as a dispersant to separate the soil aggregates,

and the mixture was subsequently left undisturbed for a few minutes. Thirdly, the mixture was dispersed using a soil mixer operating at approximately 500 rpm for a duration of 2 hours. Fourthly, the mixture was transferred into a graduated cylinder, diluted to 1000 mL with distilled water and stirred with a stir bar. Finally, hydrometer values and temperature measurements were recorded at two intervals: initially at 40 seconds, and subsequently at 2 hours.

4.5.3. Inductively coupled plasma optical emission spectrometry (ICP-OES)

ICP-OES is a sophisticated technique used for trace-level elemental analysis. By utilising the emission spectra of a sample, it can identify and quantify elements based on the intensity of radiation emitted by each specific element. ICP-OES is particularly suitable for analysing elements present in parts per million (ppm) concentrations and is widely employed for various environmental sample matrices, especially those with high matrix effects (Douvris et al., 2023). Consequently, this technique is more robust than inductively coupled plasma mass spectroscopy (ICP-MS) for analysing samples such as water, soil, and other solid/liquid samples.

4.5.3.1. Paper #1: Delineating distinct sediment pollution signatures from diverse sources in a heavily contaminated estuary near an area of high cancer and cardiovascular mortality

Concentrations of major elements (Al, Ca, *Cu, Fe, K, Mg, Na, P, S, *V, Zn) were determined in salt marsh sediments by ICP-OES using an Agilent 5110 (Agilent Technologies, Tokyo, Japan) spectrometer at the Centre for Research and Development of Agri-Food Resources and Technologies (CIDERTA) of Huelva University (Huelva, Spain). The equipment operated within the range of 160–900 nm, with external and periodic calibration ranged between 0.1–50 ppm, 0.1–100 ppm and 0.1–500 ppm. The detection and quantification limits for these measurements were 0.1 ppm and 0.5 ppm, respectively. The digested sediment samples were initially diluted at a ratio of 1:100 for analysis. If analyte concentrations exceeded the instrument's linear range, further dilutions were performed. The equipment adjusted the measured concentration by incorporating the sample's dilution factor and weight, utilising the formula outlined below [Eq. 1]:

$$Real\ (\mu g \cdot kg^{-1}) = Equipment\ (\mu g \cdot kg^{-1}) * \frac{dilution\ factor\ (g)}{sample\ weight\ (g)} \quad \text{[Eq. 1]}$$

The limit of detection for each measured element was obtained from the calibration curve (Thomsen, 2003). Detection limits were determined based on the mean and standard deviation from a minimum of five blank measurements and were found to be below 0.1 mg/L for these elements.

Multielement standard solutions were derived from single certified standards provided by SCP SCIENCE (Quebec, Canada), prepared using Milli-Q ultrapure water and 2% (v/v) nitric acid suprapur as the matrix. Moreover, element concentrations in these standards included 0 (instrumental blank), 0.05, 0.5, 1, 5, 10, 25, and 50 ppm for most elements, except for Al and Fe, which included additional concentrations of 100 and 150 ppm, respectively. Analytical precision was assessed through triplicate analyses, which exhibited variations of less than 5%. Accuracy was validated using the certified reference material NIST-1640, representative of fresh water. Digestion blanks and a reference material were also included in triplicate.

4.5.3.2. Paper #2: Influence of phosphogypsum waste on rainwater chemistry in a highly polluted area with high mortality rates in Huelva metropolitan area, Spain

The acidified rainwater samples were analysed to determine the concentration of key cations (Ca^{2+}, K^{+}, Mg^{2+}, and Na^{+}) using ICP-OES. The analysis was performed with an Agilent 5110 spectrometer (Agilent Technologies, Tokyo, Japan), which covers a wavelength range of 160–900 nm and employs regular external calibrations. Calibration ranges were set between 0.1 and 100 ppm for K^{+} and Na^{+}, and between 0.1 and 500 ppm for calcium Ca^{2+} and Mg^{2+}). Detection limits were established at 0.1 ppm for Ca^{2+} and Mg^{2+}, and 0.5 ppm for K^{+} and Na^{+}. To maintain calibration consistency, a standard solution with a concentration of 10 ppm was assessed after every ten analyses, with deviations kept under 10%. Approximately 10% of the samples underwent triplicate analysis for quality control purposes. Method accuracy was further validated using a multi-element quality control standard (Agilent Technologies, Number 5190-9418) suitable for USEPA applications and other contexts (USEPA, 1984). Recovery rates,

assessed through periodic testing of certified quality control samples during the analysis process, ranged from 80% to 120%.

4.5.4. Ion chromatography (IC)

IC is a sophisticated technique within liquid chromatography, quantifies the concentrations of ionic species by separating them based on their interactions with a resin. Different ionic species separate according to their type and size. Sample solutions pass through a pressurised chromatographic column, where ions are adsorbed by the column constituents. As an ion extraction liquid, known as eluent, flows through the column, the adsorbed ions begin to separate from the column. The retention time of various species determines the ionic concentrations within the sample. Ion chromatography was utilised to examine aqueous samples, enabling the detection of common anions present at high concentrations (0.1 to 1000 ppm; Weiß, 1987).

4.5.4.1. Paper #2: Influence of phosphogypsum waste on rainwater chemistry in a highly polluted area with high mortality rates in Huelva metropolitan area, Spain

The concentrations of anions (Cl^-, F^-, NO_2^-, NO_3^-, PO_4^{3-}, and SO_4^{2-}) and NH_4^+ in unacidified rainwater samples were analysed using a Metrohm 883 BASIC IC PLUS automated IC system (Metrohm AG, Herisau, Switzerland). Anions were separated using a Metrosep A Supp 5 250/4.0 column with a carbonate/bicarbonate eluent (3.2 mM Na_2CO_3 + 1.0 mM $NaHCO_3$) at a flow rate of 0.7 mL min^{-1}. Conversely, was separated on a Metrosep C4 250/4.0 column with an eluent of 4 mM tartaric acid + 0.75 mM dipicolinic acid, with a flow rate of 1.0 mL min^{-1}. For calibration, external standards prepared at 1000 mg L^{-1} from commercial calibration solutions were employed. The calibration ranges for minor anions were 0.1–25 ppm for F^-, 0.05–25 ppm for NO_2^-; and 0.5–25 ppm for PO_4^{3-}, while major anions were 0.5–250 ppm for Cl^-; 0.25–125 ppm for NO_3^-; and 0.5–250 ppm for SO_4^{2-}. To ensure accuracy, calibration blanks were evaluated during each analytical sequence, and triplicate analyses were conducted on 10% of the samples. Quality control standards were used, including a high-concentration standard and one near the quantification limits. Quantification limits were 0.1 ppm for F^-, 0.5 ppm for Cl^-, 0.05 ppm for NO_2^-, 0.25 ppm for NO_3^-, 0.5 ppm for PO_4^{3-}, and 0.5 ppm for SO_4^{2-}. Validation criteria required Relative Standard Deviation (RSD) below 15% for duplicate

samples and a deviation of less than 15% between control standard and theoretical values. For calibration, five-point curves were created for both anions and cations using certified multi-element IC standard solutions from Sigma-Aldrich. All reagents, standards, and eluents were prepared with high-purity water (resistivity 18.2 MΩ·cm, total organic carbon <10 µg L^{-1}) from an Elix 3/Milli-Q Element system. The method detection limits (MDL) adhered to U.S. EPA guidelines outlined in 40 CFR 136, Appendix B (USEPA, 1984). Recovery rates, evaluated through routine analyses of certified multi-element standards IC Quality Control Sample 1 (IC-QC1-1) and IC Quality Control Sample 2 (IC-QC2-1) supplied by Sigma-Aldrich (San Luis, Missouri, USA), fell within 80–120%. To ensure data integrity, samples were analysed in triplicate, with reference materials and blanks routinely interspersed throughout sample batches.

4.5.5. Inductively coupled plasma mass spectrometry (ICP-MS)

ICP-MS boasts a multi-element character and high sample throughput. While ICP-OES measures the radiation emitted by various atoms using an optical detector, ICP-MS detects ions through a mass spectrometer, based on the mass-to-charge ratio (m/z). ICP-MS is particularly suitable for isotope ratio studies and ultra-trace analysis of elements, with instrumental detection limits (IDL) ranging from 1 ppt to 10 ppb, depending on each specific element. Moreover, this technique exhibits a wide dynamic range (Jenner et al., 1990). However, it is not capable of measuring certain non-metallic elements (e.g., P, S, Sc, and Ti), which can be determined using ICP-OES.

4.5.5.1. Paper #1: Delineating distinct sediment pollution signatures from diverse sources in a heavily contaminated estuary near an area of high cancer and cardiovascular mortality

Concentrations of trace elements (As, Ba, Be, Bi, Cd, Ce, Co, Cr, Cs, Dy, Er, Eu, Ga, Gd, Ge, Ho, In, La, Li, Mo, Nb, Nd, Ni, Pd, Pr, Rb, Sb, Sc, Se, Sm, Sn, Sr, Tb, Te, Th, Tl, Tm, U, Y, Yb, and Zr) in salt march sediments were determined by ICP-MS using an Agilent 7700 (Agilent Technologies, Tokyo, Japan) spectrometer with SPS4 auto sampler and collision cell (He mode) at the CIDERTA of Huelva University (Huelva, Spain). The digested sediment samples were initially diluted at a ratio of 1:100 for analysis. If analyte concentrations exceeded the instrument's linear range, further dilutions were

performed. The equipment adjusted the measured concentration by incorporating the sample's dilution factor and weight, utilising the formula outlined below [Eq. 1]. Molecular (polyatomic) ions are commonly formed in the inductively coupled plasma and can provoke interferences in ICP-MS. In this study, molecular ions elimination through kinetic energy discrimination (KED) was applied, by adding 4.3 ml min^{-1} He gas flow in the collision cell (ORS) of the ICP-MS instrument. This method is commonly used in ICP-MS and has historically proven to be efficient. In particular, the specifications of the instrument used in this study (Agilent 7700 ICP-MS) showES interferences removal factor >30 (expressed as the ratio ^{59}Co/51ClO). Further studies of the possible interferences for each analyte isotope and each potential molecular ion interferent were not conducted, since such fundamental ICP-MS studies were considered out of scope in this work. An internal solution containing Rh was added on-line to the samples to correct signal drifts. Sediment reference materials for trace metals (EnviroMAT SS-1 Soil Standard) were also analysed to check the analytical accuracy. The calibration range was from 0.5 ppb to 250 ppb for all elements, and the quantification limit was 0.5 ppm. The calibration method was performed with a solution consisting of 10 ppb of ^{7}Li, ^{89}Y and ^{205}Tl. Internal quality controls (IQC) were used according to the work instructions included in the Quality Manual according to ISO9001 and 14001 standards. Various IQC were applied to ensure that the analytical procedure was correctly carried out, from digestion to analysis, and to enable analytical chemists to validate the results obtained. The laboratory quality controls used to determine the metals using ICP-Ms technique were the AccuTraceTM certified reference standards ICP-MS Quality Control Sample 1 (ICP-MS-QC1-1) and ICP-MS Quality Control Sample 2 (ICP-MS-QC2-1) supplied by AccuStandard®, Inc (Germany). The comparison of measurement results on the certified reference material BCR®667, an estuarine sediment (rare elements, Th and U) with the certified value supplied by Institute for Reference Materials and Measurements (IRMM; Geel, Belgium) was applied. Digestion blanks and a reference material were also included in triplicate.

4.5.5.2. Paper #2: Influence of phosphogypsum waste on rainwater chemistry in a highly polluted area with high mortality rates in Huelva metropolitan area, Spain

The concentrations of trace elements (As, Ba, Cd, Co, Cr, Cu, Mn, Mo, Ni, Pb, Sr, V, and Zn) were determined in acidified rainwater samples using an Agilent 7700 ICP-MS (Agilent Technologies, Tokyo, Japan) with SPS4 autosampler and collision cell (He mode) at the CIDERTA of Huelva University (Huelva, Spain). The equipment used the same parameters that were shown in the previous section.

4.5.5.3. Paper #3: Internal cumulated dose of toxic metal(loid)s in a population residing near naturally occurring radioactive material waste stacks and an industrial heavily polluted area with high mortality rates in Spain

Concentration of trace elements (Al, As, Cd, Co, Cr, Cu, Fe, Mn, Mo, Ni, Pb, Se, Tl, U, V, and Zn) in toenails was determined by ICP-MS system, using an XSeries 2 (Thermo Fisher Scientific Inc., Waltham, MA, USA) spectrometer at the Environmental Bioanalytical Chemistry Unit of Huelva University (Huelva, Spain). The digested sediment samples were initially diluted at a ratio of 1:100 for analysis. If analyte concentrations exceeded the instrument's linear range, further dilutions were performed. The equipment adjusted the measured concentration by incorporating the sample's dilution factor and weight, utilising the formula outlined below [Eq. 1]. To ensure high-quality analysis, several procedures were implemented: (a) the comparison of measurement results on the certified reference material NSC DC73347a, a human hair with the certified value supplied by LGC Standards a division of LGC Group (Middlesex, United Kingdom) was applied. 100 mg was utilised to address instrumental variability across sample batches, maintaining a mean accuracy of 90% within a margin of ±5% over time; (b) the ICP-MS system's performance was tracked by measuring metal(loid) concentrations at a fixed calibration point (2 ng ml^{-1}) after every 20 samples to verify its response; (c) instrumental drift was corrected by adding rhodium (100 ng ml^{-1}) as an internal standard to all samples and calibrants, with re-analysis performed if responses deviated by more than ±10%; (d) reagent blanks containing 5% HNO_3 (Suprapur), 1% HCl, and 100 ng ml^{-1} of Rh in Milli-Q water were analysed every 5 samples; (e) duplicate samples were analysed at 2.5-hour intervals throughout the sequence; and (f) reference materials spiked with analytes under investigation (50 ng ml^{-1}) were used to perform

spiked sample analyses. Additionally, interferences caused by ^{98}Mo, ^{205}Tl, and, ^{238}U—often found in nails—were mitigated by employing helium collision mode in the ICP-MS system (He flow rate: 4 mL min^{-1}). Table 6 presents the operational settings of the ICP-ORS-MS system.

Table 6. *Main the operational settings of the ICP-ORS-MS system.*

Forward power	1500 W
Plasma gas flow	15 L min^{-1}
Auxiliary gas flow 1 L min^{-1}	1 L min^{-1}
Carrier gas flow	0.15 L min^{-1}
Sampling depth 7 mm	7 mm
Sampling and skimmer cones	Ni
H_2 flow 4	4 mL min^{-1}
Nebuliser	Microflow (ESI)
Torch	Shield (with long-life platinum shield plate)
Qoct –18 V	18 V
Qp	–16 V
Points per peak	1
Integration time	0.3 s per isotope
Replicates	1
Isotopes monitored for total metals in nail	^{27}Al, ^{75}As, ^{114}Cd, ^{59}Co, ^{52}Cr, ^{63}Cu, ^{56}Fe, ^{55}Mn, ^{98}Mo, ^{58}Ni, ^{208}Pb, ^{80}Se, ^{205}Tl, ^{238}U, ^{51}V, ^{64}Zn
Dead time of detector	47 s

4.6. Statistical analyses

The following section detailed the statistical analyses used in each publication.

4.6.1. Paper #1: Delineating distinct sediment pollution signatures from diverse sources in a heavily contaminated estuary near an area of high cancer and cardiovascular mortality

A complete descriptive statistical analysis was conducted for each element measured in salt marsh sediment samples and for each sampling area studied, using mean and standard deviation.

Furthermore, homogeneity of variance and normality of the variables were assessed using Levene and Shapiro-Wilk tests, respectively. Parametric one-way ANOVAs (F-test) or non-parametric Kruskal-Wallis H-tests with post-hoc Tukey tests were used to compare salt marsh sediment characteristics and elemental contents

between sampling areas. All analyses were conducted with a significance level (α) of 95% ($p < 0.05$), and deviations were expressed as the standard error of the mean. In addition, a principal component analysis (PCA) was employed to examine the relations among elemental contents in sediment samples from the seven sampling areas. This method condenses complex data into a limited number of uncorrelated components, thereby representing the entire dataset with minimal information loss (Demir et al., 2010). The correlation matrix was examined using up to 25 maximum iterations for convergence without rotation. Independent PCA factors with eigenvalues greater than 1 were extracted. PCA regression factor scores for each sediment sample were compared among the seven sampling areas studied using Kruskal-Wallis H tests with post-hoc Tukey tests. The Statistical Package for the Social Sciences (SPSS) version 15.0 (IBM SPSS Inc., Chicago, USA) and was used for data analysis. Additionally, SigmaPlot 11.0 (Systat Software Inc., Düsseldorf, Germany) was used to quickly create accurate graphs.

4.6.2. Paper #2: Influence of phosphogypsum waste on rainwater chemistry in a highly polluted area with high mortality rates in Huelva metropolitan area, Spain

A comprehensive descriptive statistical analysis was accomplished to characterise the chemical content distribution in rainwater, using means, lower and upper limits (95%), means trimmed at 5%, medians, variances, standard deviations, RSD%, minimums, maximums, ranges, interquartile ranges, skewness, and kurtosis.

Additionally, in order to define if the dataset exhibited a normal distribution, the Kolmogorov–Smirnov test was conducted, with a significance level (α) of 95% ($p < 0.05$) applied in all cases (Paz-González et al., 2000). For elements that conformed to a normal distribution, the mean and standard deviation were reported. For those that did not, the median and interquartile range were utilised. The statistical analyses were executed with SPSS 26.0 (IBM SPSS Inc., Chicago, USA).

4.6.3. Paper #3: Internal cumulated dose of toxic metal(loid)s in a population residing near naturally occurring radioactive material waste stacks and an industrial heavily polluted area with high mortality rates in Spain

In order to assess the elemental distribution in nails a complete descriptive statistical analysis, using mean, geometric mean, median, standard deviation, minimum and maximum concentrations, skewness, and kurtosis, was conducted.

Additionally, the normality of the variables was analysed using both the Shapiro–Wilk and Kolmogorov–Smirnov tests (Paz-González et al., 2000), with a significance level (α) of 95% ($p < 0.05$) applied in all cases. In order to evaluate the potential relationships between the measured elements the Spearman's correlation coefficient was calculated. Additionally, PCA was used to study the relations among chemical contents in nails. This method condenses complex data into a limited number of uncorrelated components, thereby representing the entire dataset with minimal information loss (Demir et al., 2010). To optimise the variance of factor loadings a cross variables for each principal component (PC), a Varimax rotation with Kaiser normalisation was performed (Cui et al., 2011). Moreover, PCA was carried out on the measured elements in toenails to assess the correlation strength between them and investigate their potential anthropogenic and/or natural sources. Statistical significance level (α) of 95% ($p < 0.05$) and (α) of 99% ($p < 0.01$) was used in all the cases. The statistical analyses were executed with SPSS 26.0 (IBM SPSS Inc., Chicago, USA).

4.7. Spatial analyses

A detailed description of the spatial analyses applied is provided in this section.

4.7.1. Paper #1: Delineating distinct sediment pollution signatures from diverse sources in a heavily contaminated estuary near an area of high cancer and cardiovascular mortality

The spatial distribution of elements linked to pollution sources within the Odiel-Tinto Estuary, including PG stacks, mineral wastes, and AMD, was analysed using the kriging method. This spatial interpolation approach facilitated the creation of continuous surface maps for the elements, utilising data from 70 sediment samples from

the estuary's salt marshes. Additionally, inverse distance weighting (IDW) interpolation was employed to generate detailed maps of chemical element distributions. IDW assigns higher weights to nearby points, based on the assumption that variable influence diminishes with increasing distance from the sample site (Lu et al., 2008). All analyses were conducted using the geographic information system (GIS) software, ArcGIS 10.5 (ArcGIS Enterprise, Esri Inc., California, USA).

4.7.2. Paper #2: Influence of phosphogypsum waste on rainwater chemistry in a highly polluted area with high mortality rates in Huelva metropolitan area, Spain

The spatial distribution of elements found in rainwater collected across the metropolitan area of Huelva was analysed using graphs. These graphs depicted the median values of each element at different rain gauge locations, considering their distance from the reference station located at the PG stacks (FB). The graphs were refined through the addition of corresponding trend lines, derived using linear regression models. These were constructed utilising the statistical software R, version 2024.12.0+467 (Posit Software, PBC formerly RStudio, PBC, Boston, MA, USA).

4.7.3. Paper #3: Internal cumulated dose of toxic metal(loid)s in a population residing near naturally occurring radioactive material waste stacks and an industrial heavily polluted area with high mortality rates in Spain

The spatial distribution of elements linked to pollution sources within the Odiel-Tinto Estuary, including PG stacks, mineral wastes, and AMD, was analysed using the kriging method.

This method allowed for the creation of continuous surface models for each analysed element, utilising data derived from toenail samples collected from 55 residents in Huelva City. This approach enabled the visualisation of spatial distribution patterns for these elements in areas of the city that were not directly measured. The interpolation and mapping of these distribution patterns were carried out using ArcGIS 10.5 for Desktop software (Esri Inc., Redlands, CA, USA)

5. Discussion

This section presents the essential insights derived from the discussions of the three papers incorporated into this doctoral thesis.

5.1. Paper #1: Delineating distinct sediment pollution signatures from diverse sources in a heavily contaminated estuary near an area of high cancer and cardiovascular mortality

The research paper discusses the identification of three distinct chemical signatures in sediments from seven salt marsh areas across the Odiel–Tinto Estuary, each linked to specific pollution sources: acid AMD upstream of the Tinto River, PG waste stacks, and an abandoned foundry in the Odiel River. Peak concentrations of 20 elements were detected near the PG stacks (site A1), associated with PC1, which accounted for 34% of the data variance. These elements have been previously documented in edge outflows and nanoparticles originating from PG stacks (Millán-Becerro et al., 2016; Pérez-López et al., 2016; Ruiz Cánovas et al., 2018; Silva et al., 2022). Among radionuclides, U-series isotopes exhibit the highest mobility within PG stacks (Pérez-Moreno et al., 2018). Elements such as Al, Cr, Fe, Pb, and U tend to precipitate under neutral seawater conditions through co-precipitation and adsorption onto phosphate phases, with fluoride precipitation also contributing to their removal (Guerrero et al., 2020; Papaslioti et al., 2018). Additionally, elements like As, Cd, Co, Cr, Cu, Ni, Pb, U, and Zn precipitate when sediment pH exceeds 4 and Eh falls below +340 mV, facilitated by Fe-limited sulphide precipitation in organic-rich sediments (DeLaune and Reddy, 2005; Guerrero et al., 2019; Hierro et al., 2014; Pérez-López et al., 2011, 2018; Santos Bermejo et al., 2003).

The PG stacks are situated in the estuarine zone where seawater meets the Tinto River, characterised by a sharp shift in water properties. This leads to the neutralisation of acidic waters and the precipitation of chemical elements from both the PG stacks and those transported down the Tinto River, reflected in a significant decrease in Cu concentrations downstream (Chica-Olmo et al., 2004). Arsenic concentrations recorded

in the study (866.5 ± 64.0 mg kg^{-1}) may exhibit high ecotoxicity levels when accumulated in marsh sediments (Hwang et al., 2008).

Phosphorus has been suggested as a suitable tracer to determine the impact of PG stacks on sediments (Guerrero et al., 2019). The study also identified trace elements such as Gd, Bi, Ce, and Zr as potential geochemical tracers, exhibiting high concentrations characteristic of PG stack pollution signatures. Elements with the highest loadings in PC2 (Cd, Cr, Dy, Ga, Ho, Ni, and Tm) showed the greatest sediment concentrations near the PG stacks on both banks of the Tinto River (A1 and A2). Some of these elements, particularly Cd and Ni, tend to remain in solution with increasing pH, with an average removal of around 60% (Beltrán et al., 2010; Hierro et al., 2014; Morillo et al., 2008; Sáez et al., 2003).

Several chemical elements identified in PG stack outflows by Perez-Lopez et al. (2016), including Fe, S, Cd, Co, Pb, and Ni, were not among those with the highest loadings in PC1. However, Co, Fe, and Pb exhibited the highest sediment concentrations near the abandoned foundry's mineral waste (site A5; Curado et al., 2014). Elements typically associated with AMD, such as Co, Fe, Pb, Mn, Tl, and Rb, exhibited the highest loadings on PC3, explaining 13% of the data variance across the estuary, suggesting their utility as geochemical tracers for AMD pollution (da Silva et al., 2005; Fernández-Landero et al., 2023; Millan-Becerro et al., 2024).

The analysis revealed the highest total sulphur concentrations upstream in the Tinto River (site A6), 32% higher than the second-highest value (site A5). Sulphur was the only element with a factor loading exceeding 0.600 in PC5, explaining 6% of the data variance, serving as a unique geochemical marker in the highly polluted Tinto River Estuary. The low pH and high Eh, driven by extensive pyrite oxidation, promote the dissolution of toxic elements and radionuclides (Mehdi et al., 2013).

Estuarine sediments in the Piedras River displayed high concentrations of Se and La, strongly associated with PC4, explaining 7.3% of the data variance. Alkaline soils release more Se than acidic ones (Santos Bermejo et al., 2003), aligning with higher Se

concentrations observed in the Piedras River salt marshes (site A7), unaffected by AMD unlike the Odiel and Tinto Rivers.

Two sampling sites (A2 and A7) near intensive strawberry cultivation exhibited the highest average beryllium concentrations (1.5–2.7 mg kg-1), over 40% higher than those near the PG stacks (site A1), despite beryllium being a trace element in these deposits (Silva et al., 2022). Beryllium, associated with PC6 explaining 4% of the data variance, distinguished sediments near the PG stacks from those across the Tinto River with elevated beryllium, suggesting its suitability as a geochemical marker for agricultural pollution. Given its use in metal alloys, beryllium could originate from greenhouse structures and become trapped in sediment (ATSDR, 2022).

Many studies on heavy metal distribution in polluted locations have provided important data for pollution management and remediation (Dong et al., 2024; Liu et al., 2024; Sun et al., 2025). The study characterises sediment pollution signatures in a highly polluted Spanish estuary, differentiating between sources such as PG stacks, AMD, and agricultural activities. This knowledge is valuable for developing integrated monitoring and pollution management plans to quantify and reduce pollution impacts. The identified signatures can serve as references for assessing future interventions in the Odiel–Tinto Estuary, critical for evaluating the RESTORE 2030 plan and future restoration efforts for contaminated other areas, such the zone near the abandoned foundry.

Given the known links between industrial and mining pollution and excess mortality rates in the Huelva area (Alguacil et al., 2014; Benach et al., 2003; Lopez-Abente et al., 2001; Briffa et al., 2020), studying correlations between pollution sources and mortality is warranted. Biomonitoring of metal exposure in the population and ecosystem is justified, as recommended by scientific experts (Alguacil et al., 2014; Scientific committee, 2022).

5.2. Paper #2: Influence of phosphogypsum waste on rainwater chemistry in a highly polluted area with high mortality rates in Huelva metropolitan area, Spain

The mean pH of rainwater in the Huelva metropolitan area was 7.03, which is relatively high compared to unpolluted rainwater, which typically has a pH of 5.6 due to the natural buffering effect of CO_2 in the atmosphere (Charlson and Rodhe, 1982). The higher pH levels observed in this area were attributed to neutralising sea-salt particles, a common feature in coastal regions (Al-Momani et al., 1995; Dikaiakos et al., 1990; Tuncer et al., 2001; Zeng et al., 2024). However, this neutralisation effect was counteracted in areas closer to the PG stacks (FB), where acidic compounds, such as hydrogen fluoride, likely contributed to lower pH values. The minimum pH recorded at FB was 6.31, below the World Health Organisation (WHO) guideline of 6.5 for drinking water, indicating that rainwater in these areas could pose a health risk due to increased solubility of toxic metals like As, Cd, and Pb in acidic conditions, which poses numerous health risks, such as cancer and neurobehavioral disorders (WHO, 2003).

Rainwater EC exhibited notable differences across the sampling sites. Higher EC values were recorded in rain gauges influenced by organic material from nearby animals (e.g., birds) and vegetation (Tranel and Kimmel, 2009). The study found that these organic and inorganic particles contributed to increased EC levels, especially at rain gauges located near industrial and agricultural areas (e.g., SJ, PU, and EP). The data revealed a moderately positive correlation between EC levels and proximity to the PG stacks, with more distant locations exhibiting lower EC values.

The chemical composition of rainwater was found to vary seasonally, with the highest concentrations of major ions occurring during the first rains of autumn. This pattern was attributed to the accumulation of pollutants in the atmosphere after a dry summer period. Major ions like NO_2^- and NO_3^- also peaked in the spring, possibly due to agricultural activities in surrounding areas (Al-Khashman, 2005; Al-Momani et al., 1995; André et al., 2007; Avila and Alarcón, 1999; Morales-Baqueroet al., 2013). This seasonal variation in ion concentrations was consistent with other studies in Mediterranean climates (Al-Khashman, 2005; Alcolea et al., 2015; Al-Momani et al., 1995; Avila and

Alarcón, 1999; Castillo et al., 2013a,b; Morales-Baqueroet al., 2013; Robles-Arenas et al., 2006).

The study identified significant changes in the concentrations of major ions like Ca^{2+}, F^{-}, PO_4^{3-}, and SO_4^{2-} in rainwater, with higher concentrations closer to the PG stacks. It is primarily composed of calcium sulphate ($CaSO4{\cdot}2H_2O$), is a by-product of phosphate fertiliser production (Contreras, 2017; Contreras-Llanes et al., 2015; Lieberman et al., 2020; Pérez-López et al., 2010; Rentería-Villalobos et al., 2010), and its deposition near these stacks contributed to elevated levels of like Ca^{2+}, F^{-}, PO_4^{3-}, and SO_4^{2-}. The study found that as the distance from the stacks increased, the concentrations of these ions declined, confirming that the PG stacks were a primary source of these pollutants (Contreras, 2017; Contreras-Llanes et al., 2015; Lieberman et al., 2020; Pérez-López et al., 2010; Rentería-Villalobos et al., 2010). Furthermore, fluoride concentrations, in particular, exceeded the WHO drinking water guideline of 1.5 mg L^{-1} in areas near the PG stacks, posing potential risks for dental and skeletal fluorosis (WHO, 2003).

The study also identified a positive correlation between ions such as Cl^{-}, K^{+}, Mg^{2+}, Na^{+}, NO_2^{-}, and NO_3^{-} with distance from the PG stacks, suggesting a strong marine influence in rainwater composition. These ions likely originate from sea-salt aerosols, which are common in coastal regions, in accordance with other studies (Alcolea et al., 2015; Al-Momani et al., 1995; Custodio and Llamas, 1996; Dikaiakos et al., 1990; Todd and Mays, 2005; Tuncer et al., 2001; Zeng et al., 2024). The rain gauge located in an unpolluted area (Matalascañas village), close to the Atlantic Ocean, exhibited high concentrations of sea-derived ions, further supporting the sea-salt influence on rainwater quality.

The concentration of trace elements in rainwater was significantly influenced by the proximity to PG stacks, with elements like As, Ni, Sr, and V showing elevated levels near the PG stacks. The study revealed that as the distance from the PG stacks increased, the concentrations of these toxic metals decreased. The concentration of trace elements in rainwater within the Huelva metropolitan area was significantly elevated compared to the Matalascañas village location, an unpolluted site, as well as in comparison to findings

from other studies carried out in rural regions (Al-Khashman, 2005; André et al., 2007; Avila and Alarcón, 1999; Pelicho et al., 2006; Seto and Hara, 2006). The spatial distribution of trace metals in rainwater exhibited weak statistical correlations, but the trend of higher concentrations closer to the stacks was consistent with previous studies linking PG emissions to contamination (Contreras, 2017; Contreras-Llanes et al., 2015; Lieberman et al., 2020; Pérez-López et al., 2010; Rentería-Villalobos et al., 2010).

Trace elements like Co, Cu, Pb, and Zn were also detected at elevated levels in areas near industrial complexes, such as the 'Polígono Tartessos' industrial area. These metals were found to have positive correlations with distance from the PG stacks, suggesting that local industrial activities (e.g., metal production) contributed to their presence in rainwater. The enrichment factors for Cu, Pb, and Zn point to notable human-induced contributions, primarily from industrial discharges, as highlighted by related studies in highly polluted regions of China (Xing et al., 2017) and Bangladesh (Adhikari et al., 2023). Comparable findings were also observed in earlier research in Huelva province, specifically in the Rio Tinto Mining District, which demonstrated elevated deposition rates in the soluble forms of these elements linked to mining and metallurgical processes (Castillo et al., 2013a,b). Furthermore, the spatial distribution of Cu, Pb, and Zn aligns with prior investigations that documented unique sediment pollution patterns in the Odiel-Tinto Estuary (Contreras-Llanes et al., 2024). These studies also uncovered a cumulative exposure to hazardous metal(loid)s in Huelva’s residents from various sources, with the most pronounced concentrations located near chemical industrial sites (Contreras-Llanes et al., 2025a). Elevated levels of Cu, Pb, and Zn near these industrial zones may pose health risks, including respiratory and neurological disorders, as well as potential damage to organs like the liver and kidneys due to long-term exposure (WHO, 2003).

Additionally, As, Ni, and Sr concentrations exceeded WHO guideline levels in some rainwater samples, raising concerns about the potential health risks associated with chronic exposure. Arsenic is a known carcinogen, and nickel exposure can lead to reproductive and developmental toxicity (WHO, 2003). Additionally, the presence of

trace elements in rainwater reflects the complex interplay between local industrial emissions, PG stack contamination, and natural sources like soil and vegetation.

The results suggest that residents living near the PG stacks may be exposed to higher concentrations of toxic metals, which could lead to serious health issues over time (Briffa et al., 2020; Lopez-Abente et al., 2001). In addition to the direct contribution of PG stacks to rainwater contamination, local industrial activities, such as metal production and power generation, also played a significant role in the observed pollution levels.

5.3. Paper #3: Internal cumulated dose of toxic metal(loid)s in a population residing near naturally occurring radioactive material waste stacks and an industrial heavily polluted area with high mortality rates in Spain

This study found significantly higher mean levels of As, Co, Cr, Ni, and Se in the toenails of Huelva residents compared to populations from unpolluted areas. These elements showed strong correlations and a spatial distribution pattern, with higher concentrations near PG stacks and industrial complexes, indicating exposure to environmental contamination. These results provide valuable insights into the effects of living near a heavily polluted estuary.

Compared to other studies in polluted areas, our results revealed that Zn had the highest mean concentrations in toenails, followed by Al, Fe, Cu, Ni, Cr, Mn, Se, Pb, As, V, Mo, Co, Cd, U, and Tl (Bechtold et al., 2021; Butler et al., 2019; Coelho et al., 2014; Nakaona et al., 2020; Przybylowicz et al., 2012; Rashed and Hossam, 2007; Slotnick et al., 2005; Sureda et al., 2017; Van Horne et al., 2021). Our findings align with other studies from polluted regions like Kima, Egypt, and the Zambian Copperbelt, which are also impacted by mining and industrial pollution (Nakaona et al., 2020; Rashed and Hossam, 2007). However, differences in results from other studies in polluted areas (Di Ciaula et al., 2020; Ojekunle et al., 2022) may stem from variations in environmental conditions, sanitation, and exposure levels. In contrast, studies from unpolluted areas with similar characteristics (e.g., culture, diet, and lifestyle), like Mallorca (Spain; Sureda et al., 2017) and Forlì (Italy; Di Ciaula et al., 2020), found much lower concentrations of

these elements, supporting the idea that Huelva residents accumulate higher levels due to environmental pollution.

Previous research also supports our findings. For example, studies on urinary levels of heavy metals in children from Huelva showed higher Cd concentrations compared to other European studies (Aguilera et al., 2010). Elevated Cd levels were also found in the hair and urine of children (Rodríguez-Barranco et al., 2014) and in industrial workers (Silva-Caicedo et al., 2024). Huelva is situated near Europe's largest NORM waste stacks and various industrial facilities, such as copper smelters, petroleum refineries, and fertiliser plants, which contribute to these elevated metal(loid) levels (Contreras, 2017; Contreras-Llanes et al., 2021; Rosado et al., 2016; Torre et al., 2019).

Spearman correlation analysis revealed that common exposure sources, such as environmental, occupational, and dietary factors, likely influence the concentrations of these metal(loid)s in toenails. PCA further helped identify correlations and sources of exposure. PC1 (Al, Co, Fe, Mn, U, and V) showed strong correlations ($r > 0.7$) at the 99% confidence level, indicating these elements may share common sources or behave similarly during bioaccumulation (Li et al., 2013). For example, Al, Mn, and Fe are linked to both natural and industrial sources, including emissions from the local industrial areas Alastuey et al., 2006; Chen at al., 2016; González-Castanedo et al., 2014; Querol et al., 2002; Sánchez de la Campa et al., 2007, 2015, 2018. The interpolation analysis highlights areas of high Al concentration, which might originate from industrial activity and crustal sources. Additionally, previous studies have linked Co and V emissions in Huelva City to the crude oil refinery in the 'Nuevo Puerto Palos de la Frontera' industrial complex (Alastuey et al., 2006; Chen at al., 2016; González-Castanedo et al., 2014; Querol et al., 2002; Sánchez de la Campa et al., 2007, 2015, 2018). Meanwhile, U pollution appears to stem mainly from PG stacks and phosphoric fertiliser production (Contreras, 2017; Contreras-Llanes et al., 2021; Lieberman et al., 2020; Pérez-López et al., 2010; Rentería-Villalobos et al., 2010).

The second principal component (PC2) indicated that Cr, Pb, and Zn likely originate from industrial waste, air emissions, and traffic-related sources. Pb and Zn emissions are

associated with the copper smelter and other industrial facilities in Huelva's 'Polo Químico de Promoción y Desarrollo' industrial complex, while Cr is mainly linked to traffic emissions (Alastuey et al., 2006; Chen at al., 2016; González-Castanedo et al., 2014; Querol et al., 2002; Sánchez de la Campa et al., 2007, 2015, 2018). The spatial distribution of these elements further supports the connection to industrial and traffic-related pollution sources.

Cd, As, and Cu, characterised by the third principal component (PC3), did not correlate strongly with each other or with other elements, suggesting they originate from different sources, particularly industrial emissions (Taiwo and Harrison, 2014). As and Cu are associated with the Cu smelter, fertiliser plants, and oil refinery, while Cd is primarily linked to petrochemical and TiO_2 pigment industries (Alastuey et al., 2006; Chen at al., 2016; González-Castanedo et al., 2014; Querol et al., 2002; Sánchez de la Campa et al., 2007, 2015, 2018). The spatial distribution of elements like As and Cu further supports the influence of industrial activities, with higher concentrations found downwind of the copper smelter and near fertiliser industries.

PC4 identified a strong association between Mo and Tl, both of which are likely sourced from PG stacks and fertiliser emissions (Contreras, 2017; Contreras-Llanes et al., 2021; Lieberman et al., 2020; Pérez-López et al., 2010; Rentería-Villalobos et al., 2010). The spatial distribution of Mo supports this finding, with higher concentrations near the PG stacks.

The fifth principal component (PC5) highlighted a negative association between Pb and Se, suggesting an antagonistic relationship. Se, which primarily comes from diet and drinking water, may protect against the bioaccumulation of metal(loid)s like Pb (Adigun, 2018; Egwunye et al., 2023). Its distribution near industrial areas and PG stacks suggests some influence from industrial emissions. The primary route of human exposure to selenium is through diet, food, and drinking water, although smoking is also an inadvertent inhalation exposure route (WHO, 1987).

Finally, the sixth principal component (PC6) was dominated by Ni, with a moderate positive correlation with Co, indicating a shared origin, likely from the petrochemical

industries in the 'Nuevo Puerto Palos de la Frontera' industrial complex (Alastuey et al., 2006; Chen at al., 2016; González-Castanedo et al., 2014; Querol et al., 2002; Sánchez de la Campa et al., 2007, 2015, 2018).

5.4. Study limitations

The interpretation of our findings must take into account several limitations.

First, consistency in temporal and spatial observations between sample collection for all samples (sediments, rainwater and toenails) is crucial for extracting valuable insights from any analysis. It is presumed that the exposure levels of pollutants, particularly metal(loid)s, have remained relatively stable in recent years in the study area. Nevertheless, an ideal approach would have involved first conducting a thorough characterisation of the local pollution sources of metal(loid)s, concurrently with the collection of nail samples.

Second, several factors play a crucial role in determining the quality of rainwater sampling from the rain gauges. These include insufficient maintenance and inconsistent cleaning of the equipment, particularly following extended dry periods; the challenging environmental conditions caused by heavy road traffic, ash, dust, and organic particles of both plant and animal origin—most notably bird droppings; the materials utilised in constructing the rain gauge; and the limited volume of rainwater collected during each precipitation event. A quality score ranging from 1 to 5 (1 = poor, 5 = excellent) was assigned to each sampling point taking into consideration these factors. This 5-point Likert scale reflects a range of average scores, demonstrating the challenge of obtaining meaningful data from rain gauges with the lowest scores (1) compared to those with the highest scores (5). A minimum acceptable score of 3 is required to achieve this consistency. The Likert scale reveals an average score of 3.5, which is higher than the minimum acceptable score of 3.

Third, despite being representative of the general population, the sample size of 55 participants from a total population of 150,000, constrains the statistical power of the analysis. However, the fact of using samples from individual subjects is needed for making conclusions under a public health perspective.

Fourth, participants might have experienced exposure to metal(loid)s through various confounding factors (sociodemographic characteristics, dietary intake cumulative retrospective environmental exposures, traffic emissions, and occupational backgrounds). Nevertheless, the inclusion of multiple metal(loid)s in the principal component analysis (PCA) ensures that the loadings of the primary elements from the principal sources remain unaffected.

Fifth, PCA and Spearman's correlation analyses are valuable tools for identifying likely sources; however, their interpretation relies heavily on the expertise and judgment of the analyst. Recognising distinct patterns demands meticulous analysis, incorporating knowledge of potential local contamination sources (both anthropogenic and natural), diverse exposure pathways, and specific regional characteristics. Consequently, we drew upon a range of prior studies to characterise air quality in Huelva City (e.g., Alastuey et al., 2006; Chen et al., 2016; González-Castanedo et al., 2014; Querol et al., 2002; Sánchez de la Campa et al., 2007, 2015, 2018), assess the industrial influence on the adjacent river, estuary, and marshlands (e.g., Rosado et al., 2016; Sainz et al., 2004), and evaluate Acid Mine Drainage (AMD) stemming from upstream mining activities (e.g., Nieto et al., 2020; Torre et al., 2019). Additionally, studies on metal(loid) source identification (e.g., Contreras-Llanes et al., 2015; Rosado et al., 2016; Torre et al., 2019) were consulted.

Sixth, increasing the sampling points of the sediments would had allowed to check the consistency of the measurements on the low-middle tidal salt marsh areas in the Odiel–Tinto Estuary, most importantly for the reference point with tidal salt marsh in the estuary of the Piedras River. However, the relatively high (10 samples) of sampling points per area collected on each site increased allowed evaluating the small study area samples measurements reproducibility and their validity.

Seventh, increasing the sampling points of the rainwater sample collection sites would had allowed checking the consistency of the measurements. An extra reference sampling area inland far from the sea and the polluting sources would have allowed extra comparisons.

Eighth, we didn´t evaluate the potential effect on climate stationary on the samples of sediments.

5.5. Study strengths

Despite the acknowledged limitations, our study possesses numerous strengths.

First, this work comprises two studies that spatially determine the exposure pathways, in addition to another study that measures the bioaccumulation of metals in the general population in relation to their proximity to the identified exposure sources.

Second, this is also the first study analysing the distribution of the chemical and metal(loid)s deposition from a PG stack.

Third, wide spatial distribution of metal(loid)s, both within the estuary, where they were accumulated in the sediments, and through the atmospheric dispersion of particulate matter by air, which were transported to their final deposition.

Fourth, this is the first epidemiological study to assess industrial and mining pollution levels with Huelva's residents bioaccumulation at the individual level using biological samples that capture mid-term exposure windows.

Fifth, rainwater was systematically collected on an event-specific basis (rainfall measuring at least 1mm following a dry period lasting a minimum 24 h) between January 2021 and December 2022. This collection period was deliberately selected to ensure that each rain gauge was monitored comprehensively across a minimum of two full hydrological years.

Sixth, the sampling network, comprising of 17 rain gauges, was strategically distributed at various distances from the sea and across different soil uses and human activities, including industrial, mining, urban and agricultural areas. These rain gauges were situated at public institutions, private companies, and residential addresses. Moreover, both the wind and population centres were also considered to ensure that highly populated areas influenced by all major wind directions were included. Furthermore, due to the considerable size of the city of Huelva and its proximity to the

phosphogypsum stacks, five rain gauges were installed to cover the entire city. Seventh, this study utilised ICP-MS analysis, characterised by its low limits of detection (LOD) for the majority of the examined elements, enabling the identification of trace concentrations of various metalloids. Consequently, data were obtained from a representative sample of the Huelva population, allowing for the potential detection of up to 16 elements. Previous investigations into toenail cumulated metalloid concentrations have typically focused on a limited number of potentially harmful elements (ranging from one to six) due to the reliance on analytical techniques with higher LOD (Zierold et al., 2021). In contrast, this research identified and analysed a total of 16 metal(loid)s. Similarly, in the analysis of marsh sediments and rainwater samples, up to 41 elements were successfully detected in both cases.

Eight, toenails were employed as a biomarker, representing a non-invasive and well-established method for assessing internal exposure. This approach provides valuable insights into long-term mineral metabolism patterns, encompassing a period of approximately 6 ± 18 months (Bencko, 1995; Gutiérrez-González et al., 2019; Salcedo-Bellido et al., 2021).

Ninth, demographic factors, including socioeconomic status, gender, and age, were incorporated as key variables influencing potential exposure and, consequently, the concentration of elements in toenails. These factors were systematically controlled for during the analysis to ensure robust and reliable results (Bencko, 1995; Gutiérrez-González et al., 2019; Salcedo-Bellido et al., 2021).

Tenth, due to the possibility of differential effects arising from varied durations of exposure to environmental agents (Sexton and Hattis, 2007); a key inclusion criterion for participants was a minimum residency of 6 months in Huelva City. This approach ensures the ability to estimate prolonged environmental exposure periods within the study population. Eleventh, PCA provides an objective method for evaluating the interrelationships among elements detected in marsh sediment and toenail samples, as demonstrated in previous studies (Demir et al., 2010; Gutiérrez-González et al., 2019; Salcedo-Bellido et al., 2021; Przybylowicz et al., 2012; Van Horne et al., 2021).

Eleventh, advanced spatial statistical methods, such as kriging, were employed to perform this study. Application of Kriging geostatistical methods significantly improved our comprehension of the relationship between proximity to contamination sources and the concentrations of elements in marsh sediments and the toenails of Huelva's residents (Michael et al., 2019; Shit et al., 2016; Zierold et al., 2021).

Twelfth, the concentration profiles of specific metal(loid)s in marsh sediments, wet particles, and toenails, as identified in this study, may serve as a valuable baseline for assessing the impact of future actions targeting current contamination sources in the Odiel–Tinto Estuary, such as the RESTORE 2030 plan.

6. Conclusions

6.1. Conclusions for specific objective a)

a) To assess the environmental exposure pathways, including sediments and rainwater, in the metropolitan area of Huelva, and the internal accumulated dose of toxic metal(loid)s among the inhabitants of Huelva City (Contreras-Llanes et al., 2024; 2025a,b).

1) Overall, the research offers a comprehensive assessment of the environmental impact of industrial activities in Huelva and the bioacccumulation of metal(loid)s on the local population.

2) A specific pollution signature has been identified for phosphogypsum (PG) stacks, which distinctly separates metal exposure from other pollution sources in the Odiel–Tinto Estuary. These include acid mine drainage (AMD) originating from mining waste deposits in the Odiel River, AMD contamination along the Tinto River, and areas affected by intensive agricultural practices.

3) A significant contribution to enriching data on the proportional influence of various pollution sources within the Oidel-Tinto Estuary. It also serves as a crucial foundation for comprehending the distribution patterns of toxic element concentrations in salt marsh sediments, rainwater, and toenails, quantifying the most impacted areas. Furthermore, it highlights pressing concerns about the environmental and health repercussions of PG stacks and chemical complexes in the study area.

6.2. Conclusions for specific objective b)

b) To identify specific pollution signatures in marsh sediments using geochemical tracers within the highly polluted Odiel–Tinto Estuary, aiming to determine the extent of environmental exposure to toxic metal(loid)s. (Contreras-Llanes et al., 2024).

4) The salt marsh sediment pollution signature in the area surrounding the PG stacks was thoroughly characterised by the presence of 20 elements, including As, Cy, Gd, Mg, P, U, and Zn among others. This detailed analysis highlights the diversity of pollutants originating from the PG stacks that contribute to environmental contamination in the area.

5) Salt marsh sediments sampled in close proximity to mining residues linked to an abandoned foundry situated near a residential neighbourhood in the Odiel River demonstrated significant accumulation of six distinct elements. These elements included Fe, Mn, and Pb, among others. The outcomes could contribute to assessing upcoming restoration initiatives for this site, which was classified as contaminated by the Andalusian Government in 2007.

6) The pollution fingerprint of the Tinto River sediment, heavily influenced by AMD, was defined by a pronounced enrichment of sulphur (SO_2), reflecting the significant impact of mining-related activities on the salt marsh sediment composition in this area.

7) As beryllium has been recognised as a highly reliable and effective marker for identifying the environmental impact of intensive agricultural practices, its detection in sediment samples provides a definitive indicator, facilitating researchers in evaluating and tracking the degree of agricultural influence on adjacent ecosystems.

6.3. Conclusions for specific objective c)

c) To investigate the distribution of the suspended pollutant particles originating from the PG stacks and other local pollution sources to identify the radius of influence on the rainwater chemical fallen in Huelva metropolitan area (Contreras-Llanes et al., 2025b).

8) A distinct spatial variability in the chemical composition of rainwater within the Huelva metropolitan area exists. Notably, a downward trend in the concentrations of the most harmful elements in wet depositions is observed

as the distance from the PG stacks increases. Elevated concentrations of potentially toxic elements, including As, Ca^{2+}, Cr, F^-, Ni, PO_4^{3-}, SO_4^{2-}, Sr, and V, have been observed in the wet soluble fraction of rainwater collected near the PG stacks. Specifically, in the cases of pH, F^-, and Ni, the levels exceeded the guideline values for drinking-water quality established by the WHO.

9) Significant sources of contamination influencing the rainwater chemistry in the study area have been identified. These include a regional source linked to the influence of sea-salt particles and aerosols (marine factors: Ca^{2+}, Cl^-, K^+, Mg^{2+}, and Na^+), attributed to the proximity of the Atlantic Ocean and the Odiel-Tinto Estuary. Moreover, PG stacks are predominantly situated along coastal areas around the world, rendering the marine influence a common factor among all such sites.

10) A local source has been identified, originating from industrial emissions associated with the two main chemical complexes, contributing elements such as Co, Cu, Pb, and Zn in the rainwater chemistry.

11) PG stacks represent an important source of harmful elements affecting the quality of rainwater in the Huelva metropolitan area, including As, Cr, F^-, Ni, PO_4^{3-}, and SO_4^{2-}. These elements have the potential to cause significant environmental harm to ecosystems and pose considerable health risks to populations located in proximity to these contamination sources and under the influence of prevailing wind patterns.

6.4. Conclusions for specific objective d)

d) To examine the internal accumulated dose of toxic metal(loid)s in the nails from general population of Huelva City (Contreras-Llanes et al., 2025a).

12) The spatial distribution of cumulated hazardous elements concentrations among Huelva residents appears to be largely governed by anthropogenic influences, with notably higher levels of As, Co, Cr, Fe, Ni, and Se detected in

their toenails compared to populations of similar profiles in non-polluted areas.

6.5. Conclusions for specific objective e)

e) To analyse the association between the spatial proximity patterns to the local industrial sources of pollutants with the levels of cumulated exposure of metal(loid)s in the toenails of the general population of Huelva (Contreras-Llanes et al., 2025a).

13) The cumulated levels of As, Cd, Mo, Pb, and Se were notably elevated among individuals residing in close proximity to the PG stacks. In contrast, higher levels of Al, Cu, and Zn were observed in residents living near the industrial complexes. These findings highlight distinct spatial variations in hazardous element exposure within the city and denotes the significant effect of industrial activities on the health of Huelva City's population, mainly among citizens living in closest proximity to the pollution sources—an aspect that had not been previously demonstrated.

14) The findings from the three papers, which form the core of this doctoral thesis, are consistent with one another. They demonstrate the influence of exposure sources on the salt marsh sediments of the estuary as well as on the rainfalls in the metropolitan area of Huelva. Additionally, contamination hotspots have been identified, with the highest accumulated levels observed among residents living near these areas.

6.6. Conclusions for specific objective f)

f) To establish a reference starting point of metal(loid)s levels in marsh sediments within the Odiel-Tinto Estuary, rainwater collected in the Huelva metropolitan area, and toenails from the population of Huelva City, in order to assess the impact of the RESTORE 2030 restoration plan for the Odiel-Tinto Estuary (Contreras-Llanes et al., 2024; 2025a,b).

15) Moreover, this research could provide a valuable baseline for evaluating the effectiveness of restoration plan such as RESTORE 2030 in addressing the challenges within the Odiel–Tinto Estuary. Furthermore, comparative analyses can uncover differences and patterns, as well as assess the effectiveness of interventions resulting from the restoration activities. This approach provides deeper insights into the environmental and health consequences within the study region.

16) Additionally, these specific pollution signatures both in sediments and in rainwater and finally its accumulation in toenails may also serve as valuable indicators for evaluating the effectiveness of future measures addressing comparable pollution sources in other estuaries and marshes.

6.7. Recommendations for Future Research

There remain significant gaps in our understanding, which complicate the establishment of a clear and robust link between the environmental pollution observed in the Odiel-Tinto Estuary and its potential impact on public health in Huelva. Addressing these gaps would require further in-depth research, including comprehensive and realistic evaluations to validate and expand upon the findings achieved thus far.

The potential influence of confounding variables (sociodemographic characteristics, dietary intake cumulative retrospective environmental exposures, traffic emissions, and occupational backgrounds), on the accumulated levels of metal(loid)s in toenails warrants comprehensive investigation in future studies.

The study highlights the need for more research to better understand the specific contributions of different pollution sources to the overall environmental load in the Huelva Estuary and its potential links to local morbidity and mortality.

Continuous monitoring and mitigation efforts to address the bioaccumulation of metal(loid)s and protect public health.

The study's findings underscore the need for continued research and intervention to mitigate the health risks associated with industrial pollution.

A holistic approach connecting sources of exposure, the exposure pathways, the human and natural bioaccumulation, and the consequences on the public health, and the environment is needed.

7. Conclusiones

7.1. Conclusiones para el objetivo específico a)

a) Evaluar las vías de exposición ambiental, incluidos los sedimentos y el agua de lluvia, en el área metropolitana de Huelva, así como la dosis acumulada interna de metal(loid)es tóxicos entre los habitantes de la ciudad de Huelva (Contreras-Llanes et al., 2024; 2025a,b).

1) En general, la investigación ofrece una evaluación exhaustiva del impacto ambiental de las actividades industriales en Huelva y los riesgos de la bioacumulación de metal(oid)es en población local.

2) Se ha identificado una huella de contaminación específica para las balsas de fosfoyeso (PG), que distingue claramente la exposición a estos metal(oid)es específicos de otras fuentes de contaminación en el estuario Odiel-Tinto. Estas incluyen el drenaje ácido de minas (AMD) originado en los depósitos de residuos mineros en el río Odiel, la contaminación por AMD a lo largo del río Tinto y áreas afectadas por prácticas agrícolas intensivas.

3) Este estudio contribuye significativamente a enriquecer los datos sobre la influencia de cada una de las diversas fuentes de contaminación dentro del estuario Odiel-Tinto. También sirve como una base crucial para comprender los patrones de distribución de las concentraciones de elementos tóxicos en los sedimentos de marismas, el agua de lluvia y las uñas de los pies de los habitantes de Huelva, cuantificando las áreas más afectadas. Además, destaca preocupaciones urgentes sobre las repercusiones ambientales y de salud de las balsas de PG y complejos químicos en el área de estudio.

7.2. Conclusiones para el objetivo específico b)

b) Identificar huellas de contaminación específicas en los sedimentos de marismas utilizando trazadores geoquímicos dentro del estuario Odiel-Tinto, con el objetivo de determinar la magnitud de la exposición ambiental a metal(oid)es (Contreras-Llanes et al., 2024).

4) La huella de contaminación en los sedimentos de marismas en el área circundante a las balsas de PG se caracterizó por la presencia principal de 20 elementos, incluidos As, Cy, Gd, Mg, P, U y Zn, entre otros. Este análisis detallado destaca la diversidad de contaminantes originados en las balsas de PG que contribuyen a la contaminación ambiental en el área.

5) Los sedimentos de marismas muestreados cerca de residuos mineros vinculados a una fundición abandonada situada cerca de un barrio residencial en el río Odiel, mostraron una acumulación significativa de seis elementos distintos incluyendo Fe, Mn y Pb, entre otros. Los resultados podrían contribuir a evaluar futuras iniciativas de restauración para este sitio, clasificado como suelo contaminado por el Gobierno Andaluz en 2007.

6) La huella de contaminación de los sedimentos del río Tinto, fuertemente influenciada por el AMD, se definió por un enriquecimiento pronunciado de azufre (SO_2), reflejando el impacto significativo de las actividades mineras en la composición de los sedimentos de marismas en esta área.

7) Dado que el berilio ha sido reconocido como un marcador altamente confiable y efectivo para identificar el impacto ambiental de las prácticas agrícolas intensivas, su detección en muestras de sedimentos proporciona un indicador definitivo, facilitando a los investigadores evaluar y rastrear el grado de influencia agrícola en los ecosistemas adyacentes.

7.3. Conclusiones para el objetivo específico c)

c) Investigar la distribución de las partículas contaminantes suspendidas en el aire originadas en las balsas de PG y otras fuentes de contaminación locales, para identificar el radio de influencia en la química del agua de lluvia que cae en el área metropolitana de Huelva (Contreras-Llanes et al., 2025b).

8) Existe una variabilidad espacial distinta en la composición química del agua de lluvia dentro del área metropolitana de Huelva. Notablemente, se observa una tendencia descendente en las concentraciones de los elementos más

perjudiciales en las deposiciones húmedas a medida que aumenta la distancia de las balsas de PG. Se han observado concentraciones elevadas de elementos potencialmente tóxicos, incluidos As, Ca^{2+}, Cr, F^-, Ni, PO_4^{3-}, SO_4^{2-}, Sr, and V, en la fracción soluble del agua de lluvia recolectada cerca de las balsas de PG. Específicamente, en los casos de pH, F^- y Ni, los niveles superaron los valores guía para la calidad del agua potable establecidos por la OMS.

9) Se han identificado fuentes adicionales significativas de contaminación que influyen en la química del agua de lluvia caída en el área de estudio. Estas incluyen una fuente regional relacionada con la influencia de partículas y aerosoles de sal marina (factores marinos: Ca^{2+}, Cl^-, K^+, Mg^{2+}, and Na^+), atribuida a la proximidad del Océano Atlántico y el estuario Odiel-Tinto. Además, hay que tener en cuenta que las balsas de PG están situados normalmente cerca de áreas costeras en todo el mundo, lo que convierte a la influencia marina en un factor común en todos estos sitios.

10) Se ha identificado una fuente local, originada por las emisiones industriales asociadas con los dos principales complejos químicos, que contribuye con elementos como Co, Cu, Pb y Zn en la química del agua de lluvia.

11) Las balsas de PG representan la principal fuente de contaminación de elementos perjudiciales que afectan la calidad del agua de lluvia en el área metropolitana de Huelva, incluidos As, Cr, F^-, Ni, PO_4^{3-}, and SO_4^{2-}. Estos elementos tienen el potencial de causar daños ambientales significativos a los ecosistemas y pueden representar riesgos considerables para la salud de las poblaciones ubicadas cerca de estas fuentes de contaminación y bajo la influencia de los patrones de viento predominantes.

7.4. Conclusiones para el objetivo específico d)

d) Examinar la dosis acumulada interna de metal(oid)es tóxicos en las uñas de la población general de la ciudad de Huelva (Contreras-Llanes et al., 2025a).

12) La distribución espacial de las concentraciones acumuladas en uñas de los piés de elementos peligrosos entre los residentes de Huelva ciudad parece estar ampliamente gobernada por influencias antropogénicas, mostrando niveles notablemente más altos de As, Co, Cr, Fe, Ni y Se detectados en sus uñas en comparación con poblaciones de perfiles similares en áreas no contaminadas.

7.5. Conclusiones para el objetivo específico e)

e) Analizar la asociación entre los patrones de proximidad espacial a las fuentes locales de contaminantes con los niveles de exposición acumulada de metal(oid)es en las uñas de los piés de la población general de Huelva (Contreras-Llanes et al., 2025a).

13) Los niveles acumulados de As, Cd, Mo, Pb y Se fueron notablemente elevados entre los individuos que residían cerca de las balsas de PG. En contraste, se observaron niveles más altos de Al, Cu y Zn en residentes que vivían cerca de los complejos industriales. Estos hallazgos destacan variaciones espaciales distintas en la exposición a elementos peligrosos dentro de la ciudad y denotan el efecto significativo de las actividades industriales en la salud de la población de la ciudad de Huelva, principalmente entre los ciudadanos que viven más cerca de las fuentes de contaminación, un aspecto que no se había demostrado previamente.

14) Los hallazgos de los tres artículos, que constituyen el núcleo de esta tesis doctoral, son consistentes entre sí. Demuestran la influencia de las fuentes de contaminación en los sedimentos de marismas del estuario, así como en las precipitaciones recogidas en el área metropolitana de Huelva. Además, se han identificado puntos críticos de contaminación, que coinciden con los niveles acumulados más altos observados entre los residentes que viven cerca de estas áreas.

7.6. Conclusiones para el objetivo específico f)

f) Establecer un punto de referencia inicial de los niveles de metal(oid)es en los sedimentos de marismas dentro del estuario Odiel-Tinto, el agua de lluvia

recogida en el área metropolitana de Huelva y las uñas de los pies de la población general de la ciudad de Huelva, con el fin de evaluar el impacto del plan de restauración RESTORE 2030 para el estuario Odiel-Tinto (Contreras-Llanes et al., 2024; 2025a,b).

15) Esta investigación podría proporcionar una base valiosa para evaluar la efectividad de planes de restauración como RESTORE 2030. Además, los análisis comparativos pueden revelar diferencias y patrones significativos, así como evaluar la efectividad de las intervenciones resultantes de las actividades de restauración. Este enfoque proporciona una comprensión más profunda de las consecuencias ambientales y de salud dentro del área de estudio.

16) Además, estas huellas de contaminación específicas tanto en los sedimentos como en el agua de lluvia y, finalmente, tras su acumulación en las uñas, también pueden servir como indicadores valiosos para evaluar la efectividad de futuras medidas que aborden fuentes de contaminación comparables en otros estuarios y marismas.

7.7. Recomendaciones para futuras investigaciones

Quedan lagunas significativas en nuestra comprensión que complican el establecimiento de un vínculo claro y robusto entre la contaminación ambiental observada en el estuario Odiel-Tinto y su posible impacto en la salud pública en Huelva. Abordar estas lagunas requeriría una investigación más profunda, incluyendo evaluaciones comprensivas y realistas para validar y ampliar los hallazgos logrados hasta ahora.

La posible influencia de variables confusas (características sociodemográficas, ingesta diaria, exposiciones ambientales retrospectivas acumulativas, emisiones debido al tráfico y antecedentes ocupacionales) en los niveles acumulados de metal(oid)es en las uñas de los pies merece una investigación exhaustiva en estudios futuros.

El estudio destaca la necesidad de más investigación para comprender mejor las contribuciones específicas de diferentes fuentes de contaminación a la carga ambiental total en el estuario de Huelva y sus posibles vínculos con la morbilidad y mortalidad locales.

Monitoreo continuo y esfuerzos de mitigación para abordar la bioacumulación de metales y metaloides y proteger la salud pública.

Los hallazgos del estudio destacan la necesidad de investigaciones e intervenciones continuas para mitigar los riesgos para la salud asociados con la contaminación industrial.

Es necesario un enfoque holístico que conecte las fuentes de exposición, las vías de exposición, la bioacumulación en humanos y en el medio ambiente, y las consecuencias para la salud pública y el ecosistema.

8. References

Achterberg, E.P., Herzl, V.M.C., Braungardt, C.B., Millward, G.E., 2003. Metal behaviour in an estuary polluted by acid mine drainage: the role of particulate matter. Environ. Pollut. 121, 283–292. https://doi.org/10.1016/S0269–7491(02)00216–6

Adhikari, S., Zeng, C., Zhang, F., Adhikari, N.P., Gao, J., Ahmed, N., Bhuiyan, A.Q., Ahsan, A., Khan, H.R., 2023. Atmospheric wet deposition of trace elements in Bangladesh: A new insight into spatiotemporal variability and source apportionment. Environ. Res. 217, 114729, https://doi.org/10.1016/j.envres.2022.114729

Adigun, C.G. Nail Reactions to Poisons and Intoxicants. In: Rubin, A.I., Jellinek, N.J., Daniel, C.R., Scher, R.K. (eds) Scher and Daniel's Nails. Springer, Cham, Berlín, Germany, 2018. https://doi.org/10.1007/978–3–319–65649–6_29

Agency for Toxic. Substances and Disease Registry (ATSDR) and the Environmental Protection Agency (EPA). Toxicological Profile for Beryllium. U.S. Department of Health and Human Services, Washington D.C., USA, 2022. https://www.atsdr.cdc.gov/toxprofiles/tp4.pdf

Aguilera, I., Daponte, A., Gil, F., Hernández, A.F., Godoy, P., Pla, A., Ramos, J.L., DASAHU group., 2008. Biomonitoring of urinary metals in a population living in the vicinity of industrial sources: a comparison with the general population of Andalusia, Spain. Sci. Total Environ. 407(1), 669–678. https://doi.org/10.1016/j.scitotenv.2008.08.041

Aguilera, I., Daponte, A., Gil, F., Hernández, A.F., Godoy, P., Pla, A., Ramos, J.L., 2010. Urinary levels of arsenic and heavy metals in children and adolescents living in the industrialised area of Ria of Huelva (SW Spain). Environ. Int. 36, 563–569. https://doi.org/10.1016/j.envint.2010.04.012

Alastuey, A., Querol, X., Plana, F., Viana, M., Ruiz, C.R., Sanchez de la Campa, A., de la Rosa, J., Mantilla, E., García dos Santos, S., 2006. Identification and chemical

characterization of industrial particulate matter sources in southwest Spain. J. Air Waste Manag. Assoc. 56(7), 993–1006. https://doi.org/10.1080/10473289.2006.10464502

Alcolea, A., Fernández–López, C., Vázquez, M., Caparrós, A., Ibarra, I., García, C., Zarroca, M., Rodríguez, R., 2015. An assessment of the influence of sulfidic mine wastes on rainwater quality in a semiarid climate (SE Spain). Atmos. Environ. 107, 85–94. https://doi.org/10.1016/j.atmosenv.2015.02.028

Alguacil, J., Ballester, F., Donado–Campos, J., Pollán, M., Rodríguez–Artalejo, F. Dictamen realizado por encargo del Defensor del Pueblo Andaluz sobre El exceso de mortalidad y morbilidad detectado en varias investigaciones en La Ría de Huelva. Grupo de Trabajo de la Sociedad Española de Epidemiología. Seville, Spain, 2014. https://www.defensordelpuebloandaluz.es/informe–epidemiologico–ria–de–huelva

Al–Khashman, O.A., 2005. Study of chemical composition in wet atmospheric precipitation in Eshidiya area, Jordan. Atmos. Environ. 39(33), 6175–6183. https://doi.org/10.1016/j.atmosenv.2005.06.056

Al–Momani, I.F., Tuncel, S., Eler, Ü., Örtel, E., Sirin, G., Tuncel, G., 1995. Major ion composition of wet and dry deposition in the eastern Mediterranean basin. Sci. Total. Environ. 164(1), 75–85. https://doi.org/10.1016/0048–9697(95)04468–G

Anderson, H. R., Spix, C., Medina, S., Schouten, J. P., Castellsague, J., Rossi, G., Zmirou, D., Touloumi, G., Wojtyniak, B., Ponka, A., Bacharova, L., Schwartz, J., Katsouyanni, K., 1997. Air pollution and daily admissions for chronic obstructive pulmonary disease in 6 European cities: results from the APHEA project. Eur. Respir. J. 10(5), 1064–1071. https://doi.org/10.1183/09031936.97.10051064

André, F., Jonard, M., Ponette, Q., 2007. Influence of meteorological factors and polluting environment on rain chemistry and wet deposition in a rural area near Chimay, Belgium. Atmos. Environ. 41(7), 1426–143. https://doi.org/10.1016/j.atmosenv.2006.10.013

Avila, A., Alarcón, M., 1999. Relationship between precipitation chemistry and meteorological situations at a rural site in NE Spain. Atmos. Environ. 33(11), 1663–1677. https://doi.org/10.1016/S1352–2310(98)00341–0

Barba–Brioso, C., Fernández–Caliani, J.C., Miras, A., Cornejo, J., Galán, E., 2010. Multi–source water pollution in a highly anthropized wetland system associated with the estuary of Huelva (SW Spain). Mar. Pollut. Bull. 60, 1259–1269. https://doi.org/10.1016/j.marpolbul.2010.03.018

Bechtold, P., Gatti, M.G., Quattrini, G., Ferrari, A., Barbieri, G., Iacuzio, L., Carrozzi, G., Righi, E., 2021. Trace elements in toenails in a population living near a modern municipal solid waste incinerator in Modena (Italy). Chemosphere 263, 128292. https://doi.org/10.1016/j.chemosphere.2020.128292

Beltrán, R., de la Rosa, J.D., Santos, J.C., Beltrán, M., Gómez–Ariza, J.L., 2010. Heavy metal mobility assessment in sediments from the Odiel River (Iberian Pyritic Belt) using sequential extraction. Environ. Earth Sci. 61, 1493–1503. https://doi.org/10.1007/s12665–010–0465–y

Benach, J., Yasui, Y., Borrell, C., Rosa, E., Pasarín, M.I., Benach, N., Español, E., Martínez, J.M., Daponte, A., 2003. Examining geographic patterns of mortality: the atlas of mortality in small areas in Spain (1987–1995). Eur. J. Public Health 13, 115–123. https://doi.org/10.1093/eurpub/13.2.115

Bencko V., 1995. Use of human hair as a biomarker in the assessment of exposure to pollutants in occupational and environmental settings. Toxicology 101(1–2), 29–39. https://doi.org/10.1016/0300–483x(95)03018–b

Berke, O., 2004. Exploratory disease mapping: kriging the spatial risk function from regional count data. Int. J. Health Geogr. 3, 18. https://doi.org/10.1186/1476–072X–3–18

Blasco, J., Sáenz, V., Gómez–Parra, A., 2000. Heavy metal fluxes at the sediment–water interface of three coastal ecosystems from south–west of the Iberian Peninsula. Sci. Total Environ. 247, 189–199. https://doi.org/10.1016/S0048–9697(99)00490–8

Borrego, J., Morales, J., de la Torre, M., Grande, J., 2022. Geochemical characteristics of heavy metal pollution in surface sediments of the Tinto and Odiel river estuary (southwestern Spain). Environ. Geol. 41, 785–796. https://doi.org/10.1007/s00254–001–0445–3

Bouyoucos, G.J., 1936. Directions for Making Mechanical Analysis of Soils by the Hydrometer Method. Soil Science. 4, 225–228. https://doi.org/10.1097/00010694–193609000–00007

Briffa, J., Sinagra, E., Blundell, R., 2020. Heavy metal pollution in the environment and their toxicological effects on humans. Heliyon 6(9), e04691. https://doi.org/10.1016/j.heliyon.2020.e04691

Butler, L., Gennings, C., Peli, M., Borgese, L., Placidi, D., Zimmerman, N., Hsu, H.L., Coull, B.A., Wright, R.O., Smith, D.R., Lucchini, R.G., Claus Henn, B., 2019. Assessing the contributions of metals in environmental media to exposure biomarkers in a region of ferroalloy industry. J. Expo. Sci. Environ. Epidemiol. 29(5), 674–687. https://doi.org/10.1038/s41370–018–0081–6

Capelo, R., Rohlman, D.S., Jara, R., García, T., Viñas J., Lorca, J.A., Contreras–Llanes, M., Alguacil, J., 2022. Residence in an Area with Environmental Exposure to Heavy Metals and Neurobehavioral Performance in Children 9–11 Years Old: An Explorative Study. Int. J. Environ. Res. Public Health 19(8), 4732. https://doi.org/10.3390/ijerph19084732

Castaño–Vinyals, G., Aragonés, N., Pérez–Gómez, B., Martín, V., Llorca, J., Moreno, V., Altzibar, J.M., Ardanaz, E., de Sanjosé, S., Jiménez–Moleón, J.J., Tardón, A., Alguacil, J., Peiró, R., Marcos–Gragera, R., Navarro, C., Pollán, M., Kogevinas, M., MCC–Spain Study Group., 2015. Population–based multicase–control study in common tumors in Spain (MCC–Spain): Rationale and study design. Gac. Sanit. 29, 308–315. https://doi.org/10.1016/j.gaceta.2014.12.003

Castillo, S., de la Rosa, J.D., Sánchez de la Campa, A.M., González–Castanedo, Y., Fernández–Caliani, J.C., Gonzalez, I. Romero, A., 2013a. Contribution of mine wastes to atmospheric metal deposition in the surrounding area of an abandoned heavily polluted mining district (Rio Tinto mines, Spain). Sci. Total Environ. 449, 363–372. https://doi.org/10.1016/j.scitotenv.2013.01.076

Castillo, S., de la Rosa, J.D., Sánchez de la Campa, A.M., González–Castanedo, Y., Fernández–Camacho, R., 2013b. Heavy metal deposition fluxes affecting an Atlantic coastal area in the southwest of Spain. Atmos. Environ. 2013b, 77, 509–517. https://doi.org/10.1016/j.atmosenv.2013.05.046

Charlson, R.J., Rodhe, H., 1982. Factors controlling the acidity of natural rainwater. Nature 295, 683–685. https://doi.org/10.1038/295683a0

Chen, B., Stein, A.F., Castell, N., González–Castanedo, Y., Sánchez de la Campa, A.M., de la Rosa, J.D., 2016. Modeling and evaluation of urban pollution events of atmospheric heavy metals from a large Cu–smelter. Sci. Total Environ. 539, 17–25. https://doi.org/10.1016/j.scitotenv.2015.08.117

Chica–Olmo, M., Rodriguez, F., Abarca, F., Rigol–Sanchez, J.P., deMiguel, E., Gomez, J.A., Fernandez–Palacios, A., 2004. Integrated remote sensing and GIS techniques for biogeochemical characterization of the Tinto–Odiel estuary system, SW Spain. Environ. Geo. 45, 834–842. https://doi.org/10.1007/s00254–003–0943–6

Coelho, P., Costa, S., Costa, C., Silva, S., Walter, A., Ranville, J., Pastorinho, M.R., Harrington, C., Taylor, A., Dall'Armi, V., Zoffoli, R., Candeias, C., da Silva, E.F., Bonassi, S., Laffon, B., Teixeira, J.P., 2014. Biomonitoring of several toxic metal(loid)s in different biological matrices from environmentally and occupationally exposed populations from Panasqueira mine area, Portugal. Environ. Geochem. Health 36(2), 255–269. https://doi.org/10.1007/s10653–013–9562–7

Conesa, H.M., María–Cervantes, A., Álvarez–Rogel, J., González–Alcaraz, M.N., 2011. Influence of soil properties on trace element availability and plant accumulation in a Mediterranean salt marsh polluted by mining wastes: Implications for

phytomanagement, Sci. Total Environ. 409, 4470–4479, https://doi.org/10.1016/j.scitotenv.2011.07.049

Contreras, M. Valorisation of inorganic waste for obtaining construction materials. Doctoral thesis. “Cum Laude”, “Doctor Internacional”, University of Huelva, Huelva, Spain. 19/07/2017. http://hdl.handle.net/10272/16090

Contreras–Llanes, M., Alguacil, J., Capelo, R., Gómez–Ariza, J.L., García–Pérez, J., Pérez–Gómez, B., Martin–Olmedo, P., Santos–Sánchez, V., 2025a. Internal cumulated dose of toxic metal(loid)s in a population residing near a Naturally Occurring Radioactive Material waste stacks and an industrial heavily polluted area with high mortality rates in Spain. J. Xenobiot. 15, 29. https://doi.org/10.3390/jox15010029.

Contreras–Llanes, M., Pérez–López, R., Gázquez, M.J., Morales, V., Santos, A., Esquivias, L.M., Bolívar, J.P., 2015. Fractionation and fluxes of metals and radionuclides during the recycling process of phosphogypsum wastes applied to mineral CO_2 sequestration. Waste Manage. 45, 412–419. https://doi.org/10.1016/j.wasman.2015.06.046

Contreras–Llanes, M., Santos–Sánchez, V., Alguacil, J. and Rodríguez, R., 2025b. Influence of phosphogypsum waste on rainwater chemistry in a highly polluted area with high mortality rates in Huelva metropolitan area. Sustainability, 17, 3102. https://doi.org/10.3390/su17073102

Contreras–Llanes, M., Santos–Sánchez, V., Alguacil, J., Castillo, J.M., 2024. Delineating distinct sediment pollution signatures from diverse sources in a heavily contaminated estuary near an area of high cancer and cardiovascular mortality. Sci. Total Environ. 957, 177715. https://doi.org/10.1016/j.scitotenv.2024.177715

Cui, Z., Qiao, S., Bao, Z., Wu, N., 2011. Contamination and distribution of heavy metals in urban and suburban soils in Zhangzhou City, Fujian, China. Environ. Earth Sci. 64(6), 1607–1615. https://doi.org/10.1007/s12665–011–1179–5

Curado, G., Rubio–Casal, A.E., Figueroa, E., Castillo, J.M., 2010. Germination and establishment of the invasive cordgrass Spartina densiflora in acidic and metal polluted

sediments of the Tinto River. Mar. Pollut. Bull. 60, 1842–1848. https://doi.org/10.1016/j.marpolbul.2010.05.022

Curado, G., Rubio–Casal, A.E., Figueroa, E., Castillo, J.M., 2014. Plant Zonation in Restored, Nonrestored, and Preserved Spartina maritima Salt Marshes. J. Coastal Res. 30, 629–634. https://doi.org/10.2112/JCOASTRES–D–12–00089.1

Custodio, E., Llamas, M.R. In: Hidrología subterranea. Vol. I and II. Omega, Barcelona. 1996.

da Silva, E.F.D., Fonseca, E., Matos, J., Patinha, C., Reis, P., Santos Oliveira, J.M., 2005. The effect of unconfined mine tailings on the geochemistry of soils, sediments and surface waters of the lousal area (Iberian Pyrite Belt, Southern Portugal). Land Degrad. Develop. 16, 213–228. https://doi.org/10.1002/ldr.659

Davila, J.M., Sarmiento, A.M., Santisteban, M., Luís, A.T., Fortes, J.C., Diaz–Curiel, J., Valbuena, C., Grande, J.A., 2019. The UNESCO national biosphere reserve (Marismas del Odiel, SW Spain): an area of 18,875 ha affected by mining waste. Environ. Sci. Pollut. Res. 26, 33594–33606. https://doi.org/10.1007/s11356–019–06438–7

DeLaune, R.D., Reddy, K.R. REDOX POTENTIAL, Editor(s): Daniel Hillel, Encyclopedia of Soils in the Environment, Elsevier, Pages 366–371, ISBN 9780123485304, Amsterdam, Netherlands, 2005. https://doi.org/10.1016/B0–12–348530–4/00212–5

Demir, S., Saral, A., Ertürk, F., Kuzu, L., 2010. Combined Use of Principal Component Analysis (PCA) and Chemical Mass Balance (CMB) for Source Identification and Source Apportionment in Air Pollution Modeling Studies. Water Air Soil Pollut. 212, 429–439. https://doi.org/10.1007/s11270–010–0358–4

Di Ciaula, A., Gentilini, P., Diella, G., Lopuzzo, M., Ridolfi, R., 2020. Biomonitoring of Metals in Children Living in an Urban Area and Close to Waste Incinerators. Int. J. Environ. Res. Public Health 17(6), 1919. https://doi.org/10.3390/ijerph17061919

Dikaiakos J.G., Tsitouris C.G., Siskos P.A., Melissos D.A., Nastos P., 1990. Rainwater composition in Athens, Greece. Atmos. Environ. 241(1), 171–176. https://doi.org/10.1016/0957–1272(90)90022–M

Dockery, D.W., Pope, C.A., 1994. Acute respiratory effects of particulate air pollution. Annu. Rev. Public Health 15, 107–132. https://doi.org/10.1146/annurev.pu.15.050194.000543

Dong, Y., Lu, H., Lin, H., 2024. Comprehensive study on the spatial distribution of heavy metals and their environmental risks in high–sulfur coal gangue dumps in China. J. Environ. Scienc. 136, 486–497. https://doi.org/10.1016/j.jes.2022.12.023

Douvris, C., Vaughan, T., Bussan, D., Bartzas, G., Thomas, R., 2023. How ICP-OES changed the face of trace element analysis: Review of the global application landscape. Sci. Total Environ. 905, 167242. https://doi.org/10.1016/j.scitotenv.2023.167242

Dunea, D., Iordache, V., Frasin, L.N., Neagoe, A., Predescu, L., Iordache, S., 2021. Monitoring Rainwater Properties and Outdoor Particulate Matter in a Former Steel Manufacturing City in Romania. Atmosphere 12, 1594. https://doi.org/10.3390/atmos12121594

Egwunye, J., Cardoso, B.R., Braat, S., Ha, T., Hanieh, S., Hare, D., Duan, A.X., Doronila, A., Tran, T., Tuan, T., Fisher, J., Biggs, B.A., 2023. The role of fingernail selenium in the association between arsenic, lead and mercury and child development in rural Vi–etnam: a cross–sectional analysis. Br. J. Nutr. 129(9), 1589–1597. https://doi.org/10.1017/S0007114522001374

Elbaz–Poulichet, F., Morley, N., Cruzado, A., Velásquez, Z., Achterberg, E., Braungardt, C., 1999. Trace metal and nutrient distribution in an extremely low pH (2.5) river–estuarine system, the Ria of Huelva (South–West Spain). Sci. Total Environ. 227, 73 – 83. https://doi.org/10.1016/S0048–9697(99)00006–6

Environmental restoration project of the Huelva phosphogypsum stacks (RESTORE2030). https://restore2030.com/, 2024 (accessed 23 October 2024).

Evans, J.S., Tosteson, T., Kinney, P.L., 1984. Cross–sectional mortality studies and air pollution risk assessment. Environ. Int. 10, 1, 55–83. https://doi.org/10.1016/0160–4120(84)90233–2

Fernández–Landero, S., Fernández–Caliani, J.C., Giráldez, M.I., Morales, E., Barba–Brioso, C., González, I., 2023. Soil Contaminated with Hazardous Waste Materials at Rio Tinto Mine (Spain) Is a Persistent Secondary Source of Acid and Heavy Metals to the Environment. Minerals. 13, 456. https://doi.org/10.3390/min13040456

Figueroa, M.E., Castillo, J.M., Redondo–Gómez, S., Luque, T., Castellanos, E.M., Nieva, F.J., Luque, C., Rubio–Casal, A.E., Davy, A.J., 2003. Facilitated invasion by hybridization of Sarcocornia species in a salt-marsh succession. J. Ecol. 91, 616–626. https://doi.org/10.1046/j.1365–2745.2003.00794.x

Fuller, R., Landrigan, P. J., Balakrishnan, K., Bathan, G., Bose–O'Reilly, S., Brauer, M., Caravanos, J., Chiles, T., Cohen, A., Corra, L., Cropper, M., Ferraro, G., Hanna, J., Hanrahan, D., Hu, H., Hunter, D., Janata, G., Kupka, R., Lanphear, B., Lichtveld, M., Yan, C., 2022. Pollution and health: a progress update. Lancet Planet. Health 6(6), e535–e547. https://doi.org/10.1016/S2542–5196(22)00090–0

Gil F, Pla A., 2001. Biomarkers as biological indicators of xenobiotic exposure. J. Appl. Toxicol. 21(4), 245–255. https://doi.org/10.1002/jat.769

González–Castanedo, Y., Moreno, T., Fernández–Camacho, R., Sánchez de la Campa, A.M., Alastuey, A., Querol, X., de la Rosa, J., 2014. Size distribution and chemical composition of particulate matter stack emissions in and around a copper smelter. Atmos. Environ. 98, 271–282. https://doi.org/10.1016/j.atmosenv.2014.08.057

Guerrero, J.L., Gutiérrez–Álvarez, I., Mosqueda, F., Olías, M., García–Tenorio, R., Bolívar, J.P., 2019. Pollution evaluation on the salt–marshes under the phosphogypsum stacks of Huelva due to deep leachates. Chemosphere. 230, 219–229. https://doi.org/10.1016/j.chemosphere.2019.04.212

Guerrero, J.L., Pérez–Moreno, S.M., Gutiérrez–Álvarez, I., Gázquez, M.J., Bolívar, J.P., 2020. Behaviour of heavy metals and natural radionuclides in the mixing of phosphogypsum leachates with seawater. Environ. Pollut. 268, 115843. https://doi.org/10.1016/j.envpol.2020.115843

Guo, Z., Li, P., Yang, X., Wang, Z., Lu, B., Chen, W., Wu, Y., Li, G., Zhao, Z., Liu, G., Ritsema, C., Geissen, V., Xue, S., 2022. Soil texture is an important factor determining how microplastics affect soil hydraulic characteristics. Environ. Int. 165, 107293. https://doi.org/10.1016/j.envint.2022.107293

Gutiérrez–González, E., Fernández–Navarro, P., Pastor–Barriuso, R., García–Pérez, J., Castaño–Vinyals, G., Martín–Sánchez, V., Amiano, P., Gómez–Acebo, I., Guevara, M., Fernández–Tardón, G., Salcedo-Bellido, I., Moreno, V., Pinto-Carbó, M., Alguacil, Marcos-Gragera, R., Gómez-Gómez, J.H., Gómez-Ariza, J.L., García-Barrera, T., Varea-Jiménez, E., Núñez, O., Pérez-Gómez, B., 2022. Toenail zinc as a biomarker: Relationship with sources of environmental exposure and with genetic variability in MCC–Spain study. Environ. Int. 169, 107525. https://doi.org/10.1016/j.envint.2022.107525

Gutiérrez–González, E., Garcia–Esquinas, E., Fernadez de Larrea–Baz, N., Salcedo–Bellido, I., Navas–Acien, A., Lope, V., Gomez–Ariza, J.L., Pastor, R., Pollan, M., Perez–Gomez, B., 2019. Toenails as a biomarker to essential trace metals: A review. Environ. Res. 179, 108787. https://doi.org/10.1016/j.envres.2019.108787

Han, Y., Zhang, S., Kang, D., Hao, N., Peng, J., Zhou, Y., Liu, K., Chen, Y., 2025. A Decade Review of Human Health Risks from Heavy Metal Contamination in Industrial Sites. Water Air Soil Pollut. 236, 144. https://doi.org/10.1007/s11270-025-07759-9

Hierro, A., Olías, M., Ketterer, M.E., Vaca, F., Borrego, J., Cánovas, C.R., Bolívar, J.P., 2014. Geochemical behavior of metals and metalloids in an estuary affected by acid mine drainage (AMD). Environ. Sci. Pollut. Res. Int. 21, 2611–2627. https://doi.org/10.1007/s11356–013–2189–5

Hwang, H.M., Green, P.G., Young, T.M., 2008. Tidal salt marsh sediment in California, USA: Part 3. Current and historic toxicity potential of contaminants and their

bioaccumulation. Chemosphere 71, 2139–2149. https://doi.org/10.1016/j.chemosphere.2008.01.005

International Atomic Energy Agency (IAEA). Safety standards series. Application of the Concepts of Exclusion Exemption and Clearance, Safety Guide No. RS–G 17, STI/PUB/1202., Vienna, Austria, 2004. https://www.iaea.org/publications/7118/application-of-the-concepts-of-exclusion-exemption-and-clearance

Jenner, G.A., Longerich, H.P., Jackson, S.E., Fryer, B.J., 1990. ICP–MS — A powerful tool for high–precision trace–element analysis in Earth sciences: Evidence from analysis of se–lected U.S.G.S. reference samples. Chem. Geol. 83(1–2), 133–148, https://doi.org/10.1016/0009–2541(90)90145–W

Kerl, C.F., Basallote, M.D., Käberich, M., Oldani, E., Cerón Espejo, N.P., Colina Blanco, A.E., Ruiz Cánovas, C., Nieto, J.M., Planer–Friedrich, B., 2023. Consequences of sea level rise for high metal(loid) loads in the Ría of Huelva estuary sediments. Sci. Total Environ. 873, 162354. https://doi.org/10.1016/j.scitotenv.2023.162354

Lario, J., Alonso–Azcárate, J., Spencer, C., Zazo, C., Goy, J.L., Cabero, A., Dabrio, C.J., Borja, F., Borja, C., Civis, J., García–Ródriguez, M., 2016. Evolution of the pollution in the Piedras River Natural Site (Gulf of Cadiz, southern Spain) during the Holocene. Environ. Earth Sci. 75, 481. https://doi.org/10.1007/s12665–016–5344–8

Leistel, J.M., Marcoux, E., Thieblemont, D., Quesada, C., Sanchez, A., Almodovar, G.R., Pascual E., Saez, R., 1998. The volcanic–hosted massive sulphide deposits of the Iberian Pyrite Belt. Miner. Deposita. 33, 2–30. https://doi.org/10.1007/s001260050130

Li, F., Huang, J., Zeng, G., Yuan, X., Li, X., Liang, J., Wang, X., Tang, X., Bai, B., 2013. Spatial risk assessment and sources identification of heavy metals in surface sediments from the Dongting Lake, Middle China. J. Geochem. Explor. 132, 75–83. https://doi.org/10.1016/j.gexplo.2013.05.007

Lieberman, R.N., Izquierdo, M., Córdoba, P., Moreno Palmerola, N., Querol, X., Sánchez de la Campa, A.M., Font, O., Cohen, H., Knop, Y., Torres–Sánchez, R., Sánchez–Rodas, D., Muñoz–Quiros, C., de la Rosa, J.D., 2020. The evolution of brines from phosphogypsum deposits in Huelva (SW Spain) and its environmental implications. Sci. Total Environ. 700, 134444. https://doi.org/10.1016/j.scitotenv.2019.134444

Liu, H., Zeng, W., He, M., 2024. Distribution, sources, contamination, and risks of toxic metals in Zijiang River, a typical tributary of the midstream of the Yangtze River in China. J. Environ. Sci. 153, 30-43. https://doi.org/10.1016/j.jes.2023.12.030

López–Abente, G., Aragones, N., Ramis, R., Hernandez–Barrera, V., Perez–Gomez, B., Escolar– Pujolar, A., Pollan, M., 2006. Municipal distribution of bladder cancer mortality in Spain: possible role of mining and industry. BMC Public Health 6(17). https://doi.org/10.1186/1471–2458–6–17

López–Coto, I., Mas, J.L., Vargas, A., Bolívar, J.P., 2014. Studying radon exhalation rates variability from phosphogypsum piles in the SW of Spain. J. Hazard. Mater. 280, 464–471. https://doi.org/10.1016/j.jhazmat.2014.07.025

Lu, G.Y., Wong, D.W., 2008. An adaptive inverse–distance weighting spatial interpolation technique. Comput. Geosci. 34, 1044–1055. https://doi.org/10.1016/j.cageo.2007.07.010

Martínez–Beneito, M.A., Botella–Rocamora, P., Corpas–Burgos, F., Vergara– Hernández, C., Pérez–Panadés, J., Perpiñán–Fabuel, H. Atlas Nacional de Mortalidad en España (ANDEES). Fundación FISABIO y Dirección General de Salud Pública de la Generalitat Valenciana. Valencia, Spain, 2024. http://andees.fisabio.san.gva.es/

Mehdi, Y., Hornick, J.L., Istasse, L., Dufrasne, I., 2013. Selenium in the Environment, Metabolism and Involvement in Body Functions. Molecules. 18, 3292–3311. https://doi.org/10.3390/molecules18033292

Michael, R., O'Lenick, C.R., Monaghan, A., Wilhelmi, O., Wiedinmyer, C., Hayden, M., Estes, M., 2019. Application of geostatistical approaches to predict the spatio–temporal

distribution of summer ozone in Houston, Texas. J. Expo. Sci. Environ. Epidemiol. 29(6), 806–820. https://doi.org/10.1038/s41370–018–0091–4

Millan–Becerro, R., León, R., Romero–Matos, J., Moreno–González, R., Pérez–López, R., 2024. Towards circular and sustainable restoration of a deeply polluted river basin: The Odiel River catchment (SW Spain). Sci. Total Environ. 907, 168078. https://doi.org/10.1016/j.scitotenv.2023.168078

Millán–Becerro, R., Pérez–López, R., Cánovas, C.R., Macías, F., León, R., 2023. Phosphogypsum weathering and implications for pollutant discharge into an estuary. J. Hydrol. 617, 128943. https://doi.org/10.1016/j.jhydrol.2022.128943

Morales–Baquero, R., Pulido–Villena, E., Reche, I., 2013. Chemical signature of Saharan dust on dry and wet atmospheric deposition in the south–western Mediterranean region. Tellus B Chem. Phys. Meteorol. 65(1). https://doi.org/10.3402/tellusb.v65i0.18720

Morillo, J., Usero, J., Rojas, R., 2008. Fractionation of metals and As in sediments from a biosphere reserve (Odiel salt marshes) affected by acidic mine drainage. Environ Monit. Assess. 139, 329–337. https://doi.org/10.1007/s10661–007–9839–3

Nakaona, L., Maseka, K.K., Hamilton, E.M., Watts, M.J., 2020. Using human hair and nails as biomarkers to assess exposure of potentially harmful elements to populations living near mine waste dumps. Environ. Geochem. Health 42(4), 1197–1209. https://doi.org/10.1007/s10653–019–00376–6

Nieto, J.M., Sarmiento, A.S., Olías, M., Canovas, C.R., Riba, I., Kalman, J., Delvalls, T.A., 2020. Acid mine drainage pollution in the Tinto and Odiel rivers (Iberian Pyrite Belt, SW Spain) and bioavailability of the transported metals to the Huelva Estuary. Environ. Int. 33(4), 2007, 445–455. https://doi.org/10.1016/j.envint.2006.11.010

Ojekunle, O.Z., Rasaki, A., Taiwo, A.M., Adegoke, K.A., Balogun, M.A., Ojekunle, O.O., Anumah, A.O., Ibrahim, A.O., Adeyemi, A., 2022. Health risk assessment of heavy metals in drinking water leaching through improperly managed dumpsite waste in Kurata, Ijoko,

Sango area of Ogun State, Nigeria. Groundw. Sustain Dev. 18, 100792, https://doi.org/10.1016/j.gsd.2022.100792

Osman, K.T. Soils: principles, properties and management, Ed. 1. Springer Science & Business Media, Berlin, Germany, 2012. https://doi.org/10.1007/978-94-007-5663-2

Özkaynak, H.,Thurston., 1987. Associations Between 1980 U.S. Mortality Rates and Alternative Measures of Airborne Particle Concentration. Risk Analysis. 7, 449–461. https://doi.org/10.1111/j.1539–6924.1987.tb00482.x

Papaslioti, E.M., Pérez–López, R., Parviainen, A., Sarmiento, A.M., Nieto, J.M., Marchesi, C., Delgado–Huertas, A., Garrido, C.J., 2018. Effects of seawater mixing on the mobility of trace elements in acid phosphogypsum leachates. Mar. Pollut. Bull. 127, 695–703. https://doi.org/10.1016/j.marpolbul.2018.01.001

Paz–González, A., Vieira, S.R., Tabeada, M.T., 2000. The effect of cultivation on the spatial variability of selected properties of an umbric horizon. Geoderma. 97(3–4), 273–292. https://doi.org/10.1016/S0016–7061(00)00066–5

Pelicho, A.F., Martins, L.D., Nomi, S.N., Solci, M.C., 2006. Integrated and sequential bulk and wet–only samplings of atmospheric precipitation in Londrina, South Brazil (1998–2002). Atmos. Environ. 40(35), 6827–6835. https://doi.org/10.1016/j.atmosenv.2006.05.075

Pérez–López, R., Castillo, J., Sarmiento, A.M., Nieto, J.M., 2011. Assessment of phosphogypsum impact on the salt–marshes of the Tinto river (SW Spain): Role of natural attenuation processes. Mar. Pollut. Bull. 62, 2787–2796. https://doi.org/10.1016/j.marpolbul.2011.09.008

Pérez–López, R., Macías, F., Ruiz Cánovas, C., Sarmiento, A.M., Pérez–Moreno, S.M., 2016. Pollutant flows from a phosphogypsum disposal area to an estuarine environment: An insight from geochemical signatures. Sci. Total Environ. 553, 42–51. https://doi.org/10.1016/j.scitotenv.2016.02.070

Pérez–López, R., Millán–Becerro, R., Basallote, M.D., Carrero, S., Parviainen, A., Freydier, R., Macías, F., Cánovas, C.R., 2023. Effects of estuarine water mixing on the mobility of trace elements in acid mine drainage leachates. Mar. Pollut. Bull. 187, 114491. https://doi.org/10.1016/j.marpolbul.2022.114491

Pérez–López, R., Nieto, J.M., López–Coto, I., Aguado, J.L., Bolívar, J.P., Santisteban, M., 2010. Dynamics of contaminants in phosphogypsum of the fertilizer industry of Huelva (SW Spain): From phosphate rock ore to the environment. Appl. Geochem. 25(5), 705–715. https://doi.org/10.1016/j.apgeochem.2010.02.003

Pérez–Moreno, S.M., Gázquez, M.J., Pérez–López, R., Vioque, I., Bolívar, J.P., 2018. Assessment of natural radionuclides mobility in a phosphogypsum disposal area. Chemosphere. 211, 775–783. https://doi.org/10.1016/j.chemosphere.2018.07.193

Pope, C.A., Coleman, N., Pond, Z.A., Burnett, R.T., 2020. Fine particulate air pollution and human mortality: 25+ years of cohort studies. Environ Res. 183, 108924. https://doi.org/10.1016/j.envres.2019.108924

Pope, C.A., Dockery, D.W., 2006. Health effects of fine particulate air pollution: lines that connect. J. Air Waste Manag. Assoc. 56(6), 709–742. https://doi.org/10.1080/10473289.2006.10464485

Pope, C.A., Thun, M.J., Namboodiri, M.M., Dockery, D.W., Evans, J.S., Speizer, F.E., Heath, C.W., 1995. Particulate air pollution as a predictor of mortality in a prospective study of U.S. adults. Am. J. Respir. Crit. Care Med. 151(3 Pt 1), 669–674. https://doi.org/10.1164/ajrccm/151.3_Pt_1.669

Population–based multicase–control study (MCC–Spain). http://www.mccspain.org, 2013 (accessed 12 December 2024).

Przybylowicz, A., Chesy, P., Herman, M., Parczewski, A., Walas, S., Piekoszewski, W., 2012. Examination of distribution of trace elements in hair, fingernails and toenails as alternative biological materials. Application of chemometric methods. Cent. Eur. J. Chem. 10, 1590–1599. https://doi.org/10.2478/s11532–012–0089–z

Querol, X., Alastue, A., de la Rosa, J., Sánchez–de–la–Campa, A., Plana, F., Ruiz, C.R., 2002. Source apportionment analysis of atmos–pheric particulates in an industrialised urban site in southwestern Spain. Atmos. Environ. 36, 3113–3125. https://doi.org/10.1016/S1352–2310(02)00257–1

Rahman, M.M., Alam, K. Velayutham, E., 2021. Is industrial pollution detrimental to public health? Evidence from the world's most industrialised countries. BMC Public Health 21, 1175. https://doi.org/10.1186/s12889–021–11217–6

Rashed, M.N., Hossam, F., 2007. Heavy Metals in Fingernails and Scalp Hair of Children, Adults and Workers from Environmentally Exposed Areas at Aswan, Egypt, Environ. Bioindic. 2(3), 131–145. https://doi.org/10.1080/15555270701553972

Rentería–Villalobos, M., Vioque, I., Mantero, J., Manjón, G., 2010. Radiological, chemical and morphological characterizations of phosphate rock and phosphogypsum from phosphoric acid factories in SW Spain. J. Hazard. Mater. 181(1–3), 193–203. https://doi.org/10.1016/j.jhazmat.2010.04.11627

Resolución de 7 de agosto de 2007, de la Dirección General de Prevención y Calidad Ambiental, por la que se declaran como suelo contaminado dos parcelas del Plan Parcial Residencial núm. 9 de Aljaraque (Huelva). https://www.juntadeandalucia.es/boja/2007/168/9 (accessed 20 June 2024).

Robles–Arenas, V.M., Rodríguez, R., García, C., Manteca, J.I., Candela, L., 2006. Sulphide–mining impacts in the physical environment: Sierra de Cartagena–La Unión (SE Spain) case study. Environ. Geol. 51(1), 47–64. https://doi.org/10.1007/s00254–006–0303–4

Rodríguez–Barranco, M., Lacasaña, M., Gil, F., Lorca, A., Alguacil, J., Rohlman, D.S., González–Alzaga, B., Molina–Villalba, I., Mendoza, R., Aguilar–Garduño, C., 2014. Cadmium exposure and neuropsychological development in school children in southwest–ern Spain. Environ. Res. 134, 66–73. https://doi.org/10.1016/j.envres.2014.06.026

Rosado, D., Usero, J., Morillo, J., 2016. Assessment of heavy metals bioavailability and toxicity toward Vibrio fischeri in sediment of the Huelva estuary. Chemosphere 153, 7–10. https://doi.org/10.1016/j.chemosphere.2016.03.040

Ruiz Cánovas, C., Macías, F., Pérez López, R., Nieto, J.M., 2018. Mobility of rare earth elements, yttrium and scandium from a phosphogypsum stack: Environmental and economic implications, Sci. Total Environ. 618, 847–857. https://doi.org/10.1016/j.scitotenv.2017.08.220

Sáenz, V., Blasco, J., Gómez–Parra, A., 2003. Speciation of heavy metals in recent sediments of three coastal ecosystems in the Gulf of Cadiz, Southwest Iberian Peninsula. Environ. Toxicol. Chem. 22, 2833 – 2839. https://doi.org/10.1897/02–448

Sainz, A., Grande, J.A., de la Torre, M.L., 2004. Characterisation of heavy metal discharge into the Ria of Huelva, Environ. Int. 30(4), 557–566, https://doi.org/10.1016/j.envint.2003.10.013

Salcedo–Bellido, I., Gutiérrez–González, E., García–Esquinas, E., Fernández de Larrea–Baz, N., Navas–Acien, A., Téllez–Plaza, M., Pastor–Barriuso, R., Lope, V., Gómez–Ariza, J.L., García–Barrera, T., Pollán, M., Jiménez Moleón, J.J., Pérez–Gómez, B., 2021. Toxic metals in toenails as biomarkers of exposure: A review. Environ. Res. 197, 111028. https://doi.org/10.1016/j.envres.2021.111028

Samet, J.M., Zeger, S.L., Dominici, F., Curreiro, F., Coursac, I., Dockery, D.W. Schwartz, J., Zanobetti, A., 2000. The National Morbidity, Mortality, and Air Pollution Study. Part I: Methods and methodologic issues. Res. Rep. Health Eff. Inst. (94 Pt II), 5–84.

Sánchez de la Campa, A.M., de la Rosa, J., Querol, X., Alastuey, A., Mantilla, E., 2007. Geochemistry and origin of PM10 in the Huelva region, southwestern Spain. Environ. Res. 103(3), 305–316. https://doi.org/10.1016/j.envres.2006.06.011

Sánchez de la Campa, A.M., Sánchez–Rodas, D., Alsioufi, L., Alastuey, A., Querol, X., de la Rosa, J.D., 2018. Air quality trends in an industrialised area of SW Spain. J. Clean. Prod. 186, 465–474. https://doi.org/10.1016/j.jclepro.2018.03.122

Sánchez de la Campa, A.M., Sánchez–Rodas, D., González Castanedo, Y., de la Rosa, J.D., 2015. Geochemical anomalies of toxic ele–ments and arsenic speciation in airborne particles from Cu mining and smelting activities: influence on air quality. J. Hazard. Mater. 291, 8–27. https://doi.org/10.1016/j.jhazmat.2015.02.058

Santos Bermejo, J.C., Beltrán, R., Gómez Ariza, J.L., 2003. Spatial variations of heavy metals contamination in sediments from Odiel river (Southwest Spain). Environ. Int. 29, 69–77. https://doi.org/10.1016/S0160–4120(02)00147–2

Scientific committee of national experts coordinated from Huelva University about the RESTORE 2030 plan. Technical Report on the suitability of the RESTORE 20/30 project as a solution to the problem of the phosphogypsum ponds and for the recovery of the marshes of the Tinto River estuary (http://mesadelaria.es/documentos/Informe_280722_C_Expertos–Agosto2022.pdf), (accessed 20 June 2024).

Seto, S., Hara, H., 2006 Precipitation chemistry in western Japan: Its relationship to meteorological parameters. Atmos. Environ. 40(8), 1538–1549. https://doi.org/10.1016/j.atmosenv.2005.10.050

Sexton, K., Hattis, D., 2007. Assessing cumulative health risks from exposure to environmental mixtures – three fundamental questions. Environ. Health Perspect. 115(5), 825–832. https://doi.org/10.1289/ehp.9333

Shit, P.K., Bhunia, G.S., Maiti, R., 2016. Spatial analysis of soil properties using GIS based geostatistics models. Model. Earth Syst. Environ. 2, 107. https://doi.org/10.1007/s40808–016–0160–4

Silva, L.F.O., Oliveira, M.L.S., Crissien, T.J., Santosh, M., Bolivar, J.P., Shao, L., Dotto, G.L., Gasparotto, J., Schindler, M., 2022. A review on the environmental impact of phosphogypsum and potential health impacts through the release of nanoparticles. Chemosphere. 286, 131513. https://doi.org/10.1016/j.chemosphere.2021.131513

Silva–Caicedo, R.F., Contreras–Llanes, M., Capelo, R., Zumel–Marne, A., García–Sevillano, M.A., Santos–Sánchez, V., Alguacil, J., 2024. Impact of Fish, Mollusk and Seafood Consumption before Sample Donation on Urinary and Toenail Metal Levels in Work–ers Exposed to Heavy Metals. Appl. Sci. 14, 8174. https://doi.org/10.3390/app14188174

Slotnick, M.J., Nriagu, J.O., Johnson, M.M., Linder, A.M., Savoie, K.L., Jamil, H.J., Hammad, A.S., 2005. Profiles of trace elements in toenails of Arab–Americans in the Detroit area, Michigan. Biol. Trace Elem. Res. 107(2), 113–126. https://doi.org/10.1385/BTER:107:2:113

Sun, Y., Zhang, X., Peng, H., Zhou, W., Jiang, A., Zhou, F., Wang, H., Zhang, W., 2025. Development of a coupled model to simulate and assess arsenic contamination and impact factors in the Jinsha River Basin, China. J. Environ. Sci. 147, 50–61, https://doi.org/10.1016/j.jes.2023.09.038

Sureda, A., Bibiloni, M.D.M., Julibert, A., Aparicio–Ugarriza, R., Palacios–Le Blé, G., Pons, A., Gonzalez–Gross, M., Tur, J.A., 2017. Trace element contents in toenails are related to regular physical activity in older adults. PloS ONE 12(10), e0185318. https://doi.org/10.1371/journal.pone.0185318

Taiwo, A.M., Harrison, R.M., Shi, Z.B., 2014. A review of receptor modelling of industrially emitted particulate matter. Atmos. Environ. 97, 109–120. http://dx.doi.org/10.1016/j.atmosenv.2014.07.051

Thomsen, V., Schatzlein, D., Mercuro, D., 2003. Limits of detection in spectroscopy. Spectroscopy 18, 112–114.

Todd, D.K., Mays, L.W. Groundwater Hydrology. 3rd ed., Wiley, New Jersey. 2005.

Torre, B.M., Borrero–Santiago, A.R., Fabbri, E., Guerra R., 2019. Trace metal levels and toxicity in the Huelva Estuary (Spain): A case study with comparisons to historical levels from the past decades. Environ. Chem. Ecotox. 1, 12–18. http://dx.doi.org/10.1016/j.enceco.2019.07.002

Torres–Sánchez, R., Sánchez–Rodas, D., Sánchez de la Campa, A.M., Kandler, K., Schneiders, K., de la Rosa, J.D., 2019. Geochemistry and source contribution of fugitive phosphogypsum particles in Huelva, (SW Spain). Atmos. Res. 230, 104650. https://doi.org/10.1016/j.atmosres.2019.104650

Torres–Sánchez, R., Sánchez–Rodas, D., Sánchez de la Campa, A.M., de la Rosa, J.D., 2020. Hydrogen fluoride concentrations in ambient air of an urban area based on the emissions of a major phosphogypsum deposit (SW, Europe). Sci. Total Environ. 714, 136891. https://doi.org/10.1016/j.scitotenv.2020.136891

Tranel, M.A., Kimmel, R.O. Impacts of lead ammunition on wildlife, the environment, and human health literature review and implications for Minnesota. In: Watson, R.T., Fuller, M., Pokras, M., Hunt,W.G. (Eds.), Ingestion of Lead from Spent Ammunition: Implications for Wildlife and Humans. The Peregrine Fund, Boise, Idaho, USA. 2009.

Tuncer, B., Bayer, B., Yesilyurt, C., Tuncel, G., 2001. Ionic composition of precipitation at the central Anatolia, Turkey. Atmos. Environ. 35(34), 5989–6002. https://doi.org/10.1016/S1352–2310(01)00396–X

USEPA. Appendix B to Part 136. Definition and procedure for the determination of the method detection limit. Revision 1.11. Fed. Regist. 49 (209), 43430. Also referred to as “40 CFR Part 136”. Environmental Protection Agency, Washington D.C., USA, 1984

Van Horne, Y.O., Farzan, S.F., Johnston, J.E., 2021. Metal–mixtures in toenails of children living near an active industrial facility in Los Angeles County, California. J. Expo. Sci. Environ. Epidemiol. 31(3), 427–441. https://doi.org/10.1038/s41370–021–00330–8

Webster, R., Oliver, M. Geostatistics for environmental scientists. John Willey and Sons, Ltd., New York, USA, 2001. https://doi.org/10.1002/9780470517277

Weiß, J., 1987. Ion chromatography — A review of recent developments. Z. Anal. Chem. 451–455. https://doi.org/10.1007/BF00487225

Whitworth, K.W., Symanski, E., Lai, D., Coker, A.L., 2011. Kriged and modeled ambient air levels of benzene in an urban environment: an exposure assessment study. Environ. Health 10, 21. https://doi.org/10.1186/1476-069X-10-21

World Health Organization (WHO). Environmental Health Criterion 58—Selenium. World Health Organization, Geneva, Switzeland, 1987. https://iris.who.int/bitstream/handle/10665/37268/9241542586–eng.pdf?sequence=1&isAllowed=y

World Health Organization (WHO). Guidelines for Drinking–water Quality In: Recommendations, 3rd ed., vol. 1, World Health Organisation, Geneva, Switzerland, 2003. https://iris.who.int/bitstream/handle/10665/204411/9789241547611_eng.pdf?sequence=1

Xing, J., Song, J., Yuan, H., Wang, Q., Li, X., Li, N., Duan, L., Qu, B., 2017. Atmospheric wet deposition of dissolved trace elements to Jiaozhou Bay, North China: Fluxes, sources and potential effects on aquatic environments. Chemosphere 174, 428–436, https://doi.org/10.1016/j.chemosphere.2017.02.004

Zeng, J., Han, G., Wu, Q., Qu, R., Ma, Q., Chen, J., Mao, S., Ge, X., Wang, Z., Ma, Z., 2024. Significant influence of urban human activities and marine input on rainwater chemistry in a coastal large city, China. Water Res. 257, 121657. https://doi.org/10.1016/j.watres.2024.121657

Zierold, K.M., Myers, J.V., Brock, G.N., Sears, C.G., Sears, L.L., Zhang, C.H., 2021. Nail Samples of Children Living near Coal Ash Storage Facilities Suggest Fly Ash Exposure and Elevated Concentrations of Metal(loid)s. Environ. Sci. Technol. 55(13), 9074–9086. https://doi.org/10.1021/acs.est.1c01541

Zou, B., Zhan, F., Zeng, Y., Yorke, C., Liu, X., 2011. Performance of Kriging and EWPM for Relative Air Pollution Exposure Risk Assessment. Int. J. Environ. Res. 5(3), 769–778. https://doi.org/10.22059/ijer.2011.383

Annexes

A1. Published papers

A1.1. Paper #1

A1.1.1 Extended abstract paper #1

Delineating distinct sediment pollution signatures from diverse sources in a heavily contaminated estuary near an area of high cancer and cardiovascular mortality

Manuel Contreras-Llanes [1,2,*], Vanessa Santos-Sánchez [1], Juan Alguacil [1,2], Jesús M. Castillo [3]

[1] Research Group on Clinical, Environmental Epidemiology and Social Transformation (EPICAS), Department of Sociology, Social Work and Public Health, University of Huelva (UHU), 21007, Huelva, Spain

[2] Research Centre on Natural Resources, Health and Environment (RENSMA), University of Huelva (UHU), 21007, Huelva, Spain

[3] Department of Plant Biology and Ecology, University of Seville (US), Ap 1095, 41080 Seville, Spain

[*] **Corresponding author:** Manuel Contreras-Llanes (mcontreras@uhu.es)

Keywords: acid mine drainage, Odiel-Tinto Estuary, metals, PG, tidal marshes

Introduction: Substantial evidence establishes a clear link between industrial and mining pollution and severe health issues, such as cancer, cardiovascular and respiratory diseases (Briffa et al., 2020). Huelva City has higher mortality rates for these diseases compared to the rest of Spain (Alguacil et al., 2014; Benach et al., 2003; Lopez-Abente et al., 2001). Environmental pollution is likely a key factor contributing to the excess mortality observed in Huelva (Alguacil et al., 2014). The Odiel-Tinto Estuary, located

close to Huelva City (SW-Spain), is one of the most polluted estuaries worldwide due to industrial and mining activities (Morillo et al., 2008; Sáenz et al., 2003). The Iberian Pyrite Belt, one of the most important mining district (Leistel et al., 1998; Pérez-López et al., 2023), has contributed to significant metal contamination in the estuary through AMD (Blasco et al., 2000; Santos Bermejo et al., 2003). Chemical factories have discharged pollutants into the estuary since the mid-1960s. Additionally, PG stacks, a waste product from fertiliser production, cover a vast area and contain toxic elements, such as metal(loid)s and natural radionuclides (Lieberman et al., 2020; Pérez-López et al., 2010). Due to social and environmental concerns, the judicial authorities demanded the cessation of PG stockpiling in 2010 and mandated a restoration plan called as RESTORE 2030. However, an independent committee found the plan inadequate for complete restoration (Scientific committee, 2022). Researches have focused on understanding the processes governing metal behaviour in the estuary and identifying highly contaminated areas (Borrego et al., 2022; Elbaz-Poulichet et al., 1999). Although, identifying specific geochemical tracers is crucial for pinpointing pollution sources and assessing the impact of future interventions like RESTORE 2030. Our study aimed to identify specific pollution signatures in marsh sediments using geochemical tracers in the highly polluted Odiel–Tinto Estuary prior to a planned restoration of the affected marshes.

Methodology: Sediment samples were collected from six marshes in the Odiel-Tinto Estuary (A1–A6) and one in the near and unpolluted Piedras River Estuary (A7) in March 2021, with 10 samples taken from each area. Sediment textures were analysed using the Bouyoucos hydrometer method, pH, EC, and Eh using a digital multimeter, and 48 chemical element concentrations were determined using ICP-OES and ICP-MS. The spatial distribution of chemical elements associated with local pollution sources was analysed using the inverse distance weighting interpolation technique. Statistical analyses were conducted using SPSS and SigmaPlot, with tests for homogeneity of variance, normality, and comparisons of sediment characteristics and chemical element concentrations. Finally, PCA was used to analyse the relationships between chemical element concentrations in the sediments from the sampling areas.

Findings: Sediments were characterised by pH close to 7 in all areas except A6 (3.4 ± 0.1). Eh was highest in A1 near the PG stacks (33.8 ± 1.3 mS cm^{-1}) and lowest in A6 (5.3 ± 0.3 mS cm^{-1}). Eh values ranged from 245.6 ± 0.1 mV in A7 (Piedras River) to 352.5 ± 0.1 mV in A6. Sediments showed a clayey texture in A1, A2, A5, A6, and A7, meanwhile, loamy and loamy-clay in A3 and A4. We identified a specific pollution signature for PG stacks characterised by 20 elements such as Gd, U, As, Mg, Zn, Cy and P that distinguishes metal exposure from the other pollution sources in the Odiel–Tinto Estuary (Figure 10). AMD signature from mining waste deposits revealed six elements, including Fe, Pb and Mn (Figure 10). Sulphur is a suitable geochemical marker upstream by AMD in the Tinto River's marshes, while beryllium indicates the influence of intensive agriculture (Figure 10).

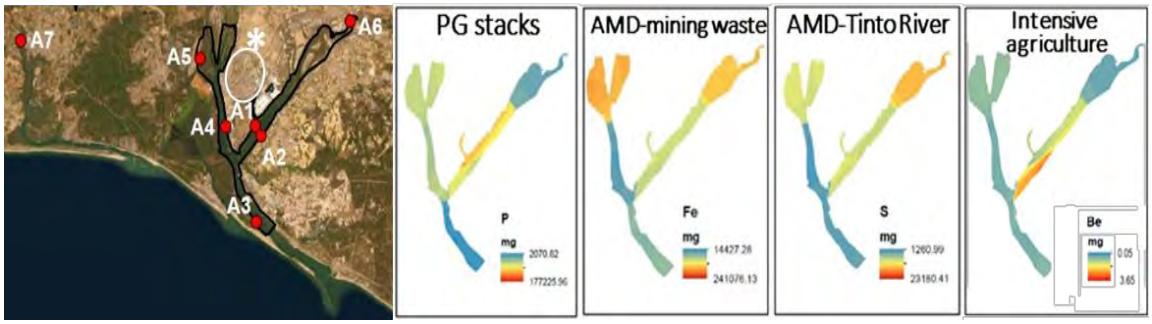

Figure A1.1. Location map of the sampled salt marsh areas (red spots) in the Odiel-Tinto Estuary (A1–6) and the Estuary of Piedras River (A7), and Huelva City (*). Spatial distribution in the Odiel-Tinto Estuary of representative chemical elements by pollution sources.

Conclusion: Our research has revealed unique pollution fingerprint for PG stacks, AMD near mining waste deposits, pollutants along the Tinto River, and areas affected by intensive agricultural activities. Our findings offer a crucial tool for distinguishing between different pollution sources, pinpointing the most affected areas of the salt marsh, assigning responsibility to the various polluting entities within the estuary, and establishing a baseline for assessing the impact of the RESTORE 2030 restoration plan in the Odiel–Tinto Estuary.

A1.1.2. Published version paper #1

Science of the Total Environment 957 (2024) 177715

Contents lists available at ScienceDirect

Science of the Total Environment

journal homepage: www.elsevier.com/locate/scitotenv

Delineating distinct sediment pollution signatures from diverse sources in a heavily contaminated estuary near an area of high cancer and cardiovascular mortality

Manuel Contreras-Llanes [a,b,*], Vanessa Santos-Sánchez [a], Juan Alguacil [a,b], Jesús M. Castillo [c]

[a] Research Group on Clinical, Environmental Epidemiology and Social Transformation (EPICAS), Department of Sociology, Social Work and Public Health, University of Huelva (UHU), 21007 Huelva, Spain
[b] Research Center on Natural Resources, Health and Environment (RENSMA), University of Huelva (UHU), 21007 Huelva, Spain
[c] Department of Plant Biology and Ecology, University of Seville (US), Ap 1095, 41080 Seville, Spain

HIGHLIGHTS

- Specific pollution signatures were detected for each of the main pollution sources.
- 20 elements including As and Mg were identified as pollution tracers for PG stacks.
- Sediments near mining wastes specially cumulated 6 elements, including Fe and Mn.
- Be and S are suitable pollution tracers for agriculture and AMD-Tinto, respectively.
- We set a starting point to evaluate the impact of the RESTORE 2030 project.

GRAPHICAL ABSTRACT

ARTICLE INFO

Editor: Manuel Esteban Lucas-Borja

Keywords:
Acid mine drainage
Odiel-Tinto estuary
Metals
Phosphogypsum
Tidal marshes

ABSTRACT

Our study aimed to identify specific pollution signatures in marsh sediments using geochemical tracers in the highly polluted Odiel–Tinto Estuary prior to a planned restoration of the affected marshes. Tidal marshes in this estuary are heavily polluted from different sources such as acid mine drainage, industrial activities (including phosphogypsum stacks) and agricultural runoffs. We analysed the total concentrations of 48 chemical elements, pH, electrical conductivity, redox potential and texture of surface sediments from six marsh areas in the Odiel–Tinto Estuary and one in the adjacent Piedras Estuary. Spatial distribution maps were created using inverse distance weighting to visualise the distribution of elements associated with different pollution sources. We identified a specific pollution signature for PG stacks that distinguishes metal exposure from the other pollution sources in the Odiel–Tinto Estuary, such as acid mine drainage near mining waste deposits, an abandoned foundry and areas under intensive agricultural cultivation. Our results provide a valuable tool for discriminating between pollution sources, quantifying the most impacted areas of the salt marsh, assigning responsibility to the various polluting entities within the estuary, and setting a starting point to evaluate the impact of the RESTORE

* Corresponding author at: Research Group on Clinical, Environmental Epidemiology and Social Transformation (EPICAS), Department of Sociology, Social Work and Public Health, University of Huelva (UHU), 21007 Huelva, Spain.
E-mail address: mcontreras@uhu.es (M. Contreras-Llanes).

https://doi.org/10.1016/j.scitotenv.2024.177715
Received 29 August 2024; Received in revised form 31 October 2024; Accepted 20 November 2024

2030 restoration plan in the Odiel–Tinto Estuary. The specific sediment pollution signatures identified may also be used as a reference to determine the impact of future interventions on existing pollution sources in estuaries or marshes polluted with phosphogypsum.

1. Introduction

There is cumulative evidence linking industrial and mining environmental pollution with health problems, specifically cancer, cardiovascular and respiratory diseases (Briffa et al., 2020). Huelva, a city of 150,000 inhabitants, has high cancer and heart disease mortality rates for both men and women as compared to the rest of Spain (Alguacil et al., 2014; Benach et al., 2003; Lopez-Abente et al., 2001). For instance, the Spanish National Atlas of Mortality shows significantly higher standard mortality ratios in the city of Huelva over the period 1989–2014 among both men and women for bladder cancer, cerebrovascular diseases, acute myocardial infarction, heart failure and other heart diseases, in addition to breast cancer in women) and lung cancer in men (Martínez-Beneito et al., 2024). Environmental pollution may be one of the factors predominately responsible for the excess mortality observed in Huelva city (Alguacil et al., 2014).

In this public health context, Huelva city lies next to the Odiel–Tinto Estuary in the southwestern Iberian Peninsula on the Gulf of Cadiz. This estuary is recognised as one of the most heavily polluted in the world due to a multitude of factors including industrial and mining pollution (Morillo et al., 2008; Sáenz et al., 2003). A confluence of stressors gives the region unique characteristics. The Iberian Pyrite Belt, situated in southwest Iberia, ranks as one of the world's most significant polymetallic sulphide mining districts (Leistel et al., 1998; Pérez-López et al., 2023). The Odiel and Tinto Rivers drain the region from north to south, carrying large amounts of metals and metalloids to the Odiel–Tinto Estuary (Blasco et al., 2000; Santos Bermejo et al., 2003). Significant acid mine drainage (AMD) has occurred for centuries, while large quantities of industrial pollutants have been discharged from various chemical factories since the mid-1960s. Additionally, intensive agricultural practices implemented in the late 1970s have resulted in agrochemical runoff entering the estuary from surrounding farmland (Barba-Brioso et al., 2010). In terms of mass, the most significant pollution problem in the Odiel–Tinto Estuary is phosphogypsum (PG), as roughly 100 million tonnes are currently stored in stacks located on the estuary itself. A waste product from fertilizer production, the PG was stockpiled on unconsolidated salt marsh sediments over a period of 42 years (1968–2010) and now covers 1200 ha in the Tinto marshes (Silva et al., 2022). The PG originates from phosphate rock, which carries trace elements that concentrate within the stacks (Rentería-Villalobos et al., 2010). These stacks contain a multitude of pollutants, such as organic substances, metals, natural radionuclides from the ^{238}U decay series and other potentially toxic elements (P, S, F, NH^{4+}, Fe, Zn, U, Cr, Cu and Cd) and natural radionuclides from the ^{238}U decay series, including the highly radiotoxic ^{226}Ra, ^{210}Po and ^{210}Pb (Lieberman et al., 2020; Pérez-López et al., 2010).

Following a social movement spurred by environmental and health concerns over the proximity of PG stacks to Huelva city, less 500 m, the stockpiling of PG from fertilizer factory activities ended in December-2010 after a judicial complaint. Judiciary authorities also demanded the fertilizer company create a restoration plan for the affected marshes. Despite having been approved by governmental authorities, the proposed plan—called RESTORE 2030 (RESTORE2030, 2020)—has not been approved by the judiciary authorities. An independent committee of national scientific experts coordinated by the University of Huelva concluded that the RESTORE 2030 plan was not adequate to achieve a complete restoration, though it could be a good place to begin while a definite solution is found (Scientific committee, 2022). Baseline data on the impact of the PG stacks would be needed to evaluate the progress of the restoration, including, but not limited to, the impact on the Odiel–Tinto Estuary sediments, taking into account the impact of other active metal pollution sources.

Several studies have investigated the concentration of metals in the sediments of the Odiel–Tinto Estuary, focusing primarily on two key aspects: understanding the processes that govern metal behaviour and pinpointing the areas with the highest levels of contamination (Borrego et al., 2022; Elbaz-Poulichet et al., 1999). Tidal marshes were found to be more contaminated compared to other sedimentary environments like channel margins and subtidal channels. Estuaries and tidal marshes act as natural filters for a wide range of pollutants, including organic compounds, metals and even radioactive isotopes, originating from both point sources and non-point sources (Li et al., 2022; Nie et al., 2018). Once within estuaries, pollutants may undergo partial or complete mixing within sediments but can also segregate into specific zones along the estuarine gradients (Beltrán et al., 2010; Santos Bermejo et al., 2003). This segregation is influenced by the chemical and physical properties of the pollutant, changing environmental conditions within the estuary (particularly pH, salinity and redox potential) and interactions between these factors (Hierro et al., 2014a). Given these complexities, identifying appropriate geochemical tracers is crucial for pinpointing the specific sources of pollution impacting tidal marshes. The PG stacks function as an anthropogenic coastal karst aquifer, allowing for hydraulic connection between the sea, groundwater flow and the underlying sediments, leading to active subsidence (Carro et al., 2021; González, 2022). Additionally, highly concentrated contaminants are released into the estuary via acidic edge outflows (i.e. small streams) emanating from the PG stacks (Millán-Becerro et al., 2023; Pérez-López et al., 2016).

Although comprehensive studies have been conducted on the spatial distribution of heavy metals in other highly polluted locations, the specific pollutant profiles affecting the tidal marshes of this anthropogenically polluted estuary have not yet been characterised in detail (Dong et al., 2024; Liu et al., 2024; Sun et al., 2025). These spatial distributions and environment risk assessments are extremely important for the management and future remediation of this site. As the excess mortality in the Huelva area is compatible with industrial and mining metal pollution and there are multiple exposure sources, it is important to investigate the depositional signatures of heavy metals and metalloids specific to the different pollution sources. Biomonitoring can help assess the potential health risks to Huelva citizens and to the ecosystem. We investigated the spatial distribution of sediment pollution originating from various sources to identify pollution depositional signatures in the Odiel–Tinto Estuary, which is critical to assess the impact of future interventions such as RESTORE 2030.

2. Materials and methods

2.1. Study area

We conducted this study in six low-middle tidal salt marsh areas in the Odiel–Tinto Estuary (A1–6) and one tidal salt marsh in the estuary of the Piedras River (A7), situated in Huelva Province, Spain. These estuaries are located on the Gulf of Cadiz in the Southwest Iberian Peninsula (Fig. 1). The region has a Mediterranean climate influenced by the Atlantic Ocean with mild, humid winters (mean air temperature is 11 °C in January; average annual precipitation is 505.6 mm) and warm, dry summers (mean air temperature is 25 °C in August with almost no rainfall). The salt marshes in the study area are flooded twice a day by semi-diurnal mesotidal tides (tidal range [equinoctial mean] of 2.97 m; Figueroa et al., 2003). The bedrock in the Odiel and Tinto basins

primarily consists of Palaeozoic volcanic and sedimentary rocks rich in pyrite (FeS_2) and other sulphide minerals (Achterberg et al., 2003). Presently, the tidal marshes in the Odiel–Tinto Estuary are being polluted with metals coming from AMD (Beltrán et al., 2010; Santos Bermejo et al., 2003). These salt marshes also receive acid discharges and a significant radioactive impact from industrial point sources and their waste deposits (e.g. PG stacks; Guerrero et al., 2021), which also emit particles and gases with relatively high concentrations of radon and hydrogen fluoride—one of the most toxic gaseous compounds—to the atmosphere (López-Coto et al., 2014; Torres-Sánchez et al., 2019, 2020). Some of the salt marsh areas are affected by agrochemical runoff from surrounding agricultural lands (Barba-Brioso et al., 2010). The tidal regime plays a crucial role in the immobilisation and dispersion of pollutants (Hierro et al., 2014a), with bioavailable metals serving as an important source of sediment toxicity (Rosado et al., 2016; Sáenz et al., 2003).

Our first sampling area (A1) was located in the salt marshes on the right bank of the Tinto River at its tidal confluence, an area known locally as 'Estero del Rincon'. These marshes are located near the PG stacks and are predominately colonised by *Sarcocornia perennis* (Mill.) A. J. Scott, *Atriplex portulacoides* L., the exotic invasive cordgrass *Spartina densiflora* Brongn and isolated patches of native *Spartina maritima* (Curtis) Fernald (Fig. S1). The second salt marsh area (A2) was located on the left bank of the Tinto River, opposite A1, in an area that is mainly colonised by *S. perennis*, *A. portulacoides*, *S. maritima* and *S. densiflora* (Fig. S1). A3 was located to the south on the right bank of the 'Canal del Padre Santo', the main channel of the Odiel–Tinto Estuary. The area is colonised by *S. densiflora* and isolated patches of *S. maritima* (Fig. S1). Location A4 was located in the salt marshes near the Chemical Park of Huelva City. This area was ecologically restored in 1992 and is now primarily covered with continuous prairies of *S. maritima* (Fig. S1; Curado et al., 2014). The location for A5 was selected because it is an area highly polluted with metals coming from AMD. It is close to the mineral wastes of an abandoned foundry that extend over 12,600 m^2 and are exposed to rain and rising river levels during spring tides (Davila et al., 2019). The area is colonised by *A. portulacoides* and *S. densiflora*. A6 was located in salt marshes upstream of the Tinto River in an acidic area with high levels of metal pollution (Curado et al., 2010). This area is primarily colonised by *A. portulacoides*, *Phragmites australis* (Cav.) Trin. ex Steud. and *S. densiflora* (Fig. S1). Location A7 was in the estuary of the Piedras River. The sediments in the area are relatively unpolluted as there is a small catchment area relative to that of neighbouring, more polluted rivers and the area has not been affected by human activity such as mining (Lario et al., 2016). This area is colonised by different *Sarcocornia* taxa, *A. portulacoides* and sparse clumps of *S. maritima* and *S. densiflora* (Fig. S1). Geographical coordinates for each sampling point are supplied in the supplementary materials (Table S1).

2.2. Sediment sampling and characteristics

Representative samples of sediments (approx. 2.5×10^{-4} m^3) were collected directly from each salt marsh area (A1-A7) in March 2021, by taking 10 randomly selected samples 10 cm deep in each sample area, coinciding with the rooting zone of the halophytes present in the studied

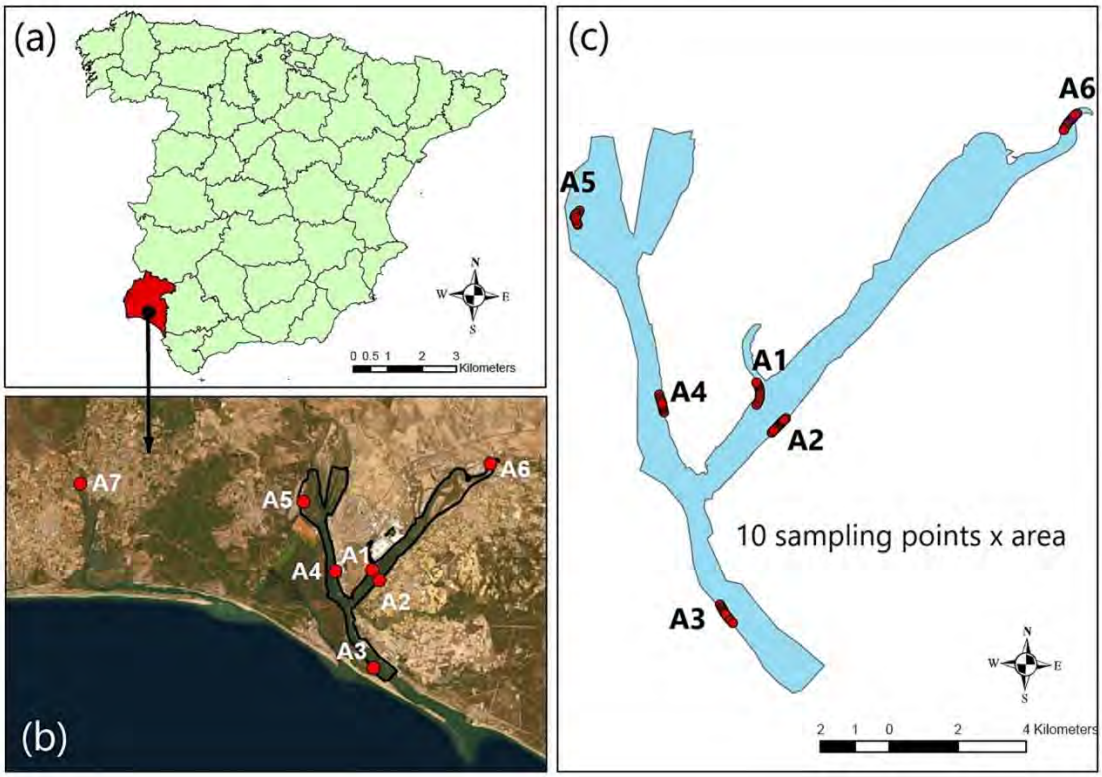

Fig. 1. (a) Location of study area in the Iberian Peninsula, (b) orthophotograph of the sampled salt marsh areas (red spots) in the Estuaries of Odiel-Tinto and Piedras Rivers, and (c) sampling locations of salt marsh sediments in the Odiel-Tinto Estuary(A1–6) and the Estuary of Piedras River (A7).

marshes. A total of 70 different sediment samples were collected. Samples were stored in a freezer at −20 °C until analysis. Within the study area, the main environmental driving factors for cation and anion mobility are pH under low salinity conditions and competitive desorption under high salinity conditions (Kerl et al., 2023). We recorded the pH, electrical conductivity (EC) as a measure of salinity, redox potential (Eh) and texture (i.e. percentages of sand, silt and clay) in the sediment samples. The pH, EC and redox potential of the sediment samples were measured in a 1:2 ratio of sediment to distilled water using a digital multimeter (LAQUA PC220. HORIBA Advanced Techno Co., Ltd.). The suspension was stirred at approximately 1200 rpm for 24 h before measuring the parameters of the supernatant solution. The corresponding value at 25 °C was obtained by temperature conversion of the results.

Sediment textures were analysed using the Bouyoucos hydrometer method (Bouyoucos, 1936). 50 g of dry soil and 100 mL of dispersant (5 % Calgon solution) were added to a flask and allowed to settle for a few minutes, before dispersing with a soil mixer running at approximately 500 rpm for 2 h. The soil suspension was then poured into a graduated cylinder, diluted to 1000 mL with distilled water and stirred with a stir bar. Hydrometer readings and temperature were recorded after 40 s and 2 h.

2.3. Chemical element concentrations in sediments

The sediment samples were analysed for the total concentrations (mg kg^{-1} dry weight) of 48 chemical elements (Table S1) at the University of Huelva. Soil samples were digested with HNO_3 at 220 °C in a microwave (UltraWAVE. Millestone Srl) and brought to 50 mL following digestion. Five replicates were conducted for each sample. Digestion blanks and a reference material were also included in duplicate. Major elements concentrations were determined by Inductively Coupled Plasma-Optical Emission Spectroscopy (ICP-OES; Agilent 5110), operating between 160 and 900 nm with external and periodic calibration ranged between 0.1 and 50 ppm, 0.1–100 ppm and 0.1–500 ppm. Detection and quantification limits were 0.1 ppm and 50 ppm, respectively. Trace elements concentrations were determined by Inductively Coupled Plasma-Mass Spectrometry (ICP-MS; Agilent 7700) with SPS4 autosampler and collision cell (He mode). Details on element concentration measurements and quality controls are supplied in the supplementary materials (Text S1).

2.4. Spatial distribution of chemical elements

The distribution of representative elements associated with the PG stacks, mineral wastes and AMD were spatially analysed. Maps of the spatial distribution of each of the chemical elements in the estuary were created using the inverse distance weighting (IDW) interpolation technique. This method gives greater weight to points close to the sampling location, assuming that the influence of the variable being represented decreases at greater distances from the sampling point (Lu and Wong, 2008). All spatial analyses were carried out with ArcGIS 10.5 software.

2.5. Data analyses

Statistical analyses were carried out using SPSS 15.0 (SPSS Inc., USA) and SigmaPlot 11.0 (Systat Software Inc., Germany). A significance level (α) of 0.05 was applied to all analyses and deviations were calculated as the standard error of the mean. Data were tested for homogeneity of variance and normality with Levene and Shapiro-Wilk tests, respectively. Sediment characteristics and chemical element concentrations were compared between salt marsh areas using parametric one-way ANOVAs (F-test) or non-parametric Kruskal–Wallis H-tests with a post-hoc Tukey test. The relationships between chemical element concentrations in the sediments of the seven sample salt marsh locations were analysed using a principal component analysis (PCA). The correlation matrix was analysed with 25 maximum iterations for convergence without rotation to extract independent PCA factors with eigenvalues >1. Regression factor scores from PCA for each sediment sample were compared between the seven salt marsh areas studied using Kruskal–Wallis H-tests with post-hoc Tukey tests.

3. Results

3.1. Sediment characteristics

Sediment characteristics differed significantly between the salt marsh areas (Table S2). Sediment pH was close to 7 for all salt marshes, with the exception of A6 (3.4 ± 0.1), located upstream of the Tinto River (Fig. 2a). Sediment EC was the highest in A1 near the PG stacks (33.8 ± 1.3 mS cm^{-1}) and the lowest in A6 (5.3 ± 0.3 mS cm^{-1}; Fig. 2b). Sediment Eh ranged from 245.6 ± 0.1 mV in A7 (Piedras River) to 352.5 ± 0.1 mV in A6 (Fig. 2c). Sediment texture was clayey in A1, A2, A5, A6 and A7, and mostly loamy and loamy-clay in A3 and A4 (Figs. 2d–f).

3.2. Sediment pollution signatures

Concentrations of the 48 chemical elements analysed differed significantly between the seven study salt marsh areas (Tables 1 and S3).

Eight factors, explaining 89.4 % of the variance, were obtained from the PCA for the concentration of chemical elements in the sediments. The first factor (PC1, explaining 33.9 % of total variance) was positively correlated with 20 chemical elements with factor loadings higher than +0.600, including Gd, U, Bi, Ba, Sr, Er, Ce, As, Mg, Zn, Cu and P (Table 2). The concentrations of these elements were highest in sediments from A1 and A2 (Fig. 3a and b). Regression factor scores for PC1 were significantly higher for A1 and A2 than for A4–7 (Fig. S2, Table S4). Using the IDW interpolation method, the spatial distribution of the concentration of elements such as P and U was clearly associated with the salt marsh sediments located at the edge of the PG stacks on the right bank of the main channel of the Tinto River (Fig. 4a and b). Concentrations of Gd and Ce were also the highest in the sediments located

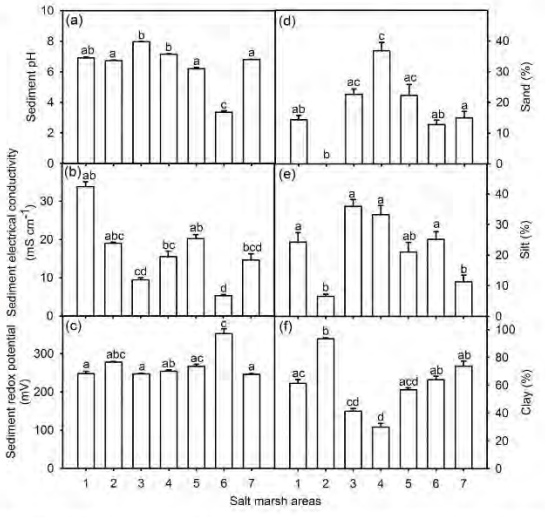

Fig. 2. Sediment (a) pH, (b) electrical conductivity, (c) redox potential and texture (% of (d) sand, (e) silt and (f) clay) in six salt marsh areas in the Odiel and Tinto Estuary (1–6) and one salt marsh in the Estuary of Piedras River (7) in Southwest Iberian Peninsula. Data are arithmetic means ± SEM (n = 10). Salt marsh areas are shown in Fig. 1. Different letters indicate significant differences between salt marsh areas (Tukey test, $p < 0.05$).

Table 1
Sediment concentrations (mg kg^{-1} DW) of forty-eight chemical elements in six salt marsh areas in the Odiel and Tinto Estuary (1–6) and one salt marsh in the Estuary of Piedras River (7) in Southwest Iberian Peninsula. Data are arithmetic means (up) ± SEM (down) ($n = 10$).

	As	Ba	Be	Bi	Ca	Cd	Ce	Co	Cr	Cs	Cu	Dy	Er	Eu	Fe	Ga	Gd	Ho	In	La	Li	Mg	Mn	Mo
Salt mash 1	866.5	430.8	0.9	17.9	7633.9	4.8	71.1	34.9	106.4	4.1	2944.9	7.7	4.2	1.9	107,338.6	17.2	10.6	1.3	2.5	38.4	106.3	10,488.2	369.6	9.0
	64.0	9.2	0.2	1.2	639.7	0.7	1.8	0.9	2.0	0.1	110.5	0.2	0.2	0.1	2523.4	0.3	0.3	0.1	0.1	1.6	1.1	179.0	28.5	0.4
Salt mash 2	632.2	407.6	2.7	17.2	4976.4	3.4	74.8	38.6	88.4	5.0	3067.7	7.0	3.8	2.1	91,131.0	18.4	10.3	1.4	2.1	35.8	129.8	10,333.6	358.8	8.5
	13.7	12.1	0.2	0.4	223.1	0.3	0.9	0.9	1.2	0.1	62.5	0.1	0.0	0.0	1513.2	0.2	0.1	0.0	0.0	0.6	2.9	128.9	36.1	0.7
Salt mash 3	421.2	202.8	0.6	6.8	15,655.3	1.0	49.4	31.6	46.6	1.5	1265.6	3.6	1.6	0.6	62,876.0	9.3	6.0	0.6	1.7	23.6	45.5	6749.5	444.5	7.2
	40.2	16.1	0.0	0.6	1826.5	0.2	2.2	1.8	2.8	0.2	85.1	0.3	0.2	0.0	4610.9	0.7	0.3	0.0	0.3	1.2	3.8	359.8	50.4	0.8
Salt mash 4	152.5	162.4	0.6	5.5	6195.2	0.6	33.4	20.3	48.8	1.0	1263.9	2.9	0.9	0.6	32,950.0	6.3	4.3	0.6	0.8	17.1	44.8	4819.0	307.7	6.6
	19.0	17.5	0.0	0.7	756.2	0.0	2.9	3.9	5.4	0.2	187.3	0.3	0.1	0.0	4286.0	0.8	0.4	0.0	0.2	1.5	4.8	577.2	66.9	2.1
Salt mash 5	16.7	25.2	0.9	4.6	4335.8	1.9	9.0	90.5	51.5	160.8	2333.0	1.2	0.6	11.2	173,693.2	10.8	1.3	3.8	2.6	68.8	60.4	7090.2	2140.6	0.6
	1.1	4.9	0.2	0.5	383.6	0.4	1.5	22.0	5.5	54.2	307.2	0.2	0.0	1.7	18,039.8	1.0	0.2	0.5	0.5	11.6	10.3	399.8	586.6	0.0
Salt mash 6	262.0	122.4	0.6	7.4	1112.0	0.6	13.6	6.9	57.0	199.3	536.9	1.0	0.6	1.6	158,327.3	11.4	1.5	0.7	2.3	17.9	25.5	4933.9	103.8	9.2
	87.6	41.5	0.0	1.0	63.6	0.0	3.7	0.4	0.9	18.2	79.7	0.2	0.0	0.4	4307.3	0.2	0.3	0.1	0.8	2.5	0.8	96.7	2.3	2.9
Salt mash 7	10.7	29.6	1.5	8.1	2274.1	0.6	7.2	16.1	75.2	178.2	46.2	0.6	0.6	6.2	42,557.4	18.9	0.6	1.5	0.8	70.8	45.8	7485.5	533.3	0.6
	4.0	1.2	0.3	0.4	149.7	0.0	0.3	2.0	2.0	5.0	3.9	0.0	0.0	0.3	1429.3	0.7	0.0	0.1	0.1	0.6	1.2	143.1	191.9	0.0
	Nb	Nd	Ni	P	Pb	Pr	Rb	S	Sc	Se	Sm	Sn	Sr	Tb	Th	Ti	Ti	Tl	Tm	U	V	Y	Yb	Zn
Salt mash 1	0.6	40.3	40.6	12,162.6	987.8	9.0	71.3	10,015.3	12.9	12.6	8.7	8.6	300.8	1.1	7.1	461.3	462.6	1.7	0.6	28.2	117.4	49.5	3.2	3471.5
	0.0	1.5	1.3	786.3	66.2	0.2	2.0	1590.2	0.3	0.7	0.3	0.4	23.2	0.1	0.1	14.1	14.6	0.2	0.0	1.1	1.1	2.5	0.1	109.3
Salt mash 2	0.6	40.2	46.5	7564.8	880.8	9.8	70.9	9998.8	13.2	11.7	9.0	9.6	226.0	1.4	7.7	475.7	474.0	1.8	0.6	12.6	109.6	39.5	3.0	3276.3
	0.0	0.5	0.4	233.1	21.5	0.1	1.3	1041.1	0.2	0.5	0.1	0.3	5.8	0.0	0.1	19.1	22.6	0.2	0.0	0.5	1.6	0.6	0.0	70.6
Salt mash 3	0.6	26.5	23.7	2495.3	386.7	5.4	39.2	3551.3	6.6	5.5	5.3	3.6	134.4	0.6	4.3	383.8	384.5	0.6	0.6	3.6	70.5	22.2	1.0	2303.2
	0.0	0.5	1.3	135.4	24.8	0.3	3.4	348.3	0.5	0.4	0.1	0.3	10.9	0.0	0.3	21.9	22.6	0.0	0.0	0.4	4.4	1.6	0.2	175.2
Salt mash 4	0.6	17.6	18.8	6319.6	245.8	3.8	27.0	2670.3	4.6	4.4	3.5	7.5	148.2	0.6	2.7	252.6	241.7	0.6	0.6	7.2	42.9	21.1	0.9	1149.8
	0.0	1.7	2.6	730.3	25.7	0.4	3.3	302.4	0.6	0.5	0.4	1.2	14.7	0.0	0.4	20.2	19.1	0.0	0.0	1.0	4.7	2.1	0.1	133.1
Salt mash 5	25.8	9.8	32.3	7857.7	945.6	41.6	163.3	10,713.6	8.4	28.1	2.0	4.2	35.9	6.0	29.7	231.8	212.2	993.2	3.0	0.0	88.7	8.3	0.6	2349.4
	7.4	1.4	4.6	1666.2	112.9	6.2	18.9	1705.7	0.9	3.1	0.3	0.3	5.6	0.5	3.6	21.9	21.0	114.1	0.4	0.0	7.5	0.7	0.0	285.2
Salt mash 6	8.5	7.0	19.6	3749.7	423.6	11.8	45.4	15,739.0	7.5	24.8	1.5	2.8	25.5	1.1	4.5	274.6	269.7	206.2	0.6	1.5	64.2	9.8	0.6	256.5
	2.7	1.6	0.8	184.2	58.6	0.7	3.3	654.9	0.2	6.5	0.3	0.7	7.0	0.2	0.6	15.4	15.2	75.3	0.0	0.6	2.3	1.2	0.0	37.3
Salt mash 7	1.5	5.7	36.6	1378.7	22.2	29.1	69.5	1357.3	11.1	73.6	1.1	0.6	16.0	3.8	2.1	265.4	293.0	24.5	1.0	0.0	97.3	20.1	0.6	103.5
	0.4	0.3	1.0	60.5	1.2	1.0	5.4	287.6	0.4	11.7	0.2	0.0	0.6	0.0	0.3	21.3	23.3	1.1	0.1	0.0	2.4	0.8	0.0	5.3

Table 2
Factor loadings of the individual variables obtained by a Principal Component Analysis (PCA) on chemical elements in sediments from the Joint Odiel and Tinto Estuary (Southwest Iberian Peninsula). Factor loadings > ± 0.600 are marked in bold. Kruskal-Wallis H-test for regression factor scores from PC for every sediment sample compared between locations (d. f. = 6).

Element	PC1	PC2	PC3	PC4	PC5	PC6	PC7	PC8
Gd	**0.958**	−0.161	−0.160	0.104	0.032	−0.061	−0.023	0.006
U	**0.886**	−0.224	−0.024	−0.127	−0.170	0.136	−0.130	0.141
Bi	**0.883**	−0.161	0.034	−0.312	0.017	−0.081	0.116	−0.103
Ba	**0.880**	−0.377	−0.113	−0.029	−0.047	−0.136	0.004	−0.075
Sr	**0.877**	−0.353	−0.105	0.094	0.036	0.031	−0.147	0.090
Er	**0.872**	0.412	−0.166	0.016	−0.069	−0.009	0.058	0.076
Ce	**0.869**	−0.407	−0.155	0.107	0.106	−0.100	−0.013	−0.031
As	**0.855**	−0.340	−0.099	−0.028	−0.163	0.084	0.125	−0.070
Y	**0.849**	−0.378	−0.067	−0.205	0.138	0.049	−0.032	0.126
Yb	**0.847**	0.458	−0.148	−0.016	−0.085	−0.070	0.018	0.061
Zr	**0.837**	0.242	−0.356	0.128	−0.197	−0.057	−0.037	−0.065
Ti	**0.834**	−0.137	−0.091	−0.013	0.192	−0.076	0.162	0.022
Mg	**0.829**	0.052	0.228	−0.175	0.281	−0.047	0.185	0.204
Zn	**0.755**	−0.270	0.332	0.325	0.178	−0.009	0.026	0.155
Cu	**0.734**	−0.219	0.505	0.243	0.161	−0.131	−0.120	−0.031
Sc	**0.701**	0.247	0.292	−0.434	0.263	−0.104	0.158	−0.074
V	**0.691**	0.233	0.400	−0.333	0.263	0.040	0.227	−0.017
Sn	**0.690**	−0.357	0.061	0.160	−0.087	−0.322	−0.225	0.064
Eu	**0.671**	−0.154	0.163	−0.222	−0.261	0.459	−0.051	0.217
P	**0.649**	−0.178	0.483	0.028	−0.085	0.108	−0.290	−0.105
Li	0.566	−0.229	−0.019	−0.092	−0.234	0.467	−0.265	0.160
Tm	0.090	**0.960**	−0.115	0.172	−0.096	0.051	−0.030	−0.030
Ho	0.132	**0.952**	−0.175	0.144	−0.107	0.043	−0.017	−0.013
In	0.197	**0.882**	−0.125	0.150	−0.196	0.011	0.098	0.129
Cr	0.464	**0.851**	−0.171	−0.078	−0.070	0.028	0.010	−0.001
Mo	0.270	**0.818**	−0.343	0.161	−0.233	0.010	0.016	−0.090
Ga	0.123	**0.788**	−0.217	0.131	−0.115	0.040	−0.026	−0.017
Cd	0.566	**0.754**	−0.037	0.072	−0.122	0.065	0.023	0.019
Dy	0.598	**0.726**	−0.271	0.148	−0.096	0.005	−0.021	0.018
Ni	0.617	**0.627**	0.157	−0.133	0.336	−0.075	0.010	−0.014
Tb	−0.240	0.396	0.242	−0.242	0.323	0.214	−0.008	0.310
Th	−0.066	0.072	**0.870**	0.297	0.049	0.001	−0.061	−0.090
Tl	−0.329	0.165	**0.845**	0.213	0.003	0.038	0.002	−0.021
Rb	0.053	0.419	**0.811**	0.127	0.152	0.022	0.006	0.037
Fe	−0.065	−0.032	**0.687**	0.097	−0.500	−0.143	0.379	0.082
Pb	0.598	−0.184	**0.682**	0.141	−0.097	−0.018	0.067	−0.096
Mn	−0.063	0.327	**0.661**	0.339	0.272	0.213	−0.239	−0.126
Co	0.170	0.487	0.579	0.387	0.268	0.147	−0.210	−0.111
Se	−0.359	0.469	0.082	**−0.629**	0.358	0.117	0.133	0.079
La	−0.273	0.098	0.043	**−0.608**	0.492	0.221	0.037	0.207
Ca	0.255	−0.299	−0.261	0.574	0.292	0.373	0.072	0.159
Nd	0.172	−0.261	−0.299	0.532	0.335	0.307	0.522	−0.093
S	0.079	−0.122	0.390	−0.104	**−0.602**	−0.294	0.450	0.095
Pr	0.345	−0.125	0.143	−0.276	−0.463	0.519	0.086	−0.234
Be	0.410	0.211	0.079	−0.247	0.359	−0.501	0.144	−0.326
Cs	−0.017	−0.008	0.429	−0.447	−0.363	0.490	0.173	−0.343
Sm	−0.036	−0.179	−0.304	0.534	0.322	0.335	0.557	−0.091
Nb	−0.365	0.115	0.478	0.214	−0.304	−0.194	0.224	0.499
Eigenvalues	16.256	9.086	6.299	3.509	2.997	2.101	1.617	1.047
Explained variance (%)	33.9	18.9	13.1	7.3	6.2	4.4	3.4	2.2
Kruskal-Wallis H-test	50.479	59.530	61.160	50.541	41.137	44.794	37.134	12.807
P	0.000	0.000	0.000	0.000	0.000	0.000	0.000	0.046

on the right and left banks of the Tinto River close to the PG stacks, however, relatively high concentrations of these two elements extended across a wide area along the main channel of the estuary (Fig. 4c).

The second principal component (PC2, explaining 18.9 % of variance) was positively correlated with 9 elements with factor loadings higher than +0.600, including Tm, Ho, Cr, Mo, Ga, Cd and Ni (Table 2). The concentrations of these elements were the highest in the sediments from A1 and A2 (Table 1, Fig. 3c). Regression factor scores for PC2 were the lowest for A1, A3 and A4 (Fig. S2).

PC3 explained 13.1 % of the variance and was positively correlated with 6 elements with factor loadings higher than +0.600 (Th, Tl, Rb, Fe, Pb and Mn; Table 2). Regression factor scores for PC3 were the highest for A5, which was close to an abandoned foundry (Fig. S2). High concentrations of Th were mostly associated with sediments close to the abandoned foundry (Fig. 4f); concentrations of Fe were also associated with the abandoned foundry but increased moving upstream along both the Odiel and Tinto Rivers (Fig. 3e and Fig. 4g). Concentrations of Pb were higher upstream in the Tinto River and downstream along the main channel of the estuary than in sediments located at intermediate locations in the Odiel and Tinto Rivers (Figs. 3f and 4h).

PC4 (explaining 7.3 % of variance) was negatively correlated with Se and La (Table 2). Its regression factor scores were the highest for A3 and A5 and the lowest for A7 (Fig. S2), where La and Se showed their maximum concentrations (Fig. 3g, Table 1). PC5 (explaining 6.2 % of variance) was negatively correlated with S concentrations (Table 2), and its regression factor scores were the lowest upstream in the Tinto River (A6; Fig. S2). Sulphur concentrations were highest in sediments located upstream in the Tinto River, and reduced gradually moving downstream towards the ocean (Figs. 3d and 4e). PC6 explained 4.4 % of the variance and was positively correlated with Pr and Cs and negatively with Be (Fig. 4d, Table 2). These two elements, Pr and Cs, had maximum concentrations in A5 and A6 (Fig. 3h). The regression factor scores for PC6

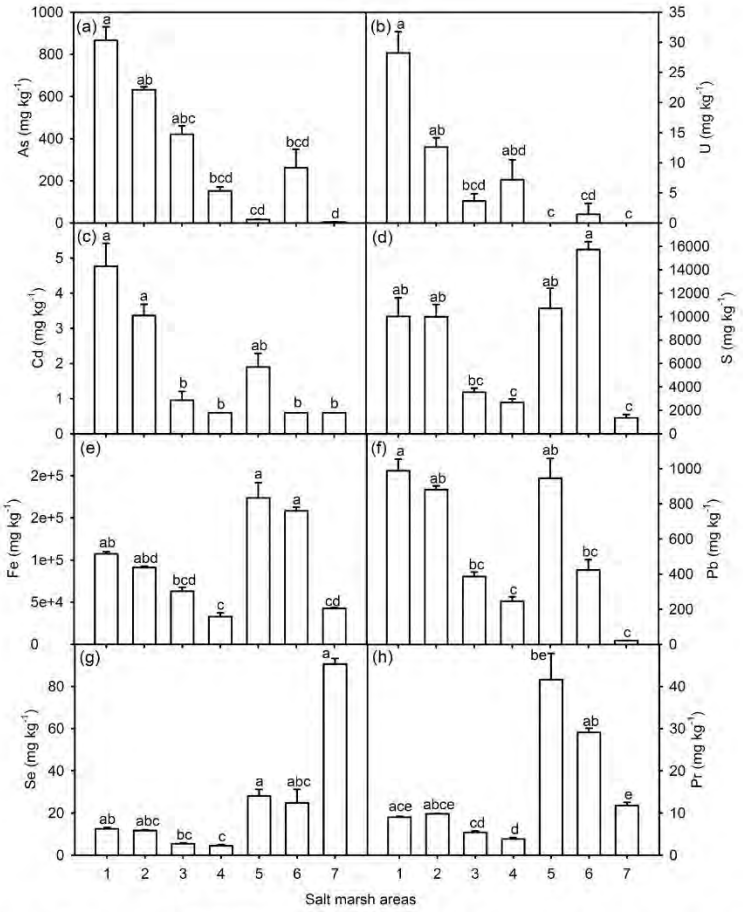

Fig. 3. Total concentrations (mg kg-1 DW) of (a) As, (b) U, (c) Cd, (d) S, (e Fe, (f) Pb, (g) Se and (h) Pr in sediments from the Odiel-Tinto Estuary (1–6) and the Estuary of Piedras River (7) in Southwest Iberian Peninsula. Data are arithmetic means ± SEM (n = 10). Salt marsh areas are shown in Fig. 1. Different letters indicate significant differences between salt marsh areas (Tukey test, $p < 0.05$).

were the highest for A1 and A3 and the lowest for A2 (Fig. S2).

4. Discussion

By modelling the spatial distribution of 48 chemical elements in sediments from seven salt marsh areas across the Odiel–Tinto Estuary, we successfully identified three unique chemical signatures linked to specific pollution sources: in salt marsh sediments from AMD upstream of the Tinto River, in sediments located near PG waste piles and in sediments near an abandoned foundry.

Peak concentrations of 20 elements were found in sediments near the PG stacks (site A1). These elements were associated with PC1, which explained the greatest proportion of the data variance (34 %). Notably, most of these 20 elements have been previously documented in edge outflows and nanoparticles originating from PG stacks within the study area (Millán-Becerro et al., 2023; Pérez-López et al., 2016; Ruiz Cánovas et al., 2018; Silva et al., 2022). Among radionuclides, U-series isotopes possess the highest mobility within PG stacks (Pérez-Moreno et al., 2018). The majority of these 20 elements associated with sediments near the PG stacks, including Al, Cr, Fe, Pb and U, tend to precipitate under neutral seawater conditions (pH 6.9 ± 0.1) through co-precipitation and/or adsorption onto phosphate phases. Fluoride precipitation also contributes to their removal (Guerrero et al., 2020; Papaslioti et al., 2018). Additionally, elements like As, Cd, Co, Cr, Cu, Ni, Pb, U and Zn precipitate when the sediment pH exceeds 4 and Eh falls below +340 mV. This is facilitated by Fe-limited sulphide precipitation, particularly in organic-rich sediments with low Eh(DeLaune and Reddy, 2005; Guerrero et al., 2019; Hierro et al., 2014a; Pérez-López et al., 2011, 2018; Santos Bermejo et al., 2003). Consequently, a significant portion of the chemical elements present in acidic leachates from the PG stacks have the potential to precipitate and become immobilised within the surrounding fine-textured, near-neutral, oxidised (Eh 248 ± 6 mV) sediments.

The PG stacks are located in the estuarine zone where seawater meets the Tinto River. This zone is characterised by a sharp shift in water properties, with salty and neutral–basic ocean waters encountering acidic, brackish river water (Chica-Olmo et al., 2004). This meeting point leads to the neutralisation of acidic waters, causing the precipitation of chemical elements from both the PG stacks and those transported down the Tinto River. This phenomenon is reflected in a significant decrease in Cu concentrations in the water just downstream of the PG stacks (Chica-Olmo et al., 2004). Interestingly, arsenic

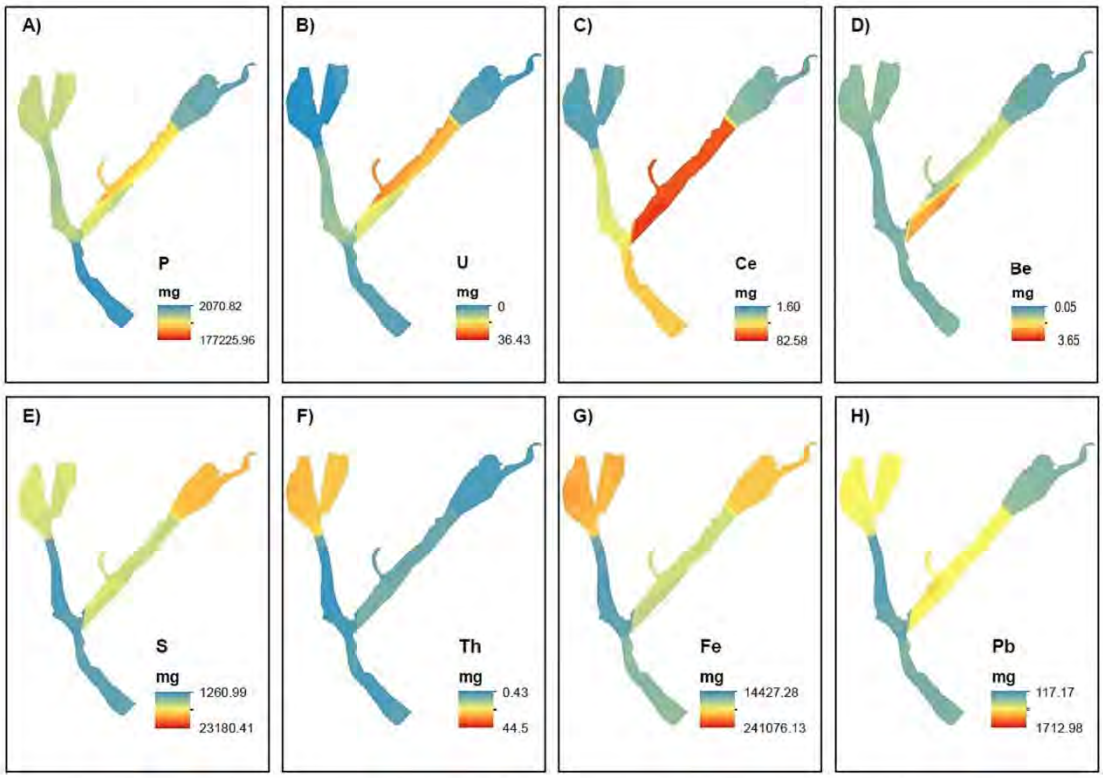

Fig. 4. Spatial distribution of representative chemical elements ((a) P, (b) U, (c) Gd, (d) Ce, (e) S, (f) Th, (g) Fe, and (h) Pb) in the Odiel-Tinto Estuary.

concentrations at the levels recorded in our study (866.5 ± 64.0 mg kg^{-1}) may show high ecotoxicity levels when accumulated in marsh sediments (Hwang et al., 2008).

Guerrero et al. (2019) suggested phosphorus as a suitable tracer to determine the impact of PG stacks on sediments. Phosphorus dissolves in the PG pore water as phosphoric acid, which is the main source of phosphoric acid for marshes, i.e. it is not associated with AMD or other sources of pollution. In addition to P, our study identified trace elements such as Gd, Bi, Ce and Zr as potential geochemical tracers. These elements exhibited relatively high concentrations, characteristic of the pollution signature of the PG stacks in the salt marsh sediments. Elements with the highest loadings in PC2 (Cd, Cr, Dy, Ga, Ho, Ni and Tm) showed the greatest sediment concentrations in salt marshes near the PG stacks on both banks of the Tinto River (A1 and A2). Some of these elements, particularly Cd and Ni, have a higher tendency to remain in solution when pH increases, compared to elements associated with PC1, with an average removal of around 60 % (Beltrán et al., 2010; Hierro et al., 2014a; Morillo et al., 2008; Sáenz et al., 2003).

Several chemical elements previously identified in PG stack outflows by Pérez-López et al. (2016), including major elements (Fe and S) and trace elements (Cd, Co, Pb and Ni), were not among those with the highest loadings in PC1, the principal component characterising the sediments near the PG stacks. However, Co, Fe and Pb exhibited the highest sediment concentrations—alongside Mn, Th, Tl and Rb—within the salt marshes closest to the abandoned foundry's mineral waste (site A5; Curado et al., 2014). Studies by Morillo et al. (2008), Beltrán et al. (2010), and Hierro et al. (2014b) have suggested that element precipitation, particularly that of Fe, is significant during rising tides in this area. Notably, elements typically associated with AMD, such as Co, Fe, Pb, Mn, Tl and Rb (da Silva et al., 2005; Fernández-Landero et al., 2023; Millan-Becerro et al., 2024) exhibited the highest loadings on PC3, a component explaining 13 % of the data variance across the estuary. This association suggests their utility as geochemical tracers for AMD pollution.

Our analysis revealed the highest total sulphur concentrations in upstream sediments in the Tinto River (site A6). These concentrations (15,739 ± 655 mg kg^{-1}) were 32 % higher than the second-highest value (site A5). Notably, sulphur was the only chemical element with a factor loading exceeding 0.600 in PC5, which explained 6 % of the data variance. This suggests that relatively high sulphur concentrations serve as a unique geochemical marker upstream in the highly polluted Tinto River Estuary. The low pH and high Eh in this environment, driven by extensive pyrite oxidation, promote the dissolution of large quantities of toxic elements and radionuclides (Mehdi et al., 2013).

Estuarine sediments in the Piedras River displayed relatively high concentrations of Se and La. These elements were strongly associated with PC4, explaining 7.3 % of the data variance. Alkaline soils are known to release more Se than acidic ones (Santos Bermejo et al., 2003). This aligns with the higher Se concentrations observed in the Piedras River salt marshes (site A7), as its hydrological basin is not impacted by AMD, unlike those of the Odiel and Tinto Rivers.

Two sampling sites (A2 and A7), situated near intensive strawberry cultivation in greenhouses exhibited the highest average beryllium concentrations (1.5–2.7 mg kg^{-1}). These values were over 40 % higher than those measured near the PG stacks (site A1), despite beryllium being identified as a trace element in these waste deposits (Silva et al.,

2022). Beryllium was associated with PC6, which explained 4 % of the data variance. Interestingly, PC6 clearly distinguished sediments near the PG stacks (site A1) from those across the Tinto River (site A2) with elevated beryllium. This suggests that beryllium may be a suitable geochemical marker for tracing the influence of intensive agriculture on the area's pollution profile. Given its widespread use in metal alloys, beryllium could potentially originate from the greenhouses' metal structures and become readily trapped in sediment (ATSDR, 2022).

Many studies have been conducted on the spatial distribution of heavy metals in other highly polluted locations providing important data for pollution management and future remediation (Dong et al., 2024; Liu et al., 2024; Sun et al., 2025). Our study characterises the sediment pollution signatures in a highly polluted Spanish estuary that has not yet been well researched. This characterisation allows us to differentiate between pollution sources including PG stacks, AMD in waste deposits and agricultural activities. This knowledge is valuable for developing integrated monitoring and pollution management plans, which can quantify and ultimately reduce the impacts of pollution from each source. The specific sediment pollution signatures identified in this study may be used as a reference to determine the impact of future interventions on existing pollution sources in the Odiel–Tinto Estuary. This study is critical for assessing the impact of the RESTORE 2030 plan, which is currently undergoing judicial review and being re-evaluated. Additionally, this study identified the sediment pollution signature of an abandoned foundry, which is located next to a residential area. The findings may also be used to evaluate future restoration plans for this area, which was declared contaminated by the Andalusian Government in 2007 (BOJA No. 168, 2007).

As the specific causes of the excess mortality rates in the Huelva area (Alguacil et al., 2014; Benach et al., 2003; Lopez-Abente et al., 2001) are known to be related to industrial and mining metal environmental pollution (Briffa et al., 2020), we believe that studying correlations between the original sources responsible for the pollutants accumulated in the sediments of the Huelva Estuary and mortality in Huelva is warranted from a public health perspective. Biomonitoring of the population and ecosystem's exposure to metals is also justified, as recommended by at least two different independent panels of scientific experts (Alguacil et al., 2014; Scientific committee, 2022).

5. Conclusions

We identified a specific pollution signature for PG stacks that distinguishes metal exposure from the other pollution sources in the Odiel–Tinto Estuary—AMD near mining waste deposits, pollution along the Tinto River and areas under intensive agricultural cultivation. The sediment pollution signature near the PG stacks was characterised by 20 elements such as Gd, U, As, Mg, Zn, Cy and P. Sediments near mining waste deposits specifically accumulated six elements, including Fe, Pb and Mn. The pollution signature in the sediment of the Tinto River was marked by high sulphur accumulation. Beryllium is a suitable marker for tracing the influence of intensive agriculture. These results provide a valuable tool for discriminating between different pollution sources, quantifying the most impacted areas of the salt marsh, assigning responsibility to the various polluting entities within the estuary, and setting a starting point to evaluate the impact of the RESTORE 2030 restoration plan for the Huelva estuary. These specific sediment pollution signatures may also be used as a reference to determine the impact of future interventions on existing pollution sources in other estuaries and marshes polluted with PG.

CRediT authorship contribution statement

Manuel Contreras-Llanes: Writing – review & editing, Writing – original draft, Visualization, Validation, Supervision, Resources, Methodology, Investigation, Conceptualization. **Vanessa Santos-Sánchez:** Writing – review & editing, Validation, Software, Formal analysis, Data curation. **Juan Alguacil:** Writing – review & editing, Visualization, Validation, Resources, Project administration, Methodology, Funding acquisition, Conceptualization. **Jesús M. Castillo:** Writing – review & editing, Writing – original draft, Visualization, Validation, Supervision, Software, Methodology, Investigation, Formal analysis, Data curation, Conceptualization.

Funding

This research was funded by the Andalusian Government, '2018 Special Action of the Andalusian Government: Support to the Huelva Phosphogypsum Experts Committee'; and by Huelva University local funds to support research groups during 2018 to 2023.

Declaration of competing interest

The authors declare the following financial interests/personal relationships which may be considered as potential competing interests: Juan Alguacil reports financial support was provided by Andalusian Government. If there are other authors, they declare that they have no known competing financial interests or personal relationships that could have appeared to influence the work reported in this paper.

Acknowledgments

We want to thank the technical advice and support from M.A. Garcia-Sevillano and J.L. Gomez-Ariza on how to proceed with the sample processing, and to Adrian Polonio for sample collection support. We thank the management of the Odiel Marshes Natural Park for its collaboration.

Appendix A. Supplementary data

Supplementary data to this article can be found online at https://doi.org/10.1016/j.scitotenv.2024.177715.

Data availability

Data will be made available on request.

References

Achterberg, E.P., Herzl, V.M.C., Braungardt, C.B., Millward, G.E., 2003. Metal behaviour in an estuary polluted by acid mine drainage: the role of particulate matter. Environ. Pollut. 121, 283–292. https://doi.org/10.1016/S0269-7491(02)00216-6.

Agency for Toxic. Substances and Disease Registry (ATSDR) and the Environmental Protection Agency (EPA), 2022. Toxicological Profile for Beryllium. U.S. Department of Health and Human Services. https://www.atsdr.cdc.gov/toxprofiles/tp4.pdf.

Alguacil, J., Ballester, F., Donado-Campos, J., Pollán, M., Rodríguez-Artalejo, F., 2014. Dictamen realizado por encargo del Defensor del Pueblo Andaluz sobre El exceso de mortalidad y morbilidad detectado en varias investigaciones en La Ría de Huelva. Grupo de Trabajo de la Sociedad Española de Epidemiología. Huelva. https://www.defensordelpuebloandaluz.es/sites/default/files/Huelva.pdf.

Barba-Brioso, C., Fernández-Caliani, J.C., Miras, A., Cornejo, J., Galán, E., 2010. Multi-source water pollution in a highly anthropized wetland system associated with the estuary of Huelva (SW Spain). Mar. Pollut. Bull. 60, 1259–1269. https://doi.org/10.1016/j.marpolbul.2010.03.018.

Beltrán, R., de la Rosa, J.D., Santos, J.C., Beltrán, M., Gómez Ariza, J.L., 2010. Heavy metal mobility assessment in sediments from the Odiel River (Iberian Pyritic Belt) using sequential extraction. Environ. Earth Sci. 61, 1493–1503. https://doi.org/10.1007/s12665-010-0465-y.

Benach, J., Yasui, Y., Borrell, C., Rosa, E., Pasarín, M.I., Benach, N., Español, E., Martínez, J.M., Daponte, A., 2003. Examining geographic patterns of mortality: the atlas of mortality in small areas in Spain (1987-1995). Eur. J. Public Health 13 (2), 115–123. https://doi.org/10.1093/eurpub/13.2.115.

Blasco, J., Sáenz, V., Gómez-Parra, A., 2000. Heavy metal fluxes at the sediment–water interface of three coastal ecosystems from south-west of the Iberian Peninsula. Sci. Total Environ. 247, 189–199. https://doi.org/10.1016/S0048-9697(99)00490-8.

BOJA No. 168, 2007. Resolution of August 7, 2007, of the General Directorate of Prevention and Environmental Quality, declaring two plots of the Partial Residential Plan No. 9 of Aljaraque (Huelva) as contaminated soil. Bulletin number 168, 80-82. Official Gazette of the Government of Andalusia - BOJA. https://www.juntadeandalucia.es/boja/2007/168/9.

Borrego, J., Morales, J., de la Torre, M., Grande, J., 2022. Geochemical characteristics of heavy metal pollution in surface sediments of the Tinto and Odiel river estuary (southwestern Spain). Environ. Geol. 41, 785–796. https://doi.org/10.1007/s00254-001-0445-3.

Bouyoucos, G.J., 1936. Directions for making mechanical analysis of soils by the hydrometer method. Soil Sci. 4, 225–228. https://doi.org/10.1097/00010694-193609000-00007.

Briffa, J., Sinagra, E., Blundell, R., 2020. Heavy metal pollution in the environment and their toxicological effects on humans. Heliyon 6 (9), e04691. https://doi.org/10.1016/j.heliyon.2020.e04691.

Carro, B.M., Reyes, A., Morales, J.A., Borrego, J., 2021. Application of the comparison of multibeam echo-sound records to the study of stability of a toxic waste stockpile located on the margin of a tidal system: Tinto estuary, Huelva, SW Spain. Remote Sens. 13, 4364. https://doi.org/10.3390/rs13214364.

Chica-Olmo, M., Rodriguez, F., Abarca, F., Rigol-Sanchez, J.P., deMiguel, E., Gomez, J. A., Fernandez-Palacios, A., 2004. Integrated remote sensing and GIS techniques for biogeo- chemical characterization of the Tinto-Odiel estuary system, SW Spain. Environ. Geo. 45, 834–842. https://doi.org/10.1007/s00254-003-0943-6.

Curado, G., Rubio-Casal, A.E., Figueroa, E., Castillo, J.M., 2010. Germination and establishment of the invasive cordgrass Spartina densiflora in acidic and metal polluted sediments of the Tinto River. Mar. Pollut. Bull. 60, 1842–1848. https://doi.org/10.1016/j.marpolbul.2010.05.022.

Curado, G., Rubio-Casal, A.E., Figueroa, E., Castillo, J.M., 2014. Plant zonation in restored, nonrestored, and preserved Spartina maritima salt marshes. J. Coast. Res. 30, 629–634. https://doi.org/10.2112/JCOASTRES-D-12-00089.1.

Davila, J.M., Sarmiento, A.M., Santisteban, M., Luís, A.T., Fortes, J.C., Diaz-Curiel, J., Valbuena, C., Grande, J.A., 2019. The UNESCO national biosphere reserve (Marismas del Odiel, SW Spain): an area of 18,875 ha affected by mining waste. Environ. Sci. Pollut. Res. 26, 33594–33606. https://doi.org/10.1007/s11356-019-06438-7.

DeLaune, R.D., Reddy, K.R., 2005. Redox Potential. In: Hillel, Daniel (Ed.), Encyclopedia of Soils in the Environment. Elsevier, pp. 366–371. ISBN 9780123485304. https://doi.org/10.1016/B0-12-348530-4/00212-5.

Dong, Y., Lu, H., Lin, H., 2024. Comprehensive study on the spatial distribution of heavy metals and their environmental risks in high-sulfur coal gangue dumps in China. Journal of Environ- mental Sciences 136, 486–497. https://doi.org/10.1016/j.jes.2022.12.023.

Elbaz-Poulichet, F., Morley, N., Cruzado, A., Velásquez, Z., Achterberg, E., Braungardt, C., 1999. Trace metal and nutrient distribution in an extremely low pH (2.5) river–estuarine system, the ria of Huelva (south–West Spain). Sci. Total Environ. 227, 73–83. https://doi.org/10.1016/S0048-9697(99)-00006-6.

Fernández-Landero, S., Fernández-Caliani, J.C., Giráldez, M.I., Morales, E., Barba-Brioso, C., González, I., 2023. Soil contaminated with hazardous waste materials at Río Tinto mine (Spain) is a persistent secondary source of acid and heavy metals to the environment. Minerals 13, 456. https://doi.org/10.3390/min13040456.

Figueroa, M.E., Castillo, J.M., Redondo-Gómez, S., Luque, T., Castellanos, E.M., Nieva, F. J., Luque, C., Rubio-Casal, A.E., Davy, A.J., 2003. Facilitated invasion by hybridization of Sarcocornia species in a salt marsh succession. J. Ecol. 91, 616–626. https://doi.org/10.1046/j.1365-2745.2003.00794.x.

González, F., 2022. InSAR-based mapping of ground deformation caused by industrial waste disposals: the case study of the Huelva phosphogypsum stack, SW Spain. Bull. Eng. Geol. Environ. 81, 304. https://doi.org/10.1007/s10064-022-02809-6.

Guerrero, J.L., Gutiérrez-Álvarez, I., Mosqueda, F., Olías, M., García-Tenorio, R., Bolívar, J.P., 2019. Pollution evaluation on the salt marshes under the phosphogypsum stacks of Huelva due to deep leachates. Chemosphere 230, 219–229. https://doi.org/10.1016/j.chemosphere.2019.04.212.

Guerrero, J.L., Pérez-Moreno, S.M., Gutiérrez-Álvarez, I., Gázquez, M.J., Bolívar, J.P., 2020. Behaviour of heavy metals and natural radionuclides in the mixing of phosphogypsum leachates with seawater. Environ. Pollut. 268, 115843. https://doi.org/10.1016/j.envpol.2020.115843.

Guerrero, J.L., Gutiérrez-Álvarez, I., Hierro, A., Pérez-Moreno, S.M., Olías, M., Bolívar, J. P., 2021. Seasonal evolution of natural radionuclides in two rivers affected by acid mine drainage and phosphogypsum pollution. CATENA 197, 104978. https://doi.org/10.1016/j.catena.2020.104978.

Hierro, A., Olías, M., Ketterer, M.E., Vaca, F., Borrego, J., Cánovas, C.R., Bolívar, J.P., 2014a. Geochemical behavior of metals and metalloids in an estuary affected by acid mine drainage (AMD). Environ. Sci. Pollut. Res. Int. 21, 2611–2627. https://doi.org/10.1007/s11356-013-2189-5.

Hierro, A., Olías, M., Cánovas, C.R., Martín, J.E., Bolívar, J.P., 2014b. Trace metal partitioning over a tidal cycle in an estuary affected by acid mine drainage (Tinto estuary, SW Spain). Sci. Total Environ. 497–498, 18–28. https://doi.org/10.1016/j.scitotenv.2014.07.070.

Hwang, H.M., Green, P.G., Young, T.M., 2008. Tidal salt marsh sediment in California, USA: part 3. Current and historic toxicity potential of contaminants and their bioaccumulation. Chemosphere 71, 2139–2149. https://doi.org/10.1016/j.chemosphere.2008.01.005.

Kerl, C.F., Basallote, M.D., Käberich, M., Oldani, E., Cerón Espejo, N.P., Colina Blanco, A. E., Ruiz Cánovas, C., Nieto, J.M., Planer-Friedrich, B., 2023. Consequences of sea level rise for high metal(loid) loads in the Ría of Huelva estuary sediments. Sci. Total Environ. 873, 162354. https://doi.org/10.1016/j.scitotenv.2023.162354.

Lario, J., Alonso-Azcárate, J., Spencer, C., Zazo, C., Goy, J.L., Cabero, A., Dabrio, C.J., Borja, F., Borja, C., Civis, J., García-Ródriguez, M., 2016. Evolution of the pollution in the Piedras River Natural Site (Gulf of Cadiz, southern Spain) during the Holocene. Environ. Earth Sci. 75, 481. https://doi.org/10.1007/s12665-016-5344-8.

Leistel, J.M., Marcoux, E., Thieblemont, D., Quesada, C., Sanchez, A., Almodovar, G.R., Pascual, E., Saez, R., 1998. The volcanic hosted massive sulphide deposits of the Iberian Pyrite Belt. Miner. Deposita 33, 2–30. https://doi.org/10.1007/s001260050130.

Li, C., Wang, H., Liao, X., Xiao, R., Liu, K., Bai, J., Li, B., He, Q., 2022. Heavy metal pollution in coastal wetlands: a systematic review of studies globally over the past three decades. J. Hazard. Mater. 424 Part A, 127312. https://doi.org/10.1016/j.jhazmat.2021.127312.

Lieberman, R.N., Izquierdo, M., Córdoba, P., Moreno Palmerola, N., Querol, X., Sánchez de la Campa, A.M., Font, O., Cohen, H., Knop, Y., Torres-Sánchez, R., Sánchez-Rodas, D., Muñoz Quiros, C., de la Rosa, J.D., 2020. The geochemical evolution of brines from phosphogypsum deposits in Huelva (SW Spain) and its environmental implications. Sci. Total Environ. 700, 134444. https://doi.org/10.1016/j.scitotenv.2019.134444.

Liu, H., Zeng, W., He, M., 2024. Distribution, sources, contamination, and risks of toxic metals in Zijiang River, a typical tributary of the midstream of the Yangtze River in China. Journal of Environmental Sciences. https://doi.org/10.1016/j.jes.2023.12.030. In Press, Corrected Proof.

Lopez-Abente, G., Pollán, M., Escolar, A., Errezola, M., Abraira, V., 2001. Atlas of cancer morta-lity and other causes of death in Spain 1978-1992. In: Instituto de Salud Carlos III (ISCIII). Centro Nacional de Epidemiología (CNE), Madrid. http://hdl.handle.net/20.500.12105/4953.

López-Coto, I., Mas, J.L., Vargas, A., Bolívar, J.P., 2014. Studying radon exhalation rates variability from phosphogypsum piles in the SW of Spain. J. Hazard. Mater. 280, 464–471. https://doi.org/10.1016/j.jhazmat.2014.07.025.

Lu, G.Y., Wong, D.W., 2008. An adaptive inverse-distance weighting spatial interpolation technique. Comput. Geosci. 34, 1044–1055. https://doi.org/10.1016/j.cageo.2007.07.010.

Martínez-Beneito, M.A., Botella-Rocamora, P., Corpas-Burgos, F., Vergara-Hernández, C., Pérez-Panadés, J., Perpiñán-Fabuel, H., 2024. Atlas Nacional de Mortalidad en España (ANDEES). Fundación FISABIO y Dirección General de Salud Pública de la Generalitat Valenciana, Valencia. http://andees.fisabio.san.gva.es/.

Mehdi, Y., Hornick, J.L., Istasse, L., Dufrasne, I., 2013. Selenium in the environment, metabolism and involvement in body functions. Molecules 18, 3292–3311. https://doi.org/10.3390/molecules18033292.

Millán-Becerro, R., Pérez-López, R., Cánovas, C.R., Macías, F., León, R., 2023. Phosphogypsum weathering and implications for pollutant discharge into an estuary. J. Hydrol. 617, 128943. https://doi.org/10.1016/j.jhydrol.2022.128943.

Millan-Becerro, R., León, R., Romero Matos, J., Moreno González, R., Pérez López, R., 2024. Towards circular and sustainable restoration of a deeply polluted river basin: the Odiel River catchment (SW Spain). Sci. Total Environ. 907, 168078. https://doi.org/10.1016/j.scitotenv.2023.168078.

Morillo, J., Usero, J., Rojas, R., 2008. Fractionation of metals and as in sediments from a biosphere reserve (Odiel salt marshes) affected by acidic mine drainage. Environ. Monit. Assess. 139, 329–337. https://doi.org/10.1007/s10661-007-9839-3.

Nie, J., Feng, H., Witherell, B.B., Alebus, M., Mahajan, M.D., Zhang, W., Yu, L., 2018. Assess- ment, and treatment of nutrient (N and P) pollution in Rivers, estuaries, and coastal waters. Curr. Pollut. Rep. 4, 154–161. https://doi.org/10.1007/s40726-018-0083-y.

Papasliotí, E.M., Pérez López, R., Parviainen, A., Sarmiento, A.M., Nieto, J.M., Marchesi, C., Delgado-Huertas, A., Garrido, C.J., 2018. Effects of seawater mixing on the mobility of trace elements in acid phosphogypsum leachates. Mar. Pollut. Bull. 127, 695–703. https://doi.org/10.1016/j. marpolbul.2018.01.001.

Pérez López, R., Nieto, J.M., López-Coto, I., Aguado, J.L., Bolívar, J.P., Santisteban, M., 2010. Dynamics of contaminants in phosphogypsum of the fertilizer industry of Huelva (SW Spain): from phosphate rock ore to the environment. Appl. Geochem. 25, 705–715. https://doi.org/10.1016/j.apgeochem.2010.02.003.

Pérez-López, R., Castillo, J., Sarmiento, A.M., Nieto, J.M., 2011. Assessment of phosphogypsum impact on the salt-marshes of the Tinto river (SW Spain): role of natural attenuation processes. Mar. Pollut. Bull. 62, 2787–2796. https://doi.org/10.1016/j.marpolbul.2011.09.008.

Pérez-López, R., Macías, F., Ruiz Cánovas, C., Sarmiento, A.M., Pérez-Moreno, S.M., 2016. Pollutant flows from a phosphogypsum disposal area to an estuarine environment: an insight from geochemical signatures. Sci. Total Environ. 553, 42–51. https://doi.org/10.1016/j.scitotenv.2016. 02.070.

Pérez-López, R., Carrero, S., Cruz-Hernández, P., Asta, M.P., Macías, F., Cánovas, C.R., Guglieri, C., Nieto, J.M., 2018. Sulfate reduction processes in salt marshes affected by phosphogypsum: geochemical influences on contaminant mobility. J. Hazard. Mater. 350, 154–161. https://doi.org/10.1016/j.jhazmat.2018.02.001.

Pérez-López, R., Millán-Becerro, R., Basallote, M.D., Carrero, S., Parviainen, A., Freydier, R., Macías, F., Cánovas, C.R., 2023. Effects of estuarine water mixing on the mobility of trace elements in acid mine drainage leachates. Mar. Pollut. Bull. 187, 114491. https://doi.org/10.1016/j.marpolbul.2022.114491.

Pérez-Moreno, S.M., Gázquez, M.J., Pérez-López, R., Vioque, I., Bolívar, J.P., 2018. Assessment of natural radionuclides mobility in a phosphogypsum disposal area. Chemosphere 211, 775–783. https://doi.org/10.1016/j.chemosphere.2018.07.193.

Rentería-Villalobos, M., Vioque, I., Mantero, J., Manjón, G., 2010. Radiological, chemical and morphological characterizations of phosphate rock and phosphogypsum from phosphoric acid factories in SW Spain. J. Hazard. Mater. 181, 193–203. https://doi.org/10.1016/j.jhazmat.2010.04.116.

RESTORE2030, 2020. Environmental restoration project of the Huelva phosphogypsum stacks (RESTORE2030) (accessed 23 June 2024). https://restore2030.com/.

Rosado, D., Usero, J., Morillo, J., 2016. Assessment of heavy metals bioavailability and toxicity toward Vibrio fischeri in sediment of the Huelva estuary. Chemosphere 153, 10–17. https://doi.org/10.1016/j.chemosphere.2016.03.040.

Ruiz Cánovas, C., Macías, F., Pérez López, R., Nieto, J.M., 2018. Mobility of rare earth elements, yttrium and scandium from a phosphogypsum stack: environmental and

economic implications. Sci. Total Environ. 618, 847–857. https://doi.org/10.1016/j.scitotenv.2017.08.220.

Sáenz, V., Blasco, J., Gómez-Parra, A., 2003. Speciation of heavy metals in recent sediments of three coastal ecosystems in the Gulf of Cadiz, Southwest Iberian Peninsula. Environ. Toxicol. Chem. 22, 2833–2839. https://doi.org/10.1897/02-448.

Santos Bermejo, J.C., Beltrán, R., Gómez Ariza, J.L., 2003. Spatial variations of heavy metals contamination in sediments from Odiel river (Southwest Spain). Environ. Int. 29, 69–77. https://doi.org/10.1016/S0160-4120(02)00147-2.

Scientific committee, 2022. Inform of the cientific committee of national experts coordinated from Huelva University about the RESTORE 2030 plan (accessed 20 June 2024). http://mesadelaria.es/documentos/Informe_280722_C_Expertos-Agosto2022.pdf.

da Silva, E.F.D., Fonseca, E., Matos, J., Patinha, C., Reis, P., Santos Oliveira, J.M., 2005. The effect of unconfined mine tailings on the geochemistry of soils, sediments and surface waters of the lousal area (Iberian Pyrite Belt, Southern Portugal). Land Degrad. Develop. 16, 213–228. https://doi.org/10.1002/ldr.659.

Silva, L.F.O., Oliveira, M.L.S., Crissien, T.J., Santosh, M., Bolivar, J.P., Shao, L., Dotto, G. L., Gasparotto, J., Schindler, M., 2022. A review on the environmental impact of phosphogypsum and potential health impacts through the release of nanoparticles. Chemosphere 286, 131513. https://doi.org/10.1016/j.chemosphere.2021.131513.

Sun, Y., Zhang, X., Peng, H., Zhou, W., Jiang, A., Zhou, F., Wang, H., Zhang, W., 2025. Develop- ment of a coupled model to simulate and assess arsenic contamination and impact factors in the Jinsha River Basin, China. Journal of Environmental Sciences 147, 50–61. https://doi.org/10.1016/j.jes. 2023.09.038.

Torres-Sánchez, R., Sánchez-Rodas, D., Sánchez de la Campa, A.M., Kandler, K., Schneiders, K., de la Rosa, J.D., 2019. Geochemistry and source contribution of fugitive phosphogypsum particles in Huelva, (SW Spain). Atmos. Res. 230, 104650. https://doi.org/10.1016/j.atmosres.2019.104650.

Torres-Sánchez, R., Sánchez-Rodas, D., Sánchez de la Campa, A.M., de la Rosa, J.D., 2020. Hydrogen fluoride concentrations in ambient air of an urban area based on the emissions of a major phosphogypsum deposit (SW, Europe). Sci. Total Environ. 714, 136891. https://doi.org/10.1016/j.scitotenv.2020.136891.

A1.2. Paper #2

A1.2.1 Extended abstract paper #2

Influence of phosphogypsum waste on rainwater chemistry in a highly polluted area with high mortality rates in Huelva metropolitan area, Spain

Manuel Contreras-Llanes [1,2], Vanessa Santos-Sánchez [1,2], Juan Alguacil [1,2,3,*,**], Roberto Rodríguez-Pacheco [4,*]

[1] Research group in Clinical, Environmental and Epidemiology Social Transformation (EPICAS), Department of Sociology, Social Work and Public Health, University of Huelva, 21007 Huelva, Spain.

[2] Research Centre for Natural Resources, Health and Environment (RENSMA), Faculty of Experimental Sciences, University of Huelva, 21007 Huelva, Spain.

[3] Consortium for Biomedical Research in Epidemiology & Public Health (CIBER in Epidemiology & Public Health - CIBERESP), 28029 Madrid, Spain

[4] The Spanish National Research Council (CSIC). Spanish Geological and Miner Institute National Center (CN IGME), Ríos Rosas, 23, 28003 Madrid, Spain

* Equally contributed to the senior authorships

** **Corresponding author:** Juan Alguacil (alguacil@uhu.es)

Keywords: Huelva; rainwater pollution; phosphogypsum; spatial variation; short-range transport; particle soluble fraction; wet deposition

Introduction:

The association between industrial and mining pollution with environmental damage and health impacts is well-documented (Briffa et al., 2020). Huelva City, located in south-western Spain within 150,000 residents, is positioned near one of the most heavily polluted regions around the world (Morillo et al., 2008; Sáenz et al., 2003). This pollution stems from substantial releases of metal(loid)s and radionuclides by two significant chemical industrial complexes, Europe's largest Naturally Occurring Radioactive Material (NORM) waste site, known as the phosphogypsum (PG) stacks, and the Odiel-Tinto Estuary, which suffers from contamination due to acid mine drainage and industrial activities (Blasco et al., 2000; Lieberman et al., 2020; Pérez-López et al., 2010; Santos Bermejo et al., 2003). Furthermore, Huelva City shows elevated mortality rates from cardiovascular diseases and cancer compared to national averages in Spain (Alguacil et al., 2014; Benach et al., 2003; Lopez-Abente et al., 2001). Despite widespread concerns linking pollution to these mortality rates, the issue remains unresolved. Additionally, efforts, primarily targeting the PG stacks, have resulted in the suspension of phosphogypsum disposal in 2010 and the implementation of RESTORE 2030, a plan aimed at rehabilitating the affected marshlands. This study examines how suspended pollutant particles emitted from the phosphogypsum stacks and other pollution sources are dispersed, aiming to determine their range of impact on the chemical composition of rainwater within the Huelva metropolitan area.

Methodology: Rainwater samples were collected using 17 rain-gauges with 16 of them (AD, AL, CA, CM, CO, EP, GI, JR, MO, FB, FE, PF, PI, PU, RA, and SJ) situated within the Odiel-Tinto estuary. An additional point was located in an unpolluted area in the village of Matalascañas (MN) within the 'Doñana' national reserve park. Both locations are in the province of Huelva, Spain. A total of 612 were collected between January-2021 to December-2022. The pH, conductivity, major ions and trace metals were detected in the soluble fraction of rainwater.

Findings: The results revealed significant spatial variations in rainwater quality. In areas near the phosphogypsum stacks, we observed elevated levels of potentially toxic metal(loid)s, including As, Ca^{2+}, Cr, F^{-}, NH_4^{+}, Ni, PO_4^{3-}, SO_4^{2-}, Sr, and V. Notably, rain gauges located close to the stacks showed pH, F^{-}, and Ni concentrations that clearly exceeded WHO guidelines for drinking-water quality. Furthermore, pollution was not solely attributable to the phosphogypsum stacks; additional contributors included regional sources, such as marine factors (Ca^{2+}, Cl^{-}, K^{+}, Mg^{2+}, and Na^{+}), and local emissions from chemical parks (Co, Cu, Pb, and Zn).

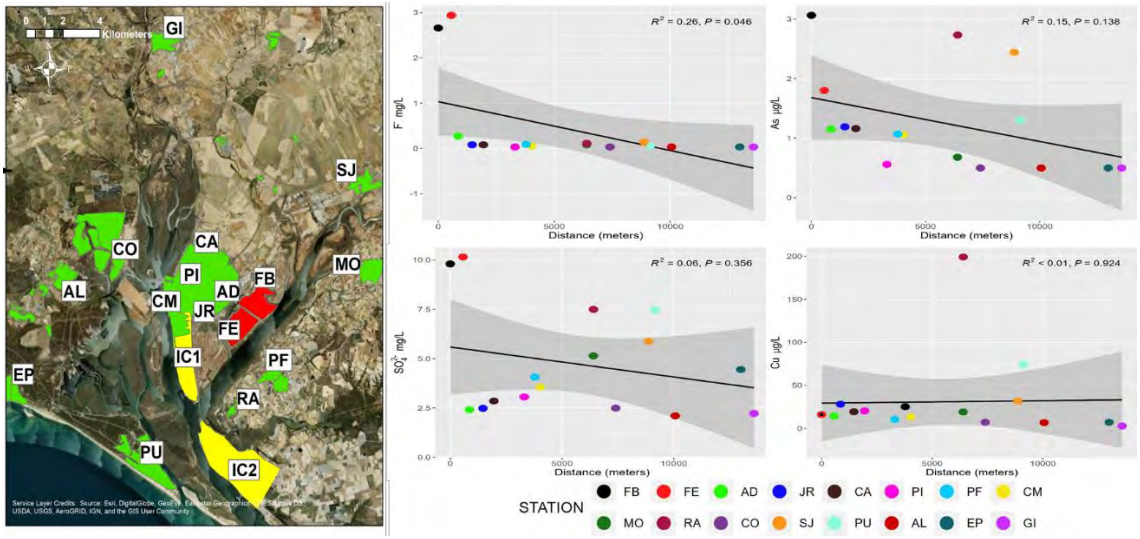

Figure A1.2. Location map of the 16 rain gauges located in Huelva metropolitan area and pollution sources (left). Scatter plots showing the distribution of F^{-}, As, SO_4^{2-}, and Cu in rainwater by rain gauge location by increasing distance (m) from PG stacks (FB) (right).

Conclusion: The concentrations of toxic metal(loid)s in wet depositions display a notable decline as the distance from the affected region increases. This pattern underscores the significance of the phosphogypsum stacks as a prominent source of metal(loid) pollution, posing potential risks to both the environment and public health. Should similar findings emerge in other studies, they could serve as a critical foundation for enhancing environmental monitoring and informing policy development. Our findings can be useful to evaluate future restoration plans to mitigate potential environmental impacts and health effects of phosphogypsum stacks, such as RESTORE2030, or other identified pollution sources, in Huelva metropolitan area.

A1.2.2 Published version paper #2

sustainability

MDPI

Article

Influence of Phosphogypsum Waste on Rainwater Chemistry in a Highly Polluted Area with High Mortality Rates in Huelva Metropolitan Area, Spain

Manuel Contreras-Llanes [1,2], Vanessa Santos-Sánchez [1,2], Juan Alguacil [1,2,3,*,†] and Roberto Rodríguez-Pacheco [4,†]

[1] Research Group in Clinical, Environmental and Epidemiology Social Transformation (EPICAS), Department of Sociology, Social Work and Public Health, University of Huelva, 21007 Huelva, Spain; mcontreras@uhu.es (M.C.-L.); vanesasantossanchez@gmail.com (V.S.-S.)
[2] Research Centre for Natural Resources, Health and Environment (RENSMA), Faculty of Experimental Sciences, University of Huelva, 21007 Huelva, Spain
[3] Consortium for Biomedical Research in Epidemiology & Public Health (CIBER in Epidemiology & Public Health—CIBERESP), 28029 Madrid, Spain
[4] The Spanish National Research Council (CSIC), Spanish Geological and Miner Institute National Center (CN IGME), Ríos Rosas 23, 28003 Madrid, Spain; roberto.rodriguez@igme.es
* Correspondence: alguacil@uhu.es
† These authors contributed equally to this work.

Abstract: This study evaluates the impact of phosphogypsum stacks on the chemical composition of rainwater in the Huelva metropolitan area, a metal-polluted area with high cancer and heart disease mortality rates. A total of 612 rainwater samples were collected using 17 rain gauges located around the study area between January 2021 and December 2022. The pH, conductivity, major ions, and trace metals were detected in the soluble fraction of rainwater. The results revealed spatial variability in the rainwater quality. The highest values of As, Ca^{2+}, Cr, F^{-}, NH_4^{+}, Ni, PO_4^{3-}, SO_4^{2-}, Sr, and V were detected in rain-gauges near phosphogypsum stacks, exceeding the levels of pH, F^{-}, and Ni according to the guideline values for drinking water quality from the WHO. Additionally, other pollution sources also contributed: a regional source (marine factors: Ca^{2+}, Cl^{-}, K^{+}, Mg^{2+}, and Na^{+}) and a local source (chemical complexes emissions: Co, Cu, Pb, and Zn). A downward trend of most toxic metal(loid) concentrations in wet depositions was detected as the distance to the affected area increased. The findings revealed that phosphogypsum stacks are a relevant source of metal(loid)s with potentially adverse environmental and public health effects that, if replicated, could be relevant for environmental monitoring and policy making.

Keywords: Huelva; rainwater pollution; phosphogypsum; spatial variation; short-range transport; particle soluble fraction; wet deposition

Academic Editors: Robson Andreazza and Filipe Selau Carlos

Received: 12 January 2025
Revised: 19 March 2025
Accepted: 25 March 2025
Published: 31 March 2025

Citation: Contreras-Llanes, M.; Santos-Sánchez, V.; Alguacil, J.; Rodríguez-Pacheco, R. Influence of Phosphogypsum Waste on Rainwater Chemistry in a Highly Polluted Area with High Mortality Rates in Huelva Metropolitan Area, Spain. *Sustainability* **2025**, *17*, 3102. https://doi.org/10.3390/su17073102

1. Introduction

Industrial and mining environmental pollution may induce adverse health effects, including cancer, cardiovascular diseases, and respiratory conditions [1]. The Huelva metropolitan area (SW Spain), with near 300,000 inhabitants, is located on the margin of the Odiel–Tinto Estuary. This area is acknowledged as one of the world's most severely polluted sites, primarily due to widespread industrial and mining activities [2,3]. This estuary has a high content of harmful elements, both metal(loid)s (As, Cd, Cr, Cu, F^{-}, Fe,

stockpiled, occupying large surfaces [15,16,21–23]. These areas frequently lack vegetation and are significantly affected by erosive forces such as wind and runoff water. The redistribution of contaminants in the environment is significantly influenced by particle resuspension from open-cast mining, waste dumps, and industrial activities [24–28]. Large quantities of resuspended particles, often linked to wind events, may negatively impact the health of nearby residents through various intake pathways, such as inhalation, dermal contact, and/or ingestion [24]. The dispersion of particulate matter through the atmosphere significantly contributes to environmental pollution. Air masses, moving more swiftly than water and soil masses, possess the highest capability to transport pollutants rapidly, ranging from hours to days. Wet deposition is considered one of the key methods by which air pollutants are deposited on the Earth's surface, including both toxic and non-toxic matters [29]. The chemical composition of rainwater is influenced by multiple factors, including the proximity to pollution sources, the volume of precipitation, and the movement of air masses, resulting in significant spatial and temporal variations [29]. The study of rainwater chemistry provides knowledge about its potential pollutants in order to identify and assess possible contamination sources, such as industry and mining activities, and prevent damage to natural ecosystems. Therefore, research on rainwater composition has increased in recent years around the world due to the increased recognition of the potential ecological consequences resulting from environmental pollution [29–35]. The first study, however, was conducted in the United States in the 1950s [36]. Nevertheless, studies analysing the pattern of metal(loid)s due to phosphogypsum stacks in rainwater have not been found.

Despite extensive research being performed on the rainwater quality in other highly polluted locations in Huelva province [37,38] and other research focusing on the chemical composition of Huelva city's air [39–45], the specific rainwater chemical profile in the Huelva metropolitan area has not yet been characterised in detail. Also, to our knowledge, this is the first study to analyse the impact of phosphogypsum stacks on the pH, conductivity, and chemical profile of the rainwater. Monitoring rainwater can help assess the possible effects of phosphogypsum stacks on the ecosystem. In addition, these environment risk assessments are crucial to evaluate the influence of restoration initiatives like RESTORE 2030. This study assess the distribution of the suspended pollutant particles originating from the phosphogypsum stacks to identify the radius of influence of the chemicals that have arrived via rainwater in the Huelva metropolitan area.

2. Materials and Methods

2.1. Study Area

This study was conducted using sixteen rain gauges (AD, AL, CA, CM, CO, EP, GI, JR, MO, FB, FE, PF, PI, PU, RA, and SJ) covering the Huelva metropolitan area and one in Matalascañas village (MN) within the "Doñana" National Reserve Park, an unpolluted area, all situated in Huelva province, SW Spain (Figure 1). The region experiences a Mediterranean climate influenced by the Atlantic Ocean, characterised by humid mild winters with an average temperature of 11 °C in January, and the annual precipitation is 505.6 mm. Summers are dry and warm, with an average temperature of 25 °C in August and nearly no precipitation. The geological composition of the soil is primarily made up of Palaeozoic volcanic and sedimentary rocks, which are abundant in pyrite (FeS_2) and other sulphide minerals [46].

NH^{4+}, Ni, P, Pb, SO_4^{2-}, and Zn) and natural radionuclides from the ^{238}U decay series, including the highly radiotoxic ^{210}Pb, ^{210}Po, and ^{226}Ra [2,3]. There is support in the international scientific literature for a deleterious effect for human heath due to environmental exposure to many of those metals [1,4]. Previous studies have revealed that the mortality rates from cancer and heart disease in Huelva city are higher for both men and women compared to the national average in Spain [4–6]. According to the Spanish National Atlas of Mortality, the city of Huelva exhibited significantly higher standardised mortality ratios between 1989 and 2014 for both men and women. These elevated ratios were observed for acute myocardial infarction, cerebrovascular diseases, bladder cancer, cardiac failure, and other cardiovascular conditions. Additionally, women experienced higher mortality rates for breast cancer, while men faced elevated mortality rates for lung cancer [7]. Furthermore, previous studies focused on the cumulated heavy metals levels (As, Cd, Cr, Cu, and Ni) in the hair and urine of children from the city of Huelva; the average levels of cadmium were found to be higher than those reported in other European research [8,9], and indicated an intellectual functioning effect in the children with high Cd concentrations [9]. Similarly, an explorative research paper linked environmental exposure to heavy metals with the cognitive behaviour of children in Huelva city [10]. In addition, industry workers of Huelva city showed elevated concentrations of arsenic and other metal(loid)s, even when accounting for seafood and fish intake [11]. Although industrial and mining pollution may be the factors that have contributed to the high mortality ratios detected in the city of Huelva [4], the issue remains uncertain. Hence, given the correlation between elevated mortality rates in Huelva city and industrial and mining pollution, along with the existence of multiple sources of exposure, it is imperative to meticulously investigate the distinct signatures of metal(loid)s specific to each pollution source. In this sense, the specific pollution signatures in marsh sediments of the Odiel–Tinto Estuary using geochemical tracers were defined by our research group [12]. In addition, we recently conducted a study that denoted the connection between the spatial variability of cumulated metal(loid)s levels in nails and exposure to pollution sources in Huelva city [13].

This scenario has incited social activism, with a primary focus on the phosphogypsum stacks, recognised as the largest Naturally Occurring Radioactive Material (NORM) waste stacks of Europe [14–16], in addition to other sources of pollution. This waste deposit is located on the highly permeable marshes just 500 m from the population [2,3]. In December 2010, judiciary authorities sanctioned the cessation of phosphogypsum stockpiling and mandated that the fertiliser company devise a restoration plan for the impacted marshlands called RESTORE 2030 (https://restore2030.com/). The Huelva City Council created a citizen participation initiative of an advisory nature and asked Huelva University to coordinate an independent committee of national scientific experts. Even though the scientific committee determined that this restoration plan was insufficient for fully restoring the affected area by the phosphogypsum stacks [17], the work has already begun.

As a consequence of the actual restoration plan and future interventions, an assessment of the environmental impact of phosphogypsum stacks in the nearby areas is necessary to monitor the impact of the restoration, encompassing, but not limited to, the effect on the Huelva metropolitan area. The restoration labours may result in resuspension of coarse particles from the phosphogypsum stacks. This occurrence could be the major source of air pollutants and could significantly affect the surrounding areas [18–20]. Industry and mining activities have a direct effect on the environment and frequently produce substantial quantities of waste containing harmful elements that reach the atmosphere [1]. Among them, fertiliser production is recognised for its significant environmental impact, as it generates a waste product known as phosphogypsum, which contains a high concentration of geo-available heavy metals and radionuclides, which are typically

is polluted with large amounts of metals generated by acid mine drainage due to the Odiel and Tinto Rivers, which drain the province of Huelva from north to south through the Iberian Pyrite Belt, one of the most important polymetallic sulphide mining areas in Europe [51,52]. Furthermore, two important industrial complexes called "Polo Químico de Promoción y Desarrollo de Huelva—Punta del Sebo" (IC1; Figure 1) and "Nuevo Puerto Palos de la Frontera" are both placed in the margin of the Odiel–Tinto Estuary (IC2; Figure 1). The principal Spanish producers of copper and fertiliser, along with a thermal power plant and an oil refinery, are among the most contaminating industries situated in these chemical complexes [3,53].

The sampling network, comprising 17 rain gauges, was strategically distributed at various distances from the sea and across different soil uses and human activities, including industrial, mining, urban, and agricultural waste areas. These rain gauges were situated at public institutions, private companies, and residential addresses. Moreover, both the wind and population centres were also considered to ensure that highly populated areas influenced by all major wind directions were included. Furthermore, due to the considerable size of the city of Huelva and its proximity to the phosphogypsum stacks, five rain gauges were installed to cover the entire city. The disposition of the rain gauges throughout the Huelva metropolitan area is depicted in Figure 1, with their main characteristics outlined in Table S1. As seen in Figure 1, the phosphogypsum stacks (FB) rain gauge is chosen as the central point of the affected area. Its UTM-30 coordinates, referenced with the ETRS89 reference system, are (x, y, z) 153073.3, 4130808.5, 6.5.

2.2. Sampling and Methodology

2.2.1. Rainwater Sampling and Hellman Rain Gauge Characteristics

Rainwater samples were collected using 17 Hellman rain gauges (DARRERA, Barcelona, Spain) during the period of January 2021 to December 2022 on an event basis. This period was chosen in order to make sure that every rain gauge was monitored for at least two complete hydrologic years. An event is classified as rainfall measuring at least 1mm following a dry period lasting a minimum 24 h.

The Hellman rain gauge with a circular collecting area of 200 cm^2 at a height of 1.5 m (World Meteorological Organisation standard) is made of plastic. Automatic rain gauges were not selected for rainwater sampling, as they discard the collected rainwater before a new rainfall event. The instrument includes an upper part with a limiter ring, a lower part, a collecting can, a holder, and a precipitation-measuring plastic vessel DIN 58667B (DARRERA, Barcelona, Spain), with a 0–10 mm scale in 1/10 mm increments. To prevent evaporation, the precipitation vessel is separated from the upper segment by an air chamber, and the exterior parts are made in pale grey that can be used on the outer surface of the rain gauge to reduce the thermal load. After an extended dry period, which is normal in the study area, it is crucial to thoroughly clean the rain gauge with deionised water and perform maintenance of before a rain event. This ensures that the composition of single-event samples can be reflected as wet-only deposition. After a rain event, rainwater was measured using graduated cylinder and collected in plastic bottles, and the rain gauges were thoroughly cleaned with deionised water. Samples were promptly collected after rainfall ended, typically the day after the event. In the laboratory, samples were filtered through 0.45 mm polypropylene membranes (Sigma-Aldrich, St. Louis, MO, USA) to eliminate insoluble particulate matter. Four replicates were conducted for each sample; two of them were acidified until they reached a pH below 2.5, and other two were unacidified, which were stored in a refrigerator at a temperature below 4 °C to maintain their chemical properties until analysis, which was conducted as soon as possible after sampling, typically within two weeks. In this study, a total of 612 rainwater samples, each up to 50 mL, were collected.

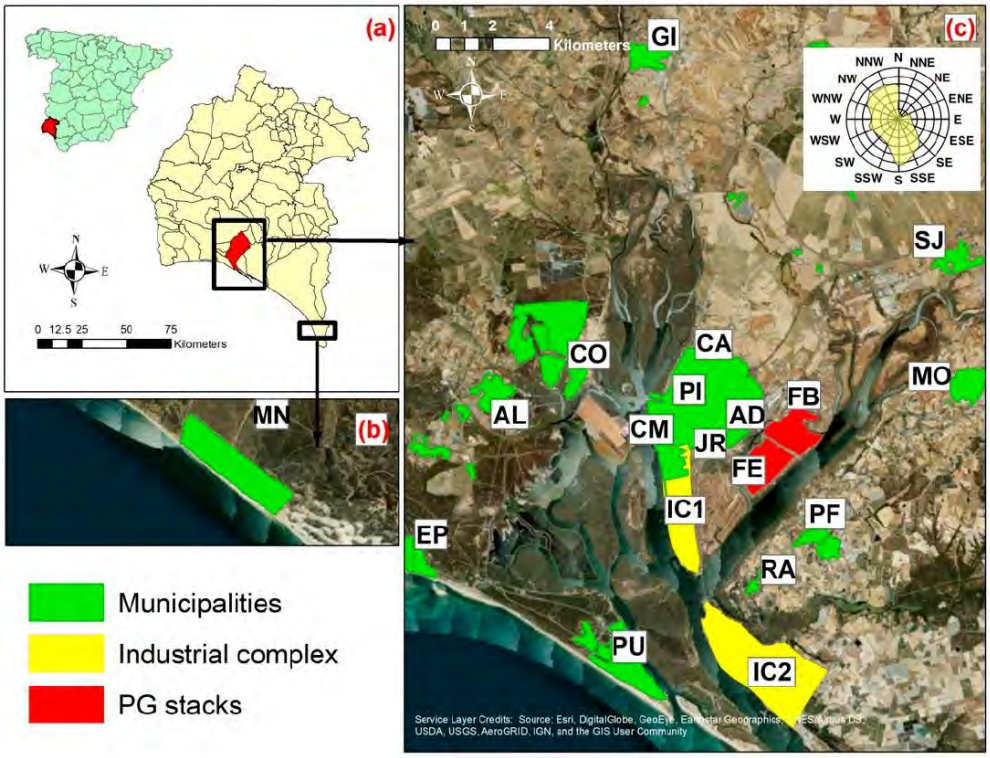

Figure 1. Location map of (**a**) Huelva province, rain gauges placed in (**b**) Matalcañas village (MN), and (**c**) Huelva metropolitan area (AD, AL, CA, CM, CO, EP, GI, JR, MO, FB, FE, PF, PI, PU, RA, and SJ) showing the wind rose diagram for the period January 2021 to December 2022. FB is the centre of phosphogypsum (PG) stacks. (IC1) Industrial complex "Polo Químico de Promoción y Desarrollo de Huelva—Punta del Sebo". (IC2) Industrial complex "Nuevo Puerto Palos de la Frontera".

Huelva metropolitan area, with nearly 300.000 inhabitants, is located in the Odiel–Tinto Estuary, recognised as an extremely polluted area [2,3]. A large portion of this estuary is covered by phosphogypsum stacks (Figure 1), an industrial waste product derived from phosphate rock during fertiliser production [15,16,21–23]. Over a period of 42 years (1968–2010), phosphogypsum was deposited on unconsolidated salt marsh sediments in the Tinto marshes, now encompassing 1,200 hectares and containing 100 million tonnes, making it one of the most substantial deposits globally [15,16,21–23]. These phosphogypsum stacks harbour a diverse array of contaminants, including organic substances, metal(loid)s, and other harmful elements (As, Cd, Cr, F^-, Fe, NH^{4+}, Ni, P, Pb, SO_4^{2-}, and Zn). Additionally, they contain natural radionuclides from the ^{238}U decay series, including the highly radiotoxic ^{210}Pb, ^{210}Po, and ^{226}Ra [13,14,19–21], which have been linked to health problems [47]. Phosphogypsum is designated as a naturally occurring radioactive material (NORM) because of its elevated concentration of natural radionuclides [14]. Additionally, it emits particles and gases with high levels of radon and hydrogen fluoride, one of the most toxic gaseous compounds, into the atmosphere [48–50]. Moreover, this estuary

Concerning the trace elements monitored in this study, the quality of rainwater samples collected using the Hellman rain gauges are significantly impacted by numerous aspects (Text S1) [30]. Consequently, a quality score ranging from 1 to 5 (1 = poor, 5 = excellent) is assigned to each rain gauge in Table S1.

2.2.2. pH and Conductivity

The pH and conductivity (EC) of the rainwater samples were assessed within 24 h after collecting utilising a digital multimeter, specifically the LAQUA PC220 (HORIBA Advanced Techno Co., Ltd., Tokyo, Japan). To measure the pH and EC of the rainwater samples, the electrode was immersed in the samples and left there until the multimeter reached a stable pH measurement. The corresponding value at 25 °C was obtained by a temperature conversion of the results. The multimeter was calibrated daily using standard solutions of 4.01, 7.00, and 9.21 pH units as the evaluated rainwaters ranged from basic to acid, and using solutions of 147 μS cm^{-1} and 1413 μS cm^{-1} as these values encompassed the majority of the EC values of the rainwaters.

2.2.3. Major Anions and Cations

The concentration of major cations (Ca^{2+}, K^{+}, Mg^{2+}, and Na^{+}) in acidified samples were determined by Inductively Coupled Plasma–Optical Emission Spectroscopy (ICP-OES) with an Agilent 5110 (Agilent Technologies, Tokyo, Japan). This instrument operates within the wavelength range of 160–900 nm and utilises external and periodic calibration with concertation ranges of 0.1–100 ppm (K^{+} and Na^{+}) and 0.1–500 ppm (Ca^{2+} and Mg^{2+}). The detection and quantification limits for these measurements were 0.1 ppm (Ca^{2+} and Mg^{2+}) and 0.5 ppm (K^{+} and Na^{+}). To ensure calibration stability, the concentration of a 10 ppm standard solution was determined every 10 analyses, yielding a deviation of less than 10%. A subset comprising 10% of the samples was analysed in triplicate. Additionally, to verify the method's accuracy, an Agilent multi-element quality control standard (Number 5190–9418; Agilent Technologies, Tokyo, Japan) was employed, applicable for both EPA methods and other applications. The recovery rates were verified through periodic analyses of certified quality control samples (Number 5190–9418) interspersed within the analysis sequence with results ranging between 80% and 120%.

On the other hand, the concentrations of anions (Cl^{-}, F^{-}, NO_2^{-}, NO_3^{-}, PO_4^{3-}, and SO_4^{2-}) as well as NH_4^{+} were determined in unacidified rainwater samples using the Metrohm automated ion chromatography system, model 883 BASIC IC PLUS (Metrohm AG, Herisau, Switzerland). Ion chromatography was employed to analyse aqueous samples containing ppm quantities of common anions [54]. Anion separation was conducted using a Metrosep A Supp 5 250/4.0 column (Metrohm AG, Herisau, Switzerland) with a flow rate of 0.7 mL min^{-1} of a carbonate/bicarbonate eluent (3.2 mM Na_2CO_3 + 1.0 mM $NaHCO_3$). In contrast, NH_4^{+} separation was performed on a Metrosep C4 250/4.0 column (Metrohm AG, Herisau, Switzerland) with an eluent composition of 4 mM tartaric acid + 0.75 mM dipicolinic acid at a flow of 1.0 mL min^{-1}. To ensure precise calibration, external standards prepared from commercial calibration standards at a concentration of 1000 mg/L were utilised. The calibration range for minor anions (F^{-}, NO_2^{-} and PO_4^{3-}) spanned from 0.05 to 25 ppm (0.1–25 ppm F^{-}, 0.05–25 ppm NO_2^{-}; 0.5–25 ppm PO_4^{3-}), while for major anions (Cl^{-}, NO_3^{-} and SO_4^{2-}) it ranged between 0.25 and 250 ppm (0.5–250 ppm Cl^{-}; 0.25–125 ppm NO_3^{-}; 0.5–250 ppm SO_4^{2-}). In each analytical sequence, calibration blanks were assessed. Moreover, 10% of the samples underwent triplication. Quality control standards were evaluated as well, with one standard positioned within the high concentration range and another at concentrations proximate to the method's quantification limits. The quantification limits for each analyte were established as follows: 0.1 ppm for F^{-}, 0.5 ppm for Cl^{-}, 0.05 ppm for NO_2^{-}, 0.25 ppm for NO_3^{-}, 0.5 ppm for PO_4^{3-}, and 0.5 ppm for SO_4^{2-}. The criteria for method

validation were as follows: relative standard deviation (RSD) for the duplicate samples must be below 15%, and the deviation of the control standard values from the theoretical values must also be under 15%. Furthermore, five-point calibration curves for anions and cations were established using two certified multi-element ion chromatography standard solutions obtained from Sigma-Aldrich (St. Louis, MO, USA). All reagents, standards, and eluents were prepared with reagent-grade water (resistivity: 18.2 MΩ cm, total organic carbon concentrations: <10 μg L^{-1}) produced from an Elix 3/Milli-Q Element system (Millipore, Billerica, MA, USA). The method detection limits (MDLs) were estimated according to the guidelines set by the U.S. EPA in 40 CFR 136, Appendix B [55]. The recovery rates were assessed by conducting routine analyses of two certified multi-element ion chromatography standard solutions supplied by Sigma-Aldrich, which were systematically integrated into the sequence of analyses. The recorded results demonstrated a variation ranging from 80% to 120%. To maintain data quality, each sample was analysed in triplicate, with sample batches frequently interspersed with reference material and digestion blanks.

2.2.4. Trace Elements

Trace element (As, Ba, Cd, Co, Cr, Cu, Mn, Mo, Ni, Pb, Sr, V, and Zn) concentrations were determined in acidified samples by Inductively Coupled Plasma–Mass Spectrometry (ICP-MS) Agilent 7700 (Agilent Technologies, Tokyo, Japan) with SPS4 autosampler and collision cell (He mode). ICP-MS is a highly sensitive type of mass spectrometry that enables the determination of a wide range of elements, including trace elements (ppb) [56]. Molecular (polyatomic) ions are commonly formed in the inductively coupled plasma and can provoke interferences in ICP-MS. In this study, molecular ion elimination through kinetic energy discrimination (KED) was applied by adding 4.3 mL min^{-1} He gas flow in the collision cell (ORS) of the ICP-MS instrument. This method is commonly used in ICP-MS and has historically proven to be efficient. In particular, the specifications of the instrument used in this study (Agilent 7700 ICP-MS) showed an interference removal factor >30 (expressed as the ratio $^{59}Co/^{51}ClO$). Further studies of the possible interferences for each analyte isotope and each potential molecular ion interferent were not conducted, since such fundamental ICP-MS studies were considered to be out of scope in this work. An internal solution containing Rh was added on-line to the samples to correct signal drifts. The calibration range was from 0.5 ppb to 250 ppb for all elements, and the quantification limit was 0.5 ppm. Internal quality controls (IQCs) were used according to the work instructions included in the Quality Manual according to ISO9001 and 14001 standards [57,58]. Various IQCs were implemented to confirm that the analytical procedure, from digestion to analysis, was conducted appropriately, enabling analytical chemists to verify the accuracy of the results. The laboratory quality controls used to determine the metals using ICP-Ms technique were the AccuTrace™ certified reference standards ICP-MS Quality Control Sample 1 (ICP-MS-QC1-1) and ICP-MS Quality Control Sample 2 (ICP-MS-QC2-1) supplied by AccuStandard®, Inc. (Berlin, Germany). To maintain data quality, each sample was analysed in triplicate, with sample batches frequently interspersed with reference material and digestion blanks.

2.2.5. Data Analyses and Spatial Variation

A descriptive statistical analysis was performed for each of the elements and stations studied, with outcomes expressed through measures of central tendency and dispersion. The normality of the variables was studied using the Kolmogorov–Smirnov test, considering, in all cases, a significance level of 95% ($p < 0.05$). In the case of the elements that

followed a normal distribution, the mean and standard deviation were used, and, otherwise, median and interquartile range were used. The Statistical Package for the Social Sciences (SPSS) version 26.0 was used for data analysis.

Graphs were created representing the medians of the values collected for each of the elements per rain gauge location according to the distance to the reference station, as well as the one located in the phosphogypsum stacks (FB). In these graphs, by means of linear regression models, the corresponding line of adjustment has been included. The statistical package R version 2024.12.0+467 was used to create the graphs.

3. Results

The average annual precipitation during the studied period was 345.8 mm (Table S1), 260.5 mm in 2021 and 431.0 mm in 2022, quite a bit lower than the average annual precipitation of 505.6 mm [46]. Moreover, in November 2021, the studied area experienced its highest rainfall of 169 mm, followed by few successive weeks without any event (19 and 18 weeks in 2021 and 2022, respectively). In addition, the dominant wind direction in the study area was NW–NNW and SE–SSE (Figure 1).

3.1. pH and Conductivity

Rainwater characteristics differed significantly among the rain gauge locations (Table S2). Rainwater pH was slightly above 7 (alkaline pH) for all sampling points, with the exception of FB, FE, PU, RA, and SJ with pH values slightly below 7 (acid pH). The lowest pH values were obtained in the rain gauges located in the border (FE; 6.84) and especially inside (FB; 6.31) of phosphogypsum stacks (Table S2; Figure 2a). Rainwater EC ranged from 58.35 µS cm^{-1} in AL to 137.65 µS cm^{-1} in SJ (Table S2; Figure 2b), and these samples exhibited low EC in accordance with the WHO guidelines for drinking water quality [59].

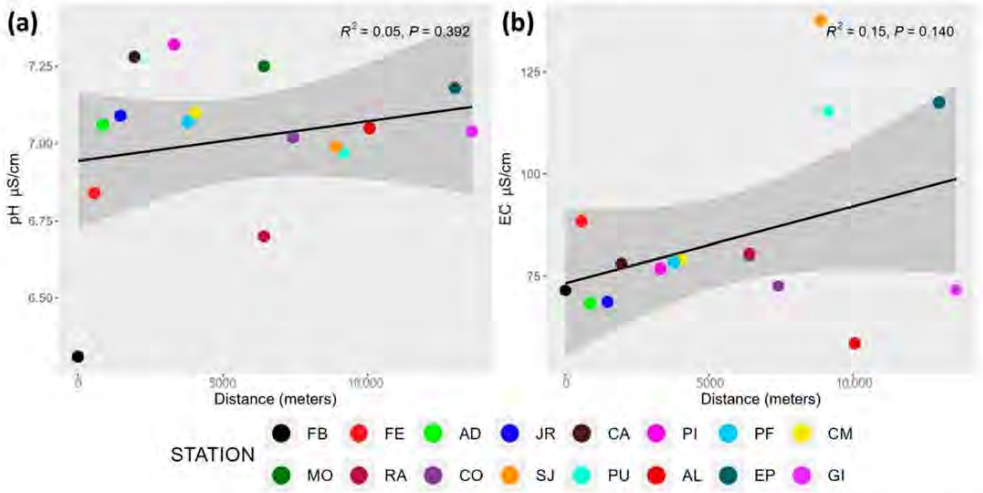

Figure 2. Scatter plots showing the distribution of (**a**) pH and (**b**) EC (µS cm^{-1}) in rainwater by rain gauge location. Sampling points are arranged by increasing distance (m) from phosphogypsum stacks (FB). Regression lines, standard error (grey shadow), correlation coefficients (R^2), and *p*-values are included in every plot.

The pH analysis shows a low relative standard deviation (5% of RSD on average), whereas the EC analysis displays a high RSD (100% on average), reflecting the significant chemical distinction across rain gauge locations. Skewness analysis is a measure of the asymmetry of the distribution. The positive skewness of the EC demonstrated asymmetric distributions and right-handed skewness. Moreover, pH displays a mean value slightly below zero, which showed asymmetric distributions and left-handed skewness (Table S2). The positive values of kurtosis in EC for most samples indicated sharp probability distributions.

3.2. Major Anions and Cations

The results of the analysis of ions, cations, and anions of rainwater are presented in Table S2. The concentration of ionic abundance (mg L^{-1}) displayed the overall pattern of $Cl^- > NO_3^- > SO_4^{2-} > PO_4^{3-} > F^- > NO_2^-$ for anions and $Ca^{2+} > Na^+ > K^+ > NH_4^+ > Mg^{2+}$ for cations. The samples were characterised by low Ca (4.73–14.84 mg L^{-1}), Cl^- (4.43–14.34 mg L^{-1}), K (1.32–6.35 mg L^{-1}), Mg (0.57–1.68 mg L^{-1}), Na (2.72–8.78 mg L^{-1}), NH_4^+ (0.10–3.94 mg L^{-1}), NO_3^- (2.33–8.21 mg L^{-1}), PO_4^{3-} (0.25–4.51 mg L^{-1}), and SO_4^{2-} (2.22–10.16 mg L^{-1}) values [59]. Meanwhile, F^- (0.03–2.94 mg L^{-1}) median is above the WHO guideline drinking value of 1.5 mg L^{-1} [59] and its concentration range is significantly influenced by the highest values in FB (2.66 mg L^{-1}) and FE (2.94 mg L^{-1}); without these (Table S2), the maximum value is 0.16 mg/L. Similarly, the NO_2^- median value obtained in SJ (0.33 mg L^{-1}) is the only one above the WHO guideline drinking value of 0.2 mg L^{-1} [59].

The variation in the major ion's concentration among the rain gauge locations revealed a high RSD (63% on average). Mean skewness and kurtoses values for each principal anion and cation are positive in all the locations studied with the exception of Ca^{2+}, indicating a rightward-extended tail (Table S2).

3.3. Trace Elements

On the other hand, a statistical summary of trace elements data in rainwater is shown in Table S2. The relative abundance in rainwater (μg L^{-1}) observed was Zn > Cu > Sr > Mn > Ba > Ni > As > Pb > V > Cr > Mo > Co > Cd. The samples were characterised by low As (0.50–3.06 μg L^{-1}), Ba (5.99+16.77 μg L^{-1}), Cd (0.25 μg L^{-1}), Co (0.25–0.50 μg L^{-1}), Cr (0.25–0.94 μg L^{-1}), Mn (5.02–35.80 μg L^{-1}), Mo (0.25–0.90 μg L^{-1}), Ni (0.76–6.21 μg L^{-1}), Pb (0.25–1.95 μg L^{-1}), and V (0.53–1.86 μg L^{-1}) values [59]. Moreover, Cu (2.78–199.13 μg L^{-1}) revealed a great influence in RA, although the values were in accordance with the WHO drinking guideline value (2000 μg L^{-1}) [59]. Similarly, the results revealed high Sr concentrations (11.36–32.54 μg L^{-1}), which do not pose a health risk and are significantly impacted by FB (Table S2). Moreover, high Zn (9.34–93.59 μg L^{-1}) median values were obtained, although the maximum values were in SJ, PU, RA, and FB (Table S2).

The trace metal concentrations analysis revealed a great RSD of over 100% on average. This is consistent with the significant natural variability among the infrequent and separated rainy events typical of a Mediterranean climate. The mean skewness and kurtoses values for each trace metal are positive across all the rain gauge locations, representing a tail extended to the right (Table S2).

3.4. Spatial Variation

Figures 2–5 illustrate how various parameters such as pH, EC, and elemental concentration change with the distance to the phosphogypsum stacks (FB). However, to truly understand the correlation, Pearson product–moment correlation coefficients (R^2) and *p*-values are contained within each plot.

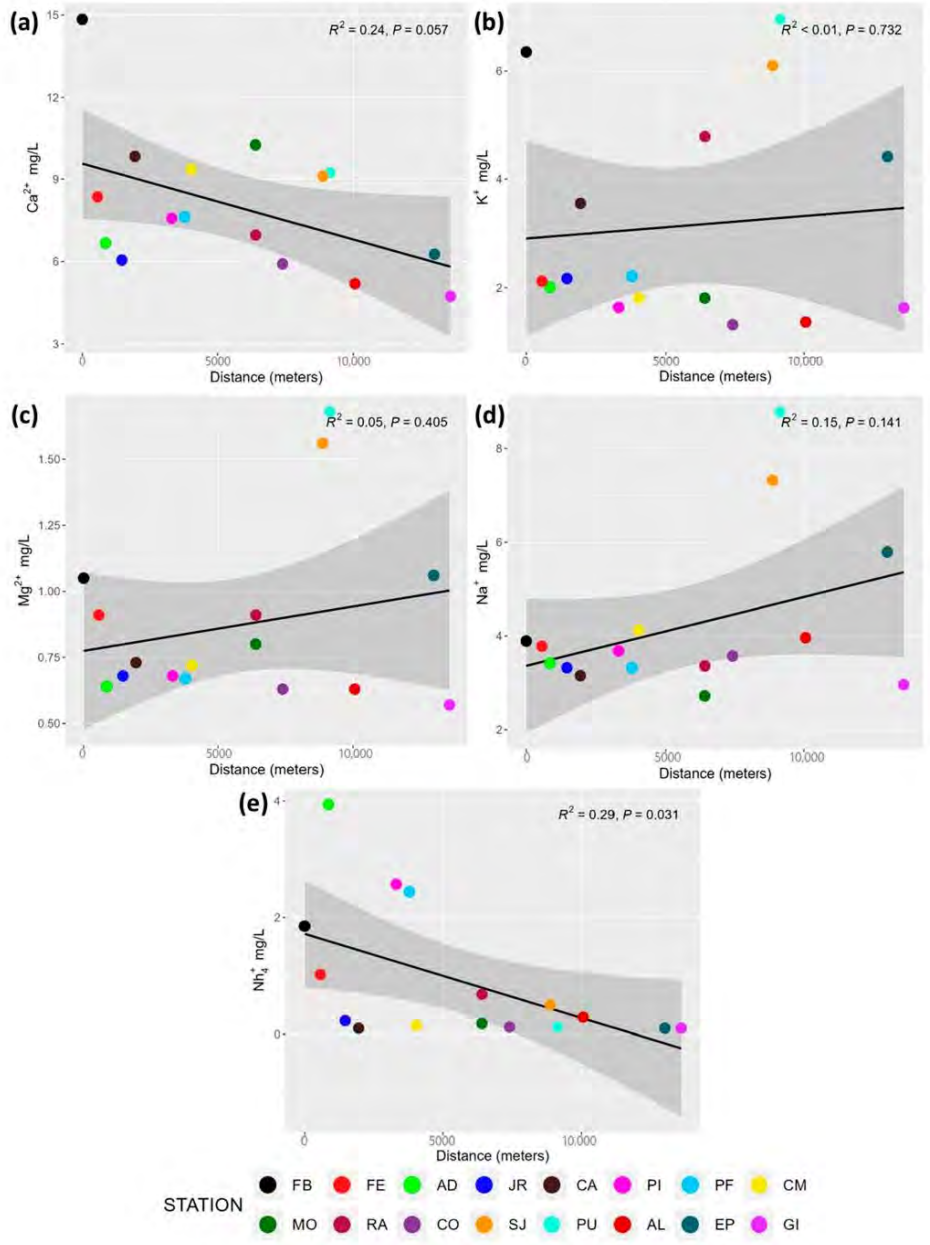

Figure 3. Scatter plots showing the distribution of major cation ((**a**) Ca^{2+}, (**b**) K^+, (**c**) Mg^2, (**d**) Na^+, and (**e**) NH_4^+) concentrations (mg L^{-1}) in rainwater by rain gauge location. Sampling points are arranged by increasing distance (m) from phosphogypsum stacks (FB). Regression lines, standard error (grey shadow), correlation coefficients (R^2), and *p*-values are included in every plot.

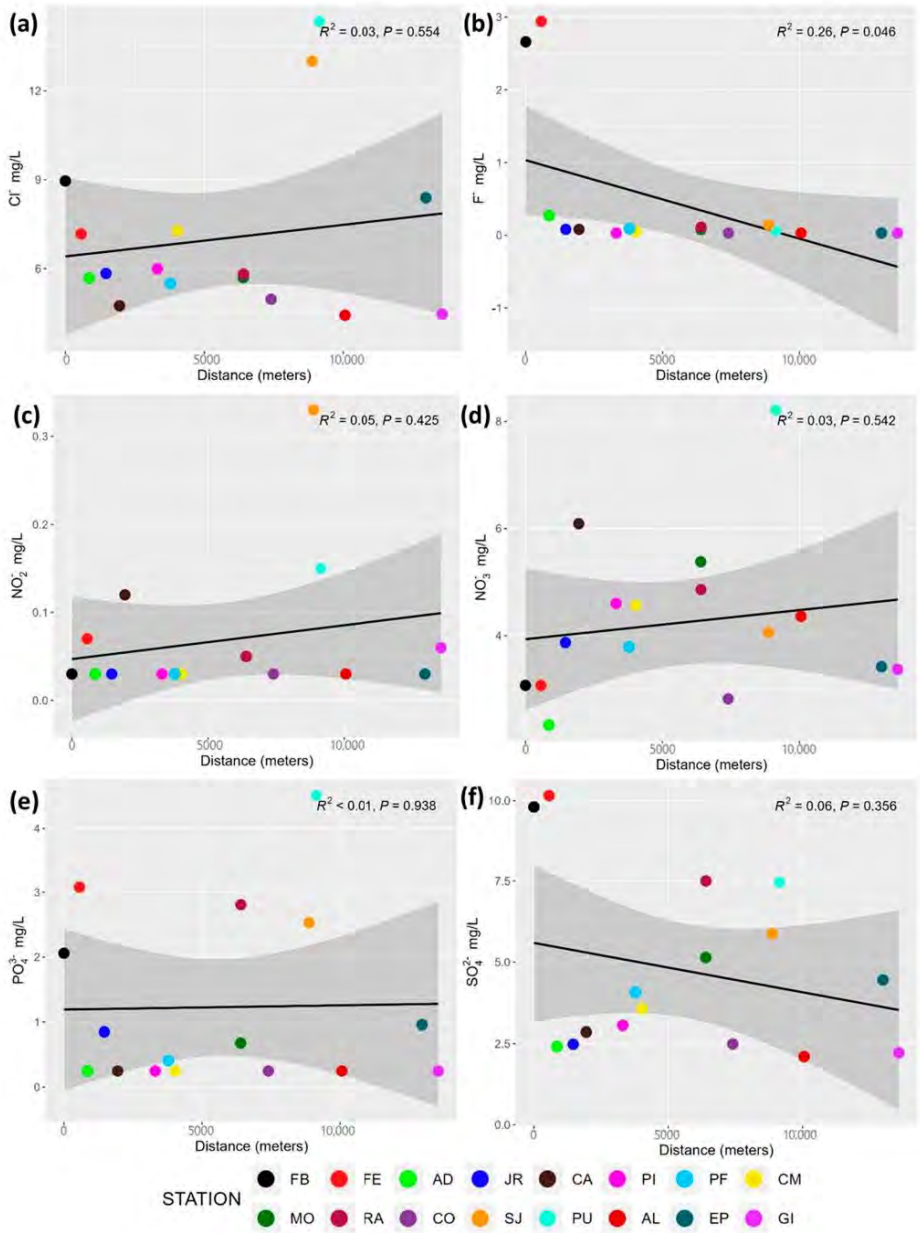

Figure 4. Scatter plots showing the distribution of major anion ((**a**) Cl^-, (**b**) F^-, (**c**) NO_2^-, (**d**) NO_3^-, (**e**) PO_4^{3-}, and (**f**) SO_4^{2-}) concentrations (mg L^{-1}) in rainwater by rain gauge location. Sampling points are arranged by increasing distance (m) from phosphogypsum stacks (FB). Regression lines, standard error (grey shadow), correlation coefficients (R^2), and *p*-values are included in every plot.

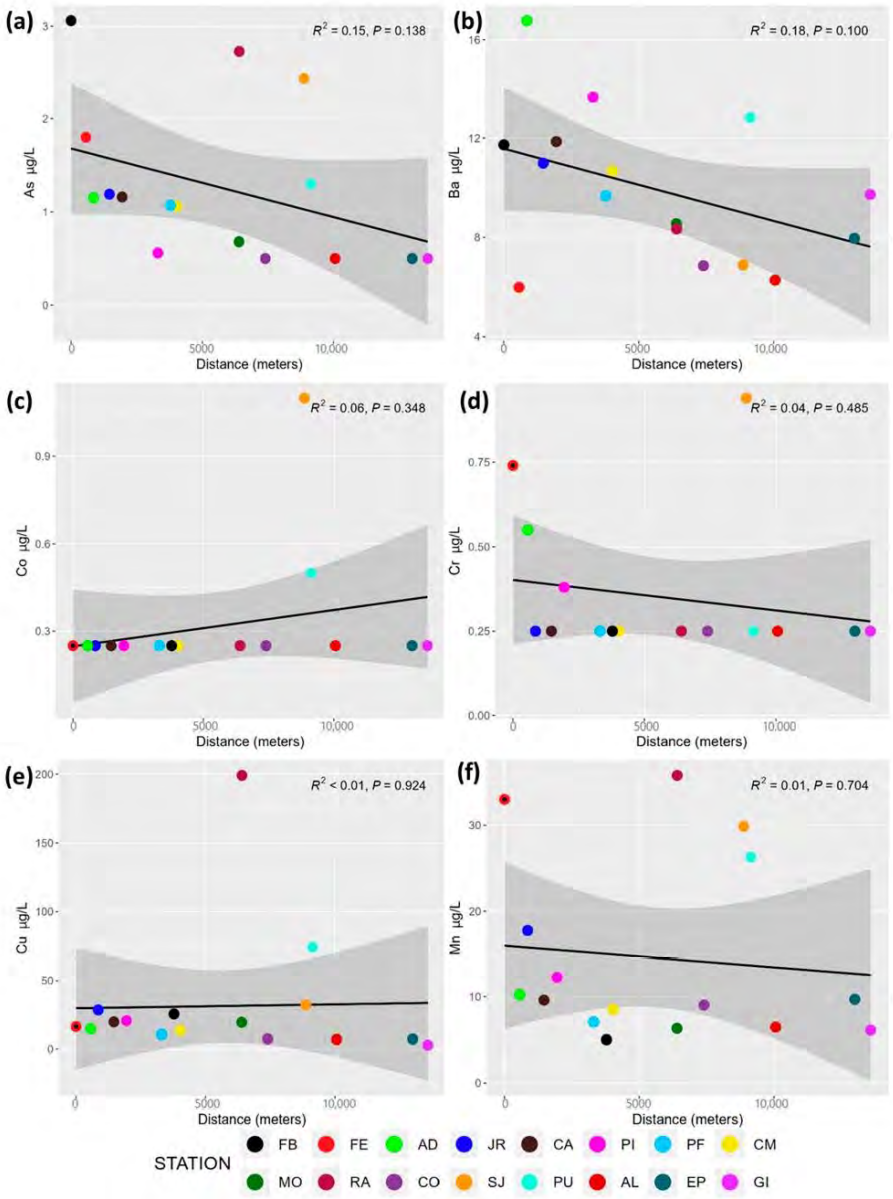
(a)
R^2 = 0.15, P = 0.138
As µg/L
Distance (meters)
(b)
R^2 = 0.18, P = 0.100
Ba µg/L
Distance (meters)
(c)
R^2 = 0.06, P = 0.348
Co µg/L
Distance (meters)
(d)
R^2 = 0.04, P = 0.485
Cr µg/L
Distance (meters)
(e)
R^2 < 0.01, P = 0.924
Cu µg/L
Distance (meters)
(f)
R^2 = 0.01, P = 0.704
Mn µg/L
Distance (meters)
STATION
FB FE AD JR CA PI PF CM
MO RA CO SJ PU AL EP GI

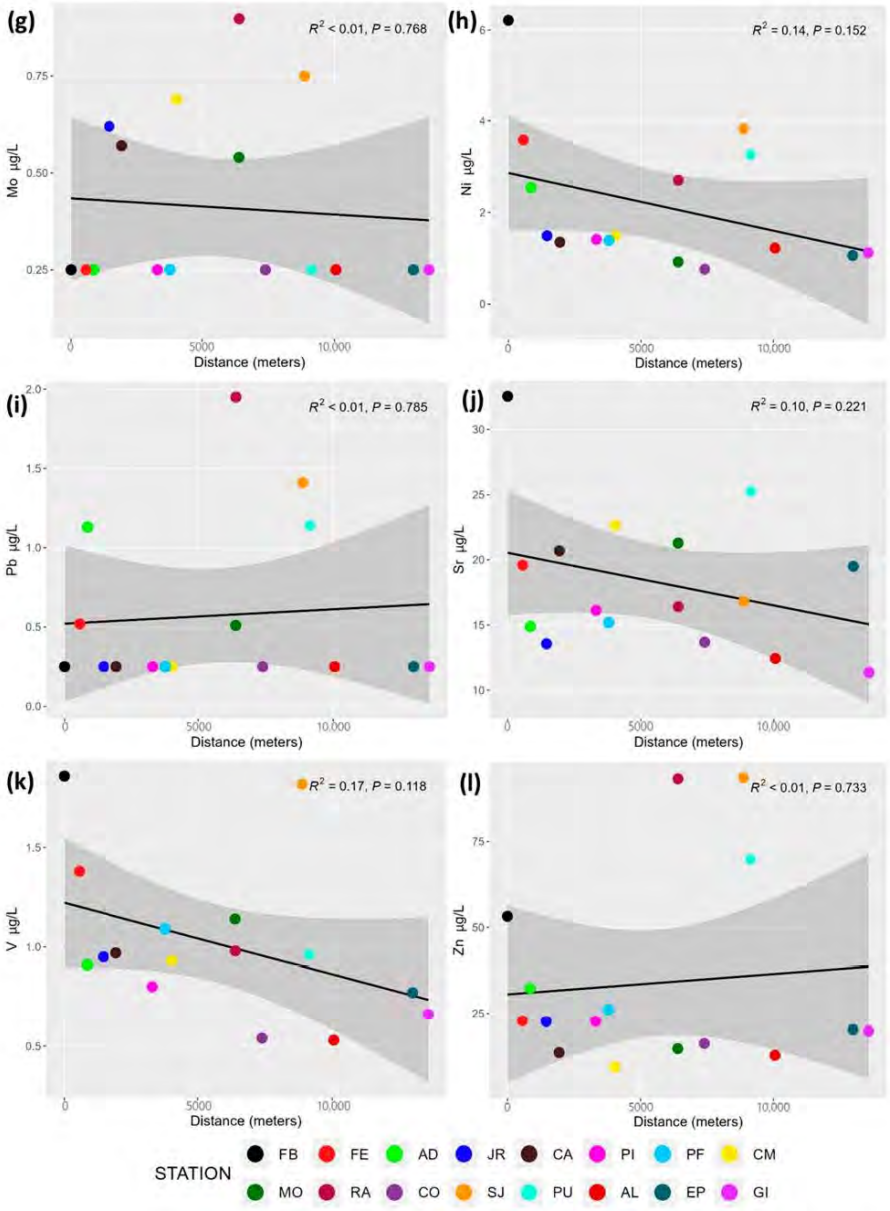

Figure 5. Scatter plots showing the variations of trace element ((**a**) As, (**b**) Ba, (**c**) Co, (**d**) Cr, (**e**) Cu, (**f**) Mn, (**g**) Mo, (**h**) Ni, (**i**) Pb, (**j**) Sr, (**k**) V, and (**l**) Zn) concentrations (µg L^{-1}) in rainwater by rain gauge location. Sampling points are arranged by increasing distance (m) from the phosphogypsum stacks (FB). Regression lines, standard error (grey shadow), correlation coefficients (R^2), and *p*-values are included in every plot.

4. Discussion

The influence of the phosphogypsum stacks on rainwater fallen in the Huelva metropolitan area was assessed through pH and EC measurements, the concentration of major anions (Cl^-, F^-, NO_2^-, NO_3^-, PO_4^{3-}, and SO_4^{2-}), major element content (Ca^{2+}, K^+, Mg^{2+}, Na^+, and NH_4^+), and trace element content (As, Cd, Co, Cr, Cu, Mn, Ni, Pb, Sr, V, and Zn) in the soluble fraction of rainwater collected in Hellmann rain gauges. In the south-western Mediterranean region, dryfall is dominant between consecutive rainy events [60]. This study revealed that the mean concentrations of F^-, Sr, and Ni were considerably higher and pH lower in rainwater collected in FB than these values in the WHO guidelines for drinking water quality [59]. Furthermore, most of the elements (As, Ca^{2+}, Cr, F^-, NH_4^+, Ni, PO_4^{3-}, SO_4^{2-}, Sr, and V) were quite a bit higher in FB compared to the other rain gauge locations, particularly when contrasted with unpolluted areas (MN). The findings indicated that the elements studied in the rainwater samples from the Huelva metropolitan area displayed consistent spatial variations. Most of these element concentrations decrease with distance to the phosphogypsum stacks (FB) and show a similar distribution pattern. The outcomes from this research are innovative and offer valuable insights into the exposure of residents living close to the phosphogypsum stacks.

4.1. pH and Conductivity

The mean median pH value of rainwater in the studied area was 7.03 (Table S2; Figure 2a), although the pH of unpolluted rainwater typically hovers around 5.6 due to the carbonate buffering effect of dissolved CO_2 in rain droplets [61]. The relatively elevated mean pH values observed in this area are not due to a lack of acidity in rainwater, but rather to the neutralisation of acidity in rainwater. The discrepancy may be due to the existence of sea-salt particles, which act as neutralising agents [33,62–64]. Elevated levels of sea-salts in rainwater have been previously documented in other locations, particularly for coastal regions [62–64]. According to previous studies, most phosphogypsum deposits are typically located in coastal zones close to the producing factories [65,66]. The key characteristic is the elevated levels of Ca^{2+}, Cl^-, Na^+, NO_3^-, Mg^{2+}, and SO_4^{2-}, indicating that neutralisation is the primary cause for the low acidity. As this study is located near the coast (Figure 1), sea-salt particles were the most dominant neutralising agents [62–64]. On the other hand, our lower pH values in rainwater compared with a similar study, which pH ranged from 7.0 to 7.5 [60–62], certainly result from rain acidity occurring by toxic acid gaseous compounds released into the atmosphere from the phosphogypsum stacks [49,50].

According to the pH (Table S2; Figure 2a), samples collected in rain gauges located close to phosphogypsum stacks (FB) revealed the minimum values (6.31), indicating acid pH values lower than the minimum value (6.5) recommend by the WHO guidelines for drinking water quality [59]. The low pH of rainwater (pH < 6. 5) can impact the solubility of harmful elements like As, Cd, and Pb, potentially making rainwater a source of toxic metal(loid)s, which pose various health risks, including cancer and neurobehavioral disorders [59]. This acidity may be associated with the existence of acid-producing particulate matter (such as sulphide particles) in suspension and acid gaseous compounds (hydrogen fluoride) released to the atmosphere coming from the phosphogypsum stacks [49,50]. Phosphogypsum is mainly calcium sulphate hydrate ($CaSO_4{\cdot}2H_2O$), which is a waste product formed when phosphate rock is combined with sulphuric acid to produce phosphoric acid [15,16,21–23]. In addition, the results revealed an inverse correlation between SO_4^{2-} concentrations and pH values in rainwater (Figures 2a and 4f). Similar results were obtained in other studies conducted in areas affected by sulphide emissions [30,37,38,67]. Moreover, Figure 2a reveals the pH dependence with the distance to FB. At greater distances from the phosphogypsum stacks, the pH values increase due to these

acid-producing minerals that are primarily neutralised by sea-salt particulate. Na^+ and Ca^{2+} denoted a similar pattern, indicating the transport of Cl^-, SO_4^{2-}, and NO_3^-, as well as buffering processes in accordance with other studies [33,62–64]. The R^2 and *p*-values indicate a slightly positive correlation (R^2 = 0.05) and a correlation that is not statistically significant (*p*-value = 0.392) between both variables.

Rainwater conductivity showed notable discrepancies among rain gauges (Table S2; Figure 2b). The elevated conductivity levels in most rainwater samples highlight the significant role of dissolved particles in the rainwater. In our case, the EC levels are influenced by the incidence of organic material from animals, primarily birds, and the nearby vegetation within the rain gauges [68]. This is the primary cause for the particularly high EC levels in SJ (137.65 μS cm^{-1}) > PU (115.35 μS cm^{-1}) > EP (117.55 μS cm^{-1}). Additional sources of inorganic contamination, such as heavy road traffic, dust, and ashes, are minor causes that affect the EC [69]. For these reasons, these rain gauges have the lowest quality score (SJ = 1; PU = 1; EP = 2). Similar EC values were obtained among the others rain gauges. The R^2 and *p*-values indicate a moderately positive correlation (R^2 = 0.15) and a slightly correlation (*p*-value = 0.140) between increases in EC levels and distance to the phosphogypsum stacks (Figure 2b).

4.2. Major Anions and Cations

Most precipitation events occurred in spring and autumn due to the study area having a Mediterranean climate. All ionic species vary throughout the year, although most ion concentrations were higher in the first rains of autumn. In accordance with previous studies conducted in Mediterranean areas [29,31,32,37,38,60,62,67], the highest concentration levels were observed at the beginning of rainy season (autumn) due to the accumulation of a large amount of soluble pollutants in the atmosphere after a long period without rain events, such as in summer, which were scavenged by the rain. Despite this, nitrite and nitrate were also high in spring. Since, during this season, the use of nitrogenous fertilisers was increased in the surrounding farm field, this could also contribute to increased NO_3^- and NO_3^- concentrations. A similar trend was obtained in other studies conducted near agricultural areas [29,31,32,60,62].

The major ion composition (Table S2) of rainwater in the Huelva metropolitan area was generally similar to that documented previously for other locations of Huelva province, except for F^- [37,38]. Variations can be attributed to different meteorological factors during the examination periods, as well as local factors such as the proximity and orientation to most important contamination sources, the effect of marine factors, dominant meteorological conditions, and other similar aspects. The outcomes showed the influence of the phosphogypsum stacks over rainwater chemical composition, increasing some of the major components such as Ca^{2+}, F^-, PO_4^{3-}, and SO_4^{2-} (Table S2; Figures 3a and 4b,e,f). A downward trend in these ion concentrations in wet depositions was detected when the distance to the affected area increased. These findings are in accordance with previous studies, where the maximum concentration of these elements was detected in sediments close to phosphogypsum stacks [35] and also cumulated in nails of citizens residing near this waste [38]. This fact is greatly influenced by gases and particulate matter released from phosphogypsum stacks. Recent studies showed the presence of hydrogen fluoride (HF) in the air of Huelva city, attributed to emissions from phosphogypsum stacks [49,50]. The F^- concentrations are a health concern and are greatly influenced by phosphogypsum stack proximity. FE achieved the highest value (2.94 mg L^{-1}) and FB a similar value (2.66 mg L^{-1}), which are above the WHO drinking guideline value of 1.5 mg L^{-1} [59]. Concentrations above this value carry an increased risk of dental fluorosis, and much higher concentrations lead to skeletal fluorosis that is associated with osteosclerosis, the calcification of tendons and ligaments, and bone deformities [59]. Although the concentration falls

with increased distance from the phosphogypsum stacks, the emissions of this gas are demonstrated, which is considered as one of the most harmful gaseous compounds present in the air [49,50]. The findings indicate that phosphogypsum stacks are the primary anthropogenic source of F^- contamination. Furthermore, phosphogypsum ($CaSO_4{\cdot}2H_2O$) is mainly composed of Ca^{2+} and SO_4^{2-}, and it contains some residual phosphorous originating from the phosphate rock utilised in the production process of phosphoric acid [15,16,21–23]. The occurrence of these elements in the phosphogypsum stacks indicates an increase in the air of these kinds of airborne particulates during dry and windy conditions [30,37,38,67], which would subsequently lead to a rise in Ca^{2+}, PO_4^{3-}, and SO_4^{2-} concentration in rainwater (Figures 3a and 4e,f). Since, over the years, south-westerly to north-westerly winds prevail along the estuary, the transport of Ca^{2+}, PO_4^{3-}, and SO_4^{2-} from phosphogypsum stacks is possible. Moreover, Ca^{2+} concentration is also related to sea-salt particles from the proximity to the ocean, as occurred in previous similar studies conducted close to the sea [3,62–64]. However, calcium also probably comes from the soil, as the Huelva metropolitan area is rich in calcareous soils [46]. In addition, PO_4^{3-} is related to organic dirt from animals, mainly birds, and the surrounding vegetation inside the rain gauges [68]. Furthermore, these major ion concentrations are inversely correlated (negative correlation) to the distance from the phosphogypsum stacks, revealing that these are the main pollution source of as F^- and SO_4^{2-} (Figure 4b,f). According to R^2 and p-values, the concentration of every major ion component in relation to distance can be ranked in the following order: $F^- > Ca^{2+} > Na^+ > SO_4^{2-} > Mg^{2+} > NO_2^- > NO_3^- > Cl^- > K^+ > PO_4^{3-} > NH_4^+$. The low R^2 values, ranging from 0.01 to 0.25 in absolute terms, indicate weak statistical correlations between each pair of variables. Moreover, the observed low significance levels, with p-values ranging from 0.046 to 0.911, validate that the possibility of the correlation is negligible.

On the other hand, positive correlations between Cl^-, K^+, Mg^{2+}, Na^+, NO_2^-, and NO_3^- concentrations and distance were found (Figures 3b–d and 4a,c,d). This situation may come from the fact that the other major components have both a sea influence and a crustal/agricultural origin, as revealed by previous studies [35,62–64]. Consequently, salts dissolved in rainwater come from marine aerosol and continental sources, both natural and anthropogenic. Considering that the majority of rain gauge locations are positioned close to the coast (Figure 1), the distances shown in Figure 3 are also linked to the proximity to the coast. This strong sea influence on rainwater concentrations for Cl^-, K^+, Mg^{2+}, and Na^+ is due to the absence of sources for these major anions and elements in the vicinity of the rain gauge locations, as well as the proximity to the sea. This might explain the positive correlation observed for Cl^-, K^+, Mg^{2+}, and Na^+, as well as the occurrence of Ca^{2+} and SO_4^{2-} inland, in accordance with other studies [30,35,62–64,67,70,71]. Additionally, the high values of Ca^{2+}, Cl^-, K^+, Mg^{2+}, and Na^+ at the control rain gauge location (MN), which is located in an unpolluted area close to the Atlantic Ocean (less than 1 km), denotes a great influence by sea-salts and aerosols (Table S2). The chemical profile of the marine source remained consistent in the region for the entire duration of the study.

However, animal and vegetation dusts and fertilisers from the surrounding farmland are generally nitrogen-rich natural and anthropogenic sources [72] and may be responsible for the origin of NO_2^- and NO_3^-. Furthermore, the high content for all the major anions and elements studied, with the exception of F^- and SO_4^{2-}, in SJ, PU, and EP (Table S2), could be attributed to the debris in the rain gauge, which is likely caused by birds and nearby vegetation [68], which were the cause of the rain gauge locations with the lowest quality score (Table S1). These results are in accordance with the EC results, which showed the highest EC values (Table S2) and the lowest quality scores (Table S1). This fact is proven in SJ, placed at 8.9 km from phosphogypsum stacks, with high concentrations of major ions. Moreover, in the northeast of Huelva city an industrial area "Polígono

Tartessos" is located that hosts a pulp and paper industry Empresa Nacional de Celulosas (Ence)-Energía y Celulosa, S.A. This facility has been in operation for over 70 years, and pulp and paper production was finally closed in 2014; it currently produces renewable energy with agroforestry biomass. The proximity of this area, situated 1 km southeast of San Juan city (aligned with the predominant wind direction), in conjunction with its closeness to the phosphogypsum stacks, make the rain gauge location of SJ mostly susceptible to the incidence of organic dust and even heavy metals [73]. With regard to NH_4^+, it may originate either from bird and vegetation debris or from combustion processes in the power plant [73].

4.3. Trace Elements

The source of pollutant emissions might be causing the seasonal variation in trace metal concentrations during different rainfall events. Rainfalls after dry periods showed high metal concentrations, whereas rainfalls that continued for several days had lower metal concentrations. The relative abundance of trace elements in rainwater is determined by their evaporation rate, their concentration within the samples, and their solubility (Table S2).

The results revealed the influence of the phosphogypsum stacks over rainwater quality, increasing some of the trace elements such as As, Ni, Sr, and V (Table S2; Figure 5a,i,j). As the distance from the affected area increases, a decline in the concentrations of most toxic metal(loid)s in wet depositions was observed. The chemical profile of rainwater samples in the studied area exhibits varying concentrations of trace elements depending on the volume of rainfall, the trajectory of the rainfront, and the interval between the precipitation events [74]. The trace element concentration in the rainwater of the Huelva metropolitan area was quite high compared with the MN location, which is an unpolluted area (Table S2), and other studies conducted in rural areas [29,31–34]. Some of the trace elements showed a possible correlation between their concentrations and the distance from the phosphogypsum stacks considering R^2 and p values (Figure 5). The correlations decreased in the following order: Ba > V > As > Ni > Sr > Co > Cr > Mn > Zn > Mo > Pb > Cu. The low values of R^2, in the range of 0.01–0.18 in absolute amounts, reveal weak statistical relationships between every pair of variables, as occurred with major components. In addition, the low significance levels observed (p-values ranged from 0.100 to 0.924) suggest a slight likelihood of correlation.

In this study, only Co, Cu, Pb, and Zn correlations with the distance to the phosphogypsum stacks are positive (Figure 5c,e,i,l), with the rest being negative (As, Ba, Cr, Mn, Mo, Ni, Sr, and V). The elements that were negatively correlated appear to be associated with the phosphogypsum stacks due to the fact that the mean concentration decreased with distance (Figure 5a,b,d,f–h,j,k). These trace elements are contained in phosphogypsum stacks [15,16] and, according to previous studies [21–23], they are widely geoavailable due to the weathering they suffered. In addition, previous studies revealed that the marsh pollution signature near the phosphogypsum stacks was characterised by 20 elements, including As, Mn, Mo, Ni, Sr, and V [12]. Similarly, other research concluded that Huelva residents living near the phosphogypsum stacks had the maximum cumulated levels of As, Ni, and Sr in nails [13]. Furthermore, very high Ni concentration is a health concern and is greatly influenced by phosphogypsum stack proximity, achieving the highest mean value in FB (86.85 μg L^{-1}), which is strongly above the WHO guideline drinking value of 70 μg L^{-1} [59]. The critical effect for the risk characterisation of chronic exposure to nickel is reproductive and developmental toxicity [5]. Moreover, there is strong metallurgical activity close to the phosphogypsum stacks located in "Polo Químico de Promoción y Desarrollo de Huelva—Punta del Sebo" (IC1; Figure 1) chemical industry

complexes, which release As, Cr, Mn, and other trace elements in accordance with previous research [39–45]. These previous studies on the air quality in the city of Huelva attributed the majority of the Sr and V emissions, with the crude oil refinery located in the "Nuevo Puerto Palos de la Frontera" (IC2; Figure 1) industrial complex identified as the primary source [39–45]. Additionally, this spatial variation may be the result of air input contaminated with industrial emissions from both the fertiliser factory and phosphogypsum stacks, combined with the closeness to the industrial complexes and the prevailing northwest wind direction; Huelva city is exposed to the significant atmospheric deposition of these elements [15,16,21,22,39–45].

In contrast, correlations for Co, Cu, Pb, and Zn were positively correlated with the distance to the phosphogypsum stacks. The elements Cu, Pb, and Zn are most likely associated with the heavy chemical industry complexes located in the vicinity of the city. This inference is substantiated by the observation that the highest concentrations of these elements were recorded at RA, followed by PU, which represents the sampling points nearest to these industrial complexes. The enrichment factors of Cu, Pb, and Zn indicated significant anthropogenic influences due to industrial emissions, as revealed by similar studies conducted in highly polluted areas in China [75] and Bangladesh [76]. Furthermore, similar results were reached in earlier studies conducted in Huelva province (Rio Tinto Mining District), which shown higher deposition fluxes in the soluble fraction of Cu, Pb, and Zn associated with mining/metallurgical activities [37,38]. The spatial variation of Cu, Pb, and Zn is in accordance with previous studies [12,13], which identified the distinct sediment pollution signatures in the Odiel–Tinto Estuary and the internal cumulated dose of harmful metal(loid)s in Huelva residents from diverse sources, revealing the highest concentration close the chemical complexes (Figure 1). Moreover, other studies on the air quality of Huelva city revealed that Cu and Pb emissions are linked to a copper smelter situated southeast of the city located in the "Nuevo Puerto Palos de la Frontera" (IC2; Figure 1) [39–45]. The literature suggests that Pb exposure can potentially lead to respiratory, neurological, digestive, cardiovascular, and urinary disorders [59]. Moreover, long-term exposition to copper can cause dizziness, headaches, and other severe diseases, such as kidney and liver damage. Breathing in copper dusts, sprays, or crystals can irritate your nose and throat [59]. In addition, elevated Zn levels pose no significant health risk and are heavily impacted by the material of the rain gauge [59].

As happens in the case of major components, rain gauge locations with the minimum quality score (SJ, PU, and EP) typically exhibit high levels for most trace elements. This fact denotes that dirt from other pollution sources, like heavy road traffic, dust, ashes, and bird droppings are factors that greatly impact rainwater chemical composition [68]. In addition, a thermal power plant is located in an industrial area "Polígono Tartessos" near the SJ rain gauge, which produces a significant amount of greenhouse gas emissions, dust, and trace elements, such as Co, Cr, and Zn. This situation might be crucial in understanding the localised increase in the concentration of these elements at this particular site, particularly cobalt, which is reduced by two orders of magnitude at other rain gauge locations. In this area, phosphogypsum stacks are the predominant source mixed with other secondary sources located inside the city of San Juan (SJ). This combination of the phosphogypsum stacks and local emission sources results in a mixture of trace elements originating from both natural sources (such as vegetation and animal dirt) and human activities (including power plant and traffic emissions).

More studies are needed to link the specific contribution of metals from the phosphogypsum stacks from different sources (trophic chain, water geochemistry, direct air resuspension, dust deposition from rain) to the pollution load of the Huelva Estuary to study its association with local morbidity and mortality.

5. Conclusions

The results of this study reveal certain spatial variability on the chemical profile of the rainwater samples collected in the Huelva metropolitan area. An enrichment of potentially harmful metal(loid)s such as As, Ca^{2+}, Cr, F^{-}, Ni, PO_4^{3-}, SO_4^{2-}, Sr, and V were detected in the soluble fraction in areas close to the phosphogypsum stacks. Only in the rain gauges near the phosphogypsum stacks did the found levels of pH, F^{-}, and Ni significantly surpassed the guideline values for drinking water quality by the WHO. In addition, other main pollution sources were identified in the studied area: a regional source comprising sea-salt particles and the aerosols from the Atlantic Ocean and Odiel–Tinto Estuary (marine factors: Ca^{2+}, Cl^{-}, K^{+}, Mg^{2+}, and Na^{+}) and a local source from the chemical complexes (industrial emissions: Co, Cu, Pb, and Zn). Moreover, phosphogypsum stacks are predominantly situated along coastal areas around the world, rendering the marine influence a common factor among all such deposits. However, other local emission factor might influence the rainwater chemistry profile. This research serves as a crucial initial step in comprehending the distribution patterns of harmful metal(loid) concentrations in rainwater and raises significant questions about the effect of the phosphogypsum stacks and the chemical industries on the environment and health in this area. These results revealed the real impact of the identified pollution sources in the quality of the rainwater of the Huelva metropolitan area, especially the areas closest to the phosphogypsum stacks. The influence of the phosphogypsum stacks is apparent in the sampling locations exposed to dust-bearing winds downwind of the area. This suggests that phosphogypsum stacks are the primary source of hazardous elements (As, Cr, F^{-}, Ni, PO_4^{3-}, and SO_4^{2-}), which could potentially have adverse environmental effects on the nearby ecosystem, and the population situated in the prevailing wind directions. Also, our results might be useful to supplement the data of the proportion of pollution sources in the study area. Despite this, more studies in other similar study areas are warranted before addressing environmental policy implications. This study could help as an initial step in evaluating the influence of the RESTORE 2030 restoration plan for the Odiel–Tinto Estuary. These chemical patterns might also be used as a reference to assess the effect of upcoming interventions on existing contamination sources in other similarly contaminated areas. Furthermore, long-term monitoring post restoration could identify changes and trends, offering a more in-depth understanding of the environmental and health implications in the study area.

Supplementary Materials: The following supporting information can be downloaded at: www.mdpi.com/xxx/s1, Table S1. Main characteristics of the weather stations; Table S2. Descriptives.

Author Contributions: Conceptualization, M.C.-L. and R.R.-P.; methodology, M.C.-L. and R.R.-P.; software, V.S.-S.; validation, M.C.-L. and R.R.-P.; formal analysis, V.S.-S.; investigation, M.C.-L.; resources, J.A.; data curation, M.C.-L. and V.S.-S.; writing—original draft, M.C.-L.; writing—review & editing, M.C.-L., J.A. and R.R.-P.; Visualization, J.A. and R.R.-P.; Supervision, J.A.; Project administration, J.A. and R.R.-P.; Funding acquisition, J.A. All authors have read and agreed to the published version of the manuscript.

Funding: This research was funded by the Andalusian Government '2018 Special Action of the Andalusian Government: Support to the Huelva Phosphogypsum Experts Committee' and by Huelva University local funds to support research groups from 2018 to 2023.

Data Availability Statement: The original contributions presented in this study are included in the article/Supplementary Materials. Further inquiries can be directed to the corresponding author.

Acknowledgments: We want to thank Adrián Polonio, Irati Chasco, and Adrián Ruiz for sample collection support. We thank the management of the CEIP Hermanos Pinzón, CEIP Pedro Alonso Niño, CEIP Tierno Galván, CEIP Juan Ramón Jiménez, IES Diego Rodríguez, IES Odiel, IES Fuente Juncal, IES Saltes, IES Pintor Pedro Gómez, Casa del Mar, Railway Infrastructure Manager (ADIF), and Fertiberia for their collaboration. Special thanks to Ismael Dominguez Báez and Alba García Omedes in charge of the "El Portil-EP" rain gauge, who provided voluntary support in this collaborative project. The authors gratefully acknowledge the analysis support of the Research and Development Centre for Agri-Food Resources and Technologies (CIDERTA) in University of Huelva (Spain).

Conflicts of Interest: The authors declare the following financial interests/personal relationships, which may be considered as potential competing interests: Juan Alguacil reports that financial support was provided by Andalusian Government. If there are other authors, they declare that they have no known competing financial interests or personal relationships that could have appeared to influence the work reported in this paper.

References

1. Briffa, J.; Sinagra, E.; Blundell, R. Heavy metal pollution in the environment and their toxicological effects on humans. *Heliyon* **2020**, *6*, e04691. https://doi.org/10.1016/j.heliyon.2020.e04691.
2. Nieto, J.M.; Sarmiento, A.S.; Olías, M.; Canovas, C.R.; Riba, I.; Kalman, J.; Delvalls, T.A. Acid mine drainage pollution in the Tinto and Odiel rivers (Iberian Pyrite Belt, SW Spain) and bioavailability of the transported metals to the Huelva Estuary. *Environ. Int.* **2020**, *33*, 445–455. https://doi.org/10.1016/j.envint.2006.11.010.
3. Torre, B.M.; Borrero-Santiago, A.R.; Fabbri, E.; Guerra, R. Trace metal levels and toxicity in the Huelva Estuary (Spain): A case study with comparisons to historical levels from the past decades. *Environ. Chem. Ecotox.* **2019**, *1*, 12–18. https://doi.org/10.1016/j.enceco.2019.07.002.
4. Alguacil, J.; Ballester, F.; Donado-Campos, J.; Pollán, M.; Rodríguez-Artalejo, F. Dictamen Realizado Por Encargo Del Defensor Del Pueblo Andaluz Sobre El Exceso de Mortalidad y Morbilidad Detectado en Varias Investigaciones en La Ría de Huelva; Grupo de Trabajo de la Sociedad Española de Epidemiología: Seville, Spain; 2014. Available online: https://www.defensordelpuebloandaluz.es/informe-epidemiologico-ria-de-huelva (accessed on 11 January 2025).
5. Benach, J.; Yasui, Y.; Borrell, C.; Rosa, E.; Pasarín, M.I.; Benach, N.; Español, E.; Martínez, J.M.; Daponte, A. Examining geographic patterns of mortality: The Atlas of mortality in small areas in Spain (1987–1995). *Eur. J. Public Health* **2003**, *13*, 115–123. https://doi.org/10.1093/eurpub/13.2.115.
6. López-Abente, G.; Aragones, N.; Ramis, R.; Hernandez-Barrera, V.; Perez-Gomez, B.; Escolar-Pujolar, A.; Pollan, M. Municipal distribution of bladder cancer mortality in Spain: Possible role of mining and industry. *BMC Public Health* **2006**, *6*, 17. https://doi.org/10.1186/1471-2458-6-17.
7. Martínez-Beneito, M.A.; Botella-Rocamora, P.; Corpas-Burgos, F.; Vergara- Hernández, C.; Pérez-Panadés, J.; Perpiñán-Fabuel, H. *Atlas Nacional de Mortalidad en España (ANDEES)*; Fundación FISABIO y Dirección General de Salud Pública de la Generalitat Valenciana: Valencia, Spain, 2024. Available online: http://andees.fisabio.san.gva.es/ (accessed on 11 January 2025).
8. Aguilera, I.; Daponte, A.; Gil, F.; Hernández, A.F.; Godoy, P.; Pla, A.; Ramos, J.L. Urinary levels of arsenic and heavy metals in children and adolescents living in the industrialised area of Ria of Huelva (SW Spain). *Environ. Int.* **2010**, *36*, 563–569. https://doi.org/10.1016/j.envint.2010.04.012.
9. Rodríguez-Barranco, M.; Lacasaña, M.; Gil, F.; Lorca, A.; Alguacil, J.; Rohlman, D.S.; González-Alzaga, B.; Molina-Villalba, I.; Mendoza, R.; Aguilar-Garduño, C. Cadmium exposure and neuropsychological development in school children in southwestern Spain. *Environ. Res.* **2014**, *134*, 66–73. https://doi.org/10.1016/j.envres.2014.06.026.
10. Capelo, R.; Rohlman, D.S.; Jara, R.; García, T.; Viñas, J.; Lorca, J.A.; Contreras-Llanes, M.; Alguacil, J. Residence in an Area with Environmental Exposure to Heavy Metals and Neurobehavioral Performance in Children 9–11 Years Old: An Explorative Study. *Int. J. Environ. Res. Public Health* **2022**, *19*, 4732. https://doi.org/10.3390/ijerph19084732.
11. Silva-Caicedo, R.F.; Contreras-Llanes, M.; Capelo, R.; Zumel-Marne, A.; García-Sevillano, M.Á.; Santos-Sánchez, V.; Alguacil, J. Impact of Fish, Mollusk and Seafood Consumption before Sample Donation on Urinary and Toenail Metal Levels in Workers Exposed to Heavy Metals. *Appl. Sci.* **2024**, *14*, 8174. https://doi.org/10.3390/app14188174.

12. Contreras-Llanes, M.; Santos-Sánchez, V.; Alguacil, J.; Castillo, J.M. Delineating distinct sediment pollution signatures from diverse sources in a heavily contaminated estuary near an area of high cancer and cardiovascular mortality. *Sci. Total Environ.* **2024**, *957*, 177715. https://doi.org/10.1016/j.scitotenv.2024.177715.
13. Contreras-Llanes, M.; Alguacil, J.; Capelo, R.; Gómez-Ariza, J.L.; García-Pérez, J.; Pérez-Gómez, B.; Martin-Olmedo, P.; Santos-Sánchez, V. Internal cumulated dose of toxic metal(loid)s in a population residing near a Naturally Occurring Radioactive Material waste stacks and an industrial heavily polluted area with high mortality rates in Spain. *J. Xenobiot.* **2025**, *in press*.
14. IAEA. *Application of the Concepts of Exclusion Exemption and Clearance*; Safety Standards Series; Safety Guide No. RS-G 17, STI/PUB/1202; International Atomic Energy Agency (IAEA): Vienna, Austria, 2004.
15. Contreras-Llanes, M.; Pérez-López, R.; Gázquez, M.J.; Morales, V.; Santos, A.; Esquivias, L.M.; Bolívar, J.P. Fractionation and fluxes of metals and radionuclides during the recycling process of phosphogypsum wastes applied to mineral CO_2 sequestration. *Waste Manag.* **2015**, *45*, 412–419. https://doi.org/10.1016/j.wasman.2015.06.046.
16. Contreras, M. Valorisation of Inorganic Waste for Obtaining Construction Materials. Doctoral Dissertation. University of Huelva, Huelva, Spain. 19 July 2017. Available online: http://hdl.handle.net/10272/16090 (accessed on 11 January 2025).
17. Scientific Committee of National Experts Coordinated from Huelva University About the RESTORE 2030 Plan. Technical Report on the Suitability of the RESTORE 20/30 Project as a Solution to the Problem of the Phosphogypsum Ponds and for the Recovery of the Marshes of the Tinto River Estuary, 2024. Available online: http://mesadelaria.es/documentos/Informe_280722_C_Expertos-Agosto2022.pdf (accessed on 20 June 2024).
18. Chopin, E.I.B.; Black, S.; Hodson, M.E.; Coleman, M.L.; Alloway, B.J. A preliminary investigation into mining and smelting impacts on trace element concentrations in the soils and vegetation around Tharsis, SW Spain. *Mineral. Mag.* **2003**, *67*, 279–288. https://doi.org/10.1180/0026461036720099.
19. Chopin, E.I.B.; Alloway, B.J. Trace element partitioning and soil particle characterisation around mining and smelting areas at Tharsis, Riotinto and Huelva, SW Spain. *Sci. Total. Environ.* **2007**, *373*, 488–500. https://doi.org/10.1016/j.scitotenv.2006.11.037.
20. López, M.; González, I.; Romero, A. Trace elements contamination of agricultural soils affected by sulphide exploitation (Iberian Pyrite Belt, SWSpain). *Environ. Geol.* **2008**, *54*, 805–818. https://doi.org/10.1007/s00254-007-0864-x.
21. Lieberman, R.N.; Izquierdo, M.; Córdoba, P.; Moreno Palmerola, N.; Querol, X.; Sánchez de la Campa, A.M.; Font, O.; Cohen, H.; Knop, Y.; Torres-Sánchez, R.; et al. The evolution of brines from phosphogypsum deposits in Huelva (SW Spain) and its environmental implications. *Sci. Total Environ.* **2020**, *700*, 134444. https://doi.org/10.1016/j.scitotenv.2019.134444.
22. Pérez-López, R.; Nieto, J.M.; López-Coto, I.; Aguado, J.L.; Bolívar, J.P.; Santisteban, M. Dynamics of contaminants in phosphogypsum of the fertilizer industry of Huelva (SW Spain): From phosphate rock ore to the environment. *Appl. Geochem.* **2010**, *25*, 705–715. https://doi.org/10.1016/j.apgeochem.2010.02.003.
23. Rentería-Villalobos, M.; Vioque, I.; Mantero, J.; Manjón, G. Radiological, chemical and morphological characterizations of phosphate rock and phosphogypsum from phosphoric acid factories in SW Spain. *J. Hazard. Mater.* **2010**, *181*, 193–203. https://doi.org/10.1016/j.jhazmat.2010.04.116.
24. Pumlee, G.S.; Morman, S.A. Mine wastes and human health. *Elements* **2011**, *7*, 399–404. https://doi.org/10.2113/gselements.7.6.399.
25. Brotons, J.M.; Diaz, A.R.; Sarria, F.A.; Serrato, F.B. Wind erosion on mining waste in southeast Spain. *Land Degrad. Dev.* **2010**, *21*, 196–209. https://doi.org/10.1002/ldr.948.
26. Csavina, J.; Field, J.; Taylor, M.P.; Gao, S.; Landázuri, A.; Betterton, E.A.; Sáez, A.E. A review on the importance of metals and metalloids in atmospheric dust and aerosol from mining operations. *Sci. Total Environ.* **2012**, *433*, 58–73. https://doi.org/10.1016/j.scitotenv.2012.06.013.
27. Taylor, M.P.; Mackay, A.K.; Hudson-Edwards, K.A.; Holz, E. Soil Cd, Cu, Pb and Zn contaminants around Mount Isa city, Queensland, Australia: Potential sources and risks to human health. *Appl. Geochem.* **2010**, *25*, 841–855. https://doi.org/10.1016/j.apgeochem.2010.03.003.
28. Zota, A.; Willis, R.; Jim, R.; Norris, G.A.; Shine, J.P.; Duvall, R.M.; Schaider, L.A.; Spengler, J.D. Impact of mine waste on airborne respirable particulates in northeastern Oklahoma, United States. *J. Air Waste Manag. Assoc.* **2009**, *59*, 1347–1357. https://doi.org/10.3155/1047-3289.59.11.1347.
29. Al-Khashman, O.A. Study of chemical composition in wet atmospheric precipitation in Eshidiya area, Jordan. *Atmos. Environ.* **2005**, *39*, 6175–6183. https://doi.org/10.1016/j.atmosenv.2005.06.056.
30. Alcolea, A.; Fernández-López, C.; Vázquez, M.; Caparrós, A.; Ibarra, I.; García, C.; Zarroca, M.; Rodríguez, R. An assessment of the influence of sulfidic mine wastes on rainwater quality in a semiarid climate (SE Spain). *Atmos. Environ.* **2015**, *107*, 85–94. https://doi.org/10.1016/j.atmosenv.2015.02.028.

31. André, F.; Jonard, M.; Ponette, Q. Influence of meteorological factors and polluting environment on rain chemistry and wet deposition in a rural area near Chimay, Belgium. *Atmos. Environ.* **2007**, *41*, 1426–143. https://doi.org/10.1016/j.atmosenv.2006.10.013.
32. Avila, A.; Alarcón, M. Relationship between precipitation chemistry and meteorological situations at a rural site in NE Spain. *Atmos. Environ.* **1999**, *33*, 1663–1677. https://doi.org/10.1016/S1352-2310(98)00341-0.
33. Pelicho, A.F.; Martins, L.D.; Nomi, S.N.; Solci, M.C. Integrated and sequential bulk and wet-only samplings of atmospheric precipitation in Londrina, South Brazil (1998–2002). *Atmos. Environ.* **2006**, *40*, 6827–6835. https://doi.org/10.1016/j.atmosenv.2006.05.075.
34. Seto, S.; Hara, H. Precipitation chemistry in western Japan: Its relationship to meteorological parameters. *Atmos. Environ.* **2006**, *40*, 1538–1549. https://doi.org/10.1016/j.atmosenv.2005.10.050.
35. Zeng, J.; Han, G.; Wu, Q.; Qu, R.; Ma, Q.; Chen, J.; Mao, S.; Ge, X.; Wang, Z.; Ma, Z. Significant influence of urban human activities and marine input on rainwater chemistry in a coastal large city, China. *Water Res.* **2024**, *257*, 121657. https://doi.org/10.1016/j.watres.2024.121657.
36. Eriksson, E. Composition of atmospheric precipitation. I: Nitrogen compounds. *Tellus* **1952**, *4*, 215–232. https://doi.org/10.3402/tellusa.v4i3.8686.
37. Castillo, S.; de la Rosa, J.D.; Sánchez de la Campa, A.M.; González-Castanedo, Y.; Fernández-Caliani, J.C.; Gonzalez, I.; Romero, A. Contribution of mine wastes to atmospheric metal deposition in the surrounding area of an abandoned heavily polluted mining district (Rio Tinto mines, Spain). *Sci. Total Environ.* **2013**, *449*, 363–372. https://doi.org/10.1016/j.scitotenv.2013.01.076.
38. Castillo, S.; de la Rosa, J.D.; Sánchez de la Campa, A.M.; González-Castanedo, Y.; Fernández-Camacho, R. Heavy metal deposition fluxes affecting an Atlantic coastal area in the southwest of Spain. *Atmos. Environ.* **2013**, *77*, 509–517. https://doi.org/10.1016/j.atmosenv.2013.05.046.
39. Alastuey, A.; Querol, X.; Plana, F.; Viana, M.; Ruiz, C.R.; Sanchez de la Campa, A.; de la Rosa, J.; Mantilla, E.; García dos Santos, S. Identification and chemical characterization of industrial particulate matter sources in southwest Spain. *J. Air Waste Manag. Assoc.* **2006**, *56*, 993–1006. https://doi.org/10.1080/10473289.2006.10464502.
40. Chen, B.; Stein, A.F.; Castell, N.; González-Castanedo, Y.; Sánchez de la Campa, A.M.; de la Rosa, J.D. Modeling and evaluation of urban pollution events of atmospheric heavy metals from a large Cu-smelter. *Sci. Total Environ.* **2016**, *539*, 17–25. https://doi.org/10.1016/j.scitotenv.2015.08.117.
41. González-Castanedo, Y.; Moreno, T.; Fernández-Camacho, R.; Sánchez de la Campa, A.M.; Alastuey, A.; Querol, X.; de la Rosa, J. Size distribution and chemical composition of particulate matter stack emissions in and around a copper smelter. *Atmos. Environ.* **2014**, *98*, 271–282. https://doi.org/10.1016/j.atmosenv.2014.08.057.
42. Querol, X.; Alastue, A.; de la Rosa, J.; Sánchez-de-la-Campa, A.; Plana, F.; Ruiz, C.R. Source apportionment analysis of atmospheric particulates in an industrialised urban site in southwestern Spain. *Atmos. Environ.* **2002**, *36*, 3113–3125. https://doi.org/10.1016/S1352-2310(02)00257-1.
43. Sánchez de la Campa, A.M.; de la Rosa, J.; Querol, X.; Alastuey, A.; Mantilla, E. Geochemistry and origin of PM10 in the Huelva region, southwestern Spain. *Environ. Res.* **2007**, *103*, 305–316. https://doi.org/10.1016/j.envres.2006.06.011.
44. Sánchez de la Campa, A.M.; Sánchez-Rodas, D.; González Castanedo, Y.; de la Rosa, J.D. Geochemical anomalies of toxic elements and arsenic speciation in airborne particles from Cu mining and smelting activities: Influence on air quality. *J. Hazard. Mater.* **2015**, *291*, 8–27. https://doi.org/10.1016/j.jhazmat.2015.02.058.
45. Sánchez de la Campa, A.M.; Sánchez-Rodas, D.; Alsioufi, L.; Alastuey, A.; Querol, X.; de la Rosa, J.D. Air quality trends in an industrialised area of SW Spain. *J. Clean. Prod.* **2018**, *186*, 465–474. https://doi.org/10.1016/j.jclepro.2018.03.122.
46. Achterberg, E.P.; Herzl, V.M.C.; Braungardt, C.B.; Millward, G.E. Metal behaviour in an estuary polluted by acid mine drainage: The role of particulate matter. *Environ. Pollut.* **2003**, *121*, 283–292. https://doi.org/10.1016/S0269-7491(02)00216-6.
47. Silva, L.F.O.; Oliveira, M.L.S.; Crissien, T.J.; Santosh, M.; Bolivar, J.P.; Shao, L.; Dotto, G.L.; Gasparotto, J.; Schindler, M. A review on the environmental impact of phosphogypsum and potential health impacts through the release of nanoparticles. *Chemosphere* **2022**, *286*, 131513. https://doi.org/10.1016/j.chemosphere.2021.131513.
48. López-Coto, I.; Mas, J.L.; Vargas, A.; Bolívar, J.P. Studying radon exhalation rates variability from phosphogypsum piles in the SW of Spain. *J. Hazard. Mater.* **2014**, *280*, 464–471. https://doi.org/10.1016/j.jhazmat.2014.07.025.
49. Torres-Sánchez, R.; Sánchez-Rodas, D.; Sánchez de la Campa, A.M.; Kandler, K.; Schneiders, K.; de la Rosa, J.D. Geochemistry and source contribution of fugitive phosphogypsum particles in Huelva, (SW Spain). *Atmos. Res.* **2019**, *230*, 104650. https://doi.org/10.1016/j.atmosres.2019.104650.

50. Torres-Sánchez, R.; Sánchez-Rodas, D.; Sánchez de la Campa, A.M.; de la Rosa, J.D. Hydrogen fluoride concentrations in ambient air of an urban area based on the emissions of a major phosphogypsum deposit (SW, Europe). *Sci. Total Environ.* **2020**, *714*, 136891. https://doi.org/10.1016/j.scitotenv.2020.136891.
51. Leistel, J.M.; Marcoux, E.; Thieblemont, D.; Quesada, C.; Sanchez, A.; Almodovar, G.R.; Pascual, E.; Saez, R. The volcanic-hosted massive sulphide deposits of the Iberian Pyrite Belt. *Miner. Depos.* **1998**, *33*, 2–30. https://doi.org/10.1007/s001260050130.
52. Pérez-López, R.; Millán-Becerro, R.; Basallote, M.D.; Carrero, S.; Parviainen, A.; Freydier, R.; Macías, F.; Cánovas, C.R. Effects of estuarine water mixing on the mobility of trace elements in acid mine drainage leachates. *Mar. Pollut. Bull.* **2023**, *187*, 114491. https://doi.org/10.1016/j.marpolbul.2022.114491.
53. Blasco, J.; Sáenz, V.; Gómez-Parra, A. Heavy metal fluxes at the sediment–water interface of three coastal ecosystems from south-west of the Iberian Peninsula. *Sci. Total Environ.* **2000**, *247*, 189–199. https://doi.org/10.1016/S0048-9697(99)00490-8.
54. Weiß, J. Ion chromatography—A review of recent developments. *Fresenius Z. Anal. Chem.* **1987**, *327*, 451–455. https://doi.org/10.1007/BF00487225.
55. USEPA. *Appendix B to Part 136. Definition and Procedure for the Determination of the Method Detection Limit*; Revision 1.11. Fed. Regist. 49 (209), 43430. Also Referred to as "40 CFR Part 136"; Environmental Protection Agency: Washington, DC, USA, 1984.
56. Jenner, G.A.; Longerich, H.P.; Jackson, S.E.; Fryer, B.J. ICP-MS—A powerful tool for high-precision trace-element analysis in Earth sciences: Evidence from analysis of se-lected U.S.G.S. reference samples. *Chem. Geol.* **1990**, *83*, 133–148. https://doi.org/10.1016/0009-2541(90)90145-W.
57. ISO 9001; *Quality management systems—Requirements*, International Organization for Standardization, Geneva, Switzerland 2015.
58. ISO 14001; *Environmental management systems—Requirements with guidance for use*, International Organization for Standardization, Geneva, Switzerland 2015.
59. WHO. *Guidelines for Drinking-Water Quality*, 3rd ed.; Recommendations; World Health Organization: Geneva, Switzerland, 2008; Volume 1. Available online: https://iris.who.int/bitstream/handle/10665/204411/9789241547611_eng.pdf?sequence=1 (accessed on 11 January 2025).
60. Morales-Baquero, R.; Pulido-Villena, E.; Reche, I. Chemical signature of Saharan dust on dry and wet atmospheric deposition in the south-western Mediterranean region. *Tellus B Chem. Phys. Meteorol.* **2013**, *65*, 18720. https://doi.org/10.3402/tellusb.v65i0.18720.
61. Charlson, R.J.; Rodhe, H. Factors controlling the acidity of natural rainwater. *Nature* **1982**, *295*, 683–685. https://doi.org/10.1038/295683a0.
62. Al-Momani, I.F.; Tuncel, S.; Eler, Ü.; Örtel, E.; Sirin, G.; Tuncel, G. Major ion composition of wet and dry deposition in the eastern Mediterranean basin. *Sci. Total. Environ.* **1995**, *164*, 75–85. https://doi.org/10.1016/0048-9697(95)04468-G.
63. Dikaiakos, J.G.; Tsitouris, C.G.; Siskos, P.A.; Melissos, D.A.; Nastos, P. Rainwater composition in Athens, Greece. *Atmos. Environ.* **1990**, *241*, 171–176. https://doi.org/10.1016/0957-1272(90)90022-M.
64. Tuncer, B.; Bayer, B.; Yesilyurt, C.; Tuncel, G. Ionic composition of precipitation at the central Anatolia, Turkey. *Atmos. Environ.* **2001**, *35*, 5989–6002. https://doi.org/10.1016/S1352-2310(01)00396-X.
65. Noli, F.; Sidirelli, M.; Tsamos, P. The impact of phosphate fertilizer factory on the chemical and radiological pollution of the surrounding marine area (seawater and sediments) in northwestern Greece. *Reg. Stud. Mar. Sci.* **2024**, *73*, 103458. https://doi.org/10.1016/j.rsma.2024.103458.
66. Tayibi, H.; Choura, M.; López, F.A.; Alguacil, F.J.; López-Delgado, A. Environmental impact and management of phosphogypsum. *J. Environ. Manag.* **2009**, *90*, 2377–2386. https://doi.org/10.1016/j.jenvman.2009.03.007.
67. Robles-Arenas, V.M.; Rodríguez, R.; García, C.; Manteca, J.I.; Candela, L. Sulphide-mining impacts in the physical environment: Sierra de Cartagena-La Unión (SE Spain) case study. *Environ. Geol.* **2006**, *51*, 47–64. https://doi.org/10.1007/s00254-006-0303-4.
68. Tranel, M.A.; Kimmel, R.O. Impacts of Lead Ammunition on Wildlife, the Environment, and Human Healthda—A Literature Review and Implications for Minnesota. In *Ingestion of Lead from Spent Ammunition: Implications for Wildlife and Humans*; Watson, R.T., Fuller, M., Pokras, M., Hunt, W.G., Eds.; The Peregrine Fund: Boise, ID, USA, 2009.
69. Wagner, S.; Funk, C.W.; Müller, K.; Raithel, D.J. The chemical composition and sources of road dust, and of tire and road wear particles–A review. *Sci. Total Environ.* **2024**, *926*, 171694. https://doi.org/10.1016/j.scitotenv.2024.171694.
70. Custodio, E.; Llamas, M.R. *Hidrología Subterranea*; Omega: Barcelona, Spain, 1996; Volume I and II.
71. Todd, D.K.; Mays, L.W. *Groundwater Hydrology*, 3rd ed.; Wiley: Hoboken, NJ, USA, 2005.
72. Wakida, F.T.; Lerner, D.N. Non-agricultural sources of groundwater nitrate: A review and case study. *Water Res.* **2005**, *39*, 3–16. https://doi.org/10.1016/j.watres.2004.07.026.

73. Raynor, G.S.; Hayes, J.V. Acidity and conductivity of precipitation on central Long Island, New York, in relation to meteorological variables. *Water Air Soil Pollut.* **1981**, *15*, 229–245. https://doi.org/10.1007/BF00161255.
74. Granat, L. On the relation between pH and the chemical composition in atmospheric precipitation. *Tellus* **1972**, *24*, 550–560. https://doi.org/10.3402/tellusa.v24i6.10682.
75. Xing, J.; Song, J.; Yuan, H.; Wang, Q.; Li, X.; Li, N.; Duan, L.; Qu, B. Atmospheric wet deposition of dissolved trace elements to Jiaozhou Bay, North China: Fluxes, sources and potential effects on aquatic environments. *Chemosphere* **2017**, *174*, 428–436. https://doi.org/10.1016/j.chemosphere.2017.02.004.
76. Adhikari, S.; Zeng, C.; Zhang, F.; Adhikari, N.P.; Gao, J.; Ahmed, N.; Bhuiyan, A.Q.; Ahsan, A.; Khan, H.R. Atmospheric wet deposition of trace elements in Bangladesh: A new insight into spatiotemporal variability and source apportionment. *Environ. Res.* **2023**, *217*, 114729. https://doi.org/10.1016/j.envres.2022.114729.

A1.3. Paper #3

A1.3.1 Extended abstract paper #3

Internal cumulated dose of toxic metal(loid)s in a population residing near a Naturally Occurring Radioactive Material waste stacks and an industrial heavily polluted area with high mortality rates in Spain

Manuel Contreras-Llanes [1,2], Juan Alguacil [1,2,3], Rocio Capelo [1,2,] José Luis Gómez-Ariza [2,4,] Javier García-Pérez [3,5,] Beatriz Pérez-Gómez [3,5,] Piedad Martin-Olmedo [6,7], Vanessa Santos-Sánchez [1,2,*]

[1] Research group in Clinical, Environmental and Epidemiology Social Transformation (EPICAS), Department of Sociology, Social Work and Public Health, University of Huelva, 21007 Huelva, Spain.

[2] Research Centre for Natural Resources, Health and Environment (RENSMA), Faculty of Experimental Sciences, University of Huelva, 21007 Huelva, Spain.

[3] Consortium for Biomedical Research in Epidemiology & Public Health (CIBER en Epidemiología y Salud Pública - CIBERESP), 28029 Madrid, Spain

[4] Department of Chemistry. Faculty of Experimental Sciences. University of Huelva

[5] Cancer and Environmental Epidemiology Unit, Department of Epidemiology of Chronic Diseases, National for Epidemiology, Carlos III Institute of Health, 28029 Madrid, Spain

[6] Andalusian School of Public (EASP), 18011 Granada, Spain.

[7] Biosanitary Research Institute of Granada (Ibs.Granada), 18012 Granada, Spain

[*] **Corresponding author:** Vanessa Santos-Sánchez (vanesa.santos@dstso.uhu.es)

Keywords: Huelva; industrial polluted area; phosphogypsum; metal(loid)s; Naturally Occurring Radioactive Material; spatial distribution; toenails; kriging; principal component analysis

Introduction: Huelva City (SW-Spain), with 150,000 inhabitants, is situated near one of the world's most contaminated sites (Morillo et al., 2008; Sáenz et al., 2003). This contamination is due to high levels of metal(loid)s and radionuclides released by two heavy chemical industry complexes, the largest NORM waste deposit (PG stacks) in Europe, and the highly polluted Odiel-Tinto Estuary by AMD and industrial activities (Blasco et al., 2000; Lieberman et al., 2020; Pérez-López et al., 2010; Santos Bermejo et al., 2003). There is strong evidence between industrial and mining pollution with environmental impact and health effects (Briffa et al., 2020). Huelva City has higher cardiovascular disease and cancer mortality rates compared to the rest of Spain (Alguacil et al., 2014; Benach et al., 2003; Lopez-Abente et al., 2001). Despite public concerns about the link between these pollution and mortality, the issue remains unresolved. Social and judicial actions have focused on the PG stacks, even though there are other pollution sources, leading to the cessation of PG stockpiling in 2010 and approving a restoration plan for the affected marshes called RESTORE 2030. Biomonitoring of metal(loid)s using bioindicators like hair and nails, which reflect long-term exposure, is crucial for assessing health risks (Bencko, 1995; Gutiérrez-González et al., 2019; Salcedo-Bellido et al., 2021). In addition, geostatistical methods, such as Kriging, are used to identify spatial patterns of metal(loid)s (Webste and Oliver, 2001). However, there are few published studies using these spatial analysis techniques to analyse the metal(loid)s signature in toenails (Zierold et al., 2021). The aim of this research was to analyse the association between the levels of cumulated exposure of 16 metal(loid)s (Al, As, Cd, Co, Cr, Cu, Fe, Mn, Mo, Ni, Pb, Se, Tl, U, V and Zn) in the toenails of Huelva's residents and their proximity to local industrial pollution sources.

Methodology: Participants were controls from Huelva City, recruited for the MCC-Spain study (2008-2013), which investigates environmental and genetic factors associated with tumours or cancers. This study included 55 participants aged 20 to 85 years from Huelva City, who had lived in the area for at least 6 months and provided written informed consent. Toenail samples were collected from both feet of each participant within 2 weeks of recruitment and the elemental content of 16 metal(loid)s was determined by ICP-MS. Descriptive statistical analysis was performed to characterise the distribution of metal(loid)s in toenails. Spearman's correlation coefficient was calculated

to assess relationships between elements, while, PCA was used to reduce data complexity and identify potential sources pollution. Spatial variability in metal(loid) concentrations was studied using kriging, a spatial interpolation method, to create distribution maps of the elements in Huelva City.

Findings: Our study revealed that the mean levels of As, Co, Cr, Ni and Se Co in Huelva citizens' toenails were considerable higher compared to these from unpolluted areas with similar population characteristics (culture, diet, and lifestyle. These results revealed correlations between the metal(loid)s analysed, exhibiting similar distribution patterns, with higher concentrations of these elements found near the PG stacks (As, Cd, Mo, Pb and Se) and industrial complexes (Al, Cu and Zn; Figure 12).

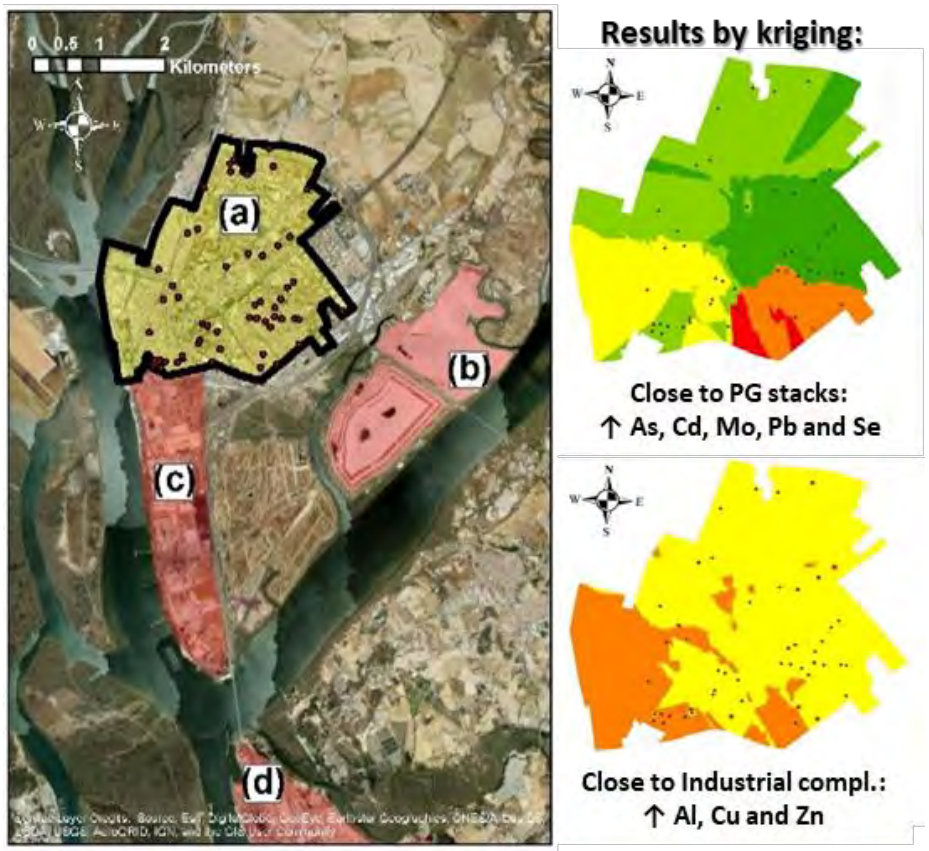

Figure A1.3. Location map of Huelva City [a) Residential area; b) PG stacks; c,d) Industrial complexes; Dots represent the locations of participants] (left). Spatial distribution of representative chemical elements by pollution sources (right).

Conclusion: The spatial distribution of most of the cumulated metal(loid)s concentration in Huelva residents appears mainly controlled by anthropogenic factors. The results are novel and provide insights into the exposures of this population to local pollutions sources, revealing the real impact of the industry on Huelva population's health, especially among those living closest to the main pollution sources (PG stacks and industrial complexes), which had not been proven before. Furthermore, this study provides a critical baseline for future health risk assessments and remediation efforts for the affected area like RESTORE 2030.

A1.3.2 Published version paper #3

Journal of Xenobiotics

MDPI

Article

Internal Cumulated Dose of Toxic Metal(loid)s in a Population Residing near Naturally Occurring Radioactive Material Waste Stacks and an Industrial Heavily Polluted Area with High Mortality Rates in Spain

Manuel Contreras-Llanes [1,2,†], Juan Alguacil [1,2,3,†], Rocío Capelo [1,2], José Luis Gómez-Ariza [2,4], Javier García-Pérez [3,5], Beatriz Pérez-Gómez [3,5], Piedad Martin-Olmedo [6,7] and Vanessa Santos-Sánchez [1,2,*]

1 Research Group in Clinical, Environmental and Epidemiology Social Transformation (EPICAS), Department of Sociology, Social Work and Public Health, University of Huelva, 21007 Huelva, Spain; mcontreras@uhu.es (M.C.-L.); alguacil@uhu.es (J.A.); rocio.capelo@dbasp.uhu.es (R.C.)
2 Research Centre for Natural Resources, Health and Environment (RENSMA), Faculty of Experimental Sciences, University of Huelva, 21007 Huelva, Spain; ariza@dqcm.uhu.es
3 Consortium for Biomedical Research in Epidemiology & Public Health (CIBER en Epidemiología y Salud Pública—CIBERESP), 28029 Madrid, Spain; jgarcia@isciii.es (J.G.-P.); bperez@isciii.es (B.P.-G.)
4 Department of Chemistry, Faculty of Experimental Sciences, University of Huelva, 21007 Huelva, Spain
5 Cancer and Environmental Epidemiology Unit, Department of Epidemiology of Chronic Diseases, National Center for Epidemiology, Carlos III Institute of Health, 28029 Madrid, Spain
6 Andalusian School of Public (EASP), 18011 Granada, Spain; piedad.martin.easp@juntadeandalucia.es
7 Biosanitary Research Institute of Granada (Ibs. Granada), 18012 Granada, Spain
* Correspondence: vanesa.santos@dstso.uhu.es
† These authors contributed equally to this work.

Abstract: Huelva is a city in SW Spain with 150,000 inhabitants, located in the proximity of two heavy chemical industry complexes, the highest naturally occurring radioactive material (NORM) waste (phosphogypsum) stacks of Europe and a highly polluted estuary, with elevated cardiovascular disease and cancer mortality rates. This study analyses the association between cumulated exposure levels to 16 metal(loid)s (Al, As, Cd, Co, Cr, Cu, Fe, Mn, Mo, Ni, Pb, Se, Tl, U, V, and Zn) measured in the toenail of a sample (n = 55 participants) of the general control population of Huelva City who were involved in the MCC-Spain study and the spatial proximity patterns to the local polluting sources. Residents of the city of Huelva have higher levels of Fe, Ni, Cr, Se, As, and Co in their toenails compared to the levels found in populations with similar characteristics living in non-polluted areas. Moreover, the highest concentrations of As, Pb, Cd, Mo, and Se were found in toenails of participants living near the NORM waste stack, while the highest Cu, Zn, and Al contents corresponded to people residing near the industrial area. The spatial distribution of most of the metal(loid)s studied appears to be mainly controlled by anthropogenic factors.

Keywords: Huelva; industrial polluted area; phosphogypsum; metal(loid)s; naturally occurring radioactive material; spatial distribution; toenails; kriging; principal component analysis

check for updates

Academic Editor: Aldo Viarengo

Received: 5 December 2024
Revised: 27 December 2024
Accepted: 4 February 2025
Published: 8 February 2025

Citation: Contreras-Llanes, M.; Alguacil, J.; Capelo, R.; Gómez-Ariza, J.L.; García-Pérez, J.; Pérez-Gómez, B.; Martin-Olmedo, P.; Santos-Sánchez, V. Internal Cumulated Dose of Toxic Metal(loid)s in a Population Residing near Naturally Occurring Radioactive Material Waste Stacks and an Industrial Heavily Polluted Area with High Mortality Rates in Spain. *J. Xenobiot.* **2025**, *15*, 29. https://doi.org/10.3390/jox15010029

1. Introduction

The estuary of the Odiel and Tinto rivers (SW Spain), located in the city of Huelva, is documented as one of the major contaminated sites in the world due to the high content of metal(loid)s and radionuclides [1,2].

Industrial and mining environmental pollution have been linked to heart disease, respiratory diseases, and cancer [3]. Huelva City, with 150,000 inhabitants, lies on this Odiel–Tinto Estuary, containing highly toxic elements like As, Cd, Cr, Cu, Ni, Pb, and the most radiotoxic radionuclides (^{210}Pb, ^{210}Po, and ^{226}Ra), associated with the natural ^{238}U decay chain [1,2], which may induce adverse health effects [4]. According to previous studies [5–7], Huelva City's heart disease and cancer mortality rates for both women and men are higher than the rest of Spain. Furthermore, the Spanish National Atlas of Mortality reveals a significantly greater standard of mortality ratios in Huelva City during the years 1989 and 2014 among both genders for acute myocardial infarction, heart failure, cerebrovascular diseases, bladder cancer, and other cardiovascular diseases, in addition to lung and breast cancer in men and women, respectively [8]. However, despite the general perception among the general population of a possible link between industrial pollution and the excess of mortality, the issue remains uncertain [5].

This situation has led to social mobilisation and judicial complaints, focusing mainly on the phosphogypsum (PG) stacks, even though there are other sources of exposure. Under pressure from citizens, associations, and environmentalists, judiciary authorities approved the end of the stockpiling of PG in December 2010. In addition, the governmental authorities have approved a restoration protocol plan for the affected saltmarshes by PG stacks, called RESTORE 2030 [9]. Furthermore, this restoration protocol is being re-evaluated due to it not having been approved by the judicial authorities, despite having government approval. Therefore, it is important to carry out a biomonitoring study of metal(loid)s to evaluate the possible health risks of Huelva's citizens.

Human health status can be monitored by measuring different bioindicators, such as urine, hair, toenails, fingernails, blood, saliva, and milk. Blood, urine, and saliva samples may reflect the short-term exposure (24 h) and are highly influenced by diet [10–12]. Nevertheless, hair and nails provide long-term exposure of mineral metabolism, reflecting a period of 6 ± 18 months [13–15]. Moreover, hair and nails have several advantages over other bioindicators in the monitoring of metal(loid)s, e.g., being a much less invasive option; they can be easily and inexpensively collected, transported, and stored for a long period before they are analysed, without any changes; the concentration levels are orders of magnitude higher [13,16,17]; and they are the most biosecure option for the analyst who manipulates the sample. Additionally, biomonitoring using toenails reduces the likelihood of external pollution in comparison to fingernails and hair [14,15,18].

Furthermore, geostatistical methods using spatial data are often used for the identification of spatial patterns. Their main objective is to provide unbiased estimates of a sampled variable at non-sampled points [19]. Kriging is a group of geostatistical techniques that interpolate unknown values from nearby known values, thus obtaining a continuous surface of estimated values for the entire area under consideration. This approach is increasingly used for the characterization of the metal(loid)s distribution in soils, as well as for atmospheric or biological sample data [20–22]. However, there are few published studies using these spatial analysis techniques to analyse the metal(loid)s signature in toenails. A recent study has been published that analyses the association between the spatial distribution of nail metal(loid)s levels and exposure to pollution sources [22]. Moreover, our research group has previously defined detailed contamination signatures in saltmarsh sediments in the Odiel–Tinto Estuary using geochemical tracers before the restoration protocol plan begins [23].

Therefore, the measurement of exposure at the individual level is a critical aspect in studying the role of these metal(loid)s in the health of the citizens of Huelva. The aim of our research was to analyse the association between the levels of cumulated exposure of 16 metal(loid)s (Al, As, Cd, Co, Cr, Cu, Fe, Mn, Mo, Ni, Pb, Se, Tl, U, V, and Zn) in the

toenails of the general population of Huelva and the spatial proximity patterns to the local industrial sources of pollutants.

2. Materials and Methods

2.1. Study Area

We conducted this study in the city of Huelva, located 500 m away from the Odiel–Tinto Estuary. A confluence of anthropogenic stressors gives this estuary a unique character. Both the Tinto and Odiel rivers drain the province of Huelva from north to south through the Iberian Pyrite Belt, one of the most important polymetallic sulphide mining areas in Europe [24,25]. Thus, large amounts of metal(loid)s are transported to the Odiel–Tinto Estuary due to acid mine drainage (AMD) that has been occurring for centuries [26,27]. Moreover, the Odiel–Tinto Estuary receives industrial effluents from factories and wastes located at the edge of the estuary channel, agrochemical drainage due to the intensive agricultural practices from the surrounding farmland, and sewage from Huelva City and other towns located in the estuary (Figure 1) [2,28–30]. On the other hand, there is an area over 12,600 m^2 that is highly polluted with metal(loid)s coming from AMD generated by mineral wastes from an abandoned foundry located in the Odiel marshes, which is exposed to rain and rising river levels during spring tides (Figure 1) [31].

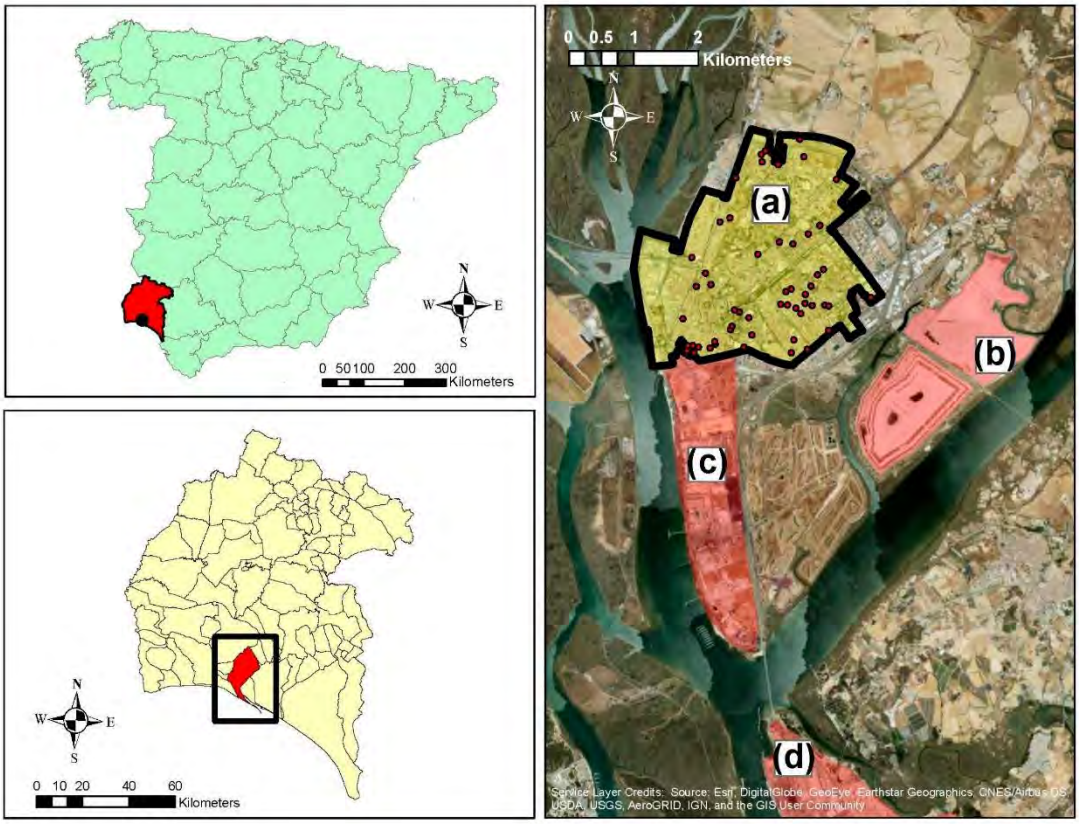

Figure 1. Location map of Huelva City (Spain) [(**a**) residential area of Huelva City (study area); (**b**) PG stacks; (**c**) industrial complex "*Polo Químico de Promoción y Desarrollo de Huelva—Punta del Sebo*"; (**d**) industrial complex "*Nuevo Puerto Palos de la Frontera*"]. Dots represent the locations of participants on a map of the residence area of Huelva City.

Furthermore, two important chemical parks called "*Polo Químico de Promoción y Desarrollo de Huelva—Punta del Sebo*" and "*Nuevo Puerto Palos de la Frontera*" are also located in the Odiel–Tinto Estuary (Figure 1). The leading Spanish copper and fertiliser producers, a thermal power plant, an oil refinery, etc., are some of the most polluting industries located in these chemical parks [2,29]. Additionally, a vast marsh area of this estuary is occupied by PG (Figure 1), an industrial waste originating from phosphate rock during fertiliser production [32–34]. PG was stockpiled on unconsolidated marshes in the Tinto River for a period of 42 years (1968–2010). This area covers 1200 hectares and contains 100 million tonnes, which ranks as one of the most significant in the world [34,35]. These PG stacks contain a wide range of contaminants, for example, organic substances, metal(loid)s and other potentially harmful elements (As, Cd, Cr, Cu, F, Fe, NH^{4+}, Ni, P, Pb, S, and Zn), and highly radiotoxic isotopes, such as ^{210}Pb, ^{210}Pb, and ^{226}Ra, from the ^{238}U decay series [32–34,36,37]. PG is classified as a naturally occurring radioactive material, sometimes known as NORM, which is the term used to describe any radioactive substance that exists naturally in the environment [38].

2.2. Study Population

Participants were the population-based controls from Huelva City recruited within the population-based multicase-control (MCC-Spain) study (http://www.mccspain.org), a study designed to explore environmental and genetic factors associated with common tumours or cancers with peculiar epidemiological features, conducted in Spain from September 2008 to December 2013 [39,40]. Participants were aged 20 to 85 years, residing in the catchment area for at least 6 months prior to recruitment. They were randomly selected from the Andalusian Public Healthcare Database (BDU), and were frequency-matched to all cancer and tumour cases, distributed by sex and age (5-year age groups). The ethical and research committees, and each participant, provided written informed consent. The study was performed in accordance with the Declaration of Helsinki.

This study is focused particularly on a representative sample (n = 55 participants) of the general population controls of Huelva City involved in the MCC-Spain study.

2.3. Toenail Sampling, Laboratory Analyses, and Calibration

After the interview, toenail samples (both feet) from the 55 participants were collected with nail clippers made of stainless steel within 2 weeks of recruitment, placed in a clean plastic bag and stored at room temperature. Moreover, anthropometric data and other information were obtained following the study protocol, which was approved by the recruiting centres.

First, toenail (50–100 mg) samples were washed twice with 2 mL of a 5% (weight/volume) Triton water solution; secondly, they were washed twice using 2 mL of Milli-Q water; thirdly, they were washed twice using 2 mL of acetone; and fourthly, an additional ultrasound treatment (5 min) was conducted. After that, toenails were air-dried and digested with 800 µL of a (4:1) mixture of HNO_3 and H_2O_2 of Ultra Trace Metals grade quality, in a Teflon reactor for microwave-assisted attack. Mineralisation was performed at 400 W, starting from room temperature, ramped up to 160 °C for 15 min, and held for 20 min at this temperature. Finally, the extracts were filtered through a 0.45 µm Polytetrafluoroethylene (PTFE) membrane filter before analysis.

The elemental content of 16 metal(loid)s (Al, As, Cd, Co, Cr, Cu, Fe, Mn, Mo, Ni, Pb, Se, Tl, U, V, and Zn) in toenails was determined by an inductively coupled plasma mass (ICP-MS) system, using an XSeries 2 (Thermo Fisher Scientific Inc., Waltham, MA, USA) spectrometer at the Environmental Bioanalytical Chemistry Unit of Huelva University (Huelva, Spain). Analyses were performed blindly from the case-control status. The

measured concentration was adjusted by the equipment, taking into account the dilution factor and sample weight, according to the following formula:

$$Real\left(\mu g{\cdot}kg^{-1}\right) = Equipment\left(\mu g{\cdot}kg^{-1}\right) * \frac{dilution\ factor\ (g)}{sample\ weight\ (g)}$$

The limit of detection for each measured element was obtained from the calibration curve [41].

To control the quality of analysis, the following operations were conducted: (a) 100 mg of human hair was used as reference material (NSC DC73347a) with the purpose of correcting the instrumental variability in each sample batch, with a mean accuracy of 90% maintained along the time ±5%; (b) the ICP-MS response was monitored over time by a measurement of metal(loid)s concentrations at a point on the calibration curve (2 ng mL^{-1}) every 20 samples analysed, ensuring an adequate evaluation of the instrument's response; (c) an instrumental drift correction was performed with the addition of 100 ng mL^{-1} rhodium, as an internal standard, to all of the samples and calibrants, of which those whose response differed ± 10% with respect to the internal standard were measured again; (d) an analysis was conducted every 5 samples of reagents blanks containing 5% (*v*/*v*) HNO_3 (Suprapur quality), 1% (*v*/*v*) HCl, and Rh 100 ng mL^{-1} in Milli-Q water; (e) an analysis was conducted of duplicate samples every 2.5 h of the sequence; (f) a spiked sample analysis was conducted by spiking the reference materials with the analytes under study (50 ng mL^{-1}). Finally, potential interferences from ^{98}Mo, ^{205}Tl, and ^{238}U, regularly existing in nails, were removed by operating the ICP-MS system in helium collision mode (He flow: 4 mL min^{-1}); the operative conditions of ICP-ORS-MS are shown in Table 1.

Table 1. Operative conditions of ICP-ORS-MS.

Forward power	1500 W
Plasma gas flow	15 L min^{-1}
Auxiliary gas flow 1 L min^{-1}	1 L min^{-1}
Carrier gas flow	0.15 L min^{-1}
Sampling depth 7 mm	7 mm
Sampling and skimmer cones	Ni
H_2 flow 4	4 mL min^{-1}
Nebuliser	Microflow (ESI)
Torch	Shield (with long-life platinum shield plate)
Qoct −18 V	18 V
Qp	−16 V
Points per peak	1
Integration time	0.3 s per isotope
Replicates	1
Isotopes monitored for total metals in nail	^{27}Al, ^{75}As, ^{114}Cd, ^{59}Co, ^{52}Cr, ^{63}Cu, ^{56}Fe, ^{55}Mn, ^{98}Mo, ^{58}Ni, ^{208}Pb, ^{80}Se, ^{205}Tl, ^{238}U, ^{51}V, ^{64}Zn
Dead time of detector	47 s

2.4. Statistical and Spatial Analyses

A complete descriptive statistical analysis, using mean, geometric mean, median, standard deviation, minimum and maximum concentrations, skewness, and kurtosis, was performed to characterise the metal(loid)s content distribution in toenails. Moreover, in order to determine if the dataset exhibited a normal distribution, the Kolmogorov–Smirnov and Shapiro–Wilk tests were applied to [42].

In addition, Spearman's correlation coefficient was calculated between the elements studied to assess their potential relationship. Furthermore, a principal component analysis (PCA) was conducted, a statistical method commonly used for the analysis of geochemical

and environmental data [43]. This method allows for the reduction of complex data to a discrete number of uncorrelated components. A complex dataset is reduced by creating a small number of uncorrelated principal components, which can describe the entire dataset with minimal loss of original information. A Varimax rotation with Kaiser normalisation was applied, which can maximise the variance of factor loadings across variables for each factor [44]. Furthermore, PCA was developed among the researched metal(loid)s in toenails to evaluate the correlation strength between them and to explore the possible natural or anthropogenic sources of the elements contained in the toenail samples. The statistical significance of a variable was based on p-values <0.05 and <0.01. The PCA and Spearman correlations were conducted using IBM SPSS Statistics 26 software.

Spatial variability in the metal(loid)s concentration was studied using kriging, a spatial interpolation method. Kriging was applied to generate continuous surfaces for each of the analysed elements based on data from 55 toenail samples collected from residents in the city of Huelva. This facilitated the visualisation of spatial patterns associated with these elements in unknown areas of the city. Spatial interpolation and distribution pattern maps were created using ArcGIS 10.5 for Desktop software (Esri Inc., Redlands, CA, USA).

3. Results

3.1. Descriptive Statistics Analysis

The summary of the metal(loid)s contents and descriptive statistics of the toenail samples of the participants collected from Huelva City is listed in Table 2. In all individuals, the Zn arithmetic mean concentration in toenails is much higher (106,042.50 $\mu g \cdot kg^{-1}$) than other metal(loid)s, such as Al (50,234.39 $\mu g \cdot kg^{-1}$), Fe (50,132.19 $\mu g \cdot kg^{-1}$), Cu (4735.88 $\mu g \cdot kg^{-1}$), Ni (3321.51 $\mu g \cdot kg^{-1}$), Cr (2196.15 $\mu g \cdot kg^{-1}$), Pb (827.65 $\mu g \cdot kg^{-1}$), and As (241.48 $\mu g \cdot kg^{-1}$). A similar result was achieved between the arithmetic mean and the geometric mean values, denoting a similar tendency and spatial variations of the data in Huelva City. Zn had the highest geometric mean concentration (102,480.18 $\mu g \cdot kg^{-1}$), followed by Al (44,229.43 $\mu g \cdot kg^{-1}$) and Fe (38,544.96 $\mu g \cdot kg^{-1}$). The geometric mean concentrations of elements in toenails decreased in the following order: Zn, Al, Fe, Cu, Ni, Cr, Se, Pb, Mn, As, V, Mo, Co, Cd, U, and Tl. The arithmetic mean concentrations decreased in the same order, only appearing to have a small discrepancy with Mn.

Table 2. Concentrations of detected metal(loid)s in toenails ($\mu g \cdot kg^{-1}$).

	n [a]	AM ± SD [b]	Median	GM (GSD) [c]	Min	Max	Skewness	Kurtosis
Al	55	50,234.39 ± 26,471.07	42,916.47	44,229.43 (1.66)	12,601.90	130,583.32	1.13 ± 0.32	0.86 ± 0.63
As	54	241.48 ± 177.86	190.91	207.50 (1.64)	99.24	1085.34	3.09 ± 0.32	11.04 ± 0.63
Cd	54	19.53 ± 16.61	16.23	16.11 (1.79)	3.80	111.46	3.94 ± 0.32	19.01 ± 0.63
Co	55	35.65 ± 29.06	28.87	28.84 (1.87)	8.47	173.57	2.97 ± 0.32	10.83 ± 0.63
Cr	55	2196.15 ± 2442.15	1521.12	1388.91 (2.71)	103.50	14,195.03	2.90 ± 0.32	10.89 ± 0.63
Cu	54	4735.88 ± 1065,34	4663,39	4624.11 (1.25)	2667,66	7972.01	0.87 ± 0.32	1.63 ± 0.63
Fe	55	50,132.19 ± 39,323.87	35,329.31	38,544.96 (2.06)	11,039.44	164,373.54	1.49 ± 0.32	1.61 ± 0.63
Mn	55	870.41 ± 1292.21	590.09	608.10 (2.12)	145.97	9608.01	5.98 ± 0.32	40.20 ± 0.63
Mo	55	56.76 ± 53.69	40.67	47.61 (1.68)	12.59	410.53	5.52 ± 0.32	35.95 ± 0.63
Ni	55	3321.51 ± 6407.36	2127.67	2054.46 (2.37)	257.05	48,325.41	6.65 ± 0.32	47.21 ± 0.63
Pb	55	827.65 ± 894.39	579.75	657.42 (1.81)	175.79	6486.15	5.09 ± 0.32	30.64 ± 0.63
Se	55	841.40 ± 180.95	815.97	822.97 (1.24)	395.14	1463.82	0.86 ± 0.32	2.10 ± 0.63
Tl	55	4.49 ± 1.91	3.98	4.15 (1.49)	1.60	11.57	1.44 ± 0.32	3.21 ± 0.63
U	52	6.46 ± 5.41	4.76	5.08 (1.94)	1.24	25.16	2.17 ± 0.32	4.38 ± 0.63
V	55	78.41 ± 64.85	59.49	64.30 (1.80)	17.84	409.82	3.25 ± 0.32	13.20 ± 0.63
Zn	55	106,042.50 ± 28,459.60	100,163.44	102,480.18 (1.30)	60,198.53	177,989.35	0.66 ± 0.32	−0.19 ± 0.63

[a] Number of samples whose concentration was above the LOD. Values reported in the table are for those participants who were above the LOD. [b] AM ± SD, arithmetic mean ± standard deviation. [c] GM (GSD), geometric mean (geometric standard deviation).

3.2. Spearman Correlation Coefficient Analysis and Principal Component Analysis (PCA)

Spearman's correlation coefficients of elements in toenail samples from Huelva City are shown in Table 3. Most of the metal(loid)s pairs displayed positive relations, which were significant, at 95%, and/or a higher confidence level (99%) in some cases, with correlation coefficients above 0.7.

Table 3. Spearman's correlation coefficients of detected metal(loid)s in the toenail samples.

	Mn	V	Al	Fe	Co	U	Zn	Cr	Pb	Cd	As	Cu	Mo	Tl	Se	Ni
Mn	1															
V	0.713 **	1														
Al	0.591 **	0.696 **	1													
Fe	0.777 **	0.673 **	0.474 **	1												
Co	0.564 **	0.623 **	0.475 **	0.514 **	1											
U	0.471 **	0.527 **	0.467 **	0.386 **	0.526 **	1										
Zn	0.003	−0.059	0.025	−0.136	−0.044	0.086	1									
Cr	0.394 **	0.453 **	0.409 **	0.405 **	0.217	0.330 *	0.286 *	1								
Pb	0.461 **	0.522 **	0.466 **	0.336 *	0.468 **	0.443 **	0.101	0.393 **	1							
Cd	0.318 *	0.321 *	0.155	0.287 *	0.202	0.389 **	−0.037	0.240	0.238	1						
As	−0.035	−0.020	−0.177	0.023	0.077	−0.008	−0.018	−0.117	−0.024	0.216	1					
Cu	0.459 **	0.373 **	0.330 *	0.296 *	0.491 **	0.376 **	0.168	0.256	0.440 **	0.277 *	0.096	1				
Mo	0.334 *	0.468 **	0.253	0.408 **	0.462 **	0.233	0.144	0.063	0.185	0.075	0.029	0.274 *	1			
Tl	0.343 *	0.274 *	0.175	0.216	0.361 **	0.281 *	0.064	0.089	0.288 *	0.066	0.181	0.268 *	0.225	1		
Se	0.002	−0.147	−0.148	−0.042	0.071	0.151	0.169	−0.082	−0.104	−0.102	0.245	0.241	0.095	0.135	1	
Ni	0.491 **	0.334 *	0.451 **	0.301 *	0.536 **	0.285 *	−0.200	0.139	0.275 *	−0.017	−0.264	0.254	0.141	0.217	−0.074	1

* Correlation is significant at the 0.05 level (2-tailed). ** Correlation is significant at the 0.01 level (2-tailed).

PCA was conducted in order to identify the likely contributing factors towards the metal(loid)s concentrations, and thereby define which metal(loid)s may have a common origin. For the PCA (Table 4), participants with metal(loid)s contents in the toenail samples above the LOD were included (n = 55). Six components/factors (PC1, PC2, PC3, PC4, PC5, and PC6) with eigenvalues >1 (Kaiser criterion), were obtained according to results of the initial eigenvalues [44], which were extracted from the study area, explaining practically 70% of total variance. The first principal component (PC1) is formed for Mn, V, Al, Fe, Co, and U, explaining 27% of the total variance. Zn, Cr, and Pb were the components of the second principal component (PC2) and explained 11.2% of the total variance. The third principal component (PC3) is characterised by Cd, As, and Cu, which described only 9.6% of the total variance. The fourth principal component (PC4) is formed for Mo and Tl, explaining 7.8% of the total variance. Moreover, Se was the element with the highest positive PCA loading of the fifth principal component (PC5), although Pb has a high negative loading (−0.517); they were responsible for 7.2% of total variance. Finally, the sixth principal component (PC6) represented 6.4% of the total variance, which is only dominated by Ni.

Table 4. Principal component analysis (PCA) results of metal(loid)s in the toenail samples.

	PC1	PC2	PC3	PC4	PC5	PC6
Mn	**0.880**	0.005	0.093	−0.043	0.050	−0.015
V	**0.845**	−0.055	0.115	0.368	−0.014	−0.088
Al	**0.773**	0.151	−0.124	−0.019	−0.120	0.049
Fe	**0.762**	0.103	0.034	0.244	−0.105	−0.072
Co	**0.724**	−0.093	0.112	0.081	−0.040	0.273
U	**0.703**	0.176	0.005	−0.013	0.234	−0.056
Zn	−0.088	**0.800**	0.046	−0.047	−0.001	−0.127
Cr	0.224	**0.652**	−0.062	−0.007	0.122	−0.124
Pb	0.108	**0.530**	0.152	0.117	**−0.517**	0.271
Cd	−0.041	0.078	**0.821**	−0.066	−0.098	−0.064
As	0.112	−0.093	**0.794**	0.029	0.190	−0.092
Cu	0.320	0.323	**0.453**	0.268	0.270	0.326
Mo	0.080	−0.152	0.069	**0.902**	−0.088	−0.116
Tl	0.208	0.204	−0.137	**0.545**	0.257	0.164

Table 4. *Cont.*

	PC1	PC2	PC3	PC4	PC5	PC6
Se	−0.030	0.110	0.156	0.077	**0.888**	0.037
Ni	−0.022	−0.200	−0.141	−0.039	−0.023	**0.841**
Eigenvalues	4.318	1.793	1.537	1.246	1.145	1.028
Total of variance (%)	26.99	11.20	9.61	7.79	7.16	6.43
Cumulative variance (%)	26.99	38.19	47.80	55.58	62.74	69.17

The values indicated in bold are crucial for explaining the PCA, as a larger number signifies a more significant contribution.

3.3. Spatial Variability

Figure 1 shows the locations of the two industrial complexes, PG stacks and the geocoded addresses of participants. According to previous studies, Huelva is situated downwind from these main emission sources, where air pollution and the diffusion of metal(loid)s are of major concern [45–51].

Figure 2 illustrates the spatially interpolated surfaces obtained by the kriging interpolation method of Al, As, Cu, Mo, Pb, Se, and Zn, and the combined PC2 from PCA, which serves as an example to observe how the distribution of combined PCA denotes similar signatures as those observed in the interpolated surfaces of each element studied. Al and Cu (Figure 2a,c) show higher values of these elements in the area of the city closest to the industrial pole. In Figure 2c, for Cu, only areas near industrial activities revealed the major concentrations, while the area far downwind from there showed relatively minor Cu values. Similarly, Al presents the highest concentration near the industrial activity area, although a small hotspot with a high concentration of Al was identified in the north of the city. Nevertheless, the concentration in toenails was generally low compared to other places, and especially close to the PG stacks (Figure 2a). Furthermore, As, Se, and Zn show a spatial pattern in which the values obtained both in the vicinity of the industry and in the vicinity of the PG stacks stand out (Figure 2b,f,g). The spatial distribution of As revealed that the highest concentration is dispersed near to the industrial complexes and PG stacks (Figure 2b). Meanwhile, a small hotspot with high As levels was located far away in the northwest (but not the immediate neighbourhoods), although the concentrations remained generally low in the studied area. Selenium also presents the highest measurements in the same area of Huelva; nevertheless, the concentrations of Se in areas far away had relatively low concentrations (Figure 2f). In the same way, Zn shows the highest values in the area of the city closest to the industrial pole and PG stacks, whereas some small patches had relatively high Zn concentrations in the northeast (Figure 2g). On the other hand, the spatial distribution of Mo and Pb (Figure 2d,e) shows higher values in the area close to the PG stacks. In Figure 2e, for Pb, neighbourhoods located nearby to the industrial activity area denoted relatively elevated concentrations, but participants with the major lead level in toenails were located downwind, close to the PG stacks. Other places away from the PG stacks had relatively minor nail levels of the measurements. Similarly, participants residing close to the PG stacks had the highest concentrations of Mo (Figure 2d). Meanwhile, Mo concentrations were lower in areas close to the industrial poles. Finally, PC2 denotes a similar pattern distribution compared to them in the interpolated surfaces of the individual elements that form it, being Cr, Pb, and Zn (Figure 2h). Overall, participants located nearby the industrial complexes and PG stacks shower relatively major measurements of the elements studied than that rest of Huelva City.

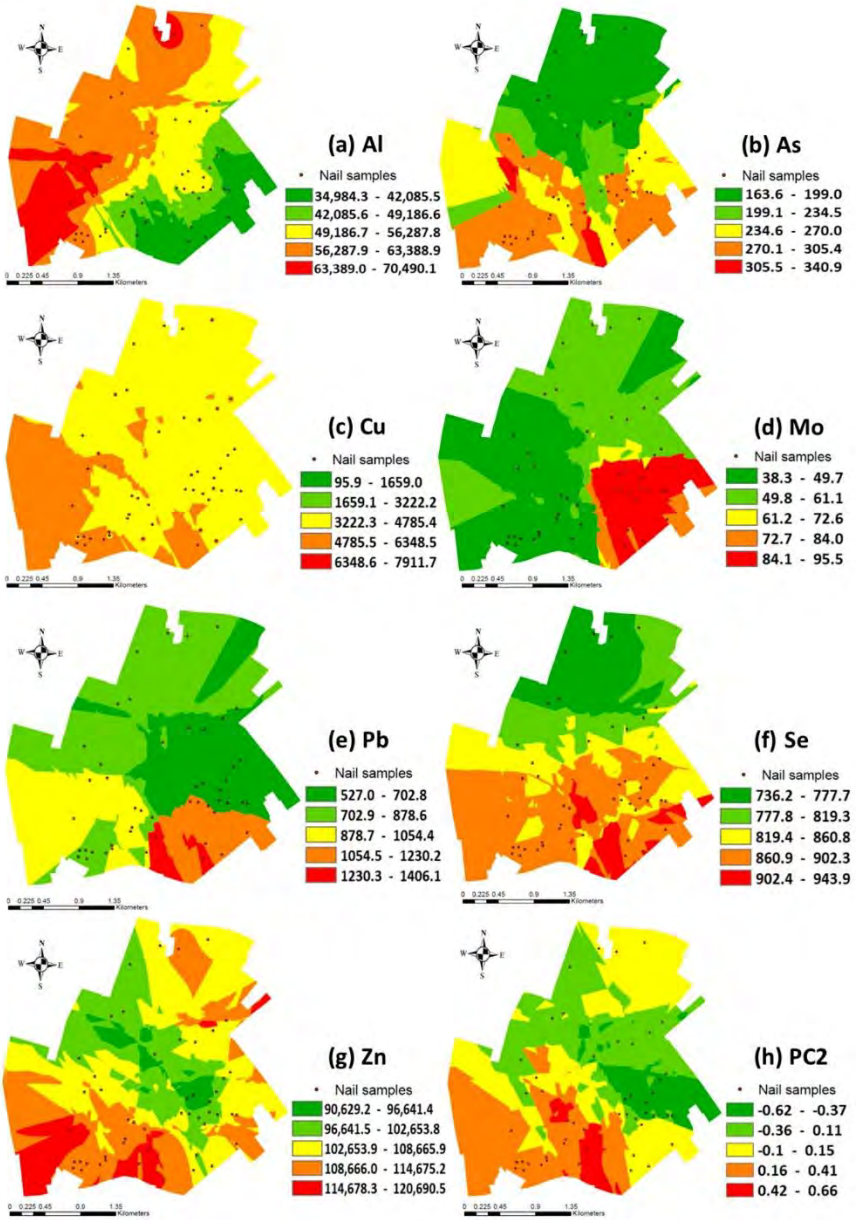

Figure 2. Spatially interpolated surfaces of metal(loid)s [(**a**) Al; (**b**) As; (**c**) Cu; (**d**) Mo; (**e**) Pb; (**f**) Se; (**g**) Zn; (**h**) PC2]. Dots represent the locations of participants on a map of the city of Huelva.

4. Discussion

Our study revealed that the mean levels of Ni, Cr, Se, As, and Co were considerably higher than those of unpolluted areas with similar population characteristics (culture, diet, and lifestyle). The results of our study show correlations between the elements analysed in the toenail samples of the residents of the city of Huelva. Many of these elements are distributed in a similar way, finding a spatial pattern in their distribution, with higher

values of metal(loid)s in the vicinity of the PG stacks and/or industrial complexes. The results are novel and provide insights into the exposures of a population located close to an extremely polluted estuary.

According to other studies among populations residing near polluted areas (Table 5), our population revealed that Zn has the maximum mean levels in toenails, followed by Al, Fe, Cu, Ni, Cr, Mn, Se, Pb, As, V, Mo, Co, Cd, U, and Tl [52–60], although this order differs from other similar studies [61–63]. Moreover, these levels were found to be similar to the other studies carried out in particularly contaminated areas [53–57,59,63]. Furthermore, it was observed that our results are similar to other populations living in polluted areas with similar conditions, as in the case of Kima (Egypt), which includes a fertiliser industry, industrial polluted areas, and heavy traffic [57]. Moreover, similar results to a population residing close to a mine waste dump in the Zambian Copperbelt, an area environmentally affected by copper mining, were also found [55]. However, the discrepancies between our results and some of the compiled research [61,62], shown in Table 5, might be due to the differences in environmental area, sanitation and statistical characteristics of human populations, predominant sources, and variance in the degree of exposure of people to these metal(loid)s. On the other hand, in other studies carried out in unpolluted areas with similar population characteristics (culture, diet, and lifestyle), such as the island of Mallorca (Spain) [59] and Forlì (Italy) [61], the mean levels of Fe, Ni, Cr, Se, As, and Co were quite minor compared to those of our data. These results suggest that the people living in Huelva bioaccumulate these metal(loid)s.

These results are supported by previous studies, such as a study focused on the urinary levels of heavy metals, such as As, Cd, Cr, Cu, and Ni, in children from Huelva, which revealed that the mean concentration of Cd was higher than rates reported in other studies conducted in Europe [64]. Similarly, another study denoted the cognitive behaviour of children living in the city of Huelva with high levels of Cd in both their hair and urine [65]. Another recent explorative study associated the environmental exposure to heavy metals and neurobehavioural performance in the children of Huelva [66]. Furthermore, industry workers show high levels of arsenic and other metals, even after taking into account fish and seafood consumption [67]. Less than 500 m from the city are the highest NORM waste stacks of Europe, and an industrial park including a copper smelter, a petrol refinery, and a fertiliser production plant, among others (Figure 1) [2,29,32,34]. In addition, the local river carries acid mine drainage from the mining activity upstream [1,2]. There are various reports showing the impact of the industrial pollution on the local river and the nearby estuary and marshes [29,30].

Spearman correlation analysis among levels of the different elements may reflect the combined effect of common sources of exposure (e.g., environmental, occupational, and dietary) and common toxicokinetic activities during absorption, transport, and bioaccumulation in toenails. Investigating how these sources contribute to exposure and their influence on metal(loid)s mixtures is important for assessing health outcomes. Additionally, PCA was used as a statistical process for reducing the dimensionality of correlated heavy metal(loid)s [43].

Table 5. Comparison of metal(loid)s levels ($\mu g \cdot g^{-1}$) in general environmentally exposed populations found in previous studies worldwide in human toenails.

Researchers	Biological Sample; *n* [a]	Study Area and Sources	Al	As	Cd	Co	Cr	Cu	Fe	Mn	Mo	Ni	Pb	Se	Tl	U	V	Zn
Our study	Toenails; *n* = 55	People living close to an extremely polluted estuary in Huelva, Spain	50.2	0.24	0.02	0.04	2.195	4.74	50.1	0.87	0.06	3.32	0.83	0.84	0.005	0.007	0.08	106.0
Bechtold et al., 2020 [52]	Toenails; *n* = 489	Population living near a municipal solid waste incinerator in Modena (Italy)	N.M.	N.M.	0.02 ± 0.02	N.M.	1.33 ± 2.92	4.10 ± 3.4	N.M.	N.M.	0.39 ± 0.57	1.04 ± 3.08	0.86 ± 1.48	0.49 ± 0.09	N.M.	N.M.	N.M.	95.6 ± 34.6
Butler et al., 2019 [53]	Toenails; *n* = 521	A region with ferroalloy industry in Brescia, Italy	70	N.M.	N.M.	N.M.	0.15	2.66	N.M.	0.19	N.M.	N.M.	0.10	N.M.	N.M.	N.M.	N.M.	110
Coelho et al., 2014 [54]	Toenails; *n* = 122	Villages near the Panasqueira mine, in central Portugal	N.M.	0.65 ± 0.56	0.05 ± 0.04	N.M.	2.17 ± 2.41	N.M.	N.M.	2.84 ± 3.17	N.M.	4.12 ± 9.20	1.25 ± 1.33	0.63 ± 0.35	N.M.	N.M.	N.M.	136.49 ± 80.72
Di Ciaula et al., 2020 [61]	Toenails; *n* = 62	Population living in an urban area and close to waste incinerators in Forlì, Italy	166.48 ± 50.42	0.01 ± 0.01	0.03 ± 0.004	0.04 ± 0.04	4.82 ± 3.88	6.34 ± 0.70	360.08 ± 126.57	4.40 ± 1.23	0.00	2.23 ± 1.51	0.32 ± 0.13	0.01 ± 0.005	0.00	0.00	0.19 ± 0.11	96.27 ± 9.42
Nakaona et al., 2020 [55]	Toenails; *n* = 40	Community living near a mine waste dump in the Zambian Copperbelt	N.M.	N.M.	0.1 ± 0.002	1.0 ± 0.02	0.6 ± 0.08	29.6 ± 4.8	N.M.	12.0 ± 2.02	N.M.	1.7 ± 0.14	4.8 ± 0.53	N.M.	N.M.	N.M.	N.M.	172 ± 27.4
Ojekunle et al., 2022 [62]	Toenails; *n* = 38	Neighbourhood close to a dumpsite waste in Nigeria	N.M.	N.M.	2.1 ± 4.5	2.9 ± 6.9	55.6 ± 35.2	95.4 ± 45.4	N.M.	108.5 ± 167.8	N.M.	156.0 ± 172.9	36.6 ± 89.4	N.M.	N.M.	N.M.	N.M.	354.3 ± 333.8
Przybylowicz et al., 2012 [56]	Toenails; *n* = 42	Adults from environmentally exposed areas at living in the same area (Krakow)	N.M.	N.M.	0.37 ± 0.41	0.04 ± 0.06	2.44 ± 1.88	4.80 ± 1.25	42.9 ± 22.4	N.M.	N.M.	2.73 ± 1.24	0.66 ± 0.15	N.M.	N.M.	N.M.	N.M.	121.4 ± 30.4
Rashed and Hossam, 2007 [57]	Toenails; *n* = 115	Adults from environmentally exposed areas at Aswan, Egypt	N.M.	N.M.	1.0 ± 0.4	N.M.	N.M.	16.2 ± 1.5	N.M.	N.M.	N.M.	N.M.	22.3 ± 3.6	N.M.	N.M.	N.M.	N.M.	158 ± 22
Slotnick et al. 2004 [58]	Toenails; *n* = 163	Residing in a highly industrialised Area in Detroit, USA	26.9 ± 21.6	0.10 ± 0.22	0.64 ± 0.79	0.17 ± 0.86	1.91 ± 1.66	5.05 ± 4.64	N.M.	N.M.	0.60 ± 1.15	32.89 ± 68.97	0.74 ± 1.23	0.82 ± 0.46	N.M.	N.M.	0.04 ± 0.04	N.M.
Van Horne et al., 2021 [60]	Toenails; *n* = 95	Communities near metalworking industries in Los Angeles, USA	N.M.	0.23 ± 0.20	0.05 ± 0.08	N.M.	N.M.	N.M.	N.M.	1.72 ± 1.65	N.M.	N.M.	0.84 ± 0.89	0.94 ± 0.52	N.M.	N.M.	0.15 ± 0.13	N.M.
Yoo et al., 2002 [63]	Toenails; *n* = 150	Distribution of heavy metals in autopsy materials from normal Korean	176 ± 94	10 ± 13	0.7 ± 0.9	N.M.	2.9 ± 2.9	8.8 ± 7.0	141 ± 99	2.9 ± 2.8	1.9 ± 2.5	5.5 ± 5.8	12 ± 11	6.9 ± 7.9	N.M.	N.M.	2.7 ± 2.8	97 ± 38
Di Ciaula et al., 2020 [61]	Toenails; *n* = 158	People residing in an unpolluted area in Forlì, Italy	103.24 ± 11.01	0.00	0.07 ± 0.02	0.00	1.28 ± 0.44	4.74 ± 0.36	164.49 ± 21.06	2.47 ± 0.35	0.00	0.43 ± 0.18	0.95 ± 0.47	0.01 ± 0.003	0.00	0.00	0.02 ± 0.02	95.30 ± 3.09
Sureda et al., 2017 [59]	Toenails; *n* = 100	Unpolluted area in Mallorca, Spain	N.M	N.M	N.M	0.01	0.55	N.M	14.0	N.M	N.M	0.99	N.M	0.57	N.M	N.M	N.M	106.3

Data shown are AM ± SD, arithmetic mean ± standard deviation. N.M., not measured. [a] Number of participants in the study.

Mn, Al, U, Co, V, and Fe were significantly correlated with each other at a 99% or higher confidence level (Table 3). A high correlation was obtained between the following metal(loid)s pairs: V-Mn (r = 0.713), V-Al (r = 0.696), and V-Fe (r = 0.673). Moreover, Mn-Fe (r = 0.777) and Mn-Al (r = 0.591) showed a strong and moderate correlation, respectively. Finally, Co-V (r = 0.623) also revealed a strong correlation. These strong correlations indicate that a general trend of high concentration in one element should indicate high concentrations in the others. Additionally, these loadings denoted that these elements come from the same source, or that they belong to the same source but with diverse origins, while a moderate correlation was observed among the U-V (r = 0.527), U-Co (r = 0.526), and the other metal(loid)s pairs (U-Mn, U-Al), as well as weakly correlated U-Fe (r = 0.386), revealing a different source (Table 3). These results may indicate a common source, probably with various origins, which were mainly a result of mixed natural and anthropogenic activities, mutual dependence, or identical behaviour during transportation [68]. On the other hand, Mn and V were very strongly associated, and Al, U, Co, and Fe were strongly associated; these components characterised factor one (PC1), which explained 27% of the total variance (Table 4). This means that all cases have the same (positive) sign and strong association, indicating that all of the elements interact in the same manner in the structure of the nails (Table 4). Furthermore, all of the results corresponding to PC1 have the same (positive) sign, indicating that each element influences PC1 in the same manner. Some previous studies based on the air quality of Huelva confirmed that Al, Mn, and Fe emissions are related to crustal sources [45–51]. Additionally, Al, Mn, and Fe levels were also higher in industrial areas, and the spatial distribution may have been controlled by both anthropogenic and natural causes [62].

The interpolation analysis revealed the information shown in Figure 2a, which demonstrates the highest Al concentration, near and far from the industrial hubs, which could be explained by different origins, the industrial activities, and the crustal source. Moreover, these previous studies based on the air quality of Huelva also attributed most of the emissions to V and Co in Huelva City, with the crude oil refinery located in the "*Nuevo Puerto Palos de la Frontera*" industrial estate [45–51]. On the other hand, the PG stack and the phosphoric fertilisers' activities could be considered the main sources of U [32–34,36,37].

The second factor (PC2) was strong for Zn and moderated for Cr and Pb; the loading indicates that each element influences PC2 in the same manner due to the same positive sign (Table 4). This showed that the availability of Cr in the toenail samples would slightly influence both Pb and Zn and their respective environmental and human-induced effects. Furthermore, positive weak correlations were also observed between Cr-Pb (r = 0.393) and Cr-Zn (r = 0.286) at $p < 0.01$ and $p < 0.05$, respectively (Table 3). PC2 denoted a mixture of sources because these elements were not correlated with both themselves and other elements, indicating that they may have had different origins. These components are suspected to emanate from the disposal of industrial waste, industrial air-borne emissions, and high traffic near the area, along with roadside dust. According to previous studies on the air quality of Huelva, Pb and Zn emissions are associated with a Cu smelter plant located in the left bank of the Odiel river in the "*Polo Químico de Promoción y Desarrollo de Huelva—Punta del Sebo*" industrial complex; meanwhile, Cr is traced to traffic emissions [45–51]. The results of Spearman's linear correlation quantified our visual interpretations of the associations between the vicinity to industrial complexes and the levels of these elements (Table 3).

The spatial distribution of Pb (Figure 2e) shows higher values in the area close to the PG stacks, although neighbourhoods residing close to the industrial complexes revealed relatively high concentrations of measures. This finding could be associated with the impact of emissions from industrial contaminating sources, in addition to the emissions generated

near PG stacks, which are particularly linked to traffic emissions, since the roads with the highest volume of vehicles are there, including heavy traffic. On the other hand, Zn shows the highest values in the area of the city closest to the industrial pole, whereas some small patches had relatively high Zn concentrations in PG stacks (Figure 2g). This fact confirmed that Zn emissions were released from the industrial pole.

On the other hand, Cd and As were strongly positive and Cu was moderately associated; these components characterised factor three (PC3), which explained only 9.6% of the total variance (Table 4). The association among these elements indicates the environmental influence of these elements on nail samples and possibly different sources of pollution. Moreover, there is no significant correlation between metal(loid)s pairs in PC3, and there is also no correlation with the other elements (Table 3). This result revealed that those elements are generated in different sources at the same time and show different behaviours during transportation into the toenails [68]. A possible source for these components is industrial emissions [69]. Moreover, there is a strong metallurgical activity located in the "*Polo Químico de Promoción y Desarrollo de Huelva—Punta del Sebo*" industrial estate, which releases As and other metal(loid)s [45–51]. Additionally, Cu^{2+} and As could be the result of industrial emissions from both the fertiliser factory and PG waste, as due to the proximity to the industrial pole and the northwest wind direction, Huelva is exposed to heavy atmospheric deposition of these elements [32–34,45–51]. On the other hand, most of the Cd emission in the city of Huelva was attributed to the petrochemical industries, as well as the TiO_2 pigment industries, which also release a small amount of Cd and As; both are located in the "*Nuevo Puerto Palos de la Frontera*" industrial complex [45–51].

The spatial distribution of As is in accordance with previous statistical results, since As is generated from different sources, such as the Cu smelter, fertiliser industries, and the oil refinery, all of them located southeast of the city of Huelva (Figure 2b). Conversely, kriging maps show upper values of Cu in the area of the city closest to the industrial complexes, downwind of the copper smelter activities, revealing this as a unique source.

The fourth principal component (PC4) explained 7.8% of the total variance and included Mo and Tl, which were very strongly and moderately associated, respectively (Table 4). This positive association identifies a moderate relationship between these elements. In addition, toenail thallium and molybdenum concentrations were weakly correlated, with a moderate Spearman coefficient. Moreover, these elements were not correlated with other elements (Table 3), revealing different sources in the Huelva area. The PG stacks and the emissions from industrial activities, such as phosphoric fertilisers, might be assumed as the sources of Mo and Tl [32,34]. The spatial distribution of Mo (Figure 2d) shows higher values, mainly in the area close to the PG stacks, which is in accordance with the previous statement.

In addition, the fifth principal component (PC5) was dominated by Se and Pb, with a strongly positive and moderately negative association, respectively (Table 4). This fact indicates that these elements interact in the opposite manner in the structure of the nails, revealing an antagonistic effect between Se and Pb. Some studies have demonstrated that selenium has a great toxicant affinity and forms biologically inert complexes [70,71], thus potentially protecting against metal(loid)s bioaccumulation. Moreover, selenium comes from a different source than the other studied elements, since it was not correlated with any of the other elements (Table 3). The principal route of human exposure to selenium is through the diet, food, and drinking water, although smoking is an inadvertent inhalation exposure route to selenium [72].

Furthermore, Se shows a spatial pattern in which the values are obtained both near the industry and in the vicinity of the PG stacks; it reveals some influence by the industrial emission (Figure 2f). No studies have been found in the bibliography that verify the

contribution of Se by industrial activity, and because this is an essential element that usually has a protective vision for health, it is not usually taken into account in studies of biomonitoring, although its presence in excess can produce toxicity.

Finally, the sixth principal component (PC6) explained 6.4% of total variance and is characterised by high-loading of nickel (Table 4). In addition, only a moderate positive correlation, at $p < 0.01$, was found between Ni-Co ($r = 0.536$), suggesting that both components may have the same origin (Table 3). The petrochemical industries located in the "*Nuevo Puerto Palos de la Frontera*" industrial area are the main emission sources of Ni [45–51].

Strengths and Limitations

Our findings must be interpreted in light of some limitations. First, this study is based on a small population of 55 participants among 150,000 inhabits, and this fact may limit our statistical power. Second, the participants may have been exposed to metal(loid)s from other confounding variables, such as sociodemographic factors, lifelong retrospective environmental exposures, occupational history, traffic, or diet, which should be addressed in upcoming investigations. Nevertheless, the loading of the main elements of the principal sources would not have been impacted, since we considered multiple metal(loid)s in the PCA. Third, PCA and Spearman's correlation analysis are techniques used to identify the probable source; however, the interpretation of the results depends on the knowledge and experience of the expert. The identification of the different patterns requires a careful interpretation based on possible local sources of contamination (both anthropogenic and natural sources), different exposure routes, and other specific local characteristics. Thus, we relied on various previous studies that have been conducted to characterise the quality of Huelva City's air [45–51], the industrial impact on the local river and the nearby estuary and marshes [29,30], the acid mine drainage from the mining activity upstream [1,2] and other studies on metal(loid)s sources' identification [2,29,32].

Regardless of the exposed limitations, our research also has several strengths. First, this is the first study developed on Huelva's citizens living in an extremely polluted area which analyses the link between potential industrial pollution exposure and metal(loid)s concentrations in toenails using statistical techniques of spatial analysis, such as kriging. Second, this study used ICP-Ms analysis, which has low LODs for most metal(loid)s studied, and may have identified low-level exposures to uranium, lead, thallium, and arsenic. Thus, we obtained data from a representative sample of Huelva's population, where we may potentially have detected 16 metal(loid)s in toenails. Normally, similar previous studies determine a limited number (one to six elements) of potentially harmful elements because they used characterisation techniques with high LODs [22]; however, we have selected and analysed a total of sixteen heavy metal(loid)s. Third, toenails were used as a bioindicator, a non-destructive method widely accepted as an internal exposure marker, which could reflect the long-term patterns of mineral metabolism, reflecting a period of 6 ± 18 months [13–15]. Fourth, as differential effects may be potentially induced by environmental agents' exposures to different lengths of time [73], the participants' inclusion criterion was residing in Huelva City for at least 6 months. Thus, we warrant to estimate the long-term environmental exposition time for the study population. Fifth, demographic variables, such as age, gender, and socioeconomic status, have been included to influence potential exposure and, consequently, the elements' levels in toenails [13–15]. These variables were controlled for in the analysis. Sixth, PCA is an unbiased approach to assess the inter-relationship of the elements identified in toenail samples [14,15,43,56,60]. Seventh, applying Kriging geostatistical techniques enhanced our understanding of the association between vicinity to contamination sources and elements' levels in toenails of Huelva's citizens [20–22]. Eighth, the specific internal dose of cumulated toxic metal(loid)s concentration signatures obtained

in this research could be used as a reference to identify the influence of future interventions on current contamination sources in the Odiel–Tinto Estuary. These findings are critical for measuring the effect of the RESTORE 2030 plan [9], which is currently being re-evaluated by judicial authorities [10]. To the best of our knowledge, there are no published references nor permissive levels of metals in toenails to compare whether the absolute concentrations found in our study are within permissive levels.

5. Conclusions

Residents of the city of Huelva have higher levels of Fe, Ni, Cr, Se, As, and Co in toenails compared to the levels found in populations with similar characteristics living in non-polluted areas. Our results indicate that citizens of Huelva residing in close-proximity to phosphogypsum stacks, a NORM waste stack, and an industrial heavily polluted area denote major contents of many metal(loid)s in toenails. The concentrations of As, Pb, Cd, Mo, and Se were high in the population living near the PG stacks, whereas Cu, Zn, and Al levels were high in people residing near the industrial area. These findings are a crucial first step towards understanding the signature of cumulated human toxic metal(loid)s' concentration in this population, and they raise significant interrogations concerning the effect of the industry on health in this city. The results bring to light the real impact of the industry on the health of the citizens of Huelva City, particularly, the residents residing closest to the pollution sources, a fact that had not yet been demonstrated. The cumulated exposure at the individual level is a critical aspect in the study of the role of these metal(loid)s on the health of the inhabitants of Huelva. Furthermore, this study might serve as a reference to assess the impact of the restoration plan (RESTORE 2030) for the affected area in the Odiel–Tinto Estuary. These specific internal doses of cumulative toxic metal(loid)s concentration patterns could also be used as a reference to evaluate the influence of future interventions in other similarly contaminated areas.

Author Contributions: Conceptualization, M.C.-L., J.A. and V.S.-S.; methodology, M.C.-L., J.A., R.C., J.L.G.-A., P.M.-O., B.P.-G., J.G.-P. and V.S.-S.; software, V.S.-S.; validation, M.C.-L., J.A. and V.S.-S.; formal analysis, M.C.-L., J.A. and V.S.-S.; investigation, M.C.-L., J.A., R.C. and V.S.-S.; resources, J.A., B.P.-G. and P.M.-O.; data curation, M.C.-L., J.A. and V.S.-S.; writing—original draft preparation, M.C.-L., J.A. and V.S.-S.; writing—review and editing, M.C.-L., J.A., J.L.G.-A., J.G.-P. and V.S.-S.; visualization, M.C.-L., J.A., J.L.G.-A., P.M.-O., B.P.-G., J.G.-P. and V.S.-S.; supervision, M.C.-L. and J.A.; project administration, J.A.; funding acquisition, J.A. All authors have read and agreed to the published version of the manuscript.

Funding: This research received no external funding. This research was funded by the Andalusian Government, '2018 Special Action of the Andalusian Government: Support to the Huelva Phosphogypsum Experts Committee'; and by Huelva University local funds to support research groups during 2018 to 2023. MCC study was funding by Carlos III Health Institute-FEDER (PI07/1160, PS09/02078, PI12/00265, and PI17/02286), and Regional Health Ministry of Andalucía (PI-0571-2009, PI-0306-2011, and salud201200057018tra).

Institutional Review Board Statement: The study was conducted in accordance with the Declaration of Helsinki and approved by the Institutional Review Board (or Ethics Committee) of the University of Huelva (PI07-1160; 27 June 2005).

Informed Consent Statement: Informed consent was obtained from all subjects involved in the study.

Data Availability Statement: The data presented in this study are available on request from the corresponding author. The data are not publicly available due to ethical considerations.

Acknowledgments: The authors thank all those who took part in this study, including the staff of all participating hospitals, all of the interviewers and research assistants in the study centres, and, finally, the study participants.

Conflicts of Interest: The authors declare no conflicts of interest.

References

1. Nieto, J.M.; Sarmiento, A.S.; Olías, M.; Canovas, C.R.; Riba, I.; Kalman, J.; Delvalls, T.A. Acid mine drainage pollution in the Tinto and Odiel rivers (Iberian Pyrite Belt, SW Spain) and bioavailability of the transported metals to the Huelva Estuary. *Environ. Int.* **2020**, *33*, 445–455. [CrossRef] [PubMed]
2. Torre, B.M.; Borrero-Santiago, A.R.; Fabbri, E.; Guerra, R. Trace metal levels and toxicity in the Huelva Estuary (Spain): A case study with comparisons to historical levels from the past decades. *Environ. Chem. Ecotox.* **2019**, *1*, 12–18. [CrossRef]
3. Briffa, J.; Sinagra, E.; Blundell, R. Heavy metal pollution in the environment and their toxicological effects on humans. *Heliyon* **2020**, *6*, e04691. [CrossRef] [PubMed]
4. Forghani Tehrani, G.; Rubinos, D.A.; Kelm, U.; Ghadimi, S. Environmental and human health risks of potentially harmful elements in mining-impacted soils: A case study of the Angouran Zn–Pb Mine, Iran. *J. Environ. Manag.* **2023**, *334*, 117470. [CrossRef]
5. Alguacil, J.; Ballester, F.; Donado-Campos, J.; Pollán, M.; Rodríguez-Artalejo, F. *Dictamen Realizado por Encargo del Defensor del Pueblo Andaluz Sobre El Exceso de Mortalidad y Morbilidad Detectado en Varias Investigaciones en La Ría de Huelva*; Grupo de Trabajo de la Sociedad Española de Epidemiología: Seville, Spain, 2014. Available online: https://www.defensordelpuebloandaluz.es/informe-epidemiologico-ria-de-huelva (accessed on 15 September 2024).
6. Benach, J.; Yasui, Y.; Borrell, C.; Rosa, E.; Pasarín, M.I.; Benach, N.; Español, E.; Martínez, J.M.; Daponte, A. Examining geographic patterns of mortality: The Atlas of mortality in small areas in Spain (1987–1995). *Eur. J. Public Health* **2003**, *13*, 115–123. [CrossRef] [PubMed]
7. López-Abente, G.; Aragones, N.; Ramis, R.; Hernandez-Barrera, V.; Perez-Gomez, B.; Escolar- Pujolar, A.; Pollan, M. Municipal distribution of bladder cancer mortality in Spain: Possible role of mining and industry. *BMC Public Health* **2006**, *6*, 17. [CrossRef] [PubMed]
8. Martínez-Beneito, M.A.; Botella-Rocamora, P.; Corpas-Burgos, F.; Vergara-Hernández, C.; Pérez-Panadés, J.; Perpiñán-Fabuel, H. *Atlas Nacional de Mortalidad en España (ANDEES)*; Fundación FISABIO y Dirección General de Salud Pública de la Generalitat Valenciana: Valencia, Spain, 2024. Available online: http://andees.fisabio.san.gva.es/ (accessed on 25 September 2024).
9. Environmental Restoration Project of the Huelva Phosphogypsum Stacks (RESTORE2030). Available online: https://restore2030.com/ (accessed on 23 June 2024).
10. Aguilera, I.; Daponte, A.; Gil, F.; Hernández, A.F.; Godoy, P.; Pla, A.; Ramos, J.L.; DASAHU group. Biomonitoring of urinary metals in a population living in the vicinity of industrial sources: A comparison with the general population of Andalusia, Spain. *Sci. Total Environ.* **2008**, *407*, 669–678. [CrossRef] [PubMed]
11. Middleton, D.R.S.; Watts, M.J.; Lark, M.R.; Milne, C.J.; Polya, D.A. Assessing urinary flow rate, creatinine, osmolality and other hydration adjustment methods for urinary biomonitoring using NHANES arsenic, iodine, lead and cadmium data. *Environ. Health* **2016**, *15*, 68–81. [CrossRef] [PubMed]
12. Wongsasuluk, P.; Chotpantarat, S.; Siriwong, W.; Robson, M. Using urine as a biomarker in human exposure risk associated with arsenic and other heavy metals contaminating drinking groundwater in intensively agricultural areas of Thailand. *Environ. Geochem. Health* **2018**, *40*, 323–348. [CrossRef]
13. Bencko, V. Use of human hair as a biomarker in the assessment of exposure to pollutants in occupational and environmental settings. *Toxicology* **1995**, *101*, 29–39. [CrossRef] [PubMed]
14. Gutiérrez-González, E.; Garcia-Esquinas, E.; Fernadez de Larrea-Baz, N.; Salcedo-Bellido, I.; Navas-Acien, A.; Lope, V.; Gomez-Ariza, J.L.; Pastor, R.; Pollan, M.; Perez-Gomez, B. Toenails as a biomarker to essential trace metals: A review. *Environ. Res.* **2019**, *179*, 108787. [CrossRef] [PubMed]
15. Salcedo-Bellido, I.; Gutiérrez-González, E.; García-Esquinas, E.; Fernández de Larrea-Baz, N.; Navas-Acien, A.; Téllez-Plaza, M.; Pastor-Barriuso, R.; Lope, V.; Gómez-Ariza, J.L.; García-Barrera, T.; et al. Toxic metals in toenails as biomarkers of exposure: A review. *Environ. Res.* **2021**, *197*, 111028. [CrossRef] [PubMed]
16. Okamoto, K.; Morita, M.; Quan, H.; Uehiro, T.; Fuwa, K. Preparation and certification of human hair powder reference material. *Clin. Chem.* **1986**, *31*, 1592–1597. [CrossRef]
17. Sukumar, A. Human Nails as a Biomarker of Element Exposure. In *Reviews of Environmental Contamination and Toxicology*; Ware, G.W., Nigg, H.N., Doerge, D.R., Eds.; Springer: New York, NY, USA, 2006; Volume 185. [CrossRef]
18. Garland, M.; Morris, J.S.; Rosner, B.A.; Stampfer, M.J.; Spate, V.L.; Baskett, C.J.; Willett, W.C.; Hunter, D.J. Toenail trace element levels as biomarkers: Reproducibility over a 6-year period. *Cancer Epidemiol. Biomark. Prev.* **1993**, *2*, 493–497.
19. Webster, R.; Oliver, M. *Geostatistics for Environmental Scientists*; John Willey and Sons, Ltd.: New York, NY, USA, 2001. [CrossRef]
20. Michael, R.; O'Lenick, C.R.; Monaghan, A.; Wilhelmi, O.; Wiedinmyer, C.; Hayden, M.; Estes, M. Application of geostatistical approaches to predict the spatio-temporal distribution of summer ozone in Houston, Texas. *J. Expo. Sci. Environ. Epidemiol.* **2019**, *29*, 806–820. [CrossRef] [PubMed]

21. Shit, P.K.; Bhunia, G.S.; Maiti, R. Spatial analysis of soil properties using GIS based geostatistics models. Model. *Earth Syst. Environ.* **2016**, *2*, 107. [CrossRef]
22. Zierold, K.M.; Myers, J.V.; Brock, G.N.; Sears, C.G.; Sears, L.L.; Zhang, C.H. Nail Samples of Children Living near Coal Ash Storage Facilities Suggest Fly Ash Exposure and Elevated Concentrations of Metal(loid)s. *Environ. Sci. Technol.* **2021**, *55*, 9074–9086. [CrossRef] [PubMed]
23. Contreras-Llanes, M.; Santos-Sánchez, V.; Alguacil, J.; Castillo, J.M. Delineating distinct sediment pollution signatures from diverse sources in a heavily contaminated estuary near an area of high cancer and cardiovascular mortality. *Sci. Total Environ.* **2024**, *957*, 177715. [CrossRef] [PubMed]
24. Leistel, J.M.; Marcoux, E.; Thieblemont, D.; Quesada, C.; Sanchez, A.; Almodovar, G.R.; Pascual, E.; Saez, R. The volcanic-hosted massive sulphide deposits of the Iberian Pyrite Belt. *Miner. Deposita* **1998**, *33*, 2–30. [CrossRef]
25. Pérez-López, R.; Millán-Becerro, R.; Basallote, M.D.; Carrero, S.; Parviainen, A.; Freydier, R.; Macías, F.; Cánovas, C.R. Effects of estuarine water mixing on the mobility of trace elements in acid mine drainage leachates. *Mar. Pollut. Bull.* **2023**, *187*, 114491. [CrossRef] [PubMed]
26. Blasco, J.; Sáenz, V.; Gómez-Parra, A. Heavy metal fluxes at the sediment–water interface of three coastal ecosystems from south-west of the Iberian Peninsula. *Sci. Total Environ.* **2000**, *247*, 189–199. [CrossRef]
27. Santos Bermejo, J.C.; Beltrán, R.; Gómez Ariza, J.L. Spatial variations of heavy metals contamination in sediments from Odiel river (Southwest Spain). *Environ. Int.* **2003**, *29*, 69–77. [CrossRef] [PubMed]
28. Barba-Brioso, C.; Fernández-Caliani, J.C.; Miras, A.; Cornejo, J.; Galán, E. Multi-source water pollution in a highly anthropized wetland system associated with the estuary of Huelva (SW Spain). *Mar. Pollut. Bull.* **2010**, *60*, 1259–1269. [CrossRef]
29. Rosado, D.; Usero, J.; Morillo, J. Assessment of heavy metals bioavailability and toxicity toward *Vibrio fischeri* in sediment of the Huelva estuary. *Chemosphere* **2016**, *153*, 7–10. [CrossRef]
30. Sainz, A.; Grande, J.A.; de la Torre, M.L. Characterisation of heavy metal discharge into the Ria of Huelva. *Environ. Int.* **2004**, *30*, 557–566. [CrossRef] [PubMed]
31. Davila, J.M.; Sarmiento, A.M.; Santisteban, M.; Luís, A.T.; Fortes, J.C.; Diaz-Curiel, J.; Valbuena, C.; Grande, J.A. The UNESCO national biosphere reserve (Marismas del Odiel, SW Spain): An area of 18,875 ha affected by mining waste. *Environ. Sci. Pollut. Res.* **2019**, *26*, 33594–33606. [CrossRef]
32. Contreras-Llanes, M.; Pérez-López, R.; Gázquez, M.J.; Morales, V.; Santos, A.; Esquivias, L.M.; Bolívar, J.P. Fractionation and fluxes of metals and radionuclides during the recycling process of phosphogypsum wastes applied to mineral CO_2 sequestration. *Waste Manag.* **2015**, *45*, 412–419. [CrossRef]
33. Rentería-Villalobos, M.; Vioque, I.; Mantero, J.; Manjón, G. Radiological, chemical and morphological characterizations of phosphate rock and phosphogypsum from phosphoric acid factories in SW Spain. *J. Hazard. Mater.* **2010**, *181*, 193–203. [CrossRef]
34. Contreras, M. Valorisation of Inorganic Waste for Obtaining Construction Materials. Ph.D. Thesis, University of Huelva, Huelva, Spain, 19 July 2017. Available online: http://hdl.handle.net/10272/16090 (accessed on 2 September 2024).
35. Silva, L.F.O.; Oliveira, M.L.S.; Crissien, T.J.; Santosh, M.; Bolivar, J.P.; Shao, L.; Dotto, G.L.; Gasparotto, J.; Schindler, M. A review on the environmental impact of phosphogypsum and potential health impacts through the release of nanoparticles. *Chemosphere* **2022**, *286*, 131513. [CrossRef]
36. Lieberman, R.N.; Izquierdo, M.; Córdoba, P.; Moreno Palmerola, N.; Querol, X.; Sánchez de la Campa, A.M.; Font, O.; Cohen, H.; Knop, Y.; Torres-Sánchez, R.; et al. The evolution of brines from phosphogypsum deposits in Huelva (SW Spain) and its environmental implications. *Sci. Total Environ.* **2020**, *700*, 134444. [CrossRef] [PubMed]
37. Pérez-López, R.; Nieto, J.M.; López-Coto, I.; Aguado, J.L.; Bolívar, J.P.; Santisteban, M. Dynamics of contaminants in phosphogypsum of the fertilizer industry of Huelva (SW Spain): From phosphate rock ore to the environment. *Appl. Geochem.* **2010**, *25*, 705–715. [CrossRef]
38. International Atomic Energy Agency (IAEA). *Safety Standards Series. Application of the Concepts of Exclusion Exemption and Clearance, Safety Guide*; No. RS-G 17, STI/PUB/1202; IAEA: Vienna, Austria, 2004.
39. Castaño-Vinyals, G.; Aragonés, N.; Pérez-Gómez, B.; Martín, V.; Llorca, J.; Moreno, V.; Altzibar, J.M.; Ardanaz, E.; de Sanjosé, S.; Jiménez-Moleón, J.J.; et al. Population-based multicase-control study in common tumors in Spain (MCC-Spain): Rationale and study design. *Gac. Sanit.* **2015**, *29*, 308–315. [CrossRef] [PubMed]
40. Gutiérrez-González, E.; Fernández-Navarro, P.; Pastor-Barriuso, R.; García-Pérez, J.; Castaño-Vinyals, G.; Martín-Sánchez, V.; Amiano, P.; Gómez-Acebo, I.; Guevara, M.; Fernández-Tardón, G.; et al. Toenail zinc as a biomarker: Relationship with sources of environmental exposure and with genetic variability in MCC-Spain study. *Environ. Int.* **2022**, *169*, 107525. [CrossRef]
41. Thomsen, V.; Schatzlein, D.; Mercuro, D. Limits of detection in spectroscopy. *Spectroscopy* **2003**, *18*, 112–114.
42. Paz-González, A.; Vieira, S.R.; Tabeada, M.T. The effect of cultivation on the spatial variability of selected properties of an umbric horizon. *Geoderma* **2000**, *97*, 273–292. [CrossRef]

43. Demir, S.; Saral, A.; Ertürk, F.; Kuzu, L. Combined Use of Principal Component Analysis (PCA) and Chemical Mass Balance (CMB) for Source Identification and Source Apportionment in Air Pollution Modeling Studies. *Water Air Soil Pollut.* **2010**, *212*, 429–439. [CrossRef]
44. Cui, Z.; Qiao, S.; Bao, Z.; Wu, N. Contamination and distribution of heavy metals in urban and suburban soils in Zhangzhou City, Fujian, China. *Environ. Earth Sci.* **2011**, *64*, 1607–1615. [CrossRef]
45. Alastuey, A.; Querol, X.; Plana, F.; Viana, M.; Ruiz, C.R.; Sanchez de la Campa, A.; de la Rosa, J.; Mantilla, E.; García dos Santos, S. Identification and chemical characterization of industrial particulate matter sources in southwest Spain. *J. Air Waste Manag. Assoc.* **2006**, *56*, 993–1006. [CrossRef] [PubMed]
46. Chen, B.; Stein, A.F.; Castell, N.; González-Castanedo, Y.; Sánchez de la Campa, A.M.; de la Rosa, J.D. Modeling and evaluation of urban pollution events of atmospheric heavy metals from a large Cu-smelter. *Sci. Total Environ.* **2016**, *539*, 17–25. [CrossRef]
47. González-Castanedo, Y.; Moreno, T.; Fernández-Camacho, R.; Sánchez de la Campa, A.M.; Alastuey, A.; Querol, X.; de la Rosa, J. Size distribution and chemical composition of particulate matter stack emissions in and around a copper smelter. *Atmos. Environ.* **2014**, *98*, 271–282. [CrossRef]
48. Querol, X.; Alastue, A.; de la Rosa, J.; Sánchez-de-la-Campa, A.; Plana, F.; Ruiz, C.R. Source apportionment analysis of atmospheric particulates in an industrialised urban site in southwestern Spain. *Atmos. Environ.* **2002**, *36*, 3113–3125. [CrossRef]
49. Sánchez de la Campa, A.M.; de la Rosa, J.; Querol, X.; Alastuey, A.; Mantilla, E. Geochemistry and origin of PM_{10} in the Huelva region, southwestern Spain. *Environ. Res.* **2007**, *103*, 305–316. [CrossRef]
50. Sánchez de la Campa, A.M.; Sánchez-Rodas, D.; González Castanedo, Y.; de la Rosa, J.D. Geochemical anomalies of toxic elements and arsenic speciation in airborne particles from Cu mining and smelting activities: Influence on air quality. *J. Hazard. Mater.* **2015**, *291*, 8–27. [CrossRef] [PubMed]
51. Sánchez de la Campa, A.M.; Sánchez-Rodas, D.; Alsioufi, L.; Alastuey, A.; Querol, X.; de la Rosa, J.D. Air quality trends in an industrialised area of SW Spain. *J. Clean. Prod.* **2018**, *186*, 465–474. [CrossRef]
52. Bechtold, P.; Gatti, M.G.; Quattrini, G.; Ferrari, A.; Barbieri, G.; Iacuzio, L.; Carrozzi, G.; Righi, E. Trace elements in toenails in a population living near a modern municipal solid waste incinerator in Modena (Italy). *Chemosphere* **2021**, *263*, 128292. [CrossRef] [PubMed]
53. Butler, L.; Gennings, C.; Peli, M.; Borgese, L.; Placidi, D.; Zimmerman, N.; Hsu, H.L.; Coull, B.A.; Wright, R.O.; Smith, D.R.; et al. Assessing the contributions of metals in environmental media to exposure biomarkers in a region of ferroalloy industry. *J. Expo. Sci. Environ. Epidemiol.* **2019**, *29*, 674–687. [CrossRef] [PubMed]
54. Coelho, P.; Costa, S.; Costa, C.; Silva, S.; Walter, A.; Ranville, J.; Pastorinho, M.R.; Harrington, C.; Taylor, A.; Dall'Armi, V.; et al. Biomonitoring of several toxic metal(loid)s in different biological matrices from environmentally and occupationally exposed populations from Panasqueira mine area, Portugal. *Environ. Geochem. Health* **2014**, *36*, 255–269. [CrossRef] [PubMed]
55. Nakaona, L.; Maseka, K.K.; Hamilton, E.M.; Watts, M.J. Using human hair and nails as biomarkers to assess exposure of potentially harmful elements to populations living near mine waste dumps. *Environ. Geochem. Health* **2020**, *42*, 1197–1209. [CrossRef]
56. Przybylowicz, A.; Chesy, P.; Herman, M.; Parczewski, A.; Walas, S.; Piekoszewski, W. Examination of distribution of trace elements in hair, fingernails and toenails as alternative biological materials. Application of chemometric methods. *Cent. Eur. J. Chem.* **2012**, *10*, 1590–1599. [CrossRef]
57. Rashed, M.N.; Hossam, F. Heavy Metals in Fingernails and Scalp Hair of Children, Adults and Workers from Environmentally Exposed Areas at Aswan, Egypt. *Environ. Bioindic.* **2007**, *2*, 131–145. [CrossRef]
58. Slotnick, M.J.; Nriagu, J.O.; Johnson, M.M.; Linder, A.M.; Savoie, K.L.; Jamil, H.J.; Hammad, A.S. Profiles of trace elements in toenails of Arab-Americans in the Detroit area, Michigan. *Biol. Trace Elem. Res.* **2005**, *107*, 113–126. [CrossRef] [PubMed]
59. Sureda, A.; Bibiloni, M.D.M.; Julibert, A.; Aparicio-Ugarriza, R.; Palacios-Le Blé, G.; Pons, A.; Gonzalez-Gross, M.; Tur, J.A. Trace element contents in toenails are related to regular physical activity in older adults. *PLoS ONE* **2017**, *12*, e0185318. [CrossRef] [PubMed]
60. Van Horne, Y.O.; Farzan, S.F.; Johnston, J.E. Metal-mixtures in toenails of children living near an active industrial facility in Los Angeles County, California. *J. Expo. Sci. Environ. Epidemiol.* **2021**, *31*, 427–441. [CrossRef] [PubMed]
61. Di Ciaula, A.; Gentilini, P.; Diella, G.; Lopuzzo, M.; Ridolfi, R. Biomonitoring of Metals in Children Living in an Urban Area and Close to Waste Incinerators. *Int. J. Environ. Res. Public Health* **2020**, *17*, 1919. [CrossRef] [PubMed]
62. Ojekunle, O.Z.; Rasaki, A.; Taiwo, A.M.; Adegoke, K.A.; Balogun, M.A.; Ojekunle, O.O.; Anumah, A.O.; Ibrahim, A.O.; Adeyemi, A. Health risk assessment of heavy metals in drinking water leaching through improperly managed dumpsite waste in Kurata, Ijoko, Sango area of Ogun State, Nigeria. *Groundw. Sustain. Dev.* **2022**, *18*, 100792. [CrossRef]
63. Yoo, Y.C.; Lee, S.K.; Yang, J.Y.; In, S.W.; Kim, K.W.; Chung, K.H.; Chung, K.G.; Choung, S.Y. Organ Distribution of Heavy Metals in Autopsy Material from Normal Korean. *J. Health Sci.* **2002**, *48*, 186–194. [CrossRef]
64. Aguilera, I.; Daponte, A.; Gil, F.; Hernández, A.F.; Godoy, P.; Pla, A.; Ramos, J.L. Urinary levels of arsenic and heavy metals in children and adolescents living in the industrialised area of Ria of Huelva (SW Spain). *Environ. Int.* **2010**, *36*, 563–569. [CrossRef] [PubMed]

65. Rodríguez-Barranco, M.; Lacasaña, M.; Gil, F.; Lorca, A.; Alguacil, J.; Rohlman, D.S.; González-Alzaga, B.; Molina-Villalba, I.; Mendoza, R.; Aguilar-Garduño, C. Cadmium exposure and neuropsychological development in school children in southwestern Spain. *Environ. Res.* **2014**, *134*, 66–73. [CrossRef] [PubMed]
66. Capelo, R.; Rohlman, D.S.; Jara, R.; García, T.; Viñas, J.; Lorca, J.A.; Contreras-Llanes, M.; Alguacil, J. Residence in an Area with Environmental Exposure to Heavy Metals and Neurobehavioral Performance in Children 9–11 Years Old: An Explorative Study. *Int. J. Environ. Res. Public Health* **2022**, *19*, 4732. [CrossRef]
67. Silva-Caicedo, R.F.; Contreras-Llanes, M.; Capelo, R.; Zumel-Marne, A.; García-Sevillano, M.Á.; Santos-Sánchez, V.; Alguacil, J. Impact of Fish, Mollusk and Seafood Consumption before Sample Donation on Urinary and Toenail Metal Levels in Workers Exposed to Heavy Metals. *Appl. Sci.* **2024**, *14*, 8174. [CrossRef]
68. Li, F.; Huang, J.; Zeng, G.; Yuan, X.; Li, X.; Liang, J.; Wang, X.; Tang, X.; Bai, B. Spatial risk assessment and sources identification of heavy metals in surface sediments from the Dongting Lake, Middle China. *J. Geochem. Explor.* **2013**, *132*, 75–83. [CrossRef]
69. Taiwo, A.M.; Harrison, R.M.; Shi, Z.B. A review of receptor modelling of industrially emitted particulate matter. *Atmos. Environ.* **2014**, *97*, 109–120. [CrossRef]
70. Adigun, C.G. Nail Reactions to Poisons and Intoxicants. In *Scher and Daniel's Nails*; Rubin, A.I., Jellinek, N.J., Daniel, C.R., Scher, R.K., Eds.; Springer: Cham, Switzerland; Berlin/Heidelberg, Germany, 2018. [CrossRef]
71. Egwunye, J.; Cardoso, B.R.; Braat, S.; Ha, T.; Hanieh, S.; Hare, D.; Duan, A.X.; Doronila, A.; Tran, T.; Tuan, T.; et al. The role of fingernail selenium in the association between arsenic, lead and mercury and child development in rural Vietnam: A cross-sectional analysis. *Br. J. Nutr.* **2023**, *129*, 1589–1597. [CrossRef]
72. World Health Organization (WHO). *Environmental Health Criterion 58—Selenium*; World Health Organization: Geneva, Switzerland, 1987. Available online: https://iris.who.int/bitstream/handle/10665/37268/9241542586-eng.pdf?sequence=1&isAllowed=y (accessed on 19 September 2024).
73. Sexton, K.; Hattis, D. Assessing cumulative health risks from exposure to environmental mixtures-three fundamental questions. *Environ. Health Perspect.* **2007**, *115*, 825–832. [CrossRef]

A2. Quality indicators

This PhD thesis is presented according to the Compendium of Publications mode, regulated under art. 35 of the Regulation of Official Doctoral Studies of the University of Huelva of 17th December 2024. The articles have been published with the express approval of the Director/Tutor of this PhD thesis and carried out further to the enrolment of doctoral studies. The references of these papers are listed below:

Publications

1. **Contreras-Llanes, M.**, Santos-Sánchez, V., Alguacil, J. and Castillo, J.M., 2024. Delineating distinct sediment pollution signatures from diverse sources in a heavily contaminated estuary near an area of high cancer and cardiovascular mortality. Sci. Total Environ. 957, 177715. https://doi.org/10.1016/j.scitotenv.2024.177715

   Journal Impact Factor:

   2023 journal Impact factor: 8.2; **journal Impact factor without self-citations**: 7.3

   Rank by Journal Impact Factor:

   CATEGORY: ENVIRONMENTAL SCIENCES (31/358)

   JCR YEAR: 2023; **JIF RANK**: 31/358; **JIF QUARTILE**: Q1; **JIF PERCENTILE**: 91.5

2. **Contreras-Llanes, M.**, Santos-Sánchez, V., Alguacil, J. and Rodríguez, R., 2025. Influence of phosphogypsum waste on rainwater chemistry in a highly polluted area with high mortality rates in Huelva metropolitan area, Spain. *Sustainability*, 17, 3102. https://doi.org/10.3390/su17073102

   Journal Impact Factor:

   2023 journal Impact factor: 3.3; **journal Impact factor without self-citations**: 2.7

Rank by Journal Impact Factor:

CATEGORY: ENVIRONMENTAL SCIENCES (159/358)

JCR YEAR: 2023; **JIF RANK**: 159/358; **JIF QUARTILE**: Q2; **JIF PERCENTILE**: 55.7

3. **Contreras-Llanes, M.**, Alguacil, J., Capelo, R., Gómez-Ariza, J.L., García-Pérez, J., Pérez-Gómez, B., Martin-Olmedo, P. and Santos-Sánchez, V., 2025. Internal cumulated dose of toxic metal(loid)s in a population residing near a Naturally Occurring Radioactive Material waste stacks and an industrial heavily polluted area with high mortality rates in Spain. J. Xenobiot, 15, 29. https://doi.org/10.3390/jox15010029

Journal Impact Factor:

2023 journal Impact factor: 6.8; **journal Impact factor without self-citations**: 6.6

Rank by Journal Impact Factor:

CATEGORY: TOXICOLOGY (6/106)

JCR YEAR: 2023; **JIF RANK**: 6/106; **JIF QUARTILE**: Q1; **JIF PERCENTILE**: 94.8

A3. Other publications

This section includes list of other publications derived from the thesis:

1. Silva-Caicedo, R.F., **Contreras-Llanes, M.**, Capelo, R., Zumel-Marne, A., García-Sevillano, M.Á., Santos-Sánchez, V., Alguacil, J., 2024. Impact of Fish, Mollusk and Seafood Consumption before Sample Donation on Urinary and Toenail Metal Levels in Workers Exposed to Heavy Metals. Appl. Sci. 14, 8174. https://doi.org/10.3390/app14188174

2. García-Pérez, J., Fernández de Larrea-Baz, N., Lope, V., Domínguez-Castillo, A., Espinosa, A., Dierssen-Sotos, T., **Contreras-Llanes, M.,** Sierra, M.A., Castaño-Vinyals, G., Tardón, A., Jiménez-Moleón, J.J., Molina-Barceló, A., Aragones, N., Kogevinas, M., Pollán, M., Pérez-Gómez, B., 2024. Risk of prostate cancer in the proximity of industrial installations: A multicase-control study in Spain (MCC-Spain). Sci. Total Environ. 946, 174347. https://doi.org/10.1016/j.scitotenv.2024.174347

3. Gasull, M., Camargo, J., Pumarega, J., Henríquez-Hernández, L.A., Campi, L., Zumbado, M., **Contreras-Llanes, M.**, Oliveras, L., González-Marín, P., Luzardo, O.P., Gómez-Gutíerrez, A., Alguaci, J., Porta, M., 2023. Blood concentrations of metals, essential trace elements, rare earth elements and other chemicals in the general adult population of Barcelona: Distribution and associated sociodemographic factors. Sci. Total Environ. 909, 168502. https://doi.org/10.1016/j.scitotenv.2023.168502

4. Peñalver-Piñol, A., Benavente, Y., Frias-Gomez, J., Alguacil, J., Santibañez, M., **Contreras-Llanes, M.**, Peremiquel-Trillas, P., López-Querol, M., Paytubi, S., Pelegrina, B., Onieva, I., Martínez, J.M., Fernandez-Gonzalez, S., de Francisco, J., Caño, V., Brunet, J., Pineda, M., Ponce, J., Matias-Guiu, X., Bosch, F.X., de Sanjosé, S., Alemany, L., Costas, L., 2023. Occupational exposure to pesticides and

endometrial cancer in the Screenwide case-control study. Environ. Health. 22, 77. https://doi.org/10.1186/s12940-023-01028-0

5. Palomar-Cros, A., Straif, K., Romaguera, D., Aragonés, N., Castaño-Vinyals, G., Martin, V., Moreno, V., Gómez-Acebo, I., Guevara, M., Aizpurua, A., Molina-Barceló, A., Jiménez-Moleón, J. J., Tardón, A., **Contreras-Llanes, M.**, Marcos-Gragera, R., Huerta, J. M., Pérez-Gómez, B., Espinosa, A., Hernández-Segura, N., Obón-Santacana, M., … Lassale, C., 2023. Consumption of aspartame and other artificial sweeteners and risk of cancer in the Spanish multicase-control study (MCC-Spain). Int. J. Cancer, 153(5), 979–993. https://doi.org/10.1002/ijc.34577

6. Capelo, R., Rohlman, D. S., Jara, R., García, T., Viñas, J., Lorca, J. A., **Contreras Llanes, M.**, Alguacil, J., 2022. Residence in an Area with Environmental Exposure to Heavy Metals and Neurobehavioral Performance in Children 9-11 Years Old: An Explorative Study. Int. J. Environ. Res. Public Health 19(8), 4732. https://doi.org/10.3390/ijerph19084732